



universität
wien

DIPLOMARBEIT

The Shape of Space

The Geometry and Topology of the Universe

angestrebter akademischer Grad

Magistra der Naturwissenschaften (Mag. rer. nat.)

Verfasser: Gudrun Weisz, Bakk.
Matrikel-Nummer: 0308220
Studienrichtung: Mathematik A405
Betreuer: Mathematik: Assoz. Prof. Dr. Dietrich Burde
Astronomie: Ao. Univ.-Prof. Dr. Ernst A. Dorfi

Wien, am 11. 11. 2012

Danksagung

Zunächst möchte ich meinen Eltern, Helga und Cornel Weisz, danken, die es mir ermöglicht haben nach Interesse zu studieren. Meiner Mutter danke ich, dass sie mich ermunterte im Zuge meiner Diplomarbeit die vielleicht einmalige Chance zu nutzen mich mit einer wissenschaftlichen Fragestellung meiner Wahl auseinanderzusetzen. Meinem Vater danke ich für die vielen inhaltlichen Gespräche über das Thema. Großer Dank gebührt meinem Partner Andreas Enzminger, der mich bei all meinen Projekten mit so viel Geduld unterstützt.

Weiters möchte ich meinem Betreuer Dietrich Burde für den wissenschaftlichen Austausch und die stetige Bereitschaft dafür danken. Er war es, der mich auf das Thema gebracht hat. Meinem Betreuer Ernst Dorfi danke ich für seine Unterstützung und den großen Freiraum den er mir gelassen hat. Ich danke den Teilnehmern des wissenschaftlichen Seminars des Institut für Mathematik der Universität für Bodenkultur für den wissenschaftlichen Austausch und das Interesse an meinem Thema.

Meinen Studienkollegen Magdalena Vass und David Hirschmann danke ich, dass ich auf ihre Erfahrung zurückgreifen durfte. Sophie Esterer ist es zu verdanken, dass die Arbeit sprachlich so ist wie sie ist.

Ich danke meinen Großeltern, Hildegard und Ernst Brandlmayer, dafür, dass ich bei Ihnen immer wieder unterchlupfen und mich in das Thema vertiefen konnte. Meinen Freunden, vor allen Christian Laffnitzegger und Sophie Esterer, danke ich für die moralische Unterstützung und Begleitung während dieser doch sehr intensiven Zeit.

Abstract

Based on the General Theory of Relativity, I argue that the spatial part of space-time can be described by a three-dimensional, orientable, locally homogeneous, connected, smooth and complete Riemannian manifold \mathcal{M} without boundary. The main topic of this work is to classify all the possible \mathcal{M} by their geometry and topology.

Complete and locally homogeneous manifolds \mathcal{M} can be represented as the quotients $\widetilde{\mathcal{M}}/\Gamma$, with Γ acting freely and properly discontinuously on the globally homogeneous universal covering space $\widetilde{\mathcal{M}}$. The geometric structure on \mathcal{M} is induced by $\widetilde{\mathcal{M}}$, hence, the classification of all geometric structures on \mathcal{M} can be done by classifying all three-dimensional geometries $(\widetilde{\mathcal{M}}, Isom(\widetilde{\mathcal{M}}))$. Finally, Thurston's Geometrization Theorem states that \mathcal{M} has a geometric structure, modeled on one of the eight three-dimensional model geometries.

Supported by observational data, we restrict ourselves to locally isotropic manifolds, reducing the classification of the possible topologies of \mathcal{M} to the three-dimensional Clifford-Klein space form problem. It can be solved by classifying the discrete subgroups of the isometry groups of the simply-connected manifolds of constant curvature $\mathbb{E}^3, \mathbb{S}^3$ and \mathbb{H}^3 which act freely on them. For \mathbb{E}^3 and \mathbb{S}^3 this classification enables us to list all candidates for the spatial part of the universe with a flat respectively spherical geometry. So far, there is no known structural classification of the hyperbolic space forms.

Every compact space form can be described as a gluing manifold, which are fundamental polyhedra with identified sides by pairs. In closing, the methods used by Cosmic Topology with the help of this "inner view" are presented. These, as opposed to the methods used by Standard Cosmology, try to determine not only the geometry, but also the topology of the space surrounding us.

Zusammenfassung

Basierend auf der allgemeinen Relativitätstheorie, wird argumentiert, dass die räumliche Komponente der Raumzeit mit einer dreidimensionalen, orientierbaren, lokal homogenen, zusammenhängenden, glatten und vollständigen Riemann'schen Mannigfaltigkeit \mathcal{M} ohne Rand beschrieben werden kann. Das Hauptbestreben der vorliegenden Arbeit ist die Klassifikation der möglichen \mathcal{M} nach ihrer Geometrie und Topologie.

Vollständige und lokal homogene Mannigfaltigkeiten \mathcal{M} können als Quotienten $\widetilde{\mathcal{M}}/\Gamma$ dargestellt werden, wobei $\Gamma \subset \text{Isom}(\widetilde{\mathcal{M}})$ frei und eigentlich diskontinuierlich auf der global homogenen universellen Überlagerung $\widetilde{\mathcal{M}}$ operiert. Die geometrische Struktur auf \mathcal{M} wird von $\widetilde{\mathcal{M}}$ induziert und somit ist eine Klassifikation der Geometrien $(\widetilde{\mathcal{M}}, \text{Isom}(\widetilde{\mathcal{M}}))$ ausreichend. Vervollständigt wird die Klassifikation durch Thurstons Geometrisierungstheorem, welches besagt, dass \mathcal{M} mit einer geometrischen Struktur versehen werden kann, welche auf einer der acht dreidimensionalen Modell-Geometrien modelliert wurde.

Die von Beobachtungsdaten gestützte Einschränkung auf lokal isotrope Mannigfaltigkeit reduziert das Problem der Klassifikation der möglichen Topologien von \mathcal{M} auf das dreidimensionale Clifford-Klein'sche Raumproblem. Dieses ist äquivalent mit der Klassifikation diskreter Untergruppen von Isometriegruppen der einfach zusammenhängender Mannigfaltigkeiten konstanter Krümmung $\mathbb{E}^3, \mathbb{S}^3$ und \mathbb{H}^3 , welche frei auf eben diesen operieren. Diese Klassifikation erlaubt es uns, eine Liste möglicher Kandidaten für die räumliche Komponente des Universums mit flacher oder sphärischer Geometrie anzugeben. Für hyperbolische Raumformen ist bis jetzt keine strukturelle Klassifikation bekannt.

Jede kompakte Raumform kann als Fundamentalpolyeder mit paarweise identifizierenden Seiten dargestellt werden. Mit Hilfe dieser Darstellung wird abschließend auf die Methoden der "Cosmic Topology" eingegangen. Im Gegensatz zu den Methoden der Standardkosmologie versuchen diese nicht nur die Geometrie, sondern auch die Topologie des uns umgebenden Raums zu bestimmen.

Contents

Abstract	iii
Zusammenfassung	v
0. Introduction	1
1. Preconditions of the Universe	5
1.1. Basics of Differential Geometry	6
1.1.1. Manifolds	6
1.1.2. Vectors and Tensors	8
1.1.3. Parallel Transport and Curvature	15
1.1.3.1. Parallel Transport	16
1.1.3.2. Curvature	17
1.1.4. Geodesics	19
1.1.5. Hypersurface	19
1.2. Introduction to General Theory of Relativity	20
1.2.1. First Assumptions on Space-Time	20
1.2.2. The Equivalence Principle	21
1.2.3. Metric within General Theory of Relativity	21
1.2.4. Geodesic Hypothesis	22
1.2.5. Einstein's Field Equations	22
1.2.6. Orientation	25
1.2.6.1. Time Orientation and Causality	25
1.2.6.2. Causality Conditions	28
1.2.6.3. Space Orientation	31
1.2.7. Further Assumptions on Space-Time	31
1.3. Observing the Universe	32
1.3.1. The Expansion of the Universe and the Big Bang	33
1.3.2. Remnant of Last Scattering	34
1.4. Is the Spatial Part of the Universe Finite or Infinite?	35
1.5. Conclusion	36
2. An Algebraic Approach to Geometry and the Topology of the Universe	37
2.1. Manifolds and Pseudogroups	37
2.2. Lie Groups – Basic Definitions and First Examples	39
2.2.1. The Action of a Group	40
2.2.2. Homogenous Spaces	42
2.3. The Universal Covering Space	44
2.3.1. The Group of Deck Transformations and its Action on M	48

2.3.2. Manifolds as Quotient Spaces	49
2.4. Conclusion	51
3. Geometry of the Universe	53
3.1. Geometric Structures on Manifolds	53
3.2. The Geometric Structure is Induced by the Universal Cover	56
3.2.1. Unrolling-Developing	56
3.2.1.1. Story of Tori – Unrolling the Two-Dimensional Torus in \mathbb{R}^4	56
3.2.2. The Developing Map	59
3.2.3. Locally Homogeneous Riemannian Manifolds and The Condition of Completeness	62
3.3. Three-Dimensional Model Geometries	64
3.3.1. Bundles	65
3.3.2. The Eight Model Geometries	67
3.3.2.1. If the Stabilizer is the Full Group $SO_3(\mathbb{R})$	68
3.3.2.2. If the Stabilizer is $SO_2(\mathbb{R})$	69
3.3.2.3. If the Stabilizer is Trivial:	72
3.3.2.4. Thurston's Geometrization Theorem	74
3.4. Conclusion	74
4. Locally Isotropic Riemannian Manifolds	77
4.1. Simply-Connected Spaces of Constant Curvature	79
4.1.1. The Classification Theorem	79
4.2. Space Forms	80
4.2.1. Homogeneous Space Forms	81
4.3. Preparations	81
4.3.1. Finite Subgroups of $SO_3(\mathbb{R})$	82
4.4. Euclidean Space Forms	85
4.4.1. Affine Spaces	85
4.4.2. Compact Euclidean Space Forms	86
4.4.2.1. Three-Dimensional Orientable, Compact Euclidean Space Forms	88
4.4.3. Open Euclidean Space Forms	90
4.4.3.1. Open Three-Dimensional Euclidean Space Forms	90
4.5. Three-Dimensional Spherical Space Forms	92
4.5.1. Finite Subgroups of $SO_4(\mathbb{R})$	92
4.5.2. Classification of the Three-Dimensional Spherical Space Forms	94
4.6. Three-Dimensional Hyperbolic Space Forms	97
4.6.1. Thick-Thin Decomposition	97
4.7. Conclusion	98
5. Gluing Manifolds	99
5.1. Gluings – Geometry of Discrete Groups	99
5.1.1. Metric on Space Forms	100
5.1.2. The Fundamental Polyhedron	101
5.1.3. Tessellation	103
5.2. Gluings	104
5.2.1. Theoretical Background	104
5.2.1.1. Side-Pairing	105

5.2.1.2. Dihedral Angle	105
5.2.1.3. Cycle Relations and Cycles of Polyhedra	106
5.2.2. Gluing Manifolds	107
5.2.3. Volumes of Space Forms	110
5.3. Euclidean Space Forms	110
5.3.0.1. Fundamental Polyhedron: Parallelepiped	110
5.3.0.2. Fundamental Polyhedron: Hexagonal Prism	112
5.4. Spherical Space Forms	112
5.4.1. Lens Spaces	113
5.4.2. Polyhedral Spaces	113
5.5. Hyperbolic Space Forms	115
5.6. Conclusion	116
6. Observing the Geometry and Topology of the Universe	119
6.1. Geometry of the Universe – The State of the Art of Standard Cosmology	121
6.1.1. Robertson-Walker Metric	121
6.1.2. Friedmann-Lemaître Universe	123
6.1.3. Measuring the Cosmological Parameter	128
6.1.3.1. Hubble Constant H_0	128
6.1.3.2. Critical Density ρ_{crit} and Hubble Time T_0	129
6.1.3.3. Mass Density ρ_M	129
6.1.3.4. Radiant Flux Density ρ_γ	131
6.1.3.5. Energy Density of Vacuum Energy ρ_Λ	131
6.1.3.6. Curvature Parameter Ω_K	132
6.2. Cosmic Topology	132
6.2.1. Introduction	132
6.2.2. Finding the Imprints of Multi-Connected Spaces	136
6.2.2.1. Spatial Scales Associated with the Fundamental Polyhedron	136
6.2.2.2. Distribution of Ghosts in the Observable Universe	136
6.2.2.3. Searching for Ghosts	137
6.2.3. Cosmic Crystallography	138
6.2.3.1. Pair Separation Histogram:	139
6.2.3.2. Collecting Correlated Pair Method CCP:	143
6.2.3.3. Cosmic Crystallography with Pull-Back:	145
6.2.3.4. Crystallographic Methods Using Filter:	146
6.2.3.5. Possible Sources of Errors of Crystallographic Methods:	147
6.3. Anisotropies in the Cosmic Microwave Background	149
6.3.1. Anisotropies Caused by Effects in the Recent Universe:	151
6.3.1.1. Dipole Anisotropy:	151
6.3.1.2. Sunyaev-Zel’dovich Effect:	152
6.3.2. Primary Anisotropies	152
6.3.2.1. Sachs-Wolf Effect:	153
6.3.2.2. Integrated Sachs-Wolf Effect:	154
6.3.3. Mathematical Description of Anisotropies	154
6.3.4. Detecting-Methods using CMB-Maps	156
6.3.4.1. Circles-in-the-Sky	157
6.3.4.2. Power Spectrum	163
6.4. The Poincaré Dodecahedral Space	165

6.5. Conclusion	169
Bibliography	172
Appendix	183
A. Topology	185
A.1. Topological Groups	186
B. The Correspondence of Lie Groups and Lie Algebras	189
B.1. Representation of Lie Groups	189
B.2. Correspondence between Lie Groups and Lie Algebras	189
B.2.1. The Tangent Space and the Vector Space of Vector Fields	190
B.2.2. The Lie Algebra of the Lie Group G	191
B.2.3. Consequences	192
B.2.4. Homogenous Spaces and their Lie Algebras	194
C. Sectional Curvature	195
Index	197
Curriculum Vitae	205

0. Introduction

From our home on the Earth, we look out into the distances and strive to imagine the sort of world into which we are born. Today we have reached far out into Space. Our immediate neighborhood we know rather intimately. But with increasing distance our knowledge fades, and fades rapidly, until at the last dim horizon we search among ghostly errors of observations for landmarks that are scarcely more substantial. The search will continue. The urge is older than history. It is not satisfied and it will not be suppressed. *Edwin Hubble, 1953* [45]

With this philosophical background, we shall focus on the question about the geometry and topology of the spatial part of the universe. The strategy shall be to formulate properties of the universe which are consistent, on the one hand, with the current physical theory on the largest scales, namely the General Theory of Relativity, and, on the other hand with the observed universe based on a Big Bang scenario. On the spaces satisfying the above formulated properties, we shall then apply the mathematical machinery to classify all the possible geometric structures and topologies.

General Theory of Relativity assumes space-time to be a connected and smooth four-dimensional Lorentzian manifold \mathcal{M}_4 which satisfies Einstein's field equations. After an introductory remark, we start the first chapter with the basics of differential geometry, which builds the formal framework of General Theory of Relativity. In the second section, the basic concept of General Theory of Relativity is introduced, which includes, for example, the correlation between matter and the metric defined on the manifold, as well as a motivation of Einstein's field equations. Furthermore, causality conditions are formulated which enable us to consider the space-component \mathcal{M}_3 of the universe on its own, which is a smooth and connected three-dimensional Riemannian manifold. Before we focus on the observational universe, further preconditions of the universe, following [43] and [107], are formulated without which the universe would appear paradoxical and contradicting our everyday-experience of the world we are living in. Observational data indicates spatial homogeneity and isotropy of the universe. At this point, it is worthwhile to note that throughout this work these properties are assumed to be local, enabling space to have a nontrivial topology and therefore to be finite and independent of the geometry defined on \mathcal{M}_3 .

In Chapter 2 we start with an algebraic definition of a manifold, which we call a G -manifold. A pseudogroup G , consisting of local homeomorphisms on \mathbb{R}^n , defines a G -atlas turning the topological space \mathcal{M} into a manifold. This group can often be assumed to be a Lie group, which we shall define in the second section, where we concretize the algebraic approach to geometry. A group G acts on a topological space \mathcal{M} , which we interpret as G moving points of the space or stabilizing them. If any point can be reached from any point, the space is called homogeneous, giving us the mathematical definition of homogeneity. We continue with the definition of a covering space and the representation of manifolds as the quotient $\mathcal{M} \simeq \widetilde{\mathcal{M}}/\Gamma$, with Γ being isomorphic to the fundamental group of \mathcal{M} and acting freely and properly discontinuously on the universal covering space $\widetilde{\mathcal{M}}$. Thus, \mathcal{M} can be constructed by identifying points in a simply-connected space $\widetilde{\mathcal{M}}$.

Next, in Chapter 3, the term “metric manifold”, which is a (\mathbb{G}, \mathbb{M}) -manifold with \mathbb{G} the isometry group of a homogeneous Riemannian manifold \mathbb{M} , is defined. A geometric structure shall be a (\mathbb{G}, \mathbb{M}) -atlas. A complete metric manifold can be characterized by the identification of the structure space \mathbb{M} and the covering space $\widetilde{\mathcal{M}}$. Therefore, the geometric structure on the complete and locally homogeneous manifold \mathcal{M} is induced by the globally homogeneous universal covering space $\widetilde{\mathcal{M}}$. This enables us to focus on the classification of simply-connected and homogeneous three-dimensional Riemannian manifolds. Thurston’s Geometrization Theorem states that there are exactly eight three-dimensional model geometries. We shall give a rough sketch of the proof of the theorem by characterizing model geometries in order of the dimension of their isotropy group and give a detailed description of each of the eight model geometries.

In Chapter 4, supported by observational data, we restrict our investigation to locally isotropic manifolds and consider their topological classification. We start by arguing that locally isotropic Riemannian manifolds are exactly Riemannian manifolds of constant curvature. The problem reduces to the three-dimensional Clifford-Klein space form problem. It can be solved by classifying the discrete subgroups of the isometry groups of the simply-connected manifolds of constant curvature \mathbb{E}^3 , \mathbb{S}^3 and \mathbb{H}^3 which act freely on them. In the compact Euclidean case, we shall see that the classification can be done by classifying the torsion-free, discrete and co-compact subgroups of $E(n)$, denoting the isometry group of \mathbb{E}^3 . These groups are called Bieberbach groups. In the spherical case, we shall classify all finite subgroups of $SO_4(\mathbb{R})$, describing the isometry group of \mathbb{S}^3 . The hyperbolic case turns out to be harder than the other cases. So far, there is no known structural classification of hyperbolic manifolds. We shall give a description of the Thick-Thin decomposition, which can be done for any complete hyperbolic manifold and we also make a remark on the existence of a classification of hyperbolic manifolds in terms of their volumes. This classification enables us to list candidates for the spatial part of the universe.

Every compact space form can be described as a gluing manifold, which is a fundamental polyhedron with identified sides by pairs. This representation enables the development of a

visualization of three-dimensional manifolds without an embedding in a higher-dimensional space. We shall introduce this representation in Chapter 5. All three-dimensional compact Euclidean space forms as well as a selected set of hyperbolic and spherical space forms are presented in detail as gluing manifolds. This “inner view” will be useful in Chapter 6, where we present methods to determine which three-dimensional manifold is surrounding us.

In Chapter 6, we start with an overview of Standard Cosmology. A family of solutions for a locally homogeneous and locally isotropic spatial part of space-time for Einstein’s field equation is justified. Furthermore, we shall give an idea of how the geometry of the universe can be determined by measuring the “cosmological parameter”. As opposed to Standard Cosmology, Cosmic Topology tries to determine not only the geometry, but also the topology of the space surrounding us. On the one hand three-dimensional data of cosmic objects is used by “crystallographic methods”. On the other hand, the topological signal of space has been searched for in the anisotropies of the Cosmic Microwave Background (CMB). Before we present the corresponding methods, such as the “circle-in-the-sky method” and methods using the “power spectrum”, we shall give a short introduction to the theory of anisotropies in the CMB. In closing, we present the results obtained so far for Poincaré dodecahedral space, which is a model frequently discussed in Cosmic Topology.

The appendix consists of three parts. The first part is a basic introduction to topology, starting with the definition of a topological space. Topological definitions and results, if not given throughout the text, shall be found in Appendix A. The second part of the appendix considers the correspondence of Lie groups and Lie algebras, which is used in Chapter 3 for the motivation of geometric structures modeled on manifolds with one-dimensional stabilizers. Appendix B ends with a remark on the Lie algebras of homogeneous spaces. The third part of the appendix, Appendix C, introduces the “sectional curvature” of a Riemannian manifold. While the General Theory of Relativity uses the “scalar curvature” defined in Chapter 1, Riemannian geometry often uses the “sectional curvature” of a manifold. The correspondence between sectional and scalar curvature is explained in Chapter 4.

A comprehensive index, starting with a table of symbols, shall enable the reader to look up definitions in case no reference is given. I have tried to write this work in a way that allows first year students of mathematics as well as astronomy to follow the arguments, sometimes to the loss of mathematical elegance and compactness. Readers with a more detailed mathematical background or a basic knowledge of General Theory of Relativity or Standard Cosmology may prefer to skip some parts of the work.

1. Preconditions of the Universe

Space is not a passive background, rather it has a structure which influences the shape of all existing objects. Every material form pays tribute to the rules dictated by the architecture of space. [62]

Which mathematical space enables a geometrical structure to describe all observed events in the universe? We define the universe as the collection of all events and we are interested in a cosmological model describing the universe. Einstein described a cosmological model as reasonable, if it is a space-time which is the exact solution of some suitable form of matter and gives a good representation of global properties in the observable universe [43].

Our everyday experience suggests three spatial dimensions and one dimension which represents time. Thus, the universe can be described by a four-dimensional space-time. First, we recognize that the shape of the universe depends on the scale. We distinguish between the microscopic, local, macroscopic and the global scale, where different physical frameworks are used. Since physics is written in terms of local geometry within mathematical space, different mathematical structures and, as we shall see, different mathematical spaces are required on these scales.

- **Microscopic:** If we are describing physical processes on scales beyond the Planck length ($< 10^{-18}$ meter), quantum physical effects have to be taken into account. On these microscopic scales we find ourselves in the field of quantum physics. Physicists try to describe space by compact Calabi-Yau manifolds, which might include hidden dimensions [43, p.57] [55].
- **Local:** Events on scales between the Planck length ($\approx 10^{-18}$ m) and the sun-earth distance ($\approx 10^{11}$ m) can be described in a very good approximation with Newtonian physics in the common Euclidean space \mathbb{E}^3 . Therefore, in a good approximation, the geometry on local scales is flat. If relativistic velocities are taken into account, a Special Theory of Relativity is required. Space-time is described by Minkowski space – a four-dimensional, connected and flat Lorentzian manifold [55].
- **Macroscopic:** ($10^{11} - 10^{25}$ m) The General Theory of Relativity is the physical framework on macroscopic scales. It is currently the most comprehensive theory for large scales. The mathematical model for space-time is a four-dimensional and connected

Lorentzian manifold which satisfies Einstein's field equations. As opposed to the Special Theory of Relativity, gravitational effects are taken into account which cause space-time to be curved by more or less massive bodies. We shall go into this in further detail in Section 1.2 [55].

- **Global:** If we look at global scales ($> 10^{25} m$), observational data indicates that matter is distributed homogeneously and density fluctuations can thus be neglected. For these scales, there is no physical framework. Here, the General Theory of Relativity is the local physical framework. To find out more about the shape of the universe on global scales, we use the following strategy: we assume physics on global scales to be in local accordance with the General Theory of Relativity. Furthermore, we can look for laws on a global scale which are implied by local physics. Additionally, we can assume properties without which the cosmological model would contradict the observed universe [55].

In the following, we shall give a short introduction to General Theory of Relativity, which is written in terms of differential geometry. We start with a basic definition of differential geometry sufficient to formulate Einstein's field equations. Afterwards, we shall define further requirements of space-time in order to specify the class of manifolds we are interested in.

1.1. Basics of Differential Geometry

1.1.1. Manifolds

The mathematical model for space-time used in the General Theory of Relativity is a smooth manifold. A manifold is a topological space (see A.0.0.1, p.185) such that each point has a neighbourhood homeomorphic (see A.0.0.7, p.186) to an open subset $U \subset \mathbb{R}^n$.

Definition 1.1.1.1. *An n-dimensional C^∞ real manifold \mathcal{M} is a set together with a collection of subsets $O_\alpha \subset \mathcal{M}$ such that:*

1. *Each point $p \in \mathcal{M}$ lies in at least one O_α , i.e., the O_α covering \mathcal{M} .*
2. *For each α there is a one-to-one, onto map $\varphi : O_\alpha \rightarrow U_\alpha$, where U_α is an open subset of \mathbb{R}^n .*
3. *If any two sets O_α and O_β overlap, $O_\alpha \cap O_\beta \neq \emptyset$, we can consider the map $\varphi_\alpha \circ \varphi_\beta^{-1}$, which takes points in $\varphi_\beta(O_\alpha \cap O_\beta) \subset U_\beta \subset \mathbb{R}^n$ to points in $\varphi_\alpha(O_\alpha \cap O_\beta) \subset U_\alpha \subset \mathbb{R}^n$. We require this map to be infinitely continuously differentiable, denoted by C^∞ . In this case $(O_\alpha, \varphi_\alpha)$ and (O_β, φ_β) are called C^∞ -compatible.*

[107]

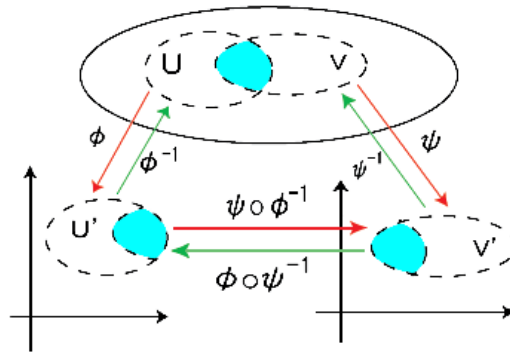


Figure 1.1.: The coordinate change of two compatible charts is visualized. In the domain of intersection, the coordinate change $\psi \circ \phi^{-1}$ takes points in $\phi(U \cap V) \subset U' \subset \mathbb{R}^n$ to points in $\psi(U \cap V) \subset V' \subset \mathbb{R}^n$ [114].

- Remark 1.1.1.2.**
1. The $(O_\alpha, \varphi_\alpha)$ are called **charts**. In a more physical context $(O_\alpha, \varphi_\alpha)$ are called **local coordinate systems**. The maps $\varphi_\alpha \circ \varphi_\beta^{-1}$ are called **transition functions** or **coordinate changes**. See Figure 1.1 for a visualization. If $p \in O_\alpha \subset M$, the **local coordinates** of p are the coordinates of $\varphi_\alpha(p) \in \mathbb{R}^n$.
 2. A C^∞ -**atlas** of M is a family of C^∞ -compatible charts $\{O_\alpha, \varphi_\alpha\}$ such that the O_α cover M . Two atlases are said to be **equivalent** if all their charts with nonempty intersection are C^∞ -compatible. A **maximal C^∞ -atlas** can be achieved by adding all C^∞ -compatible charts. Two equivalent atlases define the same structure on M . Therefore, we can define a manifold alternatively as a set M together with a maximal C^∞ -atlas.
 3. A topology of M is given by: $U \subset M$ is open if and only if $\varphi(U) \subset \mathbb{R}^n$ is open, where φ is a chart. This topology causes that all charts to be homeomorphisms. The topology turns M into a topological space. It is usually assumed that M is Hausdorff (see A.1.0.14, p.187).
 4. One gets the definition of a C^r -**manifold** by assuming the charts to be r -times continuously differentiable.
 5. We call a C^∞ -manifold a **smooth manifold**.
 6. We use the term of an abstract manifold instead of the more demonstrative term of a submanifold of \mathbb{R}^n . Space-time can be described by a four-dimensional manifold, which we do not want to view embedded in \mathbb{R}^n . A manifold is a space on its own, an embedding in a higher-dimensional space is physically not necessary since physics just uses local and therefore intrinsic geometry. Even if every abstract smooth manifold can be smoothly embedded in \mathbb{R}^n for an $n \in \mathbb{N}$, as stated by the theorem of Whitney (see [96, p.49]), we shall try to avoid this picture. [107] [54] [96]

Example 1.1.1.3. 1. The surface of the idealized earth is a two-dimensional manifold, that is a two-dimensional sphere. Irregularities like mountains or trenches, such as the Mariana Trench, are neglected. The atlas defined above is, like the geographical atlas, a collection of charts. Each chart represents a small patch of the earth's surface. In the same manner, we can describe the idealized four-dimensional space-time by an appropriate manifold.

2. The Cartesian product $\mathcal{N} \times \mathcal{M}$ of two manifolds \mathcal{N} and \mathcal{M} of dimension n and m with its natural structure, given by the structures of \mathcal{N} and \mathcal{M} , is again a manifold of dimension $m + n$. In particular, $\mathcal{N} \times \mathcal{M}$ is the set of all points (p, q) where $p \in \mathcal{N}$ and $q \in \mathcal{M}$. If $\varphi_\alpha : O_\alpha \rightarrow U_\alpha \subset \mathbb{R}^n$ is a chart on \mathcal{N} and $\psi_\beta : V_\beta \rightarrow U_\beta \subset \mathbb{R}^m$ is a chart on \mathcal{M} , a chart on $\mathcal{N} \times \mathcal{M}$ is defined by: $\varphi_{\alpha\beta} : O_\alpha \times V_\beta \rightarrow U_\alpha \times U_\beta \subset \mathbb{R}^{n+m}$. [107]

Definition 1.1.1.4. The **boundary of a smooth manifold** \mathcal{M} , denoted by $\partial\mathcal{M}$, is the (possibly empty) set of points such that, if $x \in O_\alpha$, then $\varphi_\alpha(x) \in \partial\mathbb{R}_+^n$. It is the union of the open sets $\varphi_\alpha^{-1}(\partial\mathbb{R}_+^n \cap \varphi(O_\alpha))$. [96]

Remark 1.1.1.5. 1. The restrictions of the φ_α to the boundary of \mathcal{M} are the charts of an $(n - 1)$ -dimensional manifold. $\partial\mathcal{M}$ is closed in \mathcal{M} and $\mathcal{M} \setminus \partial\mathcal{M}$ is called the **interior** of the manifold.

2. A compact manifold without boundary is called a **closed** manifold and a non-compact one is called **open**.

[96]

Remark 1.1.1.6. A family of subsets $\{B_\alpha : \alpha \in A\}$ of a metric space X , numbered by elements of a set A , is said to be **locally finite** if for each point there is a neighbourhood intersecting only finitely many subsets of this family. [103]

Definition 1.1.1.7. An atlas $\{O_\alpha, \varphi_\alpha\}$ is said to be **locally finite** if every point $p \in \mathcal{M}$ has an open neighbourhood which intersects only a finite number of the sets O_α . Furthermore, \mathcal{M} is said to be **paracompact** if for every atlas $\{O_\alpha, \varphi_\alpha\}$ there exists a locally finite atlas $\{V_\beta, \psi_\beta\}$ with each V_β contained in some O_α . [43]

1.1.2. Vectors and Tensors

By taking into account geometries with non-vanishing curvature, we lose the structure of a vector space. It turns out that we can define a vector space on every point on a manifold – the tangent space. [107]

Definition 1.1.2.1. A C^r -**curve** $\gamma(t)$ is a C^r -map $\gamma : I \subset \mathbb{R} \rightarrow \mathcal{M}$.

Definition 1.1.2.2. A **vector** $(\frac{\partial}{\partial t})|_{t_0}$, tangent to the C^1 -curve $\gamma(t)$ at the point $\gamma(t_0)$, is the operator which maps each C^1 -function f at $\gamma(t_0)$ into the derivative of f in the direction of $\gamma(t)$ with respect to the parameter t and is denoted by $(\frac{\partial f}{\partial t})_\gamma|_{t_0}$. [43]

Remark 1.1.2.3. If (x^1, \dots, x^n) are local coordinates of $\gamma(t) \in \mathcal{M}$, we can write the vector $(\frac{\partial f}{\partial t})_{\gamma|_{t_0}}$ as:

$$\left(\frac{\partial f}{\partial t}\right)_{\gamma|_{t_0}} = \sum_{i=1}^n \frac{dx^i(\gamma(t))}{dt}\Big|_{t=t_0} \cdot \frac{\partial f}{\partial x^i}\Big|_{\gamma(t)}$$

Thus, every tangent vector at the point $p \in \mathcal{M}$ can be written as a linear combination of the coordinate derivatives

$$\left(\frac{\partial}{\partial x^1}\right)\Big|_p, \left(\frac{\partial}{\partial x^2}\right)\Big|_p \dots, \left(\frac{\partial}{\partial x^n}\right)\Big|_p.$$

[43]

Definition 1.1.2.4. The **tangent space** to \mathcal{M} at x , denoted by $T_x\mathcal{M}$, is the set of all tangent vectors to \mathcal{M} at x . If \mathcal{M} is a manifold of dimension n , $T_x\mathcal{M}$ is an Euclidean vector space of the same dimension. [96, p.14]

Definition 1.1.2.5. The disjoint union of all tangent spaces $T_x\mathcal{M}$ to \mathcal{M} at all points $x \in \mathcal{M}$ is called the **tangent bundle** of \mathcal{M} , denoted by $T\mathcal{M}$. [96]

Theorem 1.1.2.6. Let \mathcal{M} be an n -dimensional C^p -manifold ($p > 1$), then its tangent bundle $T\mathcal{M}$ is a $2n$ -dimensional C^{p-1} -manifold. [96]

Definition 1.1.2.7. A (smooth) **vector field** on a manifold \mathcal{M} is a smooth map $X : \mathcal{M} \rightarrow T\mathcal{M}$ such that for any $p \in \mathcal{M}$, $X(p) \in T_p\mathcal{M}$. The set of all vector fields is a vector space, denoted by $\chi(\mathcal{M})$. [96]

Example 1.1.2.8. The gravitational field is a vector field. It assigns to each point a vector pointing in the direction of the gravitational field with a length corresponding to the absolute value of the gravitational force.

Remark 1.1.2.9. 1. A **scalar field** on a manifold is a map which assigns to each point $p \in \mathcal{M}$ a scalar $a \in \mathbb{R}$. For example, a map which assigns a temperature or density to each point in space-time is a scalar field.

Remark 1.1.2.10. 1. For a finite-dimensional vector space V , the **dual vector space** is defined by $V^* := \{f : V \rightarrow \mathbb{R} \mid f \text{ is linear}\}$. The elements of V^* are called dual vectors. V^* is a vector space with the obvious rules for adding and scalar multiplying. If $\{v_1, \dots, v_n\}$ is a basis for the vector space V , we can define elements $v^1, \dots, v^n \in V^*$ by $v^i(v_j) = \delta_j^i$, which δ_j^i denoting the Kronecker symbol. $\{v^1, \dots, v^n\}$ defines a basis of V^* , called the **dual basis** of $\{v_1, \dots, v_n\}$.

2. If we take $V = T_p\mathcal{M}$, vectors in $T_p\mathcal{M}$ are called **contravariant vectors**. Elements of $T_p\mathcal{M}^*$ are called **covariant vectors**. Given a coordinate system $\{x^1, \dots, x^n\}$, a basis of $T_p\mathcal{M}$ is given by $\{(\frac{\partial}{\partial x^1})\Big|_p, (\frac{\partial}{\partial x^2})\Big|_p \dots, (\frac{\partial}{\partial x^n})\Big|_p\}$, the corresponding dual basis is denoted by $\{dx^1, \dots, dx^n\}$. [107]

Definition 1.1.2.11. A tensor T of type (k, l) is a multi-linear map

$$T : \underbrace{V^* \times V^* \times \dots \times V^*}_k \times \underbrace{V \times V \times \dots \times V}_l \rightarrow \mathbb{R}.$$

[107] With the obvious rules for adding

$$(T + T')(v^1, \dots, v^k, v_1, \dots, v_l) = T(v^1, \dots, v^k, v_1, \dots, v_l) + T'(v^1, \dots, v^k, v_1, \dots, v_l)$$

and scalar multiplying

$$(a \cdot T)(v^1, \dots, v^k, v_1, \dots, v_l) = a \cdot T(v^1, \dots, v^k, v_1, \dots, v_l) \quad a \in \mathbb{R},$$

the collection $T(k, l)$ of all tensors of type (k, l) has the structure of a vector space of dimension n^{k+l} . [43]

Example 1.1.2.12. 1. In physics, tensors are one of the most important tools since most of physical quantities depend on vectors and dual vectors in a multilinear way. Take, for example, a material body in equilibrium and consider the plane with normal vector \vec{n} through the point p in the body. The matter of one side of the plane exerts a force per unit area F in the direction \vec{l} on the matter of the other side of the plane. F depends linearly on \vec{n} and \vec{l} and is therefore a $(0, 2)$ -tensor, the so-called **stress-tensor**. If the values of F are known of a basis for \vec{n} and \vec{l} , we can calculate the value of F for arbitrary \vec{n} and \vec{l} as a linear combination. This explains the importance of tensors in physics, especially for the General Theory of Relativity.

2. A tensor of type $(0, 1)$ is a map from V to \mathbb{R} and thus a dual vector. A tensor of type $(1, 0)$ is, therefore, an element of V^{**} , which can be identified with V and can be seen as a vector. By fixing the first or the second component accordingly, a tensor of type $(1, 1)$ can be seen either as a linear map from V to V or as a linear map from V^* to V^* .

[107]

Remark 1.1.2.13 (Operations and Notation of Tensors). 1. Assuming T to be a tensor of type (k, l) and T' to be a tensor of type (k', l') , the **outer product** of T and T' is the tensor $T \otimes T'$ of type $(k + k', l + l')$ defined by:

$$\begin{aligned} (T \otimes T')(v^1, \dots, v^{k+k'}, v_1, \dots, v_{l+l'}) &= \\ &= T(v^1, \dots, v^k, v_1, \dots, v_l) \cdot T'(v^{k+1}, \dots, v^{k+k'}, v_{l+1}, \dots, v_{l+l'}). \end{aligned} \tag{1.1}$$

2. If $\{v_1, \dots, v_n\}$ is a basis of V and $\{v^1, \dots, v^n\}$ is the corresponding dual basis for V^* , the n^{k+l} tensors $\{v_{\mu_1} \otimes \dots \otimes v_{\mu_k} \otimes v^{\nu_1} \otimes \dots \otimes v^{\nu_l}\}$ give a basis of $T(k, l)$. Thus, every

tensor can be written as

$$T = \sum_{\mu_1, \dots, \nu_l=1}^n T_{\nu_1 \dots \nu_l}^{\mu_1 \dots \mu_k} v_{\mu_1} \otimes \dots \otimes v^{\nu_l}.$$

$T(k, l)$ forms an algebra over \mathbb{R} with the outer product. [43]

3. The $T_{\nu_1 \dots \nu_l}^{\mu_1 \dots \mu_k}$ are called the **components** of T with respect to the basis $\{v_1, \dots, v_n\}$. Using **component notation**, a tensor is given by its components $T_{\nu_1 \dots \nu_l}^{\mu_1 \dots \mu_k}$. We use the standard convention for using superscript indices for contravariant vectors and subscript indices for covariant vectors. [107]

If we change the coordinate system, the tensor transforms to:

$$T'_{\nu'_1 \dots \nu'_l}{}^{\mu'_1 \dots \mu'_k} = \sum_{\mu_1, \dots, \nu_l=1}^n T_{\nu_1 \dots \nu_l}^{\mu_1 \dots \mu_k} \frac{\partial x^{\mu'_1}}{\partial x^{\mu_1}} \dots \frac{\partial x^{\nu_l}}{\partial x^{\nu'_l}}.$$

This equation is known as the **tensor transformation law**. [107]

4. Apart from the outer product, there is another important operation on tensors: the **contraction** with respect to the i^{th} (dual vector) and j^{th} (vector) slots. It is a map $C : T(k, l) \rightarrow T(k-1, l-1)$. If T is a tensor with components $T_{\nu_1 \dots \nu_l}^{\mu_1 \dots \mu_k}$, its contraction is defined by

$$CT_{\nu_1 \dots \nu_{l-1}}^{\mu_1 \dots \mu_{k-1}} = \sum_{\mu_i, \nu_i=1}^n T_{\nu_1 \dots \nu_{i-1} \sigma \nu_{i+1} \dots \nu_{l-1}}^{\mu_1 \dots \mu_{j-1} \sigma \mu_{j+1} \dots \mu_{k-1}}.$$

[107]

5. A notation similar to component notation is the **abstract index notation**: here, a tensor of type (k, l) is given by $T_{b_1 \dots b_l}^{a_1 \dots a_k}$, where superscript indices denote k contravariant vectors and subscript indices denote l covariant vectors. The abstract index notation looks very similar to the component notation, but has a few advantages. The most important is that the notation is independent of the choice of a basis. Different indices denote different slots, the same index denotes the same slot. For instance, the contraction of a $(3, 2)$ -tensor with respect to the second contravariant and first covariant slot shall be denoted by T_{bd}^{abc} . Keep in mind that this denotes a $(2, 1)$ -tensor. [107]

Remark 1.1.2.14 (Notation:). Greek letters in indices indicate that component notation is used, while latin letters indicate abstract index notation.

Definition 1.1.2.15. A **tensor field** is an assignment of a tensor over $T_p M$ for each point $p \in \mathcal{M}$ [107, p.22]

For an arbitrary set X , a metric is defined as follows:

Definition 1.1.2.16. A **metric** on a set X is a function $d : X \times X \rightarrow \mathbb{R}$ such that for all $x, y, z \in X$:

1. $d(x, y) \geq 0$ and $d(x, y) = 0 \Leftrightarrow x = y$,
2. $d(x, y) = d(y, x)$ and
3. $d(x, y) \leq d(x, z) + d(z, y)$.

X together with the map $d : (x, y) \mapsto d(x, y)$ is called a **metric space**. [84]

For manifolds, we define a metric in terms of tensor fields:

Definition 1.1.2.17. A **metric** at a point $p \in \mathcal{M}$ is a linear map $g : T_p\mathcal{M} \times T_p\mathcal{M} \rightarrow \mathbb{R}$, which satisfies:

1. $g(v_1, v_2) = g(v_2, v_1)$
2. If $g(v, v_1) = 0 \quad \forall v \in T_p\mathcal{M} \Rightarrow v_1 = 0$.

Remark 1.1.2.18. 1. We see from Definition 1.1.2.17, that a metric at $p \in \mathcal{M}$ is a symmetric, non-degenerate tensor of type $(0, 2)$. A metric on a manifold \mathcal{M} is therefore a tensor field of the same type. Given a coordinate basis $\{x^1, \dots, x^n\}$, we write the metric g in terms of its components $g_{\mu\nu}$ as

$$g = \sum_{\mu, \nu} g_{\mu\nu} dx^\mu \otimes dx^\nu.$$

It is common to write

$$ds^2 = \sum_{\mu, \nu} g_{\mu\nu} dx^\mu dx^\nu$$

where we use ds^2 for the metric tensor and omit writing the sign for the outer product. In abstract index notation the metric is denoted by g_{ab} . The metric applied to a vector v^a gives a dual vector $v_a = g_{ab}v^b$. Analogously, if we apply the metric to a dual vector w_a , it gives a vector $w^a = g^{ab}w_b$.

2. A basis $\{v_1, v_2, \dots, v_n\}$ is called an **orthonormal basis** if $g(v_\nu, v_\mu) = 0$ for $\nu \neq \mu$ and $g(v_\mu, v_\mu) = \pm 1$. The sign is called the **signature of the metric**. If the signature of g is $(+, +, \dots, +)$, the metric is called a **Riemannian metric**. Metrics with a signature $(-, +, \dots, +)$ are called **Lorentzian**.
3. Of course, a manifold together with a metric is a metric space in the sense of 1.1.2.16. [107]

Definition 1.1.2.19. A pair (\mathcal{M}, g) is called a **Lorentzian (Riemannian) manifold** if \mathcal{M} is a manifold and g a Lorentzian (Riemannian) metric defined on \mathcal{M} . [107]

Remark 1.1.2.20. 1. On a Lorentzian manifold (\mathcal{M}, g) , we distinguish three different types of vectors:

- a) If $g_{ab}v^av^b = 0$, v^a is called a **null vector**.
- b) If $g_{ab}v^av^b > 0$, v^a is called a **space-like vector**.
- c) If $g_{ab}v^av^b < 0$, v^a is called a **time-like vector**. [43]

2. Similarly we can define three different types of curves. A curve is said to be **space-like**, if for any tangent vectors along the curve $g_{ab}t^at^b > 0$; **time-like** if $g_{ab}t^at^b < 0$ and **null** if $g_{ab}t^at^b = 0$. [107]

3. A non-space-like curve is said to be a **causal curve**. [107]

Example 1.1.2.21. For literature reference see [83], [54], [103], [84]. In the following “ (\cdot, \cdot) ” shall always refer to the standard Euclidean inner product.

Euclidean Space \mathbb{E}^n : Coordinates in $\mathbb{R}^n : (x_1, \dots, x_n)$

Inner Product: $(x, y) = x_1y_1 + \dots + x_ny_n$, Norm on \mathbb{E}^n : $|x| = \sqrt{(x, x)}$

\mathbb{R}^n with the inner product (\cdot, \cdot) is called the n-dimensional Euclidean space, denoted by \mathbb{E}^n . The Riemannian metric on the space \mathbb{E}^n is induced by the Euclidean metric on the space \mathbb{R}^n , thus, it is of the following form:

$$ds^2 = dx_1^2 + \dots + dx_n^2. \quad (1.2)$$

Sphere \mathbb{S}^n : Coordinates in \mathbb{R}^{n+1} : x_0, \dots, x_n ;

Inner Product on \mathbb{R}^{n+1} : $(x, y) = x_0y_0 + \dots + x_ny_n$, Norm on \mathbb{R}^{n+1} : $|x| = \sqrt{(x, x)}$

This scalar product turns \mathbb{R}^{n+1} into an Euclidean vector space.

We obtain the n-dimensional sphere by the restriction:

$$\mathbb{S}^n := \{x \in \mathbb{R}^{n+1} : (x, x) = x_0^2 + \dots + x_n^2 = 1\}. \quad (1.3)$$

The Riemannian metric is induced by the Euclidean metric on \mathbb{R}^{n+1} $d_E(x, y) := |x - y|$:

$$ds^2 = dx_0^2 + \dots + dx_n^2.$$

Keep in mind that the coordinates on \mathbb{S}^n are not independent. Thus, this is no intrinsic metric to \mathbb{S}^n since it is defined on \mathbb{R}^{n+1} . To define an intrinsic metric on \mathbb{S}^3 we need to recall the cross product in \mathbb{R}^3 :

$$x \times y = (x_2y_3 - x_3y_2, x_3y_1 - x_1y_3, x_1y_2 - x_2y_1).$$

Furthermore, we recall that the angle $\Theta(x, y)$ between $x, y \in \mathbb{S}^3$ – both nonzero – is given by:

$$|x \times y| = |x||y| \sin \Theta(x, y).$$

The **spherical metric** on \mathbb{S}^3 is given by the **spherical distance function**:

$$d_S(x, y) := \Theta(x, y).$$

It is $0 \leq d_S(x, y) \leq \pi$. Two vectors $x, y \in \mathbb{S}^3$ are called **antipodal** if and only if $y = -x$, that is if and only if $d_S(x, y) = \pi$.

Hyperbolic Space \mathbb{H}^n : Coordinates in \mathbb{R}^{n+1} : x_0, \dots, x_n ,

Lorentzian inner product on \mathbb{R}^{n+1} : $\langle x, y \rangle = -x_0y_0 + x_1y_1 + \dots + x_ny_n$

Norm on \mathbb{R}^{n+1} : $\|x\| = \sqrt{\langle x, x \rangle}$, which is either nonnegative or positive imaginary.

Lorentzian distance: $d_L(x, y) = \|x - y\|$.

This scalar product turns \mathbb{R}^{n+1} into a pseudo-Euclidean vector space, called the **Lorentzian (n+1)-space**, denoted by $\mathbb{R}^{1,n}$.

In analogy to the spherical case we define the hyperbolic space as the sphere of the imaginary radius -1 . Thus, the Lorentzian space is defined as

$$\mathbb{H}^n := \{x \in \mathbb{R}^{n+1} : \|x\|^2 = -1, x_0 > 0\}.$$

For any $x \in \mathbb{H}^n$, the tangent space $T_x\mathbb{H}^n$ can be identified with the orthogonal complement of the vector x in $\mathbb{R}^{n,1}$, which is an n -dimensional Euclidean vector space (with respect to the same scalar product). Thus, a Riemannian metric on \mathbb{H}^n is induced by the pseudo-Euclidean metric ($d_E(x, y) = \|x - y\|$) on the space $\mathbb{R}^{n,1} : ds^2 = -dx_0^2 + dx_1^2 + \dots + dx_n^2$.

Again, this is not an intrinsic metric on \mathbb{H}^n . An intrinsic metric on \mathbb{H}^n is given by the time-like angle between the vectors x and y . It is the uniquely determined nonnegative value $\mu(x, y)$, given by:

$$\langle x, y \rangle = \|x\| \|y\| \cosh \mu(x, y).$$

The **hyperbolic distance function** $d_H(x, y) := \mu(x, y)$ defines an intrinsic metric on \mathbb{H}^n . The Riemannian metric and the intrinsic metric define the same metric topology on \mathbb{H}^n .

[103], [84]

1.1.3. Parallel Transport and Curvature

As we have pointed out already, we view space-time as a mathematical space on its own. In general, we do not have the possibility to use a higher-dimensional space to measure curvature. We therefore need an intrinsic notion of curvature. We shall define curvature as the failure of a vector to return to its original value when it is parallel-transported around a small closed curve. [107, p.36]

Definition 1.1.3.1. A derivative operator (covariant derivative) ∇ on a manifold is a map which takes each smooth tensor field $T_{b_1 \dots b_l}^{a_1 \dots a_k}$ of type (k, l) to a smooth tensor field $\nabla_c T_{b_1 \dots b_l}^{a_1 \dots a_k}$ of type $(k, l + 1)$ and satisfies:

1. *Linearity:*

$$\nabla_c (aA_{b_1 \dots b_l}^{a_1 \dots a_k} + bB_{b_1 \dots b_l}^{a_1 \dots a_k}) = a\nabla_c A_{b_1 \dots b_l}^{a_1 \dots a_k} + b\nabla_c B_{b_1 \dots b_l}^{a_1 \dots a_k} \quad A, B \in T(k, l); a, b \in \mathbb{R}$$

2. *Leibnitz rule:*

$$\nabla_e [A_{b_1 \dots b_l}^{a_1 \dots a_k} B_{d_1 \dots d_{l'}}^{c_1 \dots c_{k'}}] = \nabla_e [A_{b_1 \dots b_l}^{a_1 \dots a_k}] B_{d_1 \dots d_{l'}}^{c_1 \dots c_{k'}} + A_{b_1 \dots b_l}^{a_1 \dots a_k} \nabla_e [B_{d_1 \dots d_{l'}}^{c_1 \dots c_{k'}}], \quad \forall A \in T(k, l), B \in T(k', l')$$

3. *Commutativity with Contraction:*

$$\nabla_d (A_{b_1 \dots c \dots b_l}^{a_1 \dots c \dots a_k}) = \nabla_d A_{b_1 \dots c \dots b_l}^{a_1 \dots c \dots a_k} \quad \forall A \in T(k, l)$$

4. *Consistency with the notion of tangent vectors as directional derivatives on scalar fields:*

$$t(f) = t_a \nabla_a f \quad \forall f \in F, t_a \in T_p M$$

[107]

Remark 1.1.3.2 (Assumption:). The tensor T_{ab}^c , satisfying $\nabla_a \nabla_b f - \nabla_b \nabla_a f = -T_{ab}^c \nabla_c f$ with f a scalar field, is called **torsion tensor**. A derivative operator with vanishing torsion tensor is called **torsion-free**. General Theory of Relativity assumes the derivative operator to be torsion-free. Throughout this work, a derivative operator shall always be torsion-free, unless otherwise stated. [43] [107]

Example 1.1.3.3. 1. For a local coordinate system $(O_\alpha, \varphi_\alpha)$ and associated coordinate bases $\{\frac{\partial}{\partial x^\mu}\}$ and $\{dx^\mu\}$, a derivative operator is defined by:

$$\partial_a T_{\nu_1 \dots \nu_l}^{\mu_1 \dots \mu_k} = \frac{\partial (T_{\nu_1 \dots \nu_l}^{\mu_1 \dots \mu_k})}{\partial x^\sigma}$$

This derivative operator is called the **ordinary derivative**. It is coordinate dependent and torsion-free. [107]

2. A **connection** ∇ at $p \in \mathcal{M}$ is a special case of a derivative operator. It is a map from $\chi(\mathcal{M}) \times \chi(\mathcal{M}) \rightarrow \chi(\mathcal{M})$. It assigns a differential operator ∇_X to each vector field X at $p \in \mathcal{M}$, thereby mapping an arbitrary C^r ($r \geq 1$)-vector field Y onto a vector field $\nabla_X Y$ such that the above required conditions are satisfied. $\nabla_X Y$ can be interpreted as the covariant derivative with respect to ∇ of Y in the direction of X at p . [43]

Remark 1.1.3.4. If we consider two different derivatives $\nabla_c, \tilde{\nabla}_c$, the difference between these derivatives ($\nabla_c - \tilde{\nabla}_c$) is given by a $(1, 2)$ -tensor C_{ab}^c at p (two dual vectors are mapped to a tensor of type $(0, 2)$). Conversely, given a derivative operator and a $(1, 2)$ -tensor, we can define another derivative operator by:

$$\tilde{\nabla}_c = C_{ab}^c - \nabla_c.$$

If we choose $\tilde{\nabla}_c = \partial_c$, C_{ab}^c is denoted by Γ_{ab}^c and called **Christoffel symbol**. In this case we have:

$$\nabla_a t^b = \partial_a t^b + \Gamma_{ac}^b t^c.$$

[107]

1.1.3.1. Parallel Transport

Given a derivative operator, we can define the notion of parallel transport of a vector along a curve γ with tangent t^a :

Definition 1.1.3.5. A vector v^a , given at each point of the curve $\gamma : I \subset \mathbb{R} \rightarrow \mathcal{M}$, is said to be **parallel-transported** if

$$t^a \nabla_a v^b = 0 \tag{1.4}$$

is satisfied along the curve. [107]

Remark 1.1.3.6. Using the Christoffel symbol and ordinary derivative, we can express equation 1.4 as

$$t^a \nabla_a v^b = t^a \partial_a v^b + t^a \Gamma_{ac}^b v^c = 0.$$

Or, in terms of components of a coordinate basis:

$$\frac{dv^\nu}{dt} + \sum_{\mu, \lambda} t^\mu \Gamma_{\mu\lambda}^\nu v^\lambda = 0.$$

These partial differential equations always have a unique solution for a given initial value of v^a . Thus, a vector defines a unique parallel-transported vector everywhere along a curve. The underlying structure of parallel transport is a connection, as introduced in 1.1.3.3, item 2. A connection on a manifold can be used to identify the tangent spaces $T_p \mathcal{M}$ and $T_q \mathcal{M}$, where $p, q \in \mathcal{M}$ are lying on a curve $\gamma(t)$. [107]

Example 1.1.3.7. Let us start with a given metric g_{ab} on a manifold \mathcal{M} . Given two vectors v^a, v^b , their inner product does not change while parallel transported:

$$t^a \nabla_a (g_{bc} v^b w^c) = 0.$$

Using Leibnitz rule and the fact that the vectors v^a and w^b are parallel-transported we obtain:

$$t^a v^b w^c \nabla_a (g_{bc}) = 0,$$

which is equivalent to

$$\nabla_a g_{bc} = 0. \tag{1.5}$$

It turns out that equation 1.5 determines a unique torsion-free derivative. [107]

Remark 1.1.3.8 (Assumption:). Unless stated otherwise, we shall choose the connection given by equation 1.5.

1.1.3.2. Curvature

If a vector is parallel-transported along a closed curve on the plane, the final vector coincides with the initial one. If we perform the same on the two-dimensional sphere, the final vector does not coincide with the initial one. We can use this fact to define the plane as flat and the sphere as a manifold with a non-vanishing curvature. Since parallel transport can be written in terms of local geometry, this procedure can be used to define an intrinsic notion of curvature of manifolds. We shall define curvature as the failure of a vector to coincide with its initial values when parallel-transported along a small, closed curve. As we have a unique definition of a derivative operator for a given metric (see equation 1.5), parallel transport is defined uniquely. Thus, the definition of curvature is well-defined. A slightly different definition is the failure of the fifth Euclid postulate, the failure of initial parallel geodesics (see 1.1.4) to remain parallel.

It turns out that there is a strong correspondence between the lack of commutativity of two derivative operators ∇_a and ∇_b and the curvature. The deviation from commutativity of ∇_a and ∇_b can be expressed by:

$$(\nabla_a \nabla_b - \nabla_b \nabla_a)(f w_a),$$

where f is a smooth function and w_a is a dual vector field. Using Leibnitz rule (see 1.1.3.1), we see that

$$(\nabla_a \nabla_b - \nabla_b \nabla_a)(f w_a) = f(\nabla_a \nabla_b - \nabla_b \nabla_a)(w_a).$$

[107] This motivates the definition of the Riemannian curvature tensor:

Definition 1.1.3.9. *The Riemannian curvature tensor is defined as*

$$R_{abc}^d = (\nabla_a \nabla_b - \nabla_b \nabla_a) \cdot$$

Remark 1.1.3.10. 1. It is not hard to show that the failure of a vector to coincide with its initial values after parallel transport along a small closed path can be measured directly using the Riemannian curvature tensor. (See [107, p.37–39].)

2. For a dual vector field w_a we get $\nabla_a \nabla_b w_c - \nabla_b \nabla_a w_c = R_{abc}^d w_d$.

Theorem 1.1.3.11 (Properties of the Riemannian Curvature Tensor). *The Riemannian curvature tensor of a manifold \mathcal{M} satisfies the following properties:*

1. $R_{abc}^d = -R_{bac}^d$
2. *First Bianchi identity:* $R_{[abc]}^d = R_{abc}^d + R_{cab}^d + R_{bca}^d = 0$
3. *For the derivative ∇_a naturally associated with the metric g_{ab} we have $R_{abc}^e g_{ed} + R_{abd}^e g_{ce} = R_{abcd} + R_{abdc} = 0$.*
4. *Second Bianchi identity:* $\nabla_{[a} R_{bc]d}^e = \nabla_a R_{bcd}^e + \nabla_c R_{abd}^e + \nabla_b R_{cad}^e = 0$

[107]

Remark 1.1.3.12. 1. We can write the Riemannian curvature tensor with the notation of 1.1.3.3, item 2: if X, Y, Z are C^r -vector fields, the Riemannian curvature tensor defines a C^{r-2} -vector field:

$$R(X, Y)Z = \nabla_X(\nabla_Y Z) - \nabla_Y(\nabla_X Z) - \nabla_{[X, Y]}Z,$$

where $[X, Y]$ denotes the commutator of the vector fields X and Y :

$$[X, Y](f) = X[Y(f)] - [X(f)]Y \quad \forall f \in C^\infty.$$

[43]

2. The Riemannian curvature tensor can be decomposed into a trace part and a trace-free part. The trace part is

$$R_{abc}^b = R_{ac} \tag{1.6}$$

which is known as the **Ricci tensor**. In dimension three, the Riemannian curvature tensor of a manifold is completely given by the Ricci tensor. Furthermore, the trace of the Ricci tensor is called the **scalar curvature** $R = R_a^a$. Curvature in dimension two is completely given by scalar curvature.

3. The Ricci tensor satisfies (double contraction of the Bianchi identity):

$$\nabla_a R_c^a + \nabla_b R_c^b - \nabla_c R = 0. \quad (1.7)$$

If we define the **Einstein tensor** by

$$G_{ab} = R_{ab} - \frac{1}{2} R g_{ab} \quad (1.8)$$

Equation 1.7 reduces to

$$\nabla^a G_{ab} = 0, \quad (1.9)$$

which shall be important when deriving Einstein's field equations.

[107]

Example 1.1.3.13. The Riemannian metrics given in 1.1.2.21 are of scalar curvature +1 (sphere), 0 (Euclidean space) and -1 (hyperbolic space).

1.1.4. Geodesics

A **geodesic** is curve which satisfies the **geodesic equation**

$$t^a \nabla_a t^b = 0, \quad (1.10)$$

where ∇_a denotes, as usual, the derivative induced by the given metric g_{ab} on the manifold and t^a is an arbitrary tangent vector along the curve. With respect to the derivative ∇_a , tangent vectors t^a along geodesics remain parallel. Thus, a geodesic is “as straight as possible.”

In Riemannian manifolds, geodesics define the shortest paths between two points. Within General Theory of Relativity they define the path along which particles need minimal energy. Light rays are null geodesics, while particles move on time-like geodesics.

[107]

1.1.5. Hypersurface

Definition 1.1.5.1. A map ϕ from an n -dimensional C^k -manifold \mathcal{M} to an n' -dimensional $C^{k'}$ -manifold \mathcal{M}' is said to be a C^r -map ($r \leq k, r \leq k'$) if for any local coordinate system in \mathcal{M} and \mathcal{M}' , the coordinates of the image point $\phi(p)$ in \mathcal{M}' are C^r -functions of the coordinates of $p \in \mathcal{M}$.

Definition 1.1.5.2. If f is a function on \mathcal{M}' , the mapping ϕ (from Definition 1.1.5.1) defines a function $\phi^* f$ on \mathcal{M} as the function with value f at $\phi(p)$ at the point $p \in \mathcal{M}$:

$$\phi^*(f(p)) = f(\phi(p)).$$

Definition 1.1.5.3. A map ϕ from an n -dimensional C^k -manifold \mathcal{M} to an n' -dimensional $C^{k'}$ -manifold \mathcal{N} is said to be an **immersion** if it itself and its inverse are C^r -maps ($r \leq k$ and $r \leq k'$). This means that for each point $p \in \mathcal{M}$ there is a neighbourhood $U \subset \mathcal{M}$ of p such that the inverse ϕ^{-1} restricted to $\phi(U)$ is a C^r -map. [43]

Definition 1.1.5.4. An immersion is an **embedding** if it is a homeomorphism onto its image in the induced topology. Thus, an embedding is an injective immersion. [43]

Definition 1.1.5.5. If \mathcal{M}_{n-1} is an $(n-1)$ -dimensional manifold and $\phi : \mathcal{M}_{n-1} \rightarrow \mathcal{M}_n$ is an embedding in an n -dimensional manifold, the image $\phi(\mathcal{M}_{n-1})$ of \mathcal{M}_{n-1} is said to be a **hypersurface** in \mathcal{M}_n . [43]

Remark 1.1.5.6. If g_{ab} is a metric on \mathcal{M}_n , the embedding induces a metric ϕ^*g on \mathcal{M}_{n-1} such that for $X, Y \in T_p\mathcal{M} : \phi^*g(X, Y)|_p = g(\phi_*(X), \phi_*(Y))|_{\phi(p)}$, where $\phi_*(X)$ and $\phi_*(Y)$ denote the corresponding tangent vectors in $T_{\phi(p)}\mathcal{M}'$ to X and Y . If g_{ab} is a Lorentzian metric and n^a is orthogonal to all vectors tangent to $\phi(\mathcal{M}_{n-1})$, the induced metric ϕ^*g will be

1. Lorentzian if $g_{ab}n^an^b > 0$. In this case the hypersurface is called **time-like**.
2. degenerate if $g_{ab}n^an^b = 0$. In this case the hypersurface is called a **null hypersurface**.
3. positive definite if $g_{ab}n^an^b < 0$. In this case the hypersurface is called **space-like**.

[43]

1.2. Introduction to General Theory of Relativity

1.2.1. First Assumptions on Space-Time

Within General Theory of Relativity, the mathematical model for space-time is a pair (\mathcal{M}_4, g) , where \mathcal{M}_4 is a Hausdorff, connected, and therefore path-connected (see A.0.0.9 on page 186 and the proceeding remark), four-dimensional C^∞ -manifold and g is a Lorentzian metric on \mathcal{M}_4 . [43]

Remark 1.2.1.1. 1. This is not a very restrictive condition, because any non-compact four-dimensional manifold admits a Lorentzian metric. Furthermore, any compact four-dimensional manifold with a Euler-Poincaré characteristic (see for instance [42]) of zero admits a Lorentzian metric. [55]

2. We assume space-time to be Hausdorff. As noted in 1.1.1.2, a manifold is almost always assumed to be Hausdorff.
3. We require the metric to be at least to be C^2 in order to define the field equations continuously. But since the metric cannot be measured exactly, we cannot determine

if there would be a discontinuity at its derivatives of any order. There are theorems of Munkres and Whitney, which ensure the existence of a C^∞ -subatlas. Thus, we can choose a smooth atlas. See Chapter 2 (2.1.0.5, p.38). [43]

4. If the universe is not connected, we are only interested in the connected component we are sitting in. There is no other choice since there is no physical connection between disconnected components, and therefore information can therefore not be sent between them.

These assumptions immediately imply another: every Hausdorff manifold on which a Lorentzian metric is defined is paracompact (see 1.1.1.7). Thus, we can assume space-time to be **paracompact**. [43]

Definition 1.2.1.2 (Diffeomorphism, Transformation). *A smooth one-to-one map F for which the inverse map F^{-1} is also smooth is called a **diffeomorphism**. A diffeomorphism of a manifold onto itself is often called a smooth **transformation**. [32, p. 58]*

Definition 1.2.1.3. *Two models (\mathcal{M}_4, g) , (\mathcal{M}'_4, g') are said to be **equivalent** if they are isometric, that is, if there exists a diffeomorphism $\phi : \mathcal{M}_4 \rightarrow \mathcal{M}'_4$ with $\phi_*g = g'$. Therefore, to be precise, if we speak about a model of space-time, we speak of an equivalence class of models from which we take a representative. [43, p.56]*

Remark 1.2.1.4 (Convention:). We follow the standard convention in the General Theory of Relativity of setting the gravitational constant and the speed of light to unity: $G = c = 1$.

1.2.2. The Equivalence Principle

One of the most important principles within General Theory of Relativity, based on the equivalence of gravitation and inertia mass formulated in Newtonian physics, states that all bodies are influenced by gravity and all bodies fall precisely the same in gravitational fields. One consequence is that we cannot define isolated observers, that is, observers on whom no force acts, like in the Special Theory of Relativity. Another consequence is that for an arbitrary point in a gravitational field we can choose a local inertial coordinate system, in which gravitation is absent in a sufficiently small neighbourhood of the point. This enables us to write an equation, which is known for conditions without gravitational fields, for the condition of a gravitational field [109, p.511]. If we formulate the last sentence in the other direction, we see that Special Theory of Relativity remains locally valid within General Theory of Relativity. [43] [107]

1.2.3. Metric within General Theory of Relativity

As opposed to General Theory of Relativity, Special Theory of Relativity does not include gravitational effects. The mathematical model for space-time in the Special Theory of Relativity is a **Minkowski space**, which is a four-dimensional, connected, flat Lorentzian

manifold. The obvious way would be to introduce gravitation by a gravitational field and keep the metric flat. This attempt fails, because light rays near massive objects are deflected in accordance with Newtonian gravitation. Since light rays are defined as null geodesics, it is space itself which is curved. The deviation of the metric from a flat metric accounts for the physical effects usually ascribed to gravitational fields. Other geodesics are given by the paths of free-falling test bodies (time-like geodesics), which we shall explain in the next section. This set of preferred curves in space-time describe gravity as a property of space-time itself. Thus, we can say that the metric describes gravitational fields, or, in other words: the gravitational field is represented by space-time metric itself. This is referred to as **March's principle**. [107, p.7]; [43, p.71]

Remark 1.2.3.1. We do not rule out additional gravitational fields. If another gravitational field is detected, we can introduce it as an additional field.

1.2.4. Geodesic Hypothesis

Instead of inertial observers on whom no force acts, we define **free-falling test bodies** in General Theory of Relativity. These are small bodies with a self-gravity sufficiently weak to not influence their paths through space-time. A typical example would be a dust particle.

At any time t_0 , we can assign a spatial position (x_0, y_0, z_0) to the test body with respect to a local coordinate system. The map $t \mapsto (x(t), y(t), z(t))$ is the **worldline** of the test body.

The geodesic hypothesis states that the worldlines of free-falling test bodies in a gravitational field are exactly the time-like geodesics of the space-time metric. Thus they satisfy the **motion equation for particles** (cf. equation 1.10)

$$u^a \nabla_a u^b = 0, \tag{1.11}$$

where u^a is the **four-velocity**, that is, the unit tangent vector to the worldline of the test particle, a time-like curve. [107]

1.2.5. Einstein's Field Equations

The relation between the metric and the distribution of matter is described by Einstein's field equations. The continuous distribution of matter is given by the energy-momentum tensor which is a generalization of the stress tensor used in Newtonian physics (1.1.2.12, p.10).

Physics uses local geometry to describe processes and states. The metric and quantities derivable from it are the only space-time quantities that can appear in the equations of physics [107, p.68]. Physics is described by physical fields, such as the electromagnetic field or the neutrino field, which describes the matter content of space-time. Fields obey equations expressed as relations between tensors in \mathcal{M}_4 . Thus, physical fields are described by tensor

fields (or, in special cases, vector or scalar fields) written in terms of the manifold's structure. Furthermore, the only connection available is that one induced by the metric g_{ab} defined on \mathcal{M}_4 (see equation 1.5, p.17). If there was another connection, the difference between these two connections would once more define a tensor field (1.1.3.4, p.16) and therefore another physical field. As pointed out before, we do not exclude the possibility of the existence of an undetected field. [43, p.58]

We assume that we can express physical fields entirely in terms of tensors. Thus, we do not distinguish between gravitational fields with the same energy-momentum tensor. In accordance with the equivalence principle, we require the equations of General Theory of Relativity to reduce to the equations of Special Theory of Relativity if the metric is flat [43, p.71].

The **energy-momentum tensor** T_{ab} can be interpreted as the gravitational source (as j_a denotes the electromagnetic source used in the Maxwell equations). T_{ab} satisfies the following conditions:

1. T_{ab} is symmetric: $T_{ab} = \frac{1}{2}(T_{ab} + T_{ba})$.
2. T_{ab} vanishes on an open set $U \subset \mathcal{M}$ if and only if all matter fields vanish on U .

Remark 1.2.5.1. The only possibility of a vanishing gravitational field on an open set is the existence of some sort of negative energy such that all the existing fields cancel each other out on U .

3. The energy-momentum tensor satisfies the **motion equation**

$$\nabla^a T_{ab} = 0. \tag{1.12}$$

Remark 1.2.5.2. We assume a family of observers to be represented by a unit time-like vector field t^a . In a small region the gravitational field should not influence the energy of an observer significantly, and therefore, the energy should be approximately conserved: $\nabla_a t^b = 0$. Thus,

$$\nabla^a (T_{ab} t^b) = 0. \tag{1.13}$$

By integrating, we can interpret this equation as a **local conservation of material energy and momentum** [107].

[43]

Let t^a be the four-velocity of a particle. If $t^a \nabla_a t^b = a^b$, a force $f = m \cdot a^b$ acts on the particle with (rest) mass m . We have already pointed out that we cannot describe the absolute gravitational field in this way. But, as opposed to the absolute gravity, the relative gravitational force (tidal force) can be measured as the relative acceleration of two nearby free-falling bodies.

Let us assume the worldlines of two test bodies which are initially parallel and infinitesimally nearby. The vectors t^a are tangent to the worldlines and satisfy the geodesic equation 1.10. Because of the tidal force between the two particles, there is a non-vanishing **deviation vector** x^a . The quantity $v^a = t^b \nabla_b x^a$ gives the relative velocity of the two particles; $a^a = t^c \nabla_c v^a$ the relative acceleration between them. The correspondence between the relative acceleration of two test bodies and the curvature of space-time is given by the **geodesic deviation equation**

$$a^a = -R_{cbd}^a x^b t^c t^d, \quad (1.14)$$

where R_{cbd}^a denotes the Riemannian curvature tensor (1.1.3.9, p.17). [107]

If we give the tidal force in terms of Newtonian physics, we have

$$-(\vec{x}\nabla)\nabla\Phi,$$

where Φ denotes the gravitational potential and \vec{x} denotes the spatial separation of the two particles. Weak and slowly changing gravitational fields satisfy the Poisson equation, which is given by

$$\nabla^2\Phi = 4\pi\rho,$$

where ρ is the matter density [109]. In General Theory of Relativity the matter density is given by $\rho = T_{ab}t^a t^b$, where t^a is the four-velocity of the observer. Furthermore, we have $\nabla T_{ab} = 0$ (equation 1.12) and $\nabla G_{ab} = 0$ (equation 1.9).

This motivates **Einstein's field equations**:

$$G_{ab} = R_{ab} - \frac{1}{2}Rg_{ab} = 8\pi T_{ab}, \quad (1.15)$$

with G_{ab} being the Einstein tensor (given by equation 1.8), R_{ab} being the Ricci tensor (given by equation 1.6) and R being the scalar curvature (1.1.3.12). For more details see, for instance, [107, p. 66 – 72].

Using the trace, we get

$$R = -8\pi T. \quad (1.16)$$

[107]

Theorem 1.2.5.3. *Space-time is a manifold \mathcal{M}_4 on which there is defined a Lorentzian metric g_{ab} . The curvature of the space-time metric g_{ab} is related to the matter distribution in space-time by Einstein's field equations 1.15. [107, p.73]*

Remark 1.2.5.4. 1. It should be noted here that an exact solution of Einstein's field equations is only possible in space-times with high symmetry. Even in such perfect space-times we cannot rule out the possibility that there remain points where the physical laws brake down. These singularities are excluded from space-time such that incompleteness can be cured. [43]

2. Apart from Einstein's field equations, space-time should satisfy equations which determine the behavior of matter in space-time as the Maxwell equations and the Weyl equation. Furthermore, a suitable equation of state relates the components of the energy-momentum tensor. The equation of state is often represented as an "energy condition." [22]

1.2.6. Orientation

A manifold \mathcal{M} is called **orientable** if we can choose for any point $p \in \mathcal{M}$ a class of right-hand oriented and left-hand oriented vectors, and the orientation does not change along any path. Thus, if we choose an orientation of a vector and go along a closed path, the initial orientation is the final one. [107] More precisely, we define:

Definition 1.2.6.1. *A smooth manifold \mathcal{M} is said to be **orientable** if there exists an atlas for \mathcal{M} such that the Jacobians of all the transition functions are positive. Such an atlas is called an **orientation atlas**. [96]*

Remark 1.2.6.2. A transition function preserves a given orientation of \mathbb{R}^n .

In Figure 1.2 a picture of a non-orientable manifold is shown.

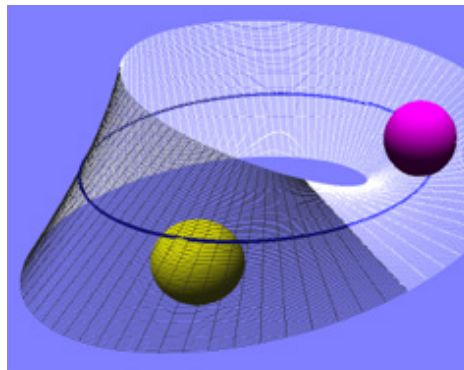


Figure 1.2.: The Möbius strip is an example of a two-dimensional non-orientable Riemannian manifold. A ball moving along the presented closed path ends on the opposite side of the surface it started at [115].

In the following, we distinguish for a Lorentzian manifold to be time-orientable and/or space-orientable. The difference shall depend on the kind of vectors under consideration.

1.2.6.1. Time Orientation and Causality

In Special Theory of Relativity **local causality** is assumed, which states:

Definition 1.2.6.3. *A signal can be sent in a convex set $U \subset \mathcal{M}_4$ between two points $p, q \in U$ if and only if p and q can be joined by a causal (non-space-like) C^1 -curve lying entirely in U and has nonzero tangent vectors. [43, p.60]*

Remark 1.2.6.4. 1. We rule out the possibility that a particle can move on space-like curves, since, so far no signal faster than light/electromagnetic radiation has been observed. Light travels on null geodesics and defines the limit of local causality.

2. Whether p is caused by q or q is caused by p depends on the local time orientation.

In a Minkowski space-time particles follow worldlines from past to future. Thus, we can define a class of past-oriented time-like vectors and a class of future-oriented time-like vectors at any point $p \in \mathcal{M}_4$. Minkowski space-time is therefore **locally time-orientable**. Since Special Theory of Relativity remains locally valid in the curved space-times of General Theory of Relativity, we can assume \mathcal{M}_4 to be locally time-orientable. \mathcal{M}_4 is called **time-orientable** if local time orientation varies continuously along curves. For a closed curve, the initial time orientation has to be the final one. Therefore, \mathcal{M}_4 is called time-orientable if every closed curve is **time-preserving**. In order to decide if space-time is (global) time-orientable, we shall go into further detail on causality. [55]

Remark 1.2.6.5. Ellis mentioned in [22] that with thermodynamic and electrodynamic experiments, one can always determine a future-oriented arrow of time. This is based on the second theorem of thermodynamics, which states that in thermal isolated systems the entropy can never decrease. [106]

Definition 1.2.6.6. A differentiable curve $\gamma(t)$ is said to be a **future-directed time-like (causal) curve** if at each point $p \in \gamma$ the tangent t^a is a future-directed time-like (or null) vector.

Remark 1.2.6.7. The definition of a **past-directed time-like or causal curve** is obtained by replacing future-directed with past-directed.

Definition 1.2.6.8 (Chronological Future and Past). 1. The **chronological future** of $p \in \mathcal{M}_4$, denoted by $I^+(p)$, is defined as the set of events that can be reached from p by a future-directed time-like curve starting at $p \in \mathcal{M}_4$. Thus,

$$I^+(p) := \{q \in \mathcal{M}_4 \mid \exists \text{ a future-directed time-like curve } \gamma(t), \text{ such that } \gamma(0) = p \text{ and } \gamma(1) = q\}.$$

2. The **chronological past** of a point $p \in \mathcal{M}_4$ is defined analogously:

$$I^-(p) := \{q \in \mathcal{M}_4 \mid \exists \text{ a past-directed time-like curve } \gamma(t), \text{ such that } \gamma(0) = p \text{ and } \gamma(1) = q\}.$$

3. For a subset $S \subset \mathcal{M}_4$ we define

$$I^+(S) = \bigcup_{p \in S} I^+(p)$$

and

$$I^-(S) = \bigcup_{p \in S} I^-(p).$$

[107]

- Remark 1.2.6.9.** 1. Generally $p \notin I^+(p)$. A point is in its own chronological future if and only if there exists a closed time-like path beginning and ending in $p \in \mathcal{M}_4$. [43]
2. In Minkowski space-time, $I^+(p)$ is the set of points (events) which can be reached from $p \in \mathcal{M}_4$ by time-like geodesics starting from p . Its boundary is generated by the null geodesics. This defines the **future light cone** $N_p \subset T_p M$ of the point $p \in \mathcal{M}_4$ (see Figure 1.3). In curved space-times, this is only true locally. Any tangent space $T_p M$ for $p \in \mathcal{M}_4$ is isomorphic to Minkowski space. [107]

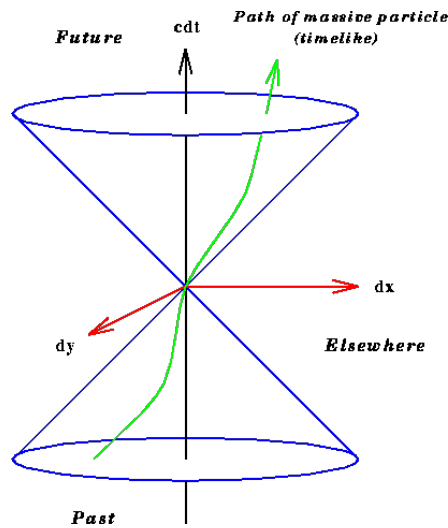


Figure 1.3.: Light cone of an observer in space-time; the red axes represent a space-like hypersurface for a fixed time. The boundary of the light cone (blue lines) represents the null geodesics. [116]

Definition 1.2.6.10. A set U is called **achronical** if $U \cap I^+(U) = \emptyset$. The **edge** of an achronical set is the set of all points $p \in \bar{U}$ such that in every neighbourhood V of p there are points $q \in I^-(p)$ and $r \in I^+(p)$ which can be joined by time-like curves in V which do not intersect U . [43]

Definition 1.2.6.11 (Causal Future and Past). 1. The **causal future** of $p \in \mathcal{M}_4$, denoted by $J^+(p)$, is defined as the set of events that can be reached from p by a future-directed causal curve starting at $p \in \mathcal{M}_4$. Thus,

$$J^+(p) := \{q \in \mathcal{M}_4 \mid \exists \text{ a future-directed causal curve } \gamma(t), \text{ such that } \gamma(0) = p \text{ and } \gamma(1) = q\}.$$

2. The **causal past** of a point $p \in \mathcal{M}_4$ is defined analogously:

$$J^-(p) := \{q \in \mathcal{M}_4 \mid \exists \text{ a past-directed causal curve } \gamma(t), \text{ such that } \gamma(0) = p \text{ and } \gamma(1) = q\}.$$

3. For a subset $S \subset \mathcal{M}_4$ we define

$$J^+(S) = \bigcup_{p \in S} J^+(p)$$

and

$$J^-(S) = \bigcup_{p \in S} J^-(p).$$

[107]

Remark 1.2.6.12. We can define an **acausal set** analogously to an achronical set.

Proposition 1.2.6.13. If $q \in J^+(p) \setminus I^+(p)$, the curve connecting p and q must be a null geodesic. [107]

Definition 1.2.6.14. 1. A point p is said to be a **future endpoint** of a future directed causal curve $\gamma : F \rightarrow \mathcal{M}_4$ if for every neighbourhood V of p , there is a $t \in F$ such that $\gamma(t_1) \in V$ for every $t_1 \geq t$

2. A causal curve is said to be **future-inextendible** (in a set S) if it has no future endpoint (in a set S). [43, p.184]

1.2.6.2. Causality Conditions

In order to rule out space-time topologies such as $\mathbb{S} \times \mathcal{M}_3$ with a three-dimensional spatial manifold \mathcal{M}_3 , which obviously is a causally misbehaving space-time, we have to permit closed time-like geodesics. Thus, we assume that cause proceeds action by assuming the **chronology condition**, which states that there are no closed time-like curves. The set of points where the chronology condition does not hold is called the **chronology violating set**.

Proposition 1.2.6.15 (Carter). The chronology violating set of \mathcal{M}_4 is the disjoint union of sets of the form $I^-(p) \cap I^+(p)$, $p \in \mathcal{M}_4$. [43]

Proposition 1.2.6.16. If \mathcal{M}_4 is compact, the chronology violating set of \mathcal{M}_4 is nonempty.

Remark 1.2.6.17 (Assumption:). We therefore assume \mathcal{M}_4 to be non-compact. There is a second argument against compact space-times: if a Lorentzian metric is defined on a compact four-dimensional manifold, it cannot be simply-connected (2.3.0.14, p.45) [43]. As opposed to the standard models of cosmology, we shall not assume a trivial topology, but there is no reason to rule them out.

In addition, it may be reasonable to rule out closed null curves, thereby stating the **causality condition**. Once more, the set of points which violate the causality condition is the disjoint union of sets of the form $J^-(p) \cap J^+(p)$, $p \in \mathcal{M}_4$. It turns out that in physical realistic space-times the causality condition is equivalent to the chronology condition. [43]

Yet, a small modification of the metric leads to a violation of the causality condition. Therefore, we shall assume **strong causality condition**, which states that for $\forall p \in \mathcal{M}_4$ and any neighbourhood U of p , there exists an $V \subset U$ such that no causal curve intersects V more than once.

The above defined causality conditions do not suffice to rule out causal pathologies (closed causal curves) in arbitrary small neighbourhoods of one or more points. It turns out that that there is a sufficiently strong condition which does ([107]):

Theorem 1.2.6.18. A space-time is said to be **stably causal** if and only if there exists a differentiable function on \mathcal{M}_4 such that $\nabla^a f$ is a past-directed time-like vector field. [107]

Remark 1.2.6.19 (Assumption:). The function f , as introduced in 1.2.6.18, can be interpreted as a **cosmic time function**. The existence of a global time function is equivalent to a global time-orientable space-time. The spatial hypersurfaces $\{f = \text{const.}\}$ can therefore be interpreted as hypersurfaces of simultaneity. If they are all compact, they are diffeomorphic [43]. We shall assume space-time \mathcal{M}_4 to be **globally time-orientable**.

A globally time-oriented space-time \mathcal{M}_4 is homeomorphic to the product of the spatial hypersurfaces of simultaneity and a one-dimensional manifold orthogonal to them which represents time. Thus, $\mathcal{M}_4 \simeq \mathcal{M}_1 \times \mathcal{M}_3$, where \mathcal{M}_3 is a three-dimensional Riemannian manifold (a space-like hypersurface). One way to prove this is to show that the space-time \mathcal{M}_4 is completely determined by the information on a hypersurface \mathcal{M}_3 (at an arbitrary fixed time t_0). We start with the definition of a Cauchy development:

- Definition 1.2.6.20.**
1. The **future Cauchy development** or **domain of dependence** $D^+(S)$ of a set S is the set of all points $p \in \mathcal{M}_4$ such that every past-inextendible causal curve through p intersects S ($S \subset D^+(S)$).
 2. We define $D(S) = D^+(S) \cup D^-(S)$, where the past Cauchy development $D^-(S)$ is defined analogously to $D^+(S)$. $D(S)$ is a subset of space-time which is entirely determined by the data on S .

3. A **partial Cauchy surface** is an acausal set S with no edge (1.2.6.10, p.27). Thus, it is a space-like hypersurface which no causal curve intersects more than once.

4. A partial Cauchy surface S is said to be a (global) **Cauchy surface** if $D(S)$ equals \mathcal{M}_4 . Thus, it is a space-like hypersurface which every causal curve intersects exactly once.

[43]

Example 1.2.6.21. In Minkowski space, the hypersurfaces $\{x_4 = \text{const.}\}$ are Cauchy surfaces, while the hypersurfaces $\{(x_1)^2 + (x_2)^2 + (x_3)^2 - (x_4)^2 = \text{const.}\}$ define only partial Cauchy surfaces. [43]

Remark 1.2.6.22. In Newtonian physics one has to know the state of the entire universe at present time to predict events in the future. In Relativity Theory, one only needs to know “enough” about a set S in order to be able to predict events in the future of S . If we wish to predict events in the entire universe, we have to know “enough” about the state of the universe at the present time. The problem is to decide whether or not the information we have is sufficient.

Closely related is the so-called **Cauchy problem**: given a three-dimensional manifold \mathcal{M}_3 with initial data (metric and extrinsic curvature), the problem is to find a four-dimensional manifold \mathcal{M}_4 , an embedding $\mathcal{M}_3 \rightarrow \mathcal{M}_4$ and a metric which satisfies Einstein’s field equations and agrees with the initial data and is also such that \mathcal{M}_3 is a Cauchy surface of \mathcal{M}_4 [43] [107].

We cannot assume a Cauchy surface yet. As we shall see, there is a property of the universe which indicates the existence of a Cauchy surface.

Definition 1.2.6.23. A set N is said to be **globally hyperbolic** if the strong causality assumption holds on N and if for two points $p, q \in N$, $J^+(p) \cap J^-(q)$ is compact and contained in N . [43]

Remark 1.2.6.24. The second requirement can be interpreted as $J^+(p) \cap J^-(p)$ does not contain any points of the edge of the space-time (i.e. at infinity or at a singularity) [43]. The latter can be granted since singularities shall be excluded from space-time.

Theorem 1.2.6.25. Let (\mathcal{M}_4, g_{ab}) be a globally hyperbolic space-time. Then (\mathcal{M}_4, g_{ab}) is stably causal. Furthermore, a global time function f can be chosen such that each surface of f is a Cauchy surface. Thus, \mathcal{M}_4 can be foliated by Cauchy surfaces and the topology of \mathcal{M}_4 is $\mathbb{R} \times \mathcal{M}_3$, where \mathcal{M}_3 denotes any Cauchy surface. [107]

Remark 1.2.6.26 (Assumption:). 1. For the one-dimensional time-like manifold there are two possibilities: \mathbb{S} or \mathbb{R} . Since \mathbb{S} leads to a causally misbehaved space-time (Gödel universe), we choose \mathbb{R} [64]. We do not have access to information about space-time events before the Big Bang or about the Big Bang itself, therefore, we may write $\mathbb{R}_+ \times \mathcal{M}_3$ [4]. Thus, we choose a space-time with a toroidal topology [48].

2. We shall assume space-time to be globally hyperbolic and can restrict our investigations to the three-dimensional space-like manifold \mathcal{M}_3 . General Theory of Relativity forbids the topology of \mathcal{M}_3 to change during cosmic evolution [64]. Thus, it is sufficient to determine the topology of space today.
3. If the cosmic time function is smooth, \mathcal{M}_4 is diffeomorphic to $\mathbb{R} \times \mathcal{M}_3$ [43, p.212]. We shall assume the existence of a smooth cosmic time function.
4. The spatial hypersurfaces of simultaneity indeed foliate space-time [107]. We shall define the term of a foliation in Chapter 3 (3.3.2.7, p.69).

1.2.6.3. Space Orientation

A space-time \mathcal{M}_4 is called **space-orientable** if the spatial part of the universe \mathcal{M}_3 is orientable in the sense of 1.2.6.1.

Remark 1.2.6.27 (Notation). An orientable manifold shall denote a space-orientable manifold throughout this work.

A non-orientable spatial part of space-time \mathcal{M}_3 contradicts our everyday experience. Pathologies like going along a path and returning upside-down would be enabled. The paradox of a space traveller who leaves his right-hand glove at home comes back and finds out that his forgotten glove fits his left hand is it is mentioned in [22, p.9]. Thus, we shall assume space-time \mathcal{M}_4 to be space-orientable.

There is the so-called CTP-theorem, a theorem of particle physics which states that along a closed path either charge, time orientation and space orientation of a particle changes or none of them. Assuming time orientation, space orientation would be implied immediately. See [55] and [43] for more information and further references.

Remark 1.2.6.28 (Assumption:). Space-times which are time-orientable and space-orientable are called **total orientable**. [55] Thus, we are assuming a total-orientable space-time.

1.2.7. Further Assumptions on Space-Time

Without Boundary: Assuming a boundary, we immediately run into contradictions. We therefore assume space-time to be a manifold without boundary.

Inextendible:

Definition 1.2.7.1. (\mathcal{M}'_4, g') is a C^r -**extension** of (\mathcal{M}_4, g) if there exists an isometric embedding $\nu : \mathcal{M}_4 \rightarrow \mathcal{M}'_4$. [43]

In this case we should points of \mathcal{M}'_4 as belonging to the space-time \mathcal{M}_4 . To ensure that all nonsingular points are included in space-time, we require that there does not exist a C^r -extension. Thus, we assume \mathcal{M}_4 to be inextendible. However, we shall

assume an even stronger version of inextendible: **locally inextendible**. We require that there does not even exist a local extension, which is defined as follows:

Definition 1.2.7.2. \mathcal{M}_4 is said to be **locally extendible** if there is an open set $U \subset \mathcal{M}_4$ with non-compact closure in \mathcal{M}_4 such that the pair $(U, g|_U)$ has an extension (U', g') in which the closure of the image of U is compact. [43]

Completeness:

Definition 1.2.7.3. A metric space (\mathcal{M}, g) is **geodesically complete** if and only if each geodesic $\gamma : I \rightarrow (\mathcal{M}, g)$ can be extended to a unique maximal geodesic $\gamma : \mathbb{R} \rightarrow \mathcal{M}$. [84]

Remark 1.2.7.4 (Notation:). We shall call a geodesically complete space-time a complete space-time.

A geodesically complete manifold is inextendible. The converse is, in general, not true. Incomplete space-times enable a variety of pathologies. In time-like or null geodesically incomplete space-times the existence of particles with a worldline beginning a finite time ago or ending in a finite time would be enabled. In space-like incomplete space-times there could be singularities in space-time, but no observer could ever reach them. For further examples see [107, p.215]. Thus, we assume space-time to be complete.

1.3. Observing the Universe

We observe the universe by detecting radiation of different frequency of the electromagnetic spectrum. For example, we detect visible light, microwaves or X-rays coming from all the different regions of the universe, except of in the direction of the bulge of the Milky Way. As we have defined in 1.2.6.3 (p.25), we can only observe our causal past (1.2.6.11, p.27).

First of all, we shall make an important and strong assumption, namely the assumption of **spatial local homogeneity**. It is the assumption that a “typical” free-falling observer in another place in the universe would at the same time make the same observations of the universe (here we can use the global time function or in other words we require the observer to sit on the same spatial hypersurface). Thus, we are assuming the **Copernican principle** which states that we are not located at a special place in the spatial universe. By a “typical” free-falling observer we mean an observer who moves with the average velocity of typical galaxies in their respective neighbourhoods. Without the assumption of homogeneity we would not be able to make any generalizations. Observational data supports this following assumption: the Sloan Digital Survey provides evidence that the distribution of galaxies on global scales is homogeneous [113]. For a visualization see Figure 6.1 in Chapter 6 (p. 119). But, and here we differ from standard theory of cosmology, we do not assume homogeneity

as a global condition. We assume homogeneity to be merely a local property, because it is a property derived from observational data and logic reasoning. [109] [55] [60]

The mathematical definition of a locally homogeneous manifold can be derived as follows:

Definition 1.3.0.5. *For a Riemannian manifold \mathcal{M} we define:*

- **Isometry:** *A local isometry on \mathcal{M} is a differentiable map f such that each of the tangent maps $T_x f : T_x \mathcal{M} \rightarrow T_{f(x)} \mathcal{M}$ is an isometry between the Euclidean vector spaces $(T_x \mathcal{M}, g_x)$ and $(T_{f(x)} \mathcal{M}, g_{f(x)})$. Thus, $T_x f$ is an isomorphism of vector spaces which preserves the inner product. Moreover if f is a diffeomorphism $f : \mathcal{M} \rightarrow \mathcal{M}$ we say that f is an isometry. In this case f is called an isometric transformation, or motion, of \mathcal{M} . [96]*
- **(Local) Homogeneity:** *\mathcal{M} is said to be (locally) homogeneous if for any two points $p, q \in \mathcal{M}$ there is a (local) isometry m such that $m(p) = q$. [111]*

Thus, any two points can be carried into each other continuously. In Chapter 2 we shall give a definition of local homogeneity using the action of the group of local isometries on the manifold \mathcal{M}_3 .

1.3.1. The Expansion of the Universe and the Big Bang

In the visual spectrum of light we observe that the farther away an object is, the greater the redshift of the light's spectrum received from it. Because of the Doppler effect (applied to light waves) we can interpret the redshift as radial velocity. Thus, the farther away an object is, the greater its radial velocity v_r with respect to us. Hubble showed empirically that this is in a good approximation directly proportional. This is the so-called **Hubble law**:

$$v_r = H_0 \cdot d,$$

where H_0 is the **Hubble constant**, which describes the cosmic expansion at the present time t_0 , and d denotes the radial distance from Earth. As an empirical law it is not in every point exact. It holds true on average and on scales where the expansion of the universe governs the motion of objects. For example, in our solar system the motion of objects is governed by gravitational fields caused by the mass of the Sun and the planets. Thus, Hubble's law does not predict the motion of these bodies. To measure the Hubble constant, secondary distance indicators are used (where peculiar velocities can be neglected). The most important standard candles to evaluate the Hubble constant are supernovae Ia [109, p.48]. Recent measurements indicate an accelerating expansion [109]. Thus, Hubble's law is only valid for a special interval of distances. We shall go into further detail in Chapter 6 (p.128).

First, Lemaître formulated that it must be space which expands. The idea that galaxies and other objects are moving away only from us is false. It would contradict the Copernican principle. In fact, it is space itself which is expanding at every point. To visualize the

expansion of the universe one can think of an inflating balloon. The surface of the balloon expands and two points, which are initially close, separate while time passes (see Figure 1.4). While the surface of the balloon is two-dimensional, the spatial part of the universe is three-dimensional.

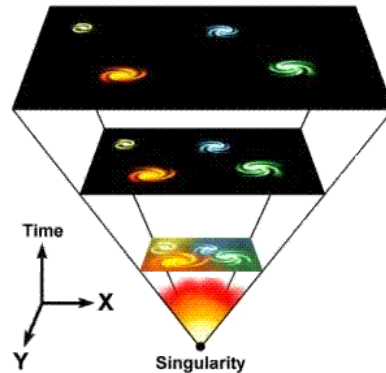


Figure 1.4.: Two-dimensional visualization of the expansion of the universe. [117]

If the universe is expanding, all points were closer to each other if we go back in time. Going back in time further and further, matter becomes denser and hotter until we come to an era when it was too hot for electrons to be bound to the nuclei in atoms. Because of the strong interactions of photons with free electrons the universe gets more opaque, keeping the past-oriented view. Going even further back in time we reach a time when the universe was so hot and dense that the mean free paths of photons was too short for light to propagate. In this era the universe was opaque. Going back even further, we come to a point where physical laws break down. This singularity is called the **Hot Big Bang**. If we now choose a future-oriented view, we can interpret this singularity as an initial explosion. [109]

1.3.2. Remnant of Last Scattering

Because of the rapid collisions of photons with electrons there was a thermal equilibrium of radiation and hot dense matter at sufficiently early times. The number density of photons in equilibrium with matter and of the temperature T and a certain frequency is given by a black body spectrum. When the universe cooled down to a mean temperature of about $T \approx 10^5 K$, the exchange of energy between electrons and photons became negligible, despite

there being some scattering (interaction between photon and electron), until a temperature was reached where hydrogen and helium nuclei were able to bind the free electrons. The function of opaqueness $\mathcal{O}(T)$ gives the probability of a photon having had at least one more scattering with an electron between a certain time $t(T)$ and the present moment. $\mathcal{O}(T)$ increases with temperature. At temperatures of about $3,000K$, 99% of the free electrons were bound. This event, which took place 400,000 years after the Big Bang, is referred to as **recombination**. From than on, the radiation could expand freely (interaction with helium and hydrogen can be neglected). This space-time event is referred to as **decoupling**. At that point in time the last scattering had happened and the universe became transparent. This space-time event is known as the **last scattering surface** [109, section 2]. The last scattering surface (LSS) defines the limit of the theoretically observable universe.

The radiation of the LSS continues to have a black body spectrum, even if the radiation has become cooler and less dense. The temperature is the original temperature with a red shift.

In the 1940s, Gamov predicted the existence of this radiation for the first time. Even earlier, Penzias and Wilson had detected the Cosmic Microwave Background (CMB) [82]. It is an almost perfect black body spectrum with maximum $T = 2.725$ [91] [72].

The CMB is almost isotropic and looks the same in every direction. The anisotropies are of order $\frac{\Delta T}{T} = 10^{-5}$. This leads to the assumption that on very large scales (global scales) density fluctuation can be neglected. Thus, the universe is in good approximation homogeneous and isotropic on these scales. Since these are properties which we deduce from observational data, we can assume these properties to be merely local properties. Thus, observational data indicates the spatial part of the universe to be locally homogeneous and locally isotropic.

We shall give a mathematical definition of locally isotropic manifolds in Chapter 4 (4.0.0.18, p.77). Descriptively, an isotropic manifold looks in any direction the same.

1.4. Is the Spatial Part of the Universe Finite or Infinite?

Standard models assume the cosmological principle, which states that the spatial part of the universe is globally isotropic and homogeneous. This assumption leads to the conclusion that space is simply-connected and of constant curvature. In this case, Einstein's field equations reduce to the Friedmann equation, which we shall deduce in Chapter 6. The metric for these space-times is given by the Robertson-Walker metric.

Standard Cosmology does not deal with the possibility that space could have a nontrivial topology. As we have seen, physics is written in terms of local geometry and is independent of the topology of space-time. We require the Lorentzian manifold \mathcal{M}_4 to satisfy Einstein's field equations, which do not include any topological information. Thus, non-simply-connected (in cosmology multi-connected) models have the same kinematics or, more generally, the

same physics as in the simply-connected case if and only if they have the same metric (up to diffeomorphism). For spatially locally homogeneous and locally isotropic space-times, Einstein's field equations also reduce to the Friedmann equation and the space-time metric is given by Robertson-Walker metric as well.

Nontrivial topologies would enable the universe to be finite without boundary. There are good arguments in favour of finiteness:

1. We assume the spatial universe to be homogeneous, but how did information propagate? The signal must have been faster than light! This contradicts the physical principles and is called the homogeneity problem. In a finite universe homogeneity is no contradiction. Gott analyzed this problem in detail in [48] and concludes that a finite universe could solve the homogeneity problem, even if it is unlikely.
2. Homogeneity in infinite space would lead to an infinite amount of matter. In a finite universe this, once more, would not lead to a contradiction. [55]
3. Space is finite if and only if it is compact. As we have seen in 1.2.6.19 (p.29), the spatial hypersurfaces of simultaneity are diffeomorphic if they are compact. It is favourable to assume the spatial hypersurfaces to be diffeomorphic.
4. Einstein and Wheeler argue for finite universes because of March's principle.
5. Ellis argues that infinite universes are unaesthetic because any event which happens once happens infinite times.
6. Some quantum cosmologists favour finite universes because spaces with small volumes have small actions, which are more likely to be created. (See [18] and references there.)

1.5. Conclusion

We assume space-time \mathcal{M}_4 to be a four-dimensional, smooth, non-compact, geodesically complete, (inextendible,) spatially locally homogeneous, connected, paracompact, Hausdorff and total-orientable Lorentzian manifold without boundary diffeomorphic to $\mathcal{M}_3 \times \mathbb{R}_+$ which satisfies Einstein's field equations. This enables us to focus on the spatial part of the universe \mathcal{M}_3 , which is a three-dimensional, smooth, connected, geodesically complete, orientable, locally homogeneous Riemannian manifold without boundary. Local homogeneity is a necessary and sufficient property to develop a space-time model on the largest scales. Local isotropy, in contrast, is not essential, but can be argued for from observational data. First, we shall assume local homogeneity and classify all possible geometric structures reasonable for the spatial part of the universe. In Chapter 4, we shall then additionally assume local isotropy and classify these manifolds by their topology.

2. An Algebraic Approach to Geometry and the Topology of the Universe

In Chapter 1 we argued that \mathcal{M}_3 is a three-dimensional, orientable, connected, geodesically complete, smooth and locally homogeneous Riemannian manifold without boundary. Most of the results we will see in this chapter are true for an arbitrary manifold.

We shall start with an alternative definition of a “(topological) manifold” and gain some insight on the algebraic concepts with which we examine these objects. After an introduction to Lie groups and homogeneous spaces, we shall then focus on the topology of \mathcal{M}_3 . We will see that the manifold describing the spatial part of the universe \mathcal{M}_3 is homeomorphic to the quotient space $\widetilde{\mathcal{M}}_3/\Gamma$ (in symbols: $\mathcal{M}_3 \simeq \widetilde{\mathcal{M}}_3/\Gamma$), where $\widetilde{\mathcal{M}}_3$ is a simply-connected space and Γ is a group of homeomorphisms acting freely and properly discontinuously on $\widetilde{\mathcal{M}}_3$.

2.1. Manifolds and Pseudogroups

We already know that manifolds are topological spaces which are locally modeled on \mathbb{R}^n . See Chapter 1 (Definition 1.1.1.1, p. 6). Thus, we have a topological space consisting of small pieces each of which is homeomorphic to an open ball in \mathbb{R}^n . These pieces are glued together by local homeomorphisms such that the resulting space has locally the same topological structure as \mathbb{R}^n . These local homeomorphisms are also called “gluing maps”. The pattern of the manifold is completely determined by the gluing maps. To ensure a well-defined mathematical object, we require the following properties of gluing maps:

Definition 2.1.0.1 (Pseudogroup). *A **pseudogroup** of a topological space X is a set \mathbb{G} of homeomorphisms between open sets of X satisfying the following conditions:*

1. *The domains of the elements $g \in \mathbb{G}$ cover X .*
2. *The restriction of an element $g \in \mathbb{G}$ to any open set contained in its domain is also in \mathbb{G} .*
3. *The composition $g_1 \circ g_2$ of two elements of \mathbb{G} , when defined, is in \mathbb{G} .*
4. *The inverse of an element of \mathbb{G} is in \mathbb{G} .*

5. The property of being in \mathbb{G} is local, that is, if $g : U \rightarrow V$ is a homeomorphism between open sets of X and U is covered by open sets U_α such that each restriction $g|_{U_\alpha}$ is in \mathbb{G} , then $g \in \mathbb{G}$. [99, p.110]

Assume $X = \mathbb{R}^n$ and \mathbb{G} a pseudogroup of \mathbb{R}^n . Since the inverse of any element is in \mathbb{G} , the identity has to be in \mathbb{G} too. The smallest pseudogroup of \mathbb{R}^n is the so-called **trivial pseudogroup**, which consists only of the identity. The largest pseudogroup of \mathbb{R}^n is the set of all homeomorphisms between open subsets of \mathbb{R}^n , denoted by **Top**. A topological space M is a manifold if the set of gluing homeomorphisms \mathbb{G} are in **Top**. Thus, locally, the space has the topological structure of \mathbb{R}^n .

Definition 2.1.0.2 (\mathbb{G} -Manifold). *Let \mathbb{G} be a pseudogroup of \mathbb{R}^n . An n -dimensional \mathbb{G} -manifold is a topological space M with a \mathbb{G} -atlas on it. A \mathbb{G} -atlas is a collection of compatible coordinate charts the domain of which covers M . A coordinate chart, or a local coordinate system, is a pair (O_i, φ_i) , where O_i is open in M and $\varphi_i : O_i \rightarrow \mathbb{R}^n$ is a homeomorphism onto its image. Compatibility means that whenever two charts (O_i, φ_i) and (O_j, φ_j) intersect the transition map or coordinate change*

$$\varphi_{ij} = \varphi_i \circ \varphi_j^{-1} : \varphi_j(O_i \cap O_j) \rightarrow \varphi_i(O_i \cap O_j)$$

is in \mathbb{G} . [99, p.110]

Remark 2.1.0.3. 1. A \mathbb{G} -structure for a manifold M is a \mathbb{G} -atlas for M .

2. The structure, that is, the pattern of the manifold depends on the choice of \mathbb{G} . Let us give an example. Let \mathbb{G} be the set of C^r -diffeomorphisms between open sets of \mathbb{R}^n (1.2.1.2, p.21). The corresponding manifold is an r -times differentiable manifold, called **C^r -manifold**. If the pseudogroup is in C^∞ , the manifold is called **smooth**. [99, p.111]

Let us now consider a group of maps which preserves the \mathbb{G} -structure: the **group of local \mathbb{G} -isomorphisms**.

Definition 2.1.0.4. *A homeomorphism which is locally expressible as an element $g \in \mathbb{G}$, is called a **local \mathbb{G} -isomorphism**. Such a map preserves the \mathbb{G} -structure. [99, p.112]*

Remark 2.1.0.5. 1. We have already mentioned that the pseudogroup of a \mathbb{G} -manifold is in **Top**. Let $\mathbb{H} \subset \mathbb{G}$ be a pseudogroup, then any \mathbb{H} -atlas is a \mathbb{G} -atlas. Thus, any \mathbb{H} -manifold is also a \mathbb{G} -manifold and has a \mathbb{G} -structure. In this case, we call the \mathbb{G} -structure the **\mathbb{G} -relaxation** of the \mathbb{H} -structure. Similarly, the \mathbb{H} -structure is called an **\mathbb{H} -stiffening** of the \mathbb{G} -structure.

2. Let $\mathbb{G} = C^r$ with $r < \infty$ and $\mathbb{H} = C^\infty$, then the C^∞ -stiffening is called a **smoothing**. Whitney proved in 1936 that every differentiable manifold has a unique smoothing up to C^r -diffeomorphisms (see [110]). [99, p.112]

3. Let \mathcal{C}^w be the pseudogroup of real-analytic diffeomorphisms of open sets of \mathbb{R}^n . A \mathcal{C}^w -manifold is then called a **real-analytic manifold**. Real-analytic diffeomorphisms are completely determined by their restriction to an open subset of \mathbb{R}^n . We shall need this property in Chapter 3, when we introduce the concept of the developing map. It is, once more, a (nontrivial) result of Whitney [110] that every smooth manifold admits a real-analytic stiffening. Since any Riemannian manifold has a smooth stiffening, there exists a real-analytic stiffening as well. [99, p.113]

2.2. Lie Groups – Basic Definitions and First Examples

Definition 2.2.0.6. *A manifold endowed with a compatible group structure is called a **Lie group**. Compatibility means that the maps $G \times G \rightarrow G$ and $G \rightarrow G$, which represent the group operations of multiplication $(g_1, g_2) \mapsto g_1 g_2$ and inversion $g \mapsto g^{-1}$, are smooth. [32, p. 96]*

Remark 2.2.0.7. The quotient G/G_0 , where G_0 is the connected component of the identity, is a discrete group. G/G_0 is called the **component group**.

Example 2.2.0.8. 1. Since any finite dimensional real or complex vector space is a Lie group under addition, so are \mathbb{R} and \mathbb{C} .

2. $\mathbb{R} \setminus \{0\}, \mathbb{C} \setminus \{0\}$ are Lie groups under multiplication.

3. $GL(\mathbb{R}^n)$ is the set of all invertible linear maps on \mathbb{R}^n . Any linear map on a finite-dimensional real vector space V is completely defined by its values on a basis of V . Fixing a basis $\{v_1, \dots, v_n\}$ of V , the map

$$L(V) \rightarrow V^n, f \mapsto (f(v_1), \dots, f(v_n))$$

defines a bijection from the set of all linear maps on V to V^n . If we choose the standard basis as a basis of \mathbb{R}^n , the above-constructed map takes the form:

$$L(\mathbb{R}^n) \rightarrow M_n(\mathbb{R})(:= (\mathbb{R}^n)^n = \mathbb{R}^{n^2}), f \mapsto A,$$

where A is the matrix representation of the linear map f . Consider the function

$$M_n(\mathbb{R}) \rightarrow \mathbb{R}, A \mapsto \det(A).$$

The map f is invertible if and only if the determinant of the matrix A is non-vanishing. The set of all invertible matrices is called the **linear group**, denoted by $GL_n(\mathbb{R})$. The image of the set of all invertible matrices under the map \det is the open set $\mathbb{R} \setminus \{0\}$. Since the map \det is continuous (see Appendix Topology, A.0.0.4, p. 185), the set of all invertible matrices is open in $M_n(\mathbb{R})$. We have found a bijection between $GL_n(\mathbb{R})$ and

an open set in \mathbb{R}^{n^2} , which turns $GL_n(\mathbb{R})$ into a manifold of dimension n^2 . The matrix multiplication is smooth and therefore, $GL_n(\mathbb{R})$ is a smooth manifold. Furthermore, the map $GL(\mathbb{R}^n) \rightarrow GL_n(\mathbb{R}) \subset M_n(\mathbb{R})$, $f \mapsto A$ is an isomorphism. Throughout this work we shall identify $GL(\mathbb{R}^n)$ with $GL_n(\mathbb{R})$.

4. Closed subgroups $H \subset G$ of Lie groups are Lie groups. For example, closed subgroups of the full linear group $GL_n(\mathbb{R})$. These groups are called **matrix groups**. Examples are:

The special linear group $SL_n(\mathbb{R}) := \{A \in GL_n(\mathbb{R}) \mid \det(A) = 1\}$ is isomorphic to the group of unimodular (or volume-preserving) transformations on \mathbb{R}^n .

The orthogonal group $O_n(\mathbb{R}) := \{A \in GL_n(\mathbb{R}) \mid A \cdot A^t = id\}$ is the group of orthogonal matrices and is isomorphic to the orthogonal transformations on \mathbb{R}^n .

The special orthogonal group $SO_n(\mathbb{R}) := O_n(\mathbb{R}) \cap SL_n(\mathbb{R})$ is the group of orthogonal matrices with determinant 1 and is isomorphic to the orthogonal, unimodular transformations on \mathbb{R}^n .

They are called the **classical simple Lie groups**. These groups will be very important for us throughout this work.

5. If G and H are Lie groups, the product $G \times H$ is a Lie group. Since $U(1) := \{z \in \mathbb{C} \mid |z| = 1\}$ is a Lie group as a closed subgroup of a Lie group, the **n-dimensional torus** $\mathbb{T}^n := U(1)^n$ ($n \in \mathbb{N}$) is a Lie group.

6. If N is a closed and normal subgroup of a Lie group G , the factor group G/N also is a Lie group too.

[16], [32] [54]

2.2.1. The Action of a Group

Definition 2.2.1.1. Let X be a set and G a group with neutral element $e \in G$.

1. A **left action of G on X** is a map $\varphi : G \times X \rightarrow X$ such that $\varphi(e, x) = x$ and $\varphi(g, \varphi(h, x)) = \varphi(gh, x)$ for all $x \in X$ and $g, h \in G$.
2. Given a left action $\varphi : G \times X \rightarrow X$ and a point $x_0 \in X$, we define the **orbit** $G \cdot x_0$ of x_0 as the subset $\{x \in X \mid \exists g \in G : \varphi(g, x_0) = x\} \subset X$ and the **isotropy subgroup (or stabilizer)** G_{x_0} of x_0 to be $\{g \in G \mid \varphi(g, x_0) = x_0\} \subset G$.

[17]

Definition 2.2.1.2. The group G is said to act **effectively** on a set X by homeomorphisms if the only element of G acting trivially is the identity. [99, p.153]

- Remark 2.2.1.3.** 1. Instead of $\varphi(g, x)$ we often write gx or $g(x)$. For us, an action shall always be a left action. Everything can be defined by right actions analogously.
2. From the definition of a group follows that for $g \in G$ with inverse g^{-1} , $\varphi(g^{-1}, \varphi(g, x)) = \varphi(e, x) = x, \forall x \in X$. We conclude that for any $g \in G$ the map $x \mapsto \varphi(g, x)$ is a bijection $X \rightarrow X$. This enables us to view $\varphi : g \mapsto \varphi(g, \cdot)$ as a map from G to the set of bijections of X , which again is a group. Thus, this is a group homomorphism.
3. The concept in 2.2.1.1(ii) becomes very natural if one thinks about the action as a way to use elements of G for moving points of X around. Thus, the orbit of $x_0 \in X$ (or left coset) is just the set of points in X which can be reached from x_0 . In other words, the orbit of a point x_0 is the set of point where x_0 can be transported to. The isotropy group is therefore the set of elements in G , which stabilize x_0 .
4. Two points $x, y \in X$ are called **equivalent** if there is an $g \in G$ such that $y = g(x)$.
5. Let $x, y \in X$ be points in the same orbit $y \in G(x)$. There is a $g \in G$ such that $y = g(x)$, thus, they are equivalent. Take h , which is an element of the stabilizer G_y . Since $h(y) = y$ and $h(g(x)) = g(x)$, $g^{-1}hg$ is an element of the stabilizer G_x . Since $h \in G_y$ was arbitrary, $g^{-1}G_yg = G_x$. Hence, G_x and G_y are conjugates in G .
6. It is a general fact that any group G is the disjoint union of its cosets. Thus, orbits are either disjoint or coincide and “lying in the same coset” is an equivalence relation. The set of all equivalent classes is called the **orbit space**, denoted by X/G . [16]
7. Let φ be an action of the group G on the set X . The **kernel of ineffectiveness** is defined as the set $\{g \in G : gx = x, \forall x \in X\}$. Factorization of G with respect to the kernel of ineffectiveness gives an effective action. [32]

Example 2.2.1.4. 1. The group \mathcal{G} of all transformations of a smooth manifold M (1.2.1.2, p.21) is an effective group and different transformations therefore refer to different elements of the group. This group can be endowed with a Lie group structure. If the action of \mathcal{G} on the manifold M , given by

$$\mathcal{G} \times M \rightarrow M, (g, x) \mapsto g(x),$$

is smooth, \mathcal{G} is called the **Lie group of transformations** and M is a \mathcal{G} -manifold. Here, the isotropy group

$$\mathcal{G}_x = \{g \in \mathcal{G} : gx = x\} \tag{2.1}$$

of any point $x \in M$ is a closed Lie subgroup of the group \mathcal{G} .

2. The group of isometries (motions) (1.3.0.5, 33) of a Riemannian manifold M is uniquely endowed with a differentiable structure, which turns it into a Lie group of transformations. It is called the **isometry group** of the manifold M and is denoted by $Isom(M)$.

[103], [32]

Remark 2.2.1.5. A subgroup $\Gamma \subset Isom(M)$ is a **discrete group of motions** if for each point $x \in M$, the family $\{\gamma(x) | \gamma \in \Gamma\}$ is locally finite (1.1.1.6, p.8). [103]

2.2.2. Homogenous Spaces

Remark 2.2.2.1 (Notation:). X shall denote a topological space and M a manifold.

Definition 2.2.2.2. Let G be a group acting on a space X . The action of G is called **transitive** if for any two points $x, y \in X$ there exists an element of G such that $g(x) = y$. The action is called **sharply transitive** if there is exactly one element $g \in G$, such that $g(x) = y$.

Remark 2.2.2.3. 1. A **sharply transitive** action is the same as a simply transitive (or regular) action, which is defined as a transitive and (fixed-point-)free action (2.3.1.3, p. 48).

2. In cosmology transitive actions are often called multiple transitive actions. This term can be found in older mathematical books too.

An action of a group G on a space X defines a bijection from the orbit $G \cdot x$ of x to the factor group G/G_x of left cosets for every $x \in X$. If the action is transitive, there is only one orbit. Every point can be transported to any other point. Therefore, we get a bijection

$$G/G_x \rightarrow X, \quad gG_x \mapsto gx. \quad (2.2)$$

The topological space X is diffeomorphic to the space of left cosets, symbolized by $X \cong G/G_x$. Assuming that X is Hausdorff is equivalent to assuming that the stabilizer G_x is a closed subgroup. (A.1.0.15, p.187). [16, p.16,17]

Definition 2.2.2.4. A smooth manifold M together with a Lie group G acting transitively on M is said to be a **homogenous space**. We denote a homogenous space with (M, G) .

Remark 2.2.2.5. 1. If the manifold M is connected or simply-connected, the homogenous space (M, G) is said to have the same property [103, p.9]. That does not mean that G is connected or simply-connected.

2. If the action of a Lie group G on a homogeneous G -manifold M is effective, G can be identified with the Lie group of transformations of the manifold M . [32, p.97]

Example 2.2.2.6. 1. A **homogeneous Riemannian space** is a Riemannian manifold (M, g) , the isometry group $Isom(M, g)$ of which acts transitively on M . $Isom(M, g)$ is compact if and only if M is compact.

2. Every isometry in \mathbb{E}^n can be written as the composition of a rotation and a translation. The set of all translations T_n is isomorphic to \mathbb{R}^n . Thus, the set of all isometries of the Euclidean space \mathbb{E}^n is the semidirect product $Isom(\mathbb{E}^n) = \mathbb{R}^n \rtimes O_n(\mathbb{R})$. $Isom(\mathbb{E}^n)$ is called the **Euclidean group** and is denoted by $E(n)$. $O_n(\mathbb{R})$ is the isotropy group of the action of $Isom(\mathbb{E}^n)$ on \mathbb{E}^n . $\mathbb{E}^n \cong E(n)/O_n(\mathbb{R})$ is a homogeneous space.
3. The group of all isometries of the n -dimensional sphere coincides with the group of all $(n + 1)$ -dimensional rotations. If we fix a one-dimensional subspace of \mathbb{R}^{n+1} , we get the isotropy group at each point. Thus, the stabilizers are isomorphic to $O_n(\mathbb{R})$. In particular $O_{n+1}(\mathbb{R})/O_n(\mathbb{R}) \cong \mathbb{S}^n$ [83, p.6]. Since the sphere is oriented, \mathbb{S}^n can be also written as $SO_{n+1}(\mathbb{R})/SO_n(\mathbb{R})$. Because $O_{n+1}(\mathbb{R})$ acts transitively, \mathbb{S}^n is a homogeneous space [96, p.65].
4. Recall Example 1.1.2.21 (p.13). A function $f : \mathbb{R}^{n+1} \rightarrow \mathbb{R}^{n+1}$ is a **Lorentz transformation** if and only if f is linear and $\{e_0, e_1, \dots, e_n\}, \{f(e_0), f(e_1), \dots, f(e_n)\}$ is an (Lorentzian) orthonormal basis of \mathbb{R}^{n+1} for the standard Lorentzian basis of \mathbb{R}^{n+1} . A matrix A is called **Lorentzian** if and only if the associated linear transformation $A : \mathbb{R}^{n+1} \rightarrow \mathbb{R}^{n+1}, x \mapsto Ax$ is Lorentzian. The group of all these matrices forms a group, denoted by $O_{n,1}(\mathbb{R})$, called the **Lorentz group** of $(n \times n)$ -matrices.

Every positive Lorentz transformation of \mathbb{R}^{n+1} restricts to an isometry of \mathbb{H}^n and every isometry of \mathbb{H}^n extends to a unique positive Lorentz transformation of \mathbb{R}^{n+1} . Thus, the group of isometries of \mathbb{H}^n is isomorphic to the positive Lorentz group $PO_{n,1}(\mathbb{R})$. The isotropy group of each point coincides with the group $O_1(\mathbb{R}) \times O_n(\mathbb{R})$. The homogeneous space \mathbb{H}^n can be written as: $\mathbb{H}^n \cong PO_{n,1}(\mathbb{R})/(O_1(\mathbb{R}) \times O_n(\mathbb{R}))$. [84]

Remark 2.2.2.7. Let G be a Lie group and $H \subset G$. Let G act on the factor space G/H through the above-defined left translation $l_g : g'H \rightarrow gg'H$. This action is transitive and therefore G/H is a homogeneous space. The left translation can be used to endow G/H with a topology. The preimage of the unity eH in G/H is the group H . If we require the topology to be Hausdorff, H has to be closed. As a closed subgroup of a Lie group, H itself is a Lie group. Here, the space G/H is a smooth manifold, because the left translation is smooth. [32] This leads to the following theorem:

Theorem 2.2.2.8. *Let G be a Lie group and $H \subset G$ a closed subgroup. Then there is a unique structure of a smooth manifold on the homogenous space G/H so that the natural map $p : G \rightarrow G/H$ is of maximal rank, i.e. $\dim(f(T_x M)) = \dim(G/H), \forall x \in M$. In particular $\dim(G/H) = \dim(G) - \dim(H)$. [16]*

Remark 2.2.2.9. 1. In this case, p is called a **submersion**. See, for instance, [54] for a definition.

2. It can be shown that the construction of 2.2.2.7 leads to all homogenous spaces of G . Thus, a homogenous space can be defined by factor groups.

3. $H \subset G$ can be identified with the isotropy group of the identity of the action of G on the quotient space G/H . The stabilizer has to be compact for every point, but since the space is homogeneous it is sufficient to require it for an arbitrary point.
4. Let $M = G/G_x$, be a homogeneous manifold of dimension n . Theorem 2.2.2.8 states that $\dim(G) = \dim(G_x) + \dim(G/G_x)$. For manifolds, which are locally modeled on \mathbb{R}^n , the isotropy group is a closed subgroup of $O_n(\mathbb{R})$, which is of dimension $\frac{n(n-1)}{2}$. This gives an upper boundary for the dimension of the isometry group of M (which can be identified with the Lie group G as mentioned in remark 2.2.2.5):

$$\dim(G) \leq n + \frac{n(n-1)}{2} = \frac{n(n+1)}{2}.$$

Therefore, the dimension of the isometry group of three-dimensional homogeneous manifolds is therefore not greater than six. The equivalence holds if and only if the isotropy group is the whole group $O_n(\mathbb{R})$. As we shall see in Chapter 4 (3.3.2.4, p.68), this is satisfied if and only if the space is of constant curvature. If the space is simply transitive, $\dim(G/G_x) = \dim(G)$. [55]

2.3. The Universal Covering Space

We assume the reader to be familiar with the basic definitions of topology as described in Appendix A (p.185).

Remark 2.3.0.10 (Notation): In the following, X and Y denote topological spaces.

Definition 2.3.0.11. Let X, Y be two topological spaces and $f : X \rightarrow Y$ a continuous map. We say f is **homotopic** to g ($f \sim g$) if there is a continuous map $H : X \times I \rightarrow Y$ such that $H(x, 0) = f(x)$ and $H(x, 1) = g(x)$. In this situation, H is called a **homotopy** between f and g . A map which is homotopic to a constant function is called **null-homotopic**. [15][p.12]

A **homotopy of paths** (see A.0.0.8, p.186) in X is a family $f_t : I \rightarrow X$, with $0 \leq t \leq 1$ and $I = [0, 1]$ such that:

1. The end points $f_t(0) = x_0$ and $f_t(1) = x_1$ are independent of t .
2. The associated map, given by $F : I \times I \rightarrow X, (s, t) \mapsto f_t(s)$, is continuous. [42]

Remark 2.3.0.12. Homotopy defines an equivalence relation. The equivalence class of the path f is denoted by $[f]$ and is called the **homotopy class** of f .

Definition 2.3.0.13 (Fundamental Group). The **fundamental group** of X with base point x_0 , denoted by $\pi_1(X, x_0)$, is defined as the set of all homotopy classes $[f]$ of loops (see A.0.0.10, p.186) $f : I \rightarrow X$ with base point x_0 .

- Remark 2.3.0.14.** 1. The fundamental group $\pi_1(X, x_0)$ is actually a group with respect to the product $[f][g] = [\nu]$, where $\nu(u) = f(2u)$ for $0 \leq u \leq 1/2$ and $\nu(u) = g(2u - 1)$ for $1/2 \leq u \leq 1$. The inverse is given by $[f]^{-1} = [f(1 - u)]$.
2. The fundamental group of a path-connected space (A.0.0.9, p.186) is independent (up to isomorphism) of the base point x_0 . Thus, the fundamental group of a path-connected space is a topological invariant.
3. If the fundamental group of a space is trivial, the space is called **simply-connected**. [42]

Definition 2.3.0.15 (Covering Space). A **covering** of a topological space X is a topological space \tilde{X} together with a map $p : \tilde{X} \rightarrow X$ satisfying the following condition: there exists an open cover $\{U_\alpha\}$ of X such that for every α , $p^{-1}(U_\alpha)$ is a disjoint union of open sets in \tilde{X} , each of which is mapped homeomorphically onto U_α by p . [42, p.56]

- Remark 2.3.0.16.** 1. If the topological space X has a base point x_0 , the covering $p : \tilde{X} \rightarrow X$ is written as $p : (\tilde{X}, \tilde{x}_0) \rightarrow (X, x_0)$ with $p(\tilde{x}_0) = x_0$. We say that \tilde{x}_0 is a lift of x_0 .
2. The covering $p : (\tilde{X}, \tilde{x}_0) \rightarrow (X, x_0)$ induces a map $p_* : \pi_1(\tilde{X}, \tilde{x}_0) \rightarrow \pi_1(X, x_0)$. Changing the base point changes the subgroup $p_*(\pi_1(\tilde{X}, \tilde{x}_0))$ to a conjugate subgroup in $\pi_1(X, x_0)$. The map p_* is always injective. [42, p.63]

Definition 2.3.0.17. A **lift** of a map $f : Y \rightarrow X$ is a map $\tilde{f} : Y \rightarrow \tilde{X}$ such that $p \circ \tilde{f} = f$. [42, p.60]

Proposition 2.3.0.18 (Homotopy Lifting Theorem). Given a covering space $p : \tilde{X} \rightarrow X$, a homotopy $f_t : Y \rightarrow X$ and a map $\tilde{f}_0 : Y \rightarrow \tilde{X}$ lifting f_0 , there exists a unique homotopy $\tilde{f}_t : Y \rightarrow \tilde{X}$ of \tilde{f}_0 that lifts f_t . [42, p.60]

Remark 2.3.0.19. For paths, we get the **path lifting property**: let $p : \tilde{X} \rightarrow X$ be a covering and $f : I \rightarrow X$ a path with starting point $f(0) = x_0$. For each lift \tilde{x}_0 of x_0 there is a unique path $\tilde{f} : I \rightarrow \tilde{X}$ lifting f and starting at \tilde{x}_0 . [42, p.60]

Proposition 2.3.0.20 (Unique Lifting Property). Let us assume a covering $p : \tilde{X} \rightarrow X$ and a map $f : Y \rightarrow X$. If two lifts $\tilde{f}_1, \tilde{f}_2 : Y \rightarrow \tilde{X}$ of f agree at one point of Y and Y is connected, then \tilde{f}_1 and \tilde{f}_2 agree on all of Y . [42, p.62]

Definition 2.3.0.21. A topological space X is called **semi-locally simply-connected** if every point $x \in X$ has an open neighbourhood $U \subset X$ such that every closed path $\sigma : I \rightarrow U$ is null-homotopic in X . [15][p.36]

Example 2.3.0.22. Let M be a connected manifold. Every $x \in M$ has a neighbourhood U which is homeomorphic to an open ball in \mathbb{R}^n and U is therefore simply-connected. In other

words, M is locally path-connected (A.0.0.10, p.186) and semi-locally simply-connected. Recall that a manifold is connected if and only if it is path-connected (A.0.0.10, p.186).

As it turns out, we already have all the necessary conditions to show that M has a simply-connected covering space.

Theorem 2.3.0.23. *Every path-connected, locally path-connected and semi-locally simply-connected space X has a simply-connected covering space \tilde{X} .*

Even though this is a basic result, we shall give an overview of its construction by virtue of its importance for this work. For details see [42, p.63–65] (English) or [15] (German). First, let us make some observations:

Remark 2.3.0.24. 1. Let (X, x_0) be a topological space with base point x_0 and a covering $p : (\tilde{X}, \tilde{x}_0) \rightarrow (X, x_0)$. Let us assume that \tilde{X} is simply-connected. By the definition of a covering (2.3.0.15), every point $x \in X$ has a neighbourhood $U \subset X$ which is homeomorphic to $\tilde{U} \subset \tilde{X}$. Hence, U is simply-connected. Take a loop $\gamma \in \pi_1(X)$ of x which lies entirely in U . Then there is a lift $\tilde{\gamma}$ in \tilde{U} which is null-homotopic in \tilde{X} , since $\pi_1(\tilde{X}) = 0$. Thus, $\gamma = \tilde{\gamma} \circ p$ is null-homotopic in X . The space X is therefore semi-locally simply-connected. Thus, any space which has a simply-connected covering space is semi-locally simply-connected.

2. An arbitrary point $\tilde{x} \in \tilde{X}$ in a simply-connected space is determined by a unique homotopy class of paths, starting at \tilde{x}_0 and ending at \tilde{x} . Since the homotopy classes of paths starting at $\tilde{x}_0 \in \tilde{X}$ are the same as the homotopy classes starting at $p(\tilde{x}_0) = x_0 \in X$ (homotopy lifting property: 2.3.0.19), we are able to describe \tilde{X} in terms of X .

3. If the fundamental group of X is not trivial, different homotopy classes of paths with starting point x_0 and end point $x \in X$ refer to different points in the covering space (see Figure 2.1). If two paths of X are homotopic, they refer to the same point in \tilde{X} .

In other words: Consider a path γ with starting point $x_0 \in X$ and end point $x \in X$. If γ lies entirely in a simply-connected domain of X , it produces a single point $[\gamma] = \tilde{x}$ in the covering \tilde{X} . Otherwise, there are non-homotopic paths with starting point x_0 and end point x , additionally producing the points $\tilde{x}', \tilde{x}'', \dots$, which are called homologous. The maps transporting $\tilde{x} \mapsto \tilde{x}', \tilde{x} \mapsto \tilde{x}'', \dots$ are isometries and form the holonomy group of X in \tilde{X} , which we will introduce in the next chapter (3.2.3.7). [55]

Construction Overview. We start with a path-connected, locally path-connected and semi-locally simply-connected topological space X with base point x_0 . Based on the previous remark, we construct a space by identifying points in \tilde{X} with the classes of paths in X starting at x_0 .

$$(\tilde{X}, [x_0]) := \{[\gamma] \mid \gamma \text{ is a path in } X \text{ starting at } x_0\}$$

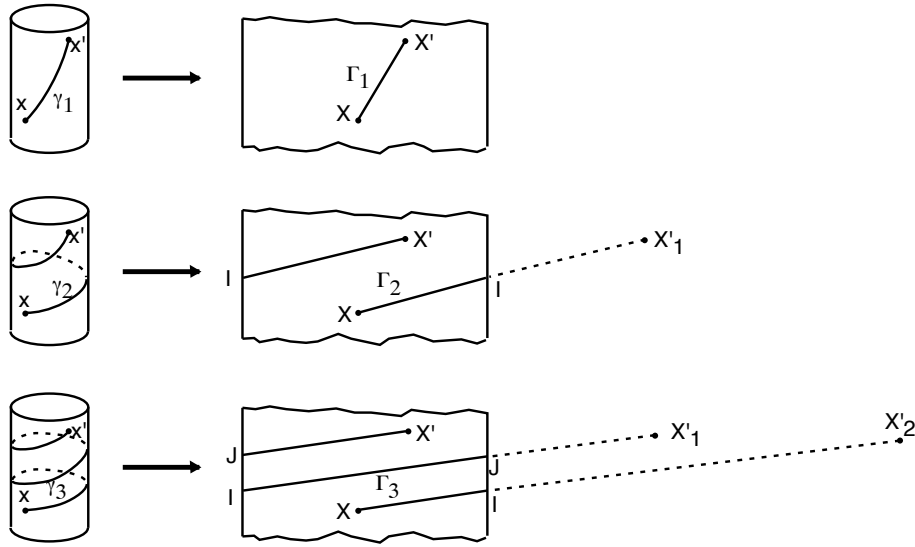


Figure 2.1.: Paths on a two-dimensional cylinder and their development in the universal cover. [99]

and the map $p : \tilde{X} \rightarrow X, [\gamma] \mapsto \gamma(1)$. Furthermore, we define

$$\mathcal{U} = \{U \subset X \mid U \text{ is path-connected and open; } \pi_1(U, x) \rightarrow \pi_1(X, x) \text{ is trivial}\}.$$

\mathcal{U} builds a basis of the topology of X (A.0.0.3, p.185) consisting of simply-connected open sets. Its existence is granted since X was assumed to be semi-locally simply-connected. To construct a basis of the topology of \tilde{X} , we take the sets

$$U_{[\gamma]} = \{[\gamma \circ v] \mid v \text{ is a path in } U \text{ with } v(0) = \gamma(1)\}.$$

If $[\gamma']$ is in $U_{[\gamma]}$, $U_{[\gamma]} = U_{[\gamma']}$. Such that, $p^{-1}(U) = \bigsqcup_{[\gamma(1) \in U} U_{[\gamma]}$ is a disjoint union of open sets. Therefore, \tilde{X} is a covering space with a covering map p .

It remains to be shown that \tilde{X} is simply-connected. Take a point $[\gamma] \in \tilde{X}$ and γ_t the path in X that equals γ on $[0, t]$ and is stationary on $[t, 1]$. The map $t \mapsto [\gamma_t]$ is a path in \tilde{X} starting at $[x_0]$ and ending at $[\gamma]$, it is the lift of γ . Since $[\gamma]$ was arbitrary, \tilde{X} is path-connected.

If $[\gamma(1)] = [x_0]$, the path is a loop. Because $\gamma = \gamma_1$ and $[\gamma] = [\gamma_1] = [x_0]$ (path lifting property 2.3.0.19), we conclude that γ is null-homotopic. Thus, the path $t \mapsto [\gamma_t]$ is null-homotopic, once again due to the path lifting property, and it follows that \tilde{X} is simply-connected. \square

Remark 2.3.0.25. 1. For a path-connected, locally path-connected and semi-locally simply-connected space M there exists $\forall H \subset \pi_1(X, x)$ a covering \tilde{X} with $p_*(\pi_1(\tilde{X}, \tilde{x})) =$

H . $H = \{1\}$ gives the simply-connected one. [111, p.39]

2. A simply-connected covering space is called **universal covering space (UCS)**. The UCS is a covering for any other covering space of X and is unique up to isomorphisms, which explains the name. [42, p.68]

2.3.1. The Group of Deck Transformations and its Action on M .

Definition 2.3.1.1. If $p : \tilde{X} \rightarrow X$ is a covering, the set

$$\{h \in \text{Hom}(\tilde{X}) \mid p \circ h = p\}$$

where $\text{Hom}(\tilde{X})$ denotes the set of all homeomorphisms $h : \tilde{X} \rightarrow \tilde{X}$ forms a group called the **group of deck transformations** (or covering group), denoted by $\Gamma(\tilde{X}/X)$. [111, p.38]

Remark 2.3.1.2 (Notation). If it is clear which covering is meant, we write Γ instead of $\Gamma(\tilde{X}/X)$.

Remark 2.3.1.3. Let G be a group of homeomorphisms acting on a connected, locally path-connected space \tilde{X} (2.2.1.1, p.40). The **quotient space** (or orbit space) \tilde{X}/G is the set of all orbits $G(\tilde{x})$, $\tilde{x} \in \tilde{X}$. The natural projection $p : \tilde{X} \rightarrow \tilde{X}/G$ is given by $p(\tilde{x}) = G(\tilde{x})$. The topology of the quotient space \tilde{X}/G is given by the quotient topology (A.0.0.6, p.185), the finest topology such that the projection p is continuous.

1. The action of G on \tilde{X} is called **discontinuous** if for each compact set $K \subset \tilde{X}$ the set $\{g \in G \mid gK \cap K \neq \emptyset\}$ is finite. [84]
2. The action of G on \tilde{X} is called **properly discontinuous** if every point $\tilde{x} \in \tilde{X}$ has a neighbourhood U such that the set $\{g \in G \mid g(\tilde{x}) \cap U \neq \emptyset\}$ is finite.
3. The action of G on \tilde{X} is called **free** if it is fixed-point-free. Thus, $\forall \tilde{x} \in \tilde{X}, \forall g \neq id \in G : g(\tilde{x}) \neq \tilde{x}$. That is, if every $g \in G$ moves any $\tilde{x} \in \tilde{X}$ [111, p.39]. Note that a free and transitive action is called sharply transitive. Compare with remark 2.2.2.3.

Example 2.3.1.4. Let M be a manifold and \tilde{M} its UCS. Take the group of deck transformations of the covering $p : \tilde{M} \rightarrow M$. The quotient space \tilde{M}/Γ consists of the orbits $\Gamma(\tilde{x})$, $\tilde{x} \in \tilde{M}$.

1. For a $\tilde{x} \in \tilde{M}$, the set $\{\Gamma(\tilde{x}) \mid p(\tilde{x}) = x\}$ is discrete (2.2.1.5, p.42) as a consequence of the quotient topology. Thus, the group of deck transformations of a covering acts properly discontinuously on the covering space since an admissible neighbourhood can always be found. As an immediate consequence, M is Hausdorff.
2. Since $p \circ h = p$, any deck transformation is a lift of the covering map p . The identity is also a lift of the covering p . Now, assume there is an $h \in \Gamma$ and $\tilde{x} \in \tilde{X}$ such that

$h(\tilde{x}) = \tilde{x}$. From the unique lifting theorem (2.3.0.20) follows $h = id$. Hence, Γ acts freely on \tilde{M} . [111]

Definition 2.3.1.5. Let Γ be a group acting on a topological space X .

1. If Γ acts properly discontinuously and the quotient space X/Γ is compact, we say that the action (or Γ itself) is **cocompact** (or **uniform**).
2. If X is a Riemannian manifold and Γ a group of isometries such that the quotient X/Γ has finite volume, Γ is said to be **cofinite**. [99, p.157]

Remark 2.3.1.6. Obviously, every cocompact group is cofinite. The converse is not true. Sometimes cofinite and cocompact groups are called **(uniform) lattices**. Caution is required, because of the more common definition of a lattice as a discrete subgroup of \mathbb{R}^n isomorphic to \mathbb{Z}^n . [99]

2.3.2. Manifolds as Quotient Spaces

Definition 2.3.2.1. A covering is called **normal** (regular) if $p_*(\pi_1(\tilde{X}, \tilde{x}))$ is a normal subgroup of $\pi_1(X, x)$ for some (hence any) $\tilde{x} \in \tilde{X}$. [111, p.35]

Proposition 2.3.2.2. Let $p : \tilde{X} \rightarrow X$ be a covering with Γ , the group of deck transformations. The covering is normal if and only if Γ acts transitively on every fibre $p^{-1}(x)$. If the covering space is simply-connected, the group of deck transformations is isomorphic to the fundamental group of X : $\Gamma(\tilde{X}/X) \approx \pi_1(X, x)$. [111, p.38;40]

Proof. $p_*(\pi_1(\tilde{X}, \tilde{x}))$ is a normal subgroup in $\pi_1(X, x)$ if and only if its normalizer is the whole set $\pi_1(X, x)$. Therefore, $p_*(\pi_1(\tilde{X}, \tilde{x}))$ is the union of conjugacy classes of $\pi_1(X, x)$. Conjugacy classes refer to changes of the base point in $p_*(\pi_1(\tilde{X}, \tilde{x}))$. Given a pair $\tilde{x}, \tilde{y} \in p^{-1}(x)$, there exists $[\sigma] \in \pi_1(X, x)$ such that: $[\sigma]p_*(\pi_1(\tilde{X}, \tilde{x}))[\sigma]^{-1} = p_*(\pi_1(\tilde{X}, \tilde{y}))$. The lift $\tilde{\sigma}$ of σ in \tilde{X} takes \tilde{x} to \tilde{y} . Since $\tilde{x}, \tilde{y} \in p^{-1}(x)$, the lift $\tilde{\sigma}$ is a deck transformation. In this case, $p^{-1}(x) = \{\gamma(\tilde{x}) \mid \gamma \in \Gamma, p(\tilde{x}) = x\}$ and Γ acts transitively on every fiber $p^{-1}(x)$.

We define a map as follows: let $x \in X$ be an arbitrary point. For $\tilde{x}, \tilde{y} \in p^{-1}(x)$ in \tilde{X} there is an $\gamma \in \Gamma$ such that $\gamma(\tilde{x}) = \tilde{y}$ (Γ acts transitively). Since they are both in $p^{-1}(x)$, $p \circ \gamma$ is a loop in X based on x . Since Γ acts freely, this map defines an isomorphism between Γ and $\pi_1(X, x)$ if \tilde{X} is simply-connected. Thus,

$$\pi_1(X, x) \approx \Gamma(\tilde{X}/X).$$

[111]

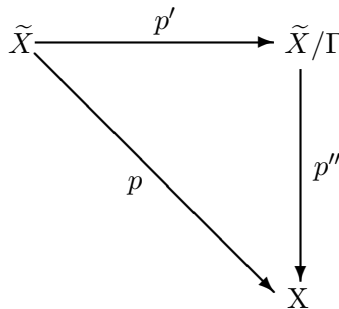
□

Theorem 2.3.2.3. Let Γ be a group of homeomorphisms acting freely and properly discontinuously on a connected, locally path-connected space \tilde{X} . Then the natural projection $p : \tilde{X} \rightarrow \tilde{X}/\Gamma$ is a normal covering, whose group of deck transformations is Γ . [111, p.39]

Proof. Let $\tilde{x} \in \tilde{X}$ be an arbitrary point. Since Γ acts properly discontinuously on \tilde{X} , there exists a neighbourhood U of \tilde{x} such that $\{\gamma \in \Gamma \mid \gamma(\bar{U}) \cap \bar{U}\} = \{id\}$. Now $\gamma(U) \simeq p(U), \forall \gamma \in \Gamma$ and $p^{-1}p(U) = \bigsqcup_{\gamma \in \Gamma} \gamma(U)$. As this is a disjoint union, p is a covering. Γ is a subset of the group of deck transformations. Since a fibre is given by $p^{-1}(p(U)) = \Gamma(U)$ and Γ acts transitively on each fibre and the group of deck transformations is free, Γ has to be the full group of deck transformations and the covering is normal. [111, p.40] \square

Corollary 2.3.2.4. *Let X be connected, locally path-connected and semi-locally simply-connected. Then $X \simeq \tilde{X}/\Gamma$, where Γ is a group of homeomorphisms acting freely and properly discontinuously on a simply-connected space \tilde{X} . [111, p.40]*

Outline of the Proof. As X is connected, locally path-connected and semi-locally simply-connected, we already know that there is a universal cover \tilde{X} with a covering map $p : \tilde{X} \rightarrow X$ and therefore a normal covering $(p_*(\pi_1(\tilde{M}, \tilde{x})) = \{1\})$. Let Γ be the group of deck transformations of $p : \tilde{X} \rightarrow X$. Take $p' : \tilde{X} \rightarrow \tilde{X}/\Gamma$, which is another normal covering. Furthermore, we can define a covering $p'' : \tilde{X}/\Gamma \rightarrow X$, by $p = p'' \circ p'$. For details see [111, p.40].



Since \tilde{X}/Γ and X have the same universal covering as well as the same group of deck transformations and p' is a normal covering, p'' has to be a homeomorphism and

$$X \simeq \tilde{X}/\Gamma.$$

\square

Remark 2.3.2.5. For a connected, simply-connected and locally path-connected space \tilde{X} , the coverings $p : \tilde{X} \rightarrow X$, with varying X , are just the projections $\tilde{X} \rightarrow \tilde{X}/\Gamma$, with varying Γ acting freely and properly discontinuously on \tilde{X} . [111, p.40]

Proposition 2.3.2.6. Let Γ be a group acting on a manifold \tilde{M} . The quotient space \tilde{M}/Γ is a manifold (which is Hausdorff) with a covering projection $\tilde{M} \rightarrow \tilde{M}/\Gamma$ if and only if Γ acts freely and properly discontinuously. [99, p.155]

2.4. Conclusion

$Isom(\mathcal{M}_3)$, the isometry group of the spatial part of the universe, is a Lie group acting on \mathcal{M}_3 . Thus, \mathcal{M}_3 is a $Isom(\mathcal{M}_3)$ -manifold and the isometry group determines the structure of \mathcal{M}_3 . Furthermore, \mathcal{M}_3 is homeomorphic to the quotient $\widetilde{\mathcal{M}}_3/\Gamma$, where $\widetilde{\mathcal{M}}_3$ is its universal covering space and Γ is the group of deck transformations of the universal covering, isomorphic to the fundamental group of \mathcal{M}_3 . Thus, all the possible candidates for the topology of the spatial universe can be constructed by a simply-connected manifold and a group acting freely and properly discontinuously on it.

3. Geometry of the Universe

In this chapter we shall give the manifold \mathcal{M}_3 a geometric structure. Let us now consider the geometry of the spatial universe.

What do we mean by the term “geometry”? Throughout history, three important approaches have been made, which we try to explain in a few words:

The first approach was exemplified by Euclid and discusses only objects such as points and lines. Geometric structure is determined by distances between points and angles between lines. The standard metric of the Euclidean plane is given by Pythagoras: $s^2 = x^2 + y^2$. The Euclidean approach is not restricted to Euclidean geometry but can also be applied to non-Euclidean geometry. In the nineteenth century the second approach was made, differential geometry developed and distances between points were first defined as the infimum of the lengths of the paths joining them. These lengths can be calculated with the help of integrals. The infimum is always taken along geodesics, which play the same role as lines in Euclidean space. The standard metric of Euclidean space now takes the form: $ds^2 = dx^2 + dy^2$. The third approach, which is the one we mainly focus on, was first formulated by Klein. Here, we have a space \mathbb{M} and a group \mathbb{G} acting on it. The group \mathbb{G} consists of isometries, which are distance-preserving maps. Geometry is interpreted as those properties which are left invariant by the action of \mathbb{G} . Every isometry of the Euclidean plane can be represented as the combination of a translation and a rotation, where any rotation stabilizes a point. From this, the Riemannian metric can be reconstructed. [92]

3.1. Geometric Structures on Manifolds

First, we shall generalize the definition of a \mathbb{G} -manifold by letting \mathbb{G} be a pseudogroup of an arbitrary Riemannian manifold which is connected and homogeneous.

Definition 3.1.0.7. *Let $(X, d_X), (Y, d_Y)$ be metric spaces (1.1.2.17, p.12) and $k > 0 \in \mathbb{R}$. A function $s : X \rightarrow Y$ such that*

$$d_Y(s(x), s(y)) = kd_X(x, y) \quad \forall x, y \in X,$$

*is called a **change of scale** with scale factor k . A bijective change of scale is called a **similarity**. [84, p.21]*

Remark 3.1.0.8. 1. An isometry is a similarity with scale factor $k = 1$. The group of isometries of a metric space X builds a subgroup of the **group of similarities** of X .

2. **Notation:** In the following, \mathbb{M} shall denote a connected and homogeneous Riemannian manifold.

Definition 3.1.0.9. Let G be the group of transformations of a Riemannian manifold M . A metric is called **G -invariant** if all transformations in G are motions (isometries) with respect to this metric. [103]

Remark 3.1.0.10 (Existence of a \mathbb{G} -Invariant Riemannian Metric). We need not assume \mathbb{M} to be a homogeneous Riemannian manifold. Less strong requirements would suffice: a homogeneous space can be written as the quotient \mathbb{G}/\mathbb{G}_x , $\mathbb{G}_x \subset \mathbb{G}$ (see section 2.2.2, p.42). This space is Hausdorff if and only if \mathbb{G}_x is compact (A.1.0.15, p.187). The stabilizer has to be compact for every point, but since the space is homogeneous it is sufficient to require this for an arbitrary point. Furthermore, there exists a unique structure of a smooth manifold on \mathbb{G}/\mathbb{G}_x . (See 2.2.2.7 and the subsequent Theorem 2.2.2.8 on page 43.) The action is effective (2.2.1.2, p.40), since the only element in \mathbb{G}/\mathbb{G}_x which acts trivially is in \mathbb{G}_x . In this case, there exists a \mathbb{G} -invariant Riemannian metric, turning \mathbb{M} into a Riemannian manifold. [96] A \mathbb{G} -invariant metric can be constructed as follows: as the homogeneous space is a manifold, one can choose an Euclidean metric in every tangent space $T_x\mathbb{M}$ which is invariant under the group \mathbb{G}_x . The metric can be moved by the transitive action of \mathbb{G} on \mathbb{M} at every point, which turns the metric to a \mathbb{G} -invariant Riemannian metric. [103]

If we strictly replace \mathbb{R}^n by \mathbb{M} in the Definition 2.1.0.2 of a \mathbb{G} -atlas, we obtain the definition of a (\mathbb{G}, \mathbb{M}) -atlas. Thus, we construct manifolds locally modeled on a connected and homogeneous Riemannian manifold.

Definition 3.1.0.11. Let \mathbb{M} be a connected and homogeneous Riemannian manifold and \mathbb{G} a pseudogroup of its similarities. A (\mathbb{G}, \mathbb{M}) -structure for a manifold M is a (\mathbb{G}, \mathbb{M}) -atlas for M . [84, p.344]

Definition 3.1.0.12. A (\mathbb{G}, \mathbb{M}) -manifold is a manifold M together with an (\mathbb{G}, \mathbb{M}) -structure for M . [84, p.344]

Remark 3.1.0.13. 1. We use Klein's idea of geometry proposed in the Erlangen program (Erlanger Programm) in 1872. The geometry of a space is given by a system of local coordinates modeled on a homogeneous Riemannian manifold $\mathbb{M} = \mathbb{G}/H$ with overlapping coordinate patches. Coordinate changes correspond to local restrictions of transformations of elements of \mathbb{G} . [36]

2. Just as every point of a \mathbb{G} -manifold has a neighbourhood homeomorphic to an open ball in \mathbb{R}^n , every point of a (\mathbb{G}, \mathbb{M}) -manifold has a neighbourhood homeomorphic to an open ball in \mathbb{M} .

3. We recall that if the action of \mathbb{G} on \mathbb{M} is effective, \mathbb{G} can be identified with the isometry group $Isom(\mathbb{M})$ (2.2.2.5, p.42).

Example 3.1.0.14 (Manifolds of Constant Curvature). 1. As we have seen in Chapter 2 (2.2.2.6, p. 42), $Isom(\mathbb{E}^n) \approx \mathbb{R}^n \times O_n(\mathbb{R})$. A $(Isom(\mathbb{E}^n), \mathbb{E}^n)$ -manifold M is called a **flat** or **Euclidean** manifold.

2. The group of all isometries of the sphere coincides with the group of all rotations in \mathbb{R}^{n+1} (2.2.2.6, p. 42). Thus, $Isom(\mathbb{S}^n) = SO_{n+1}(\mathbb{R})$. A $(Isom(\mathbb{S}^n), \mathbb{S}^n)$ -manifold is called a **spherical** or **elliptic** manifold.
3. If \mathbb{G} is the group of isometries of \mathbb{H}^n , a $(\mathbb{G}, \mathbb{H}^n)$ -manifold is called a **hyperbolic** manifold. [99, p.125–127]

In Chapter 2 (2.2.2.6, p.42), we have seen that the group of isometries of \mathbb{H}^n is isomorphic to the positive Lorentz group $PO_{n,1}(\mathbb{R})$. There are different representations of the space \mathbb{H}^n from which we shall now present the **upper half-space model**:

\mathbb{H}^n is isometric to the **upper half-space**

$$U^n := \{(x_1, \dots, x_n) \in \mathbb{E}^n : x_n > 0\}.$$

The isometry group of U^n is isomorphic to the **group of Möbius transformations** of the space $\hat{\mathbb{E}}^{n-1}$, which is the **one-point-compactification** of \mathbb{E}^{n-1} and therefore $\mathbb{E}^{n-1} \cup \infty$.

In order to give the definition of the group of Möbius transformations, we have to go into more detail:

A **reflection** ρ of \mathbb{E}^n in the hyperplane

$$P(a, t) := \{x \in \mathbb{E}^n : a \cdot x = t\}, \quad t \in \mathbb{R}, a \dots \text{unit vector in } \mathbb{E}^n$$

is defined by the formula $\rho(x) = x + 2(t - a \cdot x)a$ with $a \in \mathbb{R}$.

A Möbius transformation of $\hat{\mathbb{E}}^n$ is a finite composition of reflections of $\hat{\mathbb{E}}^n$ in spheres of $\hat{\mathbb{E}}^n$. That is in either Euclidean spheres

$$S(a, r) = \{x \in \mathbb{E}^n : |x - a| = r\}$$

centered at $a \in \mathbb{E}^n$ with radius $r \in \mathbb{R}$, or in an extended planes $\hat{P}(a, t) = P(a, t) \cup \infty$.

The group of Möbius transformations of $\hat{\mathbb{E}}^n$ is called the **Möbius group** of $\hat{\mathbb{E}}^n$, denoted by $M(\hat{\mathbb{E}}^n)$.

Thus, we have:

$$Isom(\mathbb{H}^n) \approx M(\hat{\mathbb{E}}^{n-1}). \quad [84]$$

Remark 3.1.0.15. For dimensions two and three, the group of Möbius transformation is isomorphic to the **projective special linear groups** $PSL_2(\mathbb{R})$ and $PSL_2(\mathbb{C})$ respectively. [99]

In dimension two, every simply-connected and homogeneous manifold is of constant curvature and therefore belongs to one of these three classes of manifolds. In section 3.3, we will see that in dimension three there are five more classes of simply-connected manifolds which are homogeneous but not of constant curvature.

Definition 3.1.0.16. A **metric (\mathbb{G}, \mathbb{M}) -manifold** is a connected (\mathbb{G}, \mathbb{M}) -manifold with $\mathbb{G} = \text{Isom}(\mathbb{M})$. [84, p.346]

Remark 3.1.0.17. For any metric (\mathbb{G}, \mathbb{M}) -manifold M there is an induced metric on M from \mathbb{M} . The topology of M is then the metric topology (A.0.0.2, p.185) determined by the induced metric.

Since \mathbb{M} is a homogeneous manifold, any (\mathbb{G}, \mathbb{M}) -manifold is locally homogeneous. Following Scott [92] we define:

Definition 3.1.0.18 (Geometric Structure). A metric on a manifold M is said to be **locally homogeneous** if, given x and y in M , there are neighbourhoods U of x and V of y and an isometry $(U, x) \rightarrow (V, y)$. A manifold admits a **geometric structure** if it admits a complete, locally homogeneous metric.

3.2. The Geometric Structure is Induced by the Universal Cover

3.2.1. Unrolling-Developing

3.2.1.1. Story of Tori – Unrolling the Two-Dimensional Torus in \mathbb{R}^4

In this section we closely follow Kriegl [54].

Topologically, an n -dimensional torus \mathbb{T}^n is defined as the product $\mathbb{S}_1 \times \mathbb{S}_1 \times \dots \times \mathbb{S}_1 = \mathbb{S}_1^n$ (2.2.0.8, item 5; p. 40). As a product of Lie groups, it is also a Lie group. For dimension two, we can construct $\mathbb{T}^2 = \mathbb{S}_1 \times \mathbb{S}_1$ as follows: take a rectangle and glue one pair of opposite sides together such that we get a cylinder. Glue together the cycles on the top and bottom of the cylinder, giving us a two-dimensional torus (short 2-torus) \mathbb{T}^2 (see Figure 3.1). Assuming the sides of the rectangle have the lengths a and b ($a, b \in \mathbb{R}$), the gluing maps are given by the two translations $\gamma_1, \gamma_2 : \mathbb{R}^2 \rightarrow \mathbb{R}^2$, $\gamma_1 : (x, y) \mapsto (x + b, y)$ and $\gamma_2 : (x, y) \mapsto (x, y + a)$. \mathbb{T}^2 can be written as the quotient space \mathbb{R}^2/Γ , where Γ consists of the two translations γ_1, γ_2 . Because we constructed the 2-torus by gluing opposite sides of a rectangle, it can be equipped with a homogeneous Euclidean metric and is therefore a two-dimensional, flat and homogeneous Riemannian manifold. Thus, its scalar curvature (1.1.3.12, p.18) vanishes at every point. We call the 2-torus with a flat metric a **flat 2-torus** \mathbb{T}_F^2 .

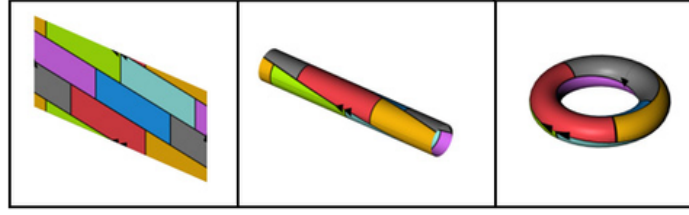


Figure 3.1.: Constructing a torus by gluing opposite facets of a rectangle. [118]

Given a manifold M , how to decide about its geometric structure? Usually, one thinks of a 2-torus to be embedded in \mathbb{R}^3 , where we fail to define a flat metric on it. We can describe the 2-torus embedded in \mathbb{R}^3 as the set of all points which have a constant distance $a \in \mathbb{R}$ to a circle with radius $A \in \mathbb{R}$, where $a < A$. Therefore, we can describe it by the equation:

$$z^2 + (\sqrt{x^2 + y^2} - A)^2 = a^2.$$

An elliptic Riemannian metric for the embedded torus in \mathbb{R}^3 is given in polar coordinates by:

$$ds^2 = (R + r \cos(\varphi))^2 (d\Psi^2 + r^2 d\varphi^2).$$

For this metric, the scalar curvature is given by

$$K = 6 \cdot \frac{\cos(\varphi)}{r(R + r \cos(\varphi))},$$

which does not vanish at every point. We call the so-constructed torus with an elliptic metric in \mathbb{R}^3 an **embedded 2-torus** \mathbb{T}_E^2 .

Let us now **unroll the embedded torus in \mathbb{R}^4** : we consider the inverse image of \mathbb{T}_E^2 with $a^2 = A^2 - 1$ under the stereographic projection $\mathbb{R}^4 \supset \mathbb{S}^3 \rightarrow \mathbb{R}^3$ based on the point $(0, 0, 0, 1) \in \mathbb{R}^4$.

The stereographic projection with respect to the point $p \in \mathbb{S}^3$ is given by the projection:

$$z \mapsto \frac{z - \langle z, p \rangle p}{1 - \langle z, p \rangle}.$$

Thus, we have $\langle z, p \rangle = y_2$ with $z = (x_1, y_1, x_2, y_2)$, where $\langle \cdot, \cdot \rangle$ denotes the standard scalar product. The projection is given by:

$$(x_1, y_1, x_2, y_2) \mapsto \frac{1}{1 - y_2} (x_1, y_1, x_2, 0).$$

The preimage of \mathbb{T}_E^2 is the set of all $(x_1, y_1, x_2, y_2) \in \mathbb{R}^4$ fulfilling the equations:

$$x_1^2 + y_1^2 + x_2^2 + y_2^2 = 1 \tag{3.1}$$

$$\left(\frac{x_2}{1-y_2}\right)^2 + \left(\frac{\sqrt{x_1^2 + y_1^2}}{1-y_2} - A\right)^2 = A^2 - 1, \quad (3.2)$$

where equation 3.1 guarantees that $(x_1, y_1, x_2, y_2) \in \mathbb{S}^4$ and equation 3.2 forces (x_1, y_1, x_2, y_2) to lie on the torus. Equation 3.2 can also be written as:

$$1 - (x_2^2 + y_2^2) = \frac{1}{A^2}.$$

Thus, \mathbb{T}_E^2 is described by the equations

$$x_1^2 + y_1^2 = \frac{1}{A^2} \quad \text{and} \quad x_2^2 + y_2^2 = \frac{a^2}{A^2}.$$

We conclude that the embedded torus can be described as the product of two circles in \mathbb{R}^4 and is, in fact, a 2-torus. One of its parametric representations is given by:

$$(\phi, \psi) \mapsto \left(\frac{1}{A} \cos(A\phi), \frac{1}{A} \sin(A\phi), \frac{a}{A} \cos\left(\frac{A\phi}{a}\right), \frac{a}{A} \sin\left(\frac{A\phi}{a}\right)\right).$$

This is an isometry $\mathbb{R}^2 \rightarrow \mathbb{R}^4$. One can prove that by calculating the Jacobi matrix, which has to build an orthonormal basis. To summarize, the 2-torus can be constructed in \mathbb{R}^4 by rolling a rectangle while preserving the Euclidean metric. One such metric is given by:

$$ds^2 = ad\Psi^2 + 2bd\Psi\varphi + cd\varphi^2 \quad \text{with } a, b, c \dots \text{ constant.}$$

For this metric, the scalar curvature vanishes at every point. The torus cannot be smoothly embedded in \mathbb{R}^3 with this metric.

Remark 3.2.1.1. The spatial part of the universe can be described by a three-dimensional manifold, which we do not want to view embedded in \mathbb{R}^n . As remarked in Chapter 1 (1.1.1.2(6), p.7), the manifold is a space on its own. The picture of an embedded manifold sometimes leads to false associations: on the one hand, we have seen that the 2-torus is locally isometric to its UCS, the Euclidean plane. On the other hand, we know that the flat 2-torus can be embedded in \mathbb{R}^3 and can be equipped with a spherical metric. Nevertheless, a two-dimensional being living on a 2-torus would experience a flat environment. In other words, we focus on the inner geometry of a manifold. The geometry is given by the intrinsic metric and does not depend on the surrounding space.

3.2.2. The Developing Map

In this section, we follow Thurston [99], if not cited otherwise.

The concept of unrolling a torus used in the previous section, enables us to decide about its geometric structure. In the following, we aim to develop a general concept of unrolling a manifold – **the developing map**:

Let M be a (\mathbb{G}, \mathbb{M}) -manifold with \mathbb{M} being a connected, real-analytic manifold and \mathbb{G} a group of real-analytic diffeomorphisms acting transitively on \mathbb{M} .

Remark 3.2.2.1. Since we have seen in Chapter 2 (2.1.0.5, p.38) that any Riemannian manifold has a real-analytic stiffening, this poses no restriction. Here, any element of \mathbb{G} is completely determined by its restriction to an open subset of \mathbb{M} .

Take an open covering \mathcal{U} with coordinate patches $U_i \in \mathcal{U}$ and coordinate charts $\varphi_i : U_i \rightarrow \mathbb{M}$ such that $\{(U_i, \varphi_i) \mid U_i \in \mathcal{U}\}$ is a (\mathbb{G}, \mathbb{M}) -atlas of M .

A transition map $\gamma_{ij} : \varphi_i \circ \varphi_j^{-1} : \varphi_j(U_i \cap U_j) \rightarrow \varphi_i(U_i \cap U_j)$ locally agrees with an element of \mathbb{G} by the definition of a (\mathbb{G}, \mathbb{M}) -manifold. Thus, we get a locally constant map, which we also call $\gamma_{ij} : U_i \cap U_j \rightarrow \mathbb{G}$.

Composing a coordinate chart $\varphi_j : U_j \rightarrow \mathbb{M}$ with a map $\gamma_{ij}(x)$ for $x \in U_i \cap U_j$ modifies φ_j in such a way that it agrees with φ_i on the whole intersection. (Observe that $U_i \cap U_j$ is connected.) Therefore, we get an extension of φ_j on $U_i \cup U_j \rightarrow \mathbb{M}$.

However, if we try to extend this concept further it breaks down. In order to generalize the coordinate charts, we have to pass to the universal cover:

Let $p : \widetilde{M} \rightarrow M$ be the universal covering and x_0 the base point of M . As we have seen in Chapter 2 (2.3.0.24, p.46), we can think of \widetilde{M} as the space of homotopy classes of paths in M starting at x_0 . Points $[\alpha]$ in \widetilde{M} are represented as the end points $\alpha(1) = p([\alpha])$.

Now we take a path α in M which starts at x_0 . We subdivide α at points

$$x_0 = \alpha(0), x_1 = \alpha(t_1), \dots, x_n = \alpha(1)$$

such that each subpath is contained entirely in a domain of a coordinate chart (U_i, φ_i) .

Going along α , we modify each chart φ_i such that it agrees on $U_{i-1} \cap U_i$ with φ_{i-1} . These adjusted charts form an “analytic continuation” of φ_0 along α (see Figure 3.2). The last adjusted chart is:

$$\varphi_0^{[\alpha]} = \gamma_{01}(x_1)\gamma_{12}(x_2)\dots\gamma_{n-1,n}(x_{n-1})\varphi_n.$$

Remark 3.2.2.2. If one takes a different choice of subpaths and/or another explicit element of the homotopy class of α , there are neighbourhoods U and V of $\alpha_1(1) = \alpha_2(1)$ such that $\varphi_0^{\alpha_1} = \varphi_0^{\alpha_2}$ on $U \cap V$. Therefore, the notation $\varphi_0^{[\alpha]}$ is well-defined.

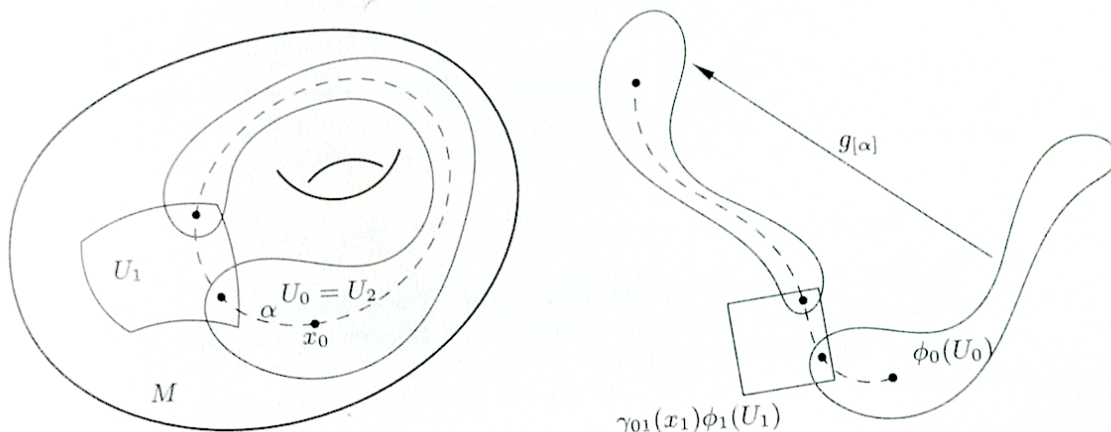


Figure 3.2.: Analytic continuation. Left: the path in M ; right: its germ in the UCS \widetilde{M} . [99]

Definition 3.2.2.3 (Developing Map). *For a fixed base point x_0 and an initial chart φ_0 , a **developing map** of a (\mathbb{G}, \mathbb{M}) -manifold M is a map $D : \widetilde{M} \rightarrow \mathbb{M}$ which agrees with the analytic continuation of φ_0 along each path in a neighbourhood of the path's end point $x = \sigma(1)$. In symbols:*

$$D = \varphi_0^\sigma \circ p$$

in a neighbourhood of $[\sigma] \in \widetilde{M}$. If we change the initial data (the base point and the initial chart), the developing map changes by composition in the range with an element of \mathbb{G} . [99, p.140]

Remark 3.2.2.4. 1. The covering map is a local homeomorphism from the topological space \widetilde{M} into the (\mathbb{G}, \mathbb{M}) -manifold M and is locally expressible as an element of \mathbb{G} . Thus, it is a local \mathbb{G} -isomorphism (2.1.0.4, p.38) and therefore preserves the \mathbb{G} -structure. [99, p.112] Consequently, it induces the (\mathbb{G}, \mathbb{M}) -structure on the UCS through the covering map. Using the notation above, the (\mathbb{G}, \mathbb{M}) -structure for \widetilde{M} can be constructed as follows:

Let $\{U_{ij}\} = p^{-1}(U_i)$ be a covering of \widetilde{M} , given by the preimages of the covering $\mathcal{U} = \{U_i\}$ of M under the covering map. We define the local homeomorphisms $p_{ij} = p|_{U_{ij}} : U_{ij} \rightarrow U_i$ to be the restrictions of the covering map on the sets U_{ij} . Furthermore, we define the maps $\varphi_{ij} : U_{ij} \rightarrow \mathbb{M}$, $\varphi_{ij} = \varphi_i \circ p_{ij}$, which map the U_{ij} homeomorphically to the open sets $\varphi(U_i) \subset \mathbb{M}$.

Suppose $U_{ij} \cap U_{kl}$ is not empty, then $U_i \cap U_k$ is not empty either and the transition map

$$\varphi_{ij} \circ \varphi_{kl}^{-1} : \varphi_{kl}(U_{ij} \cap U_{kl}) \rightarrow \varphi_{ij}(U_{ij} \cap U_{kl})$$

satisfies $\forall x \in \varphi_{kl}(U_{ij} \cap U_{kl})$:

$$\varphi_{ij} \circ \varphi_{kl}^{-1}(x) = (\varphi_i \circ p_{ij}) \circ (\varphi_k \circ p_{kl})^{-1}(x) = (\varphi_i \circ p_{ij} \circ p_{kl}^{-1} \circ \varphi_k^{-1})(x) = (\varphi_i \circ \varphi_k^{-1})(x).$$

Thus, the transition maps $\varphi_{ij} \circ \varphi_{kl}^{-1}$ are locally expressible as elements of \mathbb{G} and $\{U_{ij}, \varphi_{ij}\}$ build an (\mathbb{G}, \mathbb{M}) -atlas on \widetilde{M} [84]. This turns the covering map into a local diffeomorphism and the developing map into a local (\mathbb{G}, \mathbb{M}) -diffeomorphism between \widetilde{M} and \mathbb{M} . [99, p.140]

2. As the path above was arbitrarily chosen, we can consider a loop σ with base point x_0 . Here, the analytic continuation φ_0^σ along σ is comparable to the initial chart φ_0 , because the starting and end point are the same. Since all coordinate changes are in \mathbb{G} , the analytic continuation is of the form: $\varphi_0^\sigma = g_\sigma \circ \varphi_0$ for an $g \in \mathbb{G}$.

If we choose a lift $\tilde{x}_0 \in \widetilde{M}$ of x_0 , the path lifting property (2.3.0.19, p.45) states that σ lifts to a unique $\tilde{\sigma}$ in \widetilde{M} based on \tilde{x}_0 . Let \tilde{x}_1 be the end point of $\tilde{\sigma}$ in \widetilde{M} . Then there is a unique deck transformation $T_{\tilde{\sigma}}$ with $T_{\tilde{\sigma}}(\tilde{x}_0) = \tilde{x}_1$, which depends only on the homotopy class of σ in $\pi_1(M, x_0)$. Given another loop ν , based on x_0 in M , the lift $\tilde{\sigma} \circ \tilde{\nu}$ is given by $\tilde{\sigma} \circ (T_{\tilde{\sigma}} \circ \tilde{\nu})$ and the corresponding deck transformation is $T_{\tilde{\sigma}\tilde{\nu}} = T_{\tilde{\sigma}} \circ T_{\tilde{\nu}}$. [84]

If D is a developing map, $D \circ T_\sigma$ is another one and there exists a unique g_σ such that

$$D \circ T_\sigma = g_\sigma \circ D.$$

This defines a group homomorphism between the fundamental group $\pi_1(M)$ of M and the pseudogroup \mathbb{G} of \mathbb{M} . [99]

Definition 3.2.2.5 (Holonomy, Holonomy Group). *Let σ be an element of the fundamental group of M . The element $g_\sigma \in \mathbb{G}$ where the analytic continuation of σ can be written as $\varphi_0^\sigma = g_\sigma \circ \varphi_0$, is called the **holonomy of σ** . The homomorphism $H : \pi_1(M) \rightarrow \mathbb{G}$, $\sigma \mapsto g_\sigma$ is called **holonomy of \mathbb{M}** and its image the **holonomy group $H(\pi_1(M))$ of \mathbb{M}** .*

Remark 3.2.2.6. 1. For a Riemannian manifold in the sense of Definition 1.1.1.1 (p.6), we can give a more illustrative description of the holonomy group: consider a loop σ based on $x \in M$. We denote the parallel transport (1.1.3.5, p.16) of tangent vectors along σ by τ_σ . τ_σ is a linear transformation in the tangent space $T_x M$ and therefore an element of $O_n(\mathbb{R})$. The set $\Psi_x = \{\tau_\sigma\}$, with σ being a loop based on $x \in M$, forms a group. It is called the **linear holonomy group** at x and is a subgroup of $O_n(\mathbb{R})$. If the manifold is orientable, the holonomy group is contained in $SO_n(\mathbb{R})$. For two points $x, y \in M$, the corresponding holonomy groups Ψ_x, Ψ_y are isomorphic. The isomorphism is given as follows: let β be a curve from x to y , then $\Psi_x \rightarrow \Psi_y$, $\tau \mapsto \tau_\beta \tau \tau_\beta^{-1}$. Thus, we can speak of the **(linear) holonomy group Ψ** of M . If we only consider the null-homotopic loops, we get the **restricted holonomy group Ψ^0** . This

group is the connected component of the identity and therefore a compact subgroup. The holonomy of M can be defined alternatively as: $h : \pi_1(M, x) \rightarrow \Psi_x/\Psi_x^0$, $h([\sigma]) = \tau_\sigma$. The map h is injective and thus, $h(\pi_1(M, x)) = \Psi_x/\Psi_x^0$ (2.2.0.7, p.39). [53] [103]

2. The group Ψ/Ψ^0 is called the **holonomy representation** (B.1, p.189) of the fundamental group. [35]
3. The so-called “**developing pair**” (D, H) is unique up to composition/conjugation by elements in \mathbb{G} . The developing map D induces the (\mathbb{G}, \mathbb{M}) -structure on the universal covering space \widetilde{M} and the holonomy H determines the action of $\pi_1(M)$ on \widetilde{M} . Therefore, given a developing pair (D, H) , the geometric structure of M is determined. For a more detailed description of how exactly the structure can be reconstructed from the developing pair see [35].

3.2.3. Locally Homogeneous Riemannian Manifolds and The Condition of Completeness

Definition 3.2.3.1. A (\mathbb{G}, \mathbb{M}) -manifold M with UCS \widetilde{M} is called **complete** if the developing map $D : \widetilde{M} \rightarrow \mathbb{M}$ is a covering map. [99, p.142]

Remark 3.2.3.2. For a metric space we distinguish between geodesic completeness (1.2.7.3, p.32) and the definition of a complete metric space. The latter states that a metric space X is called complete if and only if every Cauchy sequence converges in X [84]. It is a direct consequence of the Rinow-Hopf theorem that a Riemannian manifold is geodesically complete if and only if it is a complete metric space. For example, any compact or homogeneous Riemannian manifold is complete. [83]

Remark 3.2.3.3 (Discussion of the Requirement of Completeness). 1. In Chapter 1, we restricted our considerations to complete space-times. Thus, \mathcal{M}_3 is also assumed to be complete throughout this work. We therefore assume M to be complete and locally homogeneous. In this case, M is locally isometric to a homogeneous manifold. The Definition 3.2.3.1 above is fulfilled and the two definitions of completeness are equivalent.

2. In general, a locally homogeneous manifold need not be locally isometric to a homogeneous manifold. The equivalence is true if we assume the manifold to be complete. [100]
3. \mathbb{M} is a homogeneous Riemannian manifold and is therefore a complete Riemannian manifold. Any (\mathbb{G}, \mathbb{M}) -manifold is locally homogeneous.
4. If we assume (\widetilde{M}, G) to be a homogeneous manifold and M to be a (\widetilde{M}, G) -manifold, M is complete since the covering map is a local isometry. [96]

Every covering space of the manifold M inherits a metric in a natural way such that the covering map is a local isometry. Therefore, if M admits a complete geometrical structure,

the UCS \widetilde{M} inherits a complete and locally homogeneous metric. Singer [93] showed that such a metric must be homogeneous and therefore the group of isometries acts transitively.

Let M be as specified above and, in addition, be simply-connected. Since any covering of a simply-connected space is a homeomorphism, we can identify M with \widetilde{M} . The identification is canonical up to composition with an element of G . Thus, M is a (G, M) -manifold where M can be identified with its UCS and G its group of isometries. [92, p.474]

In section 3.1 we argued that the geometric structure is given by a (G, M) -atlas, whereas in section 3.2, we argued that the geometric structure is induced on the covering space through the covering map. For complete manifolds modeled on a simply-connected manifold M these geometric structures coincide.

In this case, the complete (G, M) -manifold is entirely determined by its holonomy group.

Proposition 3.2.3.4. If G is a group of analytic diffeomorphisms of a simply-connected manifold M , any complete (G, M) -manifold may be reconstructed from its holonomy group Γ as the quotient space M/Γ . [99, p.143]

Remark 3.2.3.5. 1. Thus, given the holonomy group of such a manifold, we can decide about its geometrical structure up to stiffening or relaxation.

2. In the case of M not being simply-connected, we pass to the universal covering $p : \widetilde{M} \rightarrow M$. Due to the path lifting property (2.3.0.19) there is a unique diffeomorphism $\widetilde{g} : \widetilde{M} \rightarrow \widetilde{M}$ for every diffeomorphism $g \in G$ and every pair of points $\widetilde{x}_1, \widetilde{x}_2 \in \widetilde{M}$ satisfying $g(p(\widetilde{x}_1)) = p(\widetilde{x}_2)$ with:

- a) $\widetilde{g}(\widetilde{x}_1) = \widetilde{x}_2$ and
- b) $g(p(\widetilde{x})) = p(\widetilde{g}(x)), \forall \widetilde{x} \in \widetilde{M}$.

The diffeomorphism $\widetilde{g} \in \widetilde{G}$ is said to cover $g \in G$. \widetilde{G} is actually a group and the map $G \rightarrow \widetilde{G}$, which maps every element of $g \in G$ to a diffeomorphism $\widetilde{g} : \widetilde{M} \rightarrow \widetilde{M}$ covering g . This is a group epimorphism with the kernel being the group of deck transformations of the universal covering p [103]. \widetilde{G} is a Lie group and can be described in the form of an extension:

$$1 \rightarrow \Gamma \rightarrow \widetilde{G} \rightarrow G \rightarrow 1.$$

Thus, G is isomorphic to \widetilde{G}/Γ . There is a one-to-one correspondence between (G, M) -structures and $(\widetilde{G}, \widetilde{M})$ -structures, even though the holonomy group contains more information in respect to the $(\widetilde{G}, \widetilde{M})$ -structure. [99]

3. In the situation described above \widetilde{M} is called **model space** of M .

Corollary 3.2.3.6. Assuming G is a Lie group and M a manifold on which G acts transitively with compact stabilizers G_x , any discrete subgroup (2.2.1.5, p.42) of G acts properly discontinuously on M . [99, p.157]

We will prove Corollary 3.2.3.6 in Chapter 4 (4.3.0.4, p.81). In light of Chapter 2 (2.3.2.5, p.50), where we stated that the topology of manifolds with the same UCS depends only on the group of deck transformations, we can now state:

Corollary 3.2.3.7. *Let \mathbb{G} be a Lie group acting transitively, analytically and with compact stabilizer on a simply-connected manifold \mathbb{M} . If M is a closed differentiable manifold, (\mathbb{G}, \mathbb{M}) -structures on M (that is, (\mathbb{G}, \mathbb{M}) -stiffenings of M up to diffeomorphism) are in one-to-one correspondence with conjugacy classes of discrete subgroups of \mathbb{G} that are isomorphic to $\pi_1(M)$ and act freely on \mathbb{M} with quotient M . If M is not closed, we get the same correspondence if we look only at complete (\mathbb{G}, \mathbb{M}) -structures. [99, p.157]*

We end this section with the definition of a “geometry”:

Definition 3.2.3.8. *An **n-dimensional geometry** is a simply-connected, homogeneous, Riemannian n -manifold \mathbb{M} for which there is at least one compact manifold modeled on $(\mathbb{M}, S(\mathbb{M}))$ with $S(\mathbb{M})$ being the group of similarities of \mathbb{M} . [84, p.368]*

Definition 3.2.3.9. *A **geometric n-manifold** is a (\mathbb{G}, \mathbb{M}) -manifold with \mathbb{G} being a group of similarities of an n -dimensional geometry \mathbb{M} . [84, p.368]*

3.3. Three-Dimensional Model Geometries

We shall classify all different geometries a three-dimensional complete and locally homogeneous Riemannian manifold can have. In the previous section we argued that the geometric structure is induced by the universal covering space by the covering map. Therefore, geometric structures on three-dimensional simply-connected and homogeneous Riemannian manifolds are representative for each class of locally equivalent geometries we are interested in. This leads us to the question of which three-dimensional geometries there are?

First, we must define geometry classes. In order to achieve this, we have to specify which geometries we distinguish and which structures we view as being of the same class of geometric manifolds. For instance, if we have a (\mathbb{G}, \mathbb{M}) -manifold and a (\mathbb{H}, \mathbb{M}) -manifold where $\mathbb{H} \subset \mathbb{G}$, we want them to be in the same class of geometric manifolds. In other words, relaxations and stiffenings should belong to the same class of geometry. If we use distances to describe geometry, scaling a metric (with a constant factor) leads to different geometric structures in Riemannian geometry. We do not want to distinguish between metrics which are the same up to scaling. Let us also consider a Hopf fibration (see, for instance, [96]) of the sphere. A family of spherical metrics can be constructed by scaling the metrics in one component while keeping the metric in the orthogonal component constant. We expand or contract circles while keeping the orthogonal component constant. These geometric structures should correspond to the same class of geometries. Based on these considerations we define:

Definition 3.3.0.10. Two n -dimensional geometries \mathbb{M} and \mathbb{N} are said to be **equivalent** if there is a diffeomorphism $\phi : \mathbb{M} \rightarrow \mathbb{N}$ such that ϕ induces an isomorphism $\phi_* : \text{Isom}(\mathbb{M}) \rightarrow \text{Isom}(\mathbb{N})$ defined by

$$\phi_*(g) = \phi g \phi^{-1}. \text{ [84, p.368]}$$

This definition of equivalent geometries is in correspondence with the equivalence of space-time models defined in 1.2.1.3 (p.21). Now, we can define representatives for each class of geometry up to equivalence:

Definition 3.3.0.11 (Model Geometry). A **model geometry** (\mathbb{G}, \mathbb{M}) is a manifold \mathbb{M} combined with a Lie group \mathbb{G} of diffeomorphisms of \mathbb{M} such that:

1. \mathbb{M} is connected and simply-connected;
2. \mathbb{G} acts transitively on \mathbb{M} with compact stabilizers;
3. \mathbb{G} is not contained in any larger group of diffeomorphisms of \mathbb{M} with compact stabilizers; and
4. there exists at least one compact manifold modeled on (\mathbb{G}, \mathbb{M}) . [99, p.180]

Remark 3.3.0.12. 1. Condition (3) ensures that enlarging the group \mathbb{G} does not decrease the set of manifolds with such a structure. Condition (4) eliminates all geometries which are not serving as models for any compact manifold. Condition (2) ensures that the manifold is complete. According to (3), \mathbb{G} is chosen to be maximal. It follows that the metric is \mathbb{G} -invariant, as we have already seen, in the last section. [99]

2. In section 3.1.0.14, we introduced three different manifolds of constant curvature. All three of them are model geometries. They are homogeneous and isotropic. Isotropy, as opposed to the condition of homogeneity, is not a necessary precondition.

Definition 3.3.0.13. A manifold M is said to **admit a geometry** modeled on some model geometry (\mathbb{M}, \mathbb{G}) if $\exists \Gamma < \mathbb{G} : \mathbb{M}/\Gamma \cong M$ and $\mathbb{M} \rightarrow \mathbb{M}/\Gamma$ is a covering map.

In order to characterize all three-dimensional model geometries, we need a short introduction to bundles:

3.3.1. Bundles

Definition 3.3.1.1 (Fiber Bundle). Let E, B and X be smooth manifolds and $\pi : E \rightarrow B$ be a smooth map. The triple (π, E, B) is a **fiber bundle** with **fiber** X , **basis** B and **total space** E if:

- (a) π is surjective,

(b) there exists an open covering $(U_i)_{i \in I}$ of B and diffeomorphisms

$$h_i : \pi^{-1}(U_i) \rightarrow U_i \times X$$

such that $h_i(\pi^{-1}(x)) = \{x\} \times X$ for all $x \in U_i$ (local trivialization of the bundle). [96, p.31]

Remark 3.3.1.2. 1. In this situation we say that the space E **fibers over** B with fiber X .

2. With the vocabulary of geometric (G, X) -manifolds, a fiber bundle can be formulated in the following way: let G be a pseudogroup acting on a topological space X . A (G, X) -bundle is a fiber bundle with structure group G and fiber X . It is defined as a **bundle projection**: $\pi : E \rightarrow B$ and a **local trivialization**.

3. A **fibration** has a more general definition. It allows maps which only homotopically behave like fiber bundles. Thus, every fiber bundle is a fibration, but the converse is not true. [96]

4. A local trivialization is a tool to describe a bundle locally over a neighbourhood V as the product $V \times X$. Compare with the term of an atlas defined in 2.1.0.2 (p. 38) or 1.1.1.2 (p. 7). [99, p.158]

Example 3.3.1.3. 1. The product (G, X) -bundle over B is $B \times X$.

2. A covering space of a connected space defines a fiber bundle.

Definition 3.3.1.4 (Vector Bundle). Let E and B be two smooth manifolds and $\pi : E \rightarrow B$ a smooth map. We call (π, E, B) a **vector bundle** of rank n if:

1. E is a fiber bundle with base space B and fiber \mathbb{R}^n
2. such that for $i, j \in J$, the diffeomorphisms

$$h_i \circ h_j^{-1} : (U_i \cap U_j) \times \mathbb{R}^n \rightarrow (U_i \cap U_j) \times \mathbb{R}^n$$

are of the form

$$h_i \circ h_j^{-1}(x, v) = (x, g_{ij}(x) \cdot v),$$

where $g_{ij} : U_i \cap U_j \rightarrow GL_n(\mathbb{R})$ is smooth.

Each fiber is equipped with a linear space structure. The maps h_i are called local trivializations for the vector bundle. [96, p.16]

Remark 3.3.1.5. A vector bundle is a special case of a fiber bundle, which can be seen directly from the definitions. A (G, X) -bundle with a vector space X and $G = GL(X)$, which is the group of linear automorphisms of X , is a vector bundle.

Example 3.3.1.6. 1. The tangent bundle TM (1.1.2.5, p.9) with the projection $\pi : TM \rightarrow M, T_x M \mapsto x$ is a vector bundle. Here, the fiber at $x \in M$ is the tangent space $T_x M$.

2. If the fiber is the structure group itself and the action is by left translation, the bundle is called **principal bundle**. [99, p.161]

3.3.2. The Eight Model Geometries

Theorem 3.3.2.1 (Three-Dimensional Model Geometries). *There are eight three-dimensional model geometries (\mathbb{G}, \mathbb{M}) :*

(a) *If the point stabilizers are three-dimensional, \mathbb{M} is $\mathbb{S}^3, \mathbb{E}^3$ or \mathbb{H}^3 .*

(b) *If the point stabilizers are one-dimensional, \mathbb{M} fibers over one of the two-dimensional model geometries in a way that is invariant under \mathbb{G} . There is a \mathbb{G} -invariant metric on \mathbb{M} such that the connection orthogonal to the fibers has curvature 0 or 1.*

- *If the curvature is zero, \mathbb{M} is $\mathbb{S}^2 \times \mathbb{R}$ or $\mathbb{H}^2 \times \mathbb{R}$.*
- *If the curvature is 1, we have Nil geometry (which fibers over \mathbb{E}^2) or the geometry $\widetilde{SL}_2(\mathbb{R})$ (which fibers over \mathbb{H}^2).*

(c) *The only geometry with zero-dimensional stabilizers is Sol geometry, which fibers over the line.*

[99, p.181]

In the following, we shall explicate (for details see [99]) that there are only the eight three-dimensional model geometries. For a detailed description of the eight geometries see, for instance, the survey article by Scott [92].

\mathbb{M} is a homogenous space and therefore \mathbb{M} can be written as the quotient space \mathbb{G}/\mathbb{G}_x . Since \mathbb{M} is of dimension three, we have to find all Lie groups \mathbb{G} with $\mathbb{G}_x \subset \mathbb{G}$ a compact subgroup such that $\dim(\mathbb{G}) - \dim(\mathbb{G}_x) = 3$ (2.2.2.9, p.43). In other words, in order to get all the different three-dimensional geometries, we construct all the different Lie groups acting on three-dimensional manifolds. Since the parameter space is \mathbb{R}^3 with point stabilizer $O_3(\mathbb{R})$, the point stabilizer of any simply-connected three-dimensional manifold is a closed subgroup of $O_3(\mathbb{R})$.

Remark 3.3.2.2. Even though the space \mathbb{M} is simply-connected and therefore, by definition, the homogeneous space (\mathbb{G}, \mathbb{M}) (2.2.2.5, p.42), the Lie group \mathbb{G} need not even be connected. For this reason, we shall first consider the connected component \mathbb{G}' of the identity. The connected component \mathbb{G}' still acts transitively on \mathbb{M} and \mathbb{G}'_x is connected. \mathbb{G}_x is then of the same dimension as \mathbb{G}'_x .

The orthogonal group $O_n(\mathbb{R})$ consists of two connected components:

- **proper motions** $SO_n(\mathbb{R})$: these are the orthogonal transformations with determinant 1, preserving the orientation;
- **improper motions**: orthogonal transformations which reverse the orientation. [54]

We focus on the compact and connected Lie subgroups of $SO_3(\mathbb{R})$, namely $SO_3(\mathbb{R})$, $SO_2(\mathbb{R})$ and $SO_1(\mathbb{R})$.

Remark 3.3.2.3. The dimensions of the possible stabilizers (2.2.2.9 item (4), p.43) are $\dim(SO_3(\mathbb{R})) = 3$, $\dim(SO_2(\mathbb{R})) = 1$ and $\dim(SO_1(\mathbb{R})) = 0$. Which gives the possible dimensions of the Lie group G as six, four or three.

Let us start by giving \mathbb{M} a G -invariant Riemannian metric.

3.3.2.1. If the Stabilizer is the Full Group $SO_3(\mathbb{R})$

For details see [103], for instance.

Definition 3.3.2.4. A connected homogenous space is said to be a **space of constant curvature** if its isotropy group is the group of orthogonal transformations (at each point) with respect to some Euclidean metric.

Remark 3.3.2.5. We will give another definition of Riemannian manifolds of constant curvature in Chapter 4 and we will show that this is equivalent to Definition 3.3.2.4.

Theorem 3.3.2.6 (The Classification Theorem). Any simply-connected space of constant curvature is isomorphic to one of the spaces $\mathbb{E}^n, \mathbb{S}^n, \mathbb{H}^n$. [103]

Here, the stabilizer \mathbb{G}_x acts transitively on the tangent space $T_x\mathbb{M}$, which is equivalent to the property of isotropy. We shall now describe manifolds with such a geometry in dimension three. Recall Definition 3.3.0.13.

- $\mathbb{M} = \mathbb{S}^3 \quad \mathbb{G} = SO_4(\mathbb{R})$

Any three-dimensional manifold with spherical geometry can be described as the quotient $M = \mathbb{S}^3/\Gamma$. Since \mathbb{S}^3 is compact, we only need to consider finite subgroups of \mathbb{G} acting freely on \mathbb{S}^3 by rotation [103]. The resulting manifolds are all oriented. These spherical spaces are completely classified in any dimension. In dimension three, they can be grouped in five classes, which we shall describe in detail in Chapter 4. Examples are lens spaces and the Poincaré dodecahedral space, which are described in detail in section 5.4 (p. 112).

- $\mathbb{M} = \mathbb{E}^3 \quad \mathbb{G} = \mathbb{R}^3 \times SO_3(\mathbb{R})$

The three-dimensional manifolds with Euclidean geometry are the quotients $M = \mathbb{E}^3/\Gamma$, where Γ is a torsion-free and discrete subgroup $\Gamma \subset Isom(\mathbb{E}^3)$. Bieberbach

showed that there is only a finite number of compact Euclidean manifolds (up to diffeomorphism) in any dimension corresponding to the so-called Bieberbach groups and that each of them can be finitely covered by a torus of the same dimension [111]. We will see in the next chapter that for dimension three there are only ten non-homeomorphic and therefore non-diffeomorphic, compact Euclidean three-dimensional manifolds from which six are orientable. Apart from those, there are four non-compact Euclidean three-dimensional manifolds, as we will see.

- $\mathbb{M} = \mathbb{H}^3 \quad G = PSL_2(\mathbb{C})$

In dimension three, the group of orientation-preserving isometries of the hyperbolic space can be identified with the group of Möbius transformation of $\mathbb{C} \cup \infty$, $PSL_2(\mathbb{C})$. A Möbius transformation of $\mathbb{C} \cup \infty$ is a function of the form

$$z \mapsto \frac{az + b}{cz + d}, \quad a, b, c, d \in \mathbb{C} \text{ with } ad - bc \neq 0.$$

[92]

In the same way, a manifold with a hyperbolic structure can be written as the quotient $M = \mathbb{H}^3/\Gamma$, $\Gamma \subset \mathbb{G}$ acting freely and properly discontinuously on \mathbb{H}^3 . These manifolds are much more difficult to handle. There is no classification of these manifolds (not even for dimension two). It is known that for dimension three there are countably infinitely many. Examples are Löbell space and Weeks space, which we shall describe in detail in 5.5 (p. 115).

3.3.2.2. If the Stabilizer is $SO_2(\mathbb{R})$

In this section we introduce the term “foliation of a manifold”. For a short introduction see the article “Introduction to foliations and Lie grupoids” by I.Moerdijk and by J.Mrčun, in which they describe a foliation of a manifold as follows:

Intuitively speaking, a foliation of a manifold M is a decomposition of M into immersed submanifolds, the leaves of the foliation. These leaves are required to be of the same dimension, and fit together nicely. [46, p.4]

Definition 3.3.2.7 (Foliation). Write \mathbb{R}^n as the product $\mathbb{R}^{n-k} \times \mathbb{R}^k$ and let \mathbb{G} be the pseudogroup generated by diffeomorphisms φ between open subsets of \mathbb{R}^n which take horizontal factors to horizontal factors, that is, diffeomorphisms of the form

$$\varphi(x, y) = (\varphi_1(x, y), \varphi_2(y)),$$

with $x \in \mathbb{R}^{n-k}$, $y \in \mathbb{R}^k$. A \mathbb{G} -structure is called **foliation of codimension k or dimension $(n - k)$** . [99]

- Remark 3.3.2.8.** 1. The pseudogroup \mathbb{G} consists of all diffeomorphisms between open subsets of \mathbb{R}^n such that at every point the Jacobian is a $(n \times n)$ -matrix with the lower left $(n - k) \times k$ block being 0. [99, p.114]
2. An atlas \mathcal{A} consisting of charts with the property described in Definition 3.3.2.7 is called a **foliation atlas** and the charts are called **foliation charts**. A (smooth) **foliated manifold** is a pair (M, \mathcal{F}) with a smooth manifold M and a foliation atlas \mathcal{F} . A smooth map between foliated manifolds $f : (M, \mathcal{F}) \rightarrow (M', \mathcal{F}')$ must preserve the foliation. [46, p.6]
3. The preimage of $\mathbb{R}^{n-k} \times \{y\}$ under the charts is called a **paque**. They piece together globally and give the **leaves of the foliation**. Thus, $x, y \in \widetilde{M}$ are in the same leaf if and only if there is a sequence of foliation charts and a sequence of points p_1, \dots, p_q , $q \in \mathbb{N}$ such that p_i and p_{i-1} lie on the same plaque in U_i for all $1 \leq i \leq q$. The leaves are of dimension $(n - k)$. The quotient space M/\mathcal{F} is called the **space of leaves** and is of dimension k . It is constructed by identifying points if they lie on the same leaf. [46]
4. There is a description of foliations in terms of group actions. Let G act on M . If the map $M \rightarrow \mathbb{R}$, $x \mapsto \dim(G_x)$ is a constant function of x , the action of G on M defines a foliation of M . The connected components of the orbits of the action are the leaves of the foliation of M . [46, p.16]
5. For a bundle with an n -dimensional base space B and an m -dimensional fiber X , the total space E is an $(n + m)$ -dimensional manifold. In this situation, the manifold E has a foliation the leaves of which are the fibers. These are equipped with the (G, X) -structure. In this situation, we speak of a tangentially (G, X) -foliation (3.3.2.7, p.69). [99]

For details of the proof see [99] or [36].

Let \mathbb{G}' act on a manifold \mathbb{M} with point stabilizers $\mathbb{G}'_x = SO_2(\mathbb{R})$. Now, the dimension of the stabilizer is one. For any $x \in \mathbb{M}$, the stabilizer \mathbb{G}'_x acts on the tangent space $T_x\mathbb{M}$, giving us a map

$$\mathbb{G}'_x \times T_x\mathbb{M} \rightarrow T_x\mathbb{M}.$$

Definition 3.3.2.9. Let G be a Lie group. A vector field $X \in \chi(G)$ is called **left-invariant** if and only if $g \star X = Tg \circ X \circ g^{-1} = X \forall g \in G$. [16]

Since we can assume the action to be effective (2.2.1.2, p.40), there is at least one non-zero, \mathbb{G}' -invariant vector field $\mathbb{M} \rightarrow T\mathbb{M}$. The direction of the vector field gives the axis of rotation of the elements in \mathbb{G}'_x .

Proposition 3.3.2.10. Let $X \in \chi(M)$ be a vector field. For any $x \in M$ there exists a maximal interval I_x containing 0 and a unique smooth curve $c_x : I_x \rightarrow M$ such that $c_x(0) = x$ and for $t \in I_x : c'_x(t) = X(c_x(t))$. [96, p.22]

Definition 3.3.2.11 (Integral Curve). *The curve $c_x : I_x \rightarrow M$ with $c_x(0) = x$ described in 3.3.2.10 is called **integral curve** of the vector field $X \in \chi(M)$. It is the local solution of the differential equation $c' = X \circ c$, induced by the vector field X . [54, p.140]*

The integral curve of the vector field gives a one-dimensional foliation \mathcal{F} of \mathbb{M} (3.3.2.7, p.69), thus, a foliation with one-dimensional leaves [50]. The space of leaves \mathbb{M}/\mathcal{F} is two-dimensional. As \mathbb{M} is simply-connected, the leaves and the space of leaves are also simply-connected. Thus, the space of leaves \mathbb{M}/\mathcal{F} is one of the spaces \mathbb{E}^2 , \mathbb{S}^2 or \mathbb{H}^2 . The leaves are either \mathbb{R} or \mathbb{S}^1 . Here, the foliation defines a fiber bundle (3.3.1.1, p.65) over the base space \mathbb{M}/\mathcal{F} with the leaves being the fibers. See remark 3.3.2.8 item (4). Thus, we find that the manifold M is a principal fiber bundle (3.3.1.6, p.67) over \mathbb{M}/\mathcal{F} with fiber \mathbb{R} respectively \mathbb{S}^1 .

The type of manifold depends on the connection (1.1.3.3, item (2) p.16) on the bundle. For a more detailed introduction to connections see, for instance, [23]. Since the group of isometries of the manifold acts transitively, the connection is of constant curvature. Determining the orientation of the fibre and the base space, the curvature of the connection can be assumed to be nonnegative. Without loss of generality there remain the two cases 0 and 1 after scaling the metric.

1. First, let us assume that the curvature of the connection vanishes. Here, the group of isometries of the manifold is the product of the isometry group of the base space and the isometry group of the fiber: $Isom(M) = Isom(B) \times Isom(F)$. There are three cases:

- $\mathbb{M} = \mathbb{S}^2 \times \mathbb{R}, \quad \mathbb{G} = SO_3(\mathbb{R}) \times \mathbb{R}$

Since \mathbb{S}^1 is covered by \mathbb{R} , $\mathbb{S}^2 \times \mathbb{S}^1$ is one of these manifolds and does not have to be considered further. In addition, there are seven manifolds which occur as quotients, four of which are compact.

A metric is given by: $d\sigma^2 = dr^2 + \sin^2 r d\varphi + dz^2$.

- $\mathbb{M} = \mathbb{H}^2 \times \mathbb{R} \quad \mathbb{G} = PSL_2(\mathbb{R}) \times \mathbb{R}$

The Möbius group $PSL_2(\mathbb{R})$ is isomorphic to the orientation-preserving subgroup of the group of isometries of \mathbb{H}^2 . The \mathbb{M}/Γ include, for example, the product of any compact hyperbolic surface (the g-torus or the g-handle) by \mathbb{S}^1 or \mathbb{R} .

A metric is given by: $d\sigma^2 = dr^2 + \sinh^2 r d\varphi + dz^2$.

- In the third case we consider the base space \mathbb{E}^2 while still assuming the connection is flat. This results in the above-mentioned three-dimensional Euclidean space \mathbb{E}^3 .

2. If the connection is of positive curvature, we get:

- $\mathbb{M} = \widetilde{SL}_2(\mathbb{R})$

Here, the base space is \mathbb{H}^2 and the unit tangent bundle is $PSL_2(\mathbb{R})$. The resulting space is the three-dimensional Lie group of real matrices with determinant 1, $SL_2(\mathbb{R})$. The universal cover of this group is $\widetilde{SL}_2(\mathbb{R})$, giving the geometry.

A metric is given by: $d\sigma^2 = dx^2 + \cosh^2 x dy^2 + (dz + \sinh x dy)^2$.

- **Nil geometry:** The base space is the Euclidean plane and the fibers are lines. In order to ensure that we do not get Euclidean geometry we take the Lie group consisting of all Heisenberg matrices for \mathbb{G} :

$$\mathbf{M} = \begin{pmatrix} 1 & x & z \\ 0 & 1 & y \\ 0 & 0 & 1 \end{pmatrix} \quad x, y, z \in \mathbb{R}$$

\mathbb{G} is called the **Heisenberg group**. A metric is given by:

$$d\sigma^2 = dx^2 + dy^2 + (dz + xdy)^2. \text{ [92]}$$

There is one last case to consider: the one of base space being \mathbb{S}^2 . Without going into detail, this does not lead to a model geometry and we can therefore neglect this case.

3.3.2.3. If the Stabilizer is Trivial:

Since \mathbb{M} is a homogeneous space with a trivial isotropy group and any homogeneous space can be written as \mathbb{G}/\mathbb{G}_x [16], \mathbb{M} can be identified by its Lie group. Therefore, in examining \mathbb{M} we have to find a three-dimensional Lie group which is not the Lie group of any other of the seven geometries considered so far.

The Lie group is then simply-connected and therefore uniquely determined by its Lie algebra \mathfrak{g} . The correspondence of Lie algebras and Lie groups is presented in Appendix B (p.189), where the main theorem is described in B.2.3.2 on page 192. There are two ways of viewing the Lie algebra: as the tangent space at the identity or the set of all left-invariant vector fields. We denote the corresponding matrix to the map $L : \mathfrak{g} \times \mathfrak{g} \rightarrow \mathfrak{g}$, $(V, W) \mapsto [V, W]$ with $[\cdot, \cdot]$ being the Lie bracket, as L .

In order to ensure a compact quotient, we require the existence of a discrete, co-compact (2.3.1.5, p.49) subgroup. In addition, to ensure a compact manifold admitting the (\mathbb{G}, \mathbb{M}) -structure, we assume that every left-invariant vector field preserves volume. Thus, \mathbb{G} has to be unimodular and therefore $\det(L) = 1$ (5.4, p.40). For further details see [99, p.187]. Without going into detail here, we know that from unimodality follows that L is symmetric.

One theorem in linear algebra states that every Euclidean vector space V with a self-adjoint map $\varphi : V \rightarrow V$ (that is the corresponding matrix is symmetric) has a basis consisting of

eigenvectors of φ . Take a basis of \mathfrak{g} consisting of eigenvectors $\{e_1, e_2, e_3\}$ with:

$$[e_i, e_j] = \lambda_k e_k, \quad i \neq j \neq k,$$

where λ_k is the eigenvalue to the eigenvector e_k . L is diagonal with entries $l_{ii} = \lambda_i$ in respect to this basis.

After appropriate scaling, we can assume the eigenvalues to be $\lambda_i \in \{1, -1, 0\}$. There are six possible choices up to choosing an orientation and permutation of the basis elements:

1. $\lambda_1 = \lambda_2 = \lambda_3 = \pm 1 \Rightarrow \mathbb{S}^3$
2. $\lambda_1 = \lambda_2 = \lambda_3 = 0 \Rightarrow \mathbb{E}^3$
3. $\lambda_1 = \lambda_2 = 0, \lambda_3 = \pm 1 \Rightarrow$ Heisenberg group \Rightarrow Nil geometry
4. $\lambda_1 = \lambda_2 = \pm 1, \lambda_3 = \mp 1 \Rightarrow \mathbb{S}^2 \times \mathbb{R}$
5. $\lambda_1 = 1, \lambda_2 = -1, \lambda_3 = 0 \Rightarrow$ in this case, e_1 and e_2 act on \mathbb{E}^2 by translation and e_3 by rotation. There is no corresponding geometry.
6. $\lambda_1 = \lambda_2 = \pm 1, \lambda_3 = 0 \Rightarrow$ Sol geometry

Thus, we finally have found a new geometry: **Sol geometry**. The Lie group can be described by the set of matrices:

$$\text{Sol} = \left\{ \begin{pmatrix} e^z & 0 & x \\ 0 & e^{-z} & y \\ 0 & 0 & 1 \end{pmatrix} \mid x, y, z \in \mathbb{R} \right\}.$$

We shall now describe this geometry (see [92] or [99] for further details):

The geometry is the semidirect product $\mathbb{R}^2 \rtimes \mathbb{R}$, with the action of \mathbb{R} on \mathbb{R}^2 given by:

$$(x, y) \mapsto (e^t x, e^{-t} y).$$

Identifying Sol with \mathbb{R}^3 and \mathbb{R}^2 with the xy -plane corresponds to the multiplication:

$$(x, y, z) \cdot (x', y', z') = (x + e^{-z} x', y + e^z y', z + z').$$

A metric is given by: $d\sigma^2 = e^{2z} dx^2 + e^{-2z} dy^2 + dz^2$.

Remark 3.3.2.12. 1. Manifolds with a geometric structure modeled on either $\mathbb{E}^3, \mathbb{S}^3, \mathbb{S}^2 \times \mathbb{R}, \mathbb{H}^2 \times \mathbb{R}, \widetilde{SL}_2(\mathbb{R})$ or Nil are called **Seifert manifolds**.

2. The Lie groups of $\mathbb{E}^3, \mathbb{S}^3, \widetilde{SL}_2(\mathbb{R}),$ Nil geometry and Sol geometry are unimodular. Manifolds with such a geometric structure have been classified by Raymond and Vasquez [85]. [92]

3.3.2.4. Thurston's Geometrization Theorem

In the last section we argued for the correctness of the following theorem:

Theorem 3.3.2.13 (Thurston). *Any maximal, simply-connected, three-dimensional geometry which admits a compact quotient is equivalent to one of the geometries $(\mathbb{M}, \text{Isom}(\mathbb{M}))$, where \mathbb{M} is one of*

$$\mathbb{E}^3, \mathbb{S}^3, \mathbb{H}^3, \mathbb{S}^2 \times \mathbb{R}, \mathbb{H}^2 \times \mathbb{R}, \widetilde{SL_2(\mathbb{R})}, \text{Sol or Nil. [92, p.474]}$$

Theorem 3.3.2.14 (The Geometric Structure is Unique). *If M is a closed manifold admitting a geometric structure modeled on one of the eight geometries, the geometry involved is unique. [92]*

This uniqueness can be shown by considering the holonomy groups. In the next chapter we shall focus on the holonomy groups of three-dimensional manifolds.

In 1976, Thurston formulated his famous theorem stating that every connected and locally homogeneous three-dimensional manifold admits a canonical decomposition into pieces (prime manifolds) by cutting along surfaces of nonnegative Euler characteristic. Each of these pieces admits a geometric structure induced by one of the three-dimensional model geometries. [36]

This theorem was proved by Perelman in 2003. For more information see, for instance, [75].

Remark 3.3.2.15. The corresponding theorem in the spherical case was first formulated by Poincaré in 1900. Since then it has been known as **Poincaré's Theorem**, which states that if a closed three-dimensional manifold has a trivial fundamental group, it must be homeomorphic to the three-dimensional sphere [73]. It has also been proven by Perelman as a special case of Thurston's Geometrization Theorem.

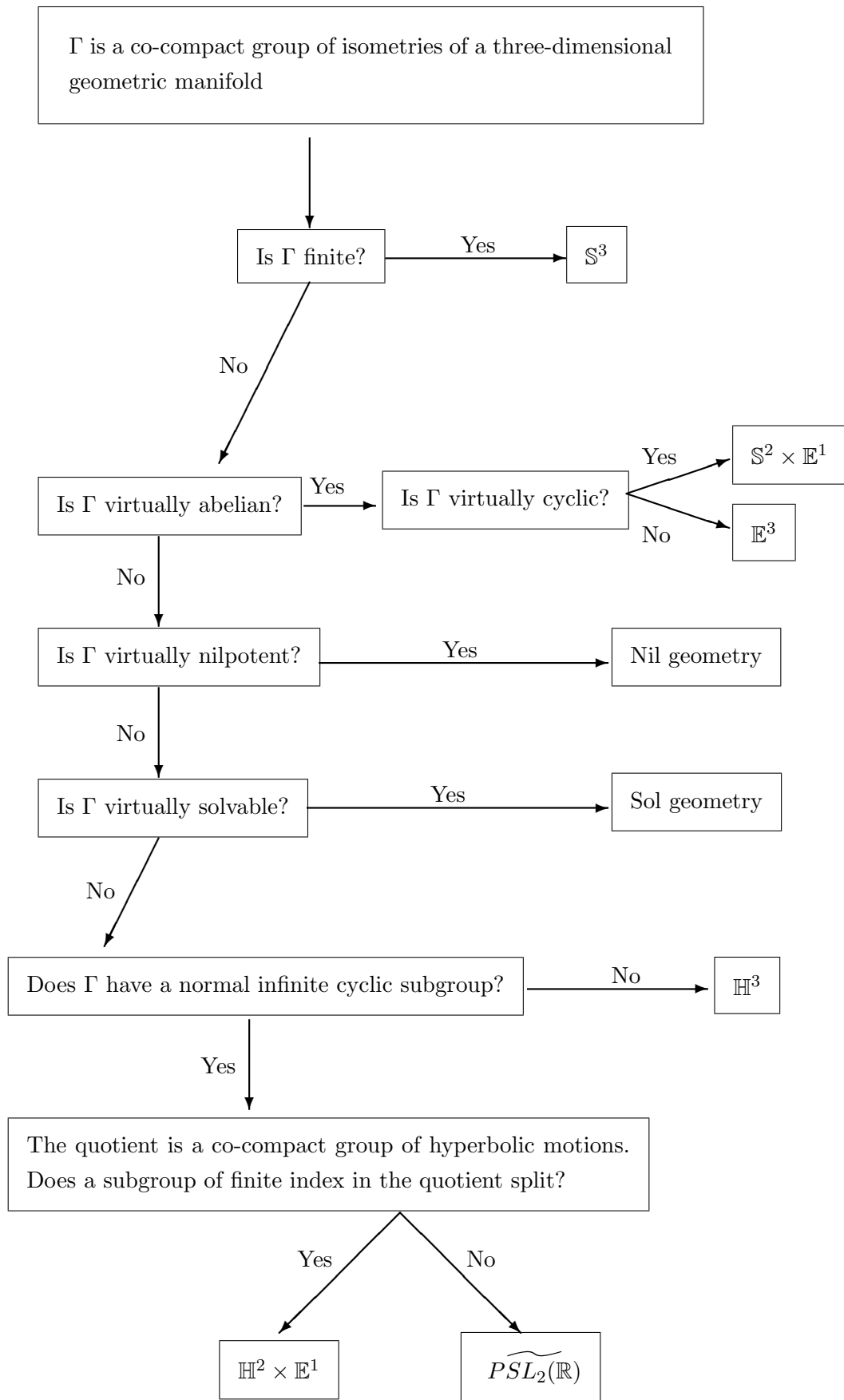
3.4. Conclusion

In Chapter 2 we argued that every connected manifold and therefore in particular \mathcal{M}_3 , can be written as $\mathcal{M}_3 \approx \widetilde{\mathcal{M}}_3/\Gamma$, where Γ is isomorphic to the fundamental group of \mathcal{M}_3 and $\widetilde{\mathcal{M}}_3$ is its universal covering space. Assuming completeness enabled us to conclude that \mathcal{M}_3 admits a geometric structure modeled on a three-dimensional geometry \mathbb{M} , which can be identified with the UCS $\widetilde{\mathcal{M}}_3$. Thurston's Geometrization Theorem states that \mathbb{M} is one of the above-described eight geometries. Thus, the spatial part of the universe \mathcal{M}_3 admits a geometric structure modeled on one of the eight three-dimensional model geometries.

Theorems 3.2.3.4 and 3.2.3.7 state that the holonomy group Γ of a complete (\mathbb{G}, \mathbb{M}) -manifold M determines the geometric structure on M . If we assume M to be compact, we can determine the geometric structure of the manifold by the algebraic properties of Γ :

Theorem 3.4.0.16. *A discrete co-compact (2.3.1.5, p.49) group Γ of automorphisms of any one of the eight basic three-dimensional geometries is not isomorphic to a co-compact group of one of the others. [99]*

The following flowchart gives an overview [99, p.281]. We note that a group is virtually cyclic/solvable/nilpotent/abelian etc. if it contains a subgroup of finite index with this property.



4. Locally Isotropic Riemannian Manifolds

Now, we require \mathcal{M}_3 to be additionally locally isotropic. In Chapter 3 we presented the classification of the geometric structures on three-dimensional, locally homogeneous and complete Riemannian manifolds. Now, we shall restrict ourselves to locally isotropic manifolds and focus on the classification of the $\Gamma \subset Isom(\widetilde{M})$, acting freely and properly discontinuously on \widetilde{M} , in order to derive a classification of all manifolds with the same geometry. First, we shall present the classification theorems for the general case of an n -dimensional manifold before we restrict our considerations to the three-dimensional case.

Remark 4.0.0.17 (Notation). \widetilde{M} denotes the UCS of a locally isotropic, locally homogeneous, complete and connected Riemannian manifold M . Recall that since we assume M to be complete, \widetilde{M} can be identified with the geometry \mathbb{M} of M .

We start with the definition of a locally isotropic Riemannian manifold:

Definition 4.0.0.18. A Riemannian manifold M is called **(locally) isotropic** if given $x \in M$ and nonzero tangent vectors X and Y at x with $\|X\|^2 = \|Y\|^2$, there is a (local) isometry (at x) which fixes x and sends X to Y . [111]

Remark 4.0.0.19. 1. Therefore, an n -dimensional manifold M is said to be (globally) isotropic (under the action of G) if the stabilizer of every point acts transitively on the tangent space at that point [99]. Thus, if $G_x = O_n(\mathbb{R})$, $\forall x \in M$. Therefore, isotropic manifolds are spaces of constant curvature in the sense of 3.3.2.4 (p.68).

2. Sitting at a point of a locally isotropic manifold, the metric looks the same in every direction.

If M is a locally isotropic manifold, its universal covering space \widetilde{M} is also locally isotropic. Since we assume the UCS \widetilde{M} to be homogeneous (3.2.3.3, p.62), the metric looks the same at every point and in every direction [111]. We conclude, that the UCS \widetilde{M} is (globally) isotropic and M is locally isometric to a simply-connected and globally isotropic Riemannian manifold. Therefore, M is also a space of constant curvature.

Remark 4.0.0.20. Conversely, (locally) isotropic manifolds are (locally) homogeneous (see, for instance, [111, p.289,p.377]). In the case of global isotropy, we can conclude that these manifolds are complete.

Until now, we have two concepts of curvature: scalar curvature used in General Theory of Relativity, defined in 1.1.3.12 (p.18), and constant curvature in the sense of 3.3.2.4 (p.68) used with an algebraic approach to geometry.

Now, we shall introduce a third concept of curvature which is usually used with manifolds in Riemannian geometry: “sectional curvature”. For a short introduction to the term “sectional curvature of a manifold” see Appendix C (p.195). The correspondence between these three concepts of curvature will be explained immediately.

Definition 4.0.0.21. *A Riemannian manifold M is said to be of constant curvature C , if at each point its **sectional curvature** along any plane section equals C .*

Theorem 4.0.0.22. *Let (M, g) be an n -dimensional Riemannian manifold of constant sectional curvature C . Then the scalar curvature K is given by*

$$K = n \cdot (n - 1) \cdot C. [40]$$

Remark 4.0.0.23 (Notation:). In the following, a manifold of constant curvature shall denote a manifold of constant sectional curvature. A manifold of constant sectional curvature is of constant scalar curvature. The converse is not true.

Remark 4.0.0.24. Since the curvature of a manifold is completely determined by its metric, an isotropic Riemannian manifold is at least local of constant curvature. Schur’s Theorem states that if the sectional curvature C of a Riemannian manifold with $\dim(M) \geq 3$ M is constant at each point, then C is actually constant on M . [38]

Remark 4.0.0.25. Now, we shall show that the connected and homogeneous spaces with stabilizer $G_x = O_n(\mathbb{R})$ are exactly the complete Riemannian manifolds of constant sectional curvature.

First, let M be simply-connected, satisfying Definition 3.3.2.4, then the isotropy group is $O_n(\mathbb{R})$. Since $O_n(\mathbb{R})$ is a compact group, there exists a G -invariant Riemannian metric (3.1.0.10, p.54), where, as usual, G denotes the group of isometries of M . Since $O_n(\mathbb{R})$ is irreducible, the metric is unique (see [103, p.10]). $O_n(\mathbb{R})$ acts transitively on every tangent space with respect to this metric, thus, (M, g) is locally isotropic and therefore a Riemannian manifold of constant curvature. Because M is homogeneous, (M, g) is complete.

Conversely, the isotropy group of any simply-connected, complete Riemannian manifold of constant curvature acts transitively on the tangent space of a point, thus, is the entire $O_n(\mathbb{R})$.

If M is not simply-connected but a connected homogeneous space satisfying the maximum mobility axiom, we consider its UCS \tilde{M} . The lifts of all diffeomorphisms on M build a Lie group \tilde{G} consisting of diffeomorphisms on \tilde{M} (see 3.2.3.5(2), p.63). The action of \tilde{G} on \tilde{M} is smooth and transitive and the covering map φ is also smooth. Thus, (\tilde{M}, \tilde{G}) satisfies the maximum mobility axiom. As \tilde{M} is homogeneous and simply-connected it is a

Riemannian manifold of constant curvature. Thus, M is a Riemannian manifold of constant curvature. [103, p.11]

Example 4.0.0.26. In Chapter 2 (Example 2.2.2.6, p.42) we presented three homogeneous spaces with stabilizer $O_n(\mathbb{R})$: \mathbb{H}^n , \mathbb{E}^n and \mathbb{S}^n , which are therefore of constant curvature. In Chapter 1 (1.1.3.13, p.19) we mentioned that these three spaces are of constant scalar curvature.

Since $M = \widetilde{M}/\Gamma$, M is locally isometric to a Riemannian manifold of constant curvature. Hence, M is of constant curvature. To classify all locally isotropic M , we start with classifying all simply-connected and homogeneous Riemannian manifolds \widetilde{M} of constant curvature.

4.1. Simply-Connected Spaces of Constant Curvature

4.1.1. The Classification Theorem

We already know three types of spaces of constant curvature : $\mathbb{S}^n, \mathbb{H}^n, \mathbb{E}^n$. As it turns out, this already constitutes a complete list of simply-connected and homogeneous manifolds of constant curvature, which is stated by the ‘‘Classification Theorem’’ below.

Definition 4.1.1.1. *Two homogenous spaces $(M_1, G_1), (M_2, G_2)$ are called **isomorphic** if there exists a diffeomorphism $f : M_1 \rightarrow M_2$ and an isomorphism of Lie groups $\varphi : G_1 \rightarrow G_2$ such that*

$$f(gx) = \varphi(g)f(x) \quad \forall x \in M_1, g \in G_1 \quad (4.1)$$

Theorem 4.1.1.2 (The Classification Theorem). *Any simply-connected space of constant curvature is isomorphic to one of the spaces $\mathbb{E}^n, \mathbb{S}^n, \mathbb{H}^n$. [103]*

We assume \widetilde{M} to be a simply-connected space of constant curvature. As a homogenous space (\widetilde{M}, G) is uniquely determined by the pair (G, G_x) (up to isomorphism), where G_x is the stabilizer of a point $x \in \widetilde{M}$ (see Chapter 2, section 2.2.2, p.42). Let \mathfrak{g} and \mathfrak{k} be the Lie algebras of the Lie groups G and G_x . If G is simply-connected, the Lie algebra \mathfrak{g} would uniquely determine G (B.2.3.2, p.192), but the group of motions G does not even have to be connected. Therefore, we have to prove the correspondence for our use:

Lemma 4.1.1.3. *Any simply-connected, homogeneous space (\widetilde{M}, G) of constant curvature is uniquely defined by the pair $(\mathfrak{g}, \mathfrak{k})$ (up to isomorphism).*

Proof. Since \widetilde{M} is connected, the connected component G_+ acts transitively on \widetilde{M} . The isotropy group of the homogenous space (\widetilde{M}, G_+) at the point $x \in \widetilde{M}$ is the connected component of the group $G_x = O_n(\mathbb{R})$, hence, $SO_n(\mathbb{R})$. This group is compact as a closed subgroup of a compact group. The homogenous space (\widetilde{M}, G_+) is uniquely determined by the pair $(\mathfrak{g}, \mathfrak{so}(n))$, see B.2.4 (p. 194).

We need to show that the group of transformations G can be reconstructed from G_+ . The action of $SO_n(\mathbb{R}) \subset O_n(\mathbb{R})$ in \mathbb{R}^n is irreducible, just as the action of $O_n(\mathbb{R})$. Thus, there is a unique G_+ -invariant Riemannian metric on \widetilde{M} . As every G -invariant metric is G_+ -invariant, they coincide. Therefore, the group G can be reconstructed from G_+ as the group of all motions with respect to this metric. [103, p.16] \square

It remains to be shown that for any dimension $n \in \mathbb{N}$ there are only three non-isomorphic pairs of $(\mathfrak{g}, \mathfrak{k})$ which correspond to simply-connected and homogeneous Riemannian manifolds of constant curvature. We already know $\mathfrak{k} = \mathfrak{so}_n(\mathbb{R})$. The remaining part of the proof can be read, for instance, in [103]. In terms of Riemannian geometry the proof can be read in [96].

4.2. Space Forms

We drop the assumption of simply-connectedness. In this section we shall closely follow [111], if not cited otherwise.

Definition 4.2.0.4. *A space form is a complete Riemannian manifold M of constant sectional curvature.*

Theorem 4.2.0.5 (W. Killing, H. Hopf). *Let M be a Riemannian manifold of dimension $n \geq 2$ and C be a real number. Then M is complete, connected and of constant curvature C if and only if it is isometric to a quotient*

$$\mathbb{S}^n/\Gamma \quad \text{with} \quad \Gamma \subset O_{n+1}(\mathbb{R}), \quad \text{if } C > 0$$

$$\mathbb{E}^n/\Gamma \quad \text{with} \quad \Gamma \subset E(n), \quad \text{if } C = 0$$

$$\mathbb{H}^n/\Gamma \quad \text{with} \quad \Gamma \subset PO_{n,1}(\mathbb{R}), \quad \text{if } C < 0$$

where Γ acts freely and properly discontinuously. [111]

In other words, every space form is locally isometric to one of $\mathbb{E}^n, \mathbb{H}^n, \mathbb{S}^n$. They are called **Euclidean** ($C = 0$), **hyperbolic** ($C < 0$) or **spherical** ($C > 0$) **space forms**.

Remark 4.2.0.6. In 1890, Clifford and Klein formulated the problem of describing compact and connected Riemannian manifolds of constant curvature. Killing then showed in 1891 that these manifolds are always of the form described in 4.2.0.5 and called them Clifford-Klein space forms. Today, space forms denote the connected, complete Riemannian manifolds of constant curvature. The problem of classifying them is referred to as the Clifford-Klein space form problem. The Euclidean space form problem for the compact case was reduced by Bieberbach to the classification of torsion-free crystallographic groups (which we shall go into in more detail in the following). It is solved for the dimensions 2, 3 and 4. The solution of the non-compact case was made by Wolf ([111]), who also published the complete solution

of the spherical space form problem for the first time in 1972. The hyperbolic case turns out to be much more difficult. So far, there is no known classification, not even for dimension $n = 2$. [103, p.157]

4.2.1. Homogeneous Space Forms

Definition 4.2.1.1. Let X be a metric space and f an isometry in X . The **displacement function** of f is given by:

$$\delta_f(x) : x \mapsto d(x, f(x)),$$

where d is the distance given by the metric on X . The isometry f is called **Clifford translation** if its displacement function is constant.

Theorem 4.2.1.2. Let Γ be a discontinuous group of isometries acting freely on a complete simply-connected Riemannian manifold \widetilde{M} of constant curvature. Then \widetilde{M}/Γ is a homogeneous Riemannian manifold if and only if Γ is a group of Clifford translations. [111, p.230]

Example 4.2.1.3. The two-dimensional torus described in 3.2.1.1 (p.56) is a two-dimensional homogeneous space form, because Euclidean translations are Clifford translations.

Before we consider the three classes of Riemannian manifolds of constant curvature in detail, let us state some theorems which will turn out to be helpful later.

4.3. Preparations

The universal covering space \widetilde{M} is a homogeneous space and therefore of the form G/H , where H is a closed subgroup of the Hausdorff topological group G (A.1.0.11, p.186). Γ acts on G/H by left translation: $\gamma : gH \rightarrow (\gamma g)H$. The space $(G/H)/\Gamma$ is therefore the double coset space $\Gamma \backslash G/H$. The topology is given by the quotient topology (A.0.0.6, p.185) of G/H , which again has the quotient topology of G . [111]

We recall the definitions given in 2.3.1.3 and 2.3.1.5 (p.48) and 49.

Lemma 4.3.0.4. Let Γ and H be subgroups of G with H compact and G locally compact.

1. The following conditions are equivalent:

- (i) Γ is discontinuous at some point of G/H ,
- (ii) Γ is discontinuous on G/H ,
- (iii) Γ is properly discontinuous on G/H ,
- (iv) Γ is discrete in G ,

2. If Γ is closed in G , then $(G/H)/\Gamma$ is compact if and only if Γ is cocompact in G .

[111]

Proof. 1. (i) \Rightarrow (iv) : Suppose Γ is discontinuous at $x \in G/H$. Then there exists a neighbourhood UH of x in G/H such that $U \subset G$ is open and the set $\{\gamma \in \Gamma | \gamma(x) \in UH\}$ is finite. Since x is in G/H , there is an $g \in G$ such that $x = gH$. Then Ug^{-1} is an open neighbourhood of 1 in G which has finite intersection with Γ . Since G is Hausdorff, there exists a neighbourhood such that the intersection is only the identity, which is just the definition of Γ is discrete in G .

(iv) \Rightarrow (iii) : Let Γ be a discrete subgroup of G . Since G is locally compact we can choose a neighbourhood U of 1 with compact closure. Let $x = gH$ be an arbitrary point in G/H . Then the set $V_g = gUHU^{-1}g^{-1}$ has compact closure too. Observe that gU is a neighbourhood of $g \in G$ and gUH a neighbourhood of $x \in G/H$. Now consider the set $\Gamma_1 = \{\gamma \in \Gamma | \gamma(x) \text{ intersects } gUH\}$. γ is in Γ_1 if and only if γ is in V_g . Since Γ is discrete in G , $H \cap V_g$ is finite and Γ acts properly discontinuously on G/H .

(iii) \Rightarrow (ii) \Rightarrow (i) follows trivially.

2. Now Γ is closed in G . Consider the continuous and open map $G/\Gamma \rightarrow \Gamma \backslash G/H$, $g^{-1}\Gamma \mapsto \Gamma gH$. The inverse image of a point γgH is compact, since H is compact. Hence G/Γ is compact if and only if $\Gamma \backslash G/H$ is compact. □

4.3.1. Finite Subgroups of $SO_3(\mathbb{R})$

The finite subgroups of $SO_3(\mathbb{R})$ will play an essential role in the following. On the one hand, the classification of three-dimensional Euclidean space forms can be done by classifying all the finite subgroups of $SO_3(\mathbb{R})$. On the other hand, we ought to see, that there is an one-to-one correspondence between finite subgroups of $SO_4(\mathbb{R})$ and those of $SO_3(\mathbb{R})$. Since the fundamental group of a spherical three-dimensional space form is finite as a discrete subgroup of the compact group $SO_4(\mathbb{R})$, this correspondence turns out to be essential for the classification of three-dimensional spherical space forms.

We consider symmetry groups of regular polyhedron:

Definition 4.3.1.1. Let X be a set, G the set of transformations on X and $Y \subset X$. We define the **symmetry group** $\mathcal{S}(Y)$ of Y as

$$\mathcal{S}(Y) := \{T \in G | T(Y) = Y\}.$$

Remark 4.3.1.2. The identity is in $\mathcal{S}(Y)$ and for two symmetries $S_1, S_2 \in \mathcal{S}(Y)$ the inverse S_1^{-1} and the composition $S_1 \circ S_2$ are in $\mathcal{S}(Y)$ too, thus, $\mathcal{S}(Y)$ is a subgroup of G . [112]

A regular polyhedron Δ_m can be inscribed in a two-dimensional sphere such that the vertices of the polyhedron intersect with the sphere. A symmetry can therefore be described as an element of $O_3(\mathbb{R})$ which stabilizes the set of vertices of Δ_m . In that way, the symmetry

group $\mathcal{S}(\Delta_m)$ can be defined as a finite subgroup of $O_3(\mathbb{R})$. $\mathcal{S}(\Delta_m)$ contains as a subgroup $\mathcal{S}^+(\Delta_m) = \mathcal{S}(\Delta_m) \cap SO_3(\mathbb{R})$, called the rotation group of Δ_m . As the rotation group of Δ_m determines the symmetry group of Δ_m , we do not distinguish between these two groups. [112]

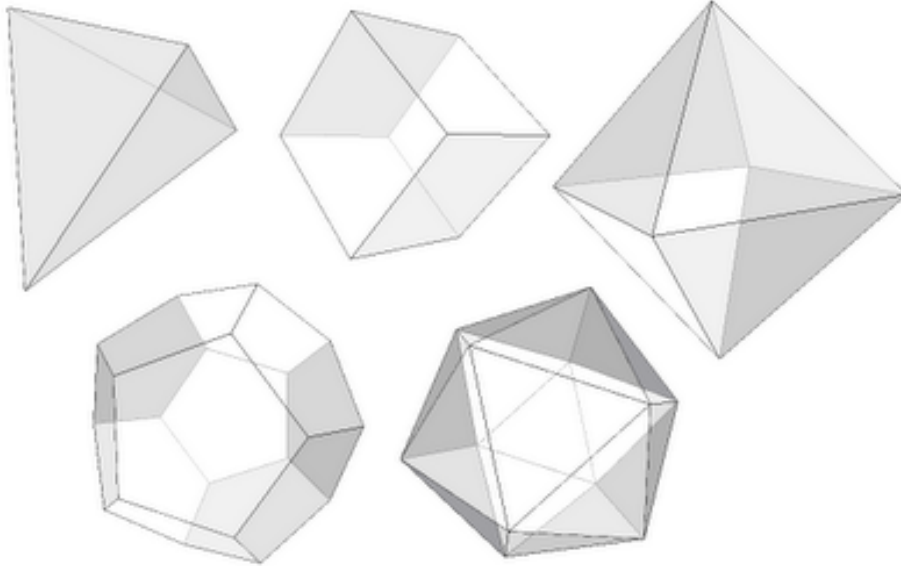


Figure 4.1.: The regular polyhedra: from top left to bottom right: tetrahedron, hexahedron, octahedron, dodecahedron, icosahedron [119]

The Dihedral Group \mathcal{D}_m : is the symmetry group of the regular m -gon. It is the semidirect product of

- *the cyclic group:* A rotation A by the angle $2\pi/m$ generates the cyclic group \mathcal{C}_m of order m .
- and \mathcal{C}_2 : The group generated by the reflection B about a symmetry axis. B takes the m -gon into itself and is therefore an element of the symmetry group of the m -gon. Obviously it is of order two.

\mathcal{D}_m is a subgroup of $SO_3(\mathbb{R})$ of order $|\mathcal{D}_m| = 2m$.

Cyclic Group \mathcal{C}_m : The cyclic group is a subgroup of $SO_3(\mathbb{R})$, since it is a subgroup of \mathcal{D}_m .

Next, we consider the symmetry groups of the five **regular polyhedra** (see Figure 4.1), which are called the **polyhedral groups**.

Tetrahedral Group \mathcal{T} : The tetrahedron Δ_4 consists of four vertices, six edges and four faces (equilateral triangles). Its symmetry group is called tetrahedral group. \mathcal{T} is generated by the three rotations A , P and Q . The relations among these generators are given by:

$$A^3 = P^2 = Q^2 = 1, \quad PQ = QP, \quad APA^{-1} = Q, \quad AQA^{-1} = PQ.$$

It is a group of order $|\mathcal{T}| = 12$ and isomorphic to the alternating group \mathcal{A}_4 .

Octahedral Group \mathcal{O} : The octahedral group is the symmetry group of the regular octahedron Δ_8 , which consists of six vertices, twelve edges and eight faces. The octahedral group is a finite subgroup of $SO_3(\mathbb{R})$ of order $|\mathcal{O}| = 24$ and isomorphic to the permutation group \mathcal{S}_4 . The tetrahedral group is a normal subgroup of \mathcal{O} of finite index $|\mathcal{O} : \mathcal{T}| = 2$. \mathcal{O} is generated by the four rotations A, P, Q and R. The relations among these generators are given by:

$$A^3 = P^2 = Q^2 = R^2 = 1, \quad PQ = QP, \quad APA^{-1} = Q$$

$$AQA^{-1} = PQ, \quad RAR^{-1} = A^{-1}, \quad RPR^{-1} = QP, \quad RQR^{-1} = Q^{-1}.$$

Icosahedral Group \mathcal{I} : The icosahedral group is the symmetry group of the regular icosahedron Δ_{20} (12 vertices, 30 edges and 20 faces). \mathcal{I} is generated by the three rotations A, B, C. The relations among these generators are given by:

$$A^3 = B^2 = C^5 = ABC = 1.$$

The order of the group is $|\mathcal{I}| = 60$ and it is isomorphic to the alternating group \mathcal{A}_5 .

There are two regular polyhedra (hexahedron \square_6 and octahedron Δ_{12}) left to consider.

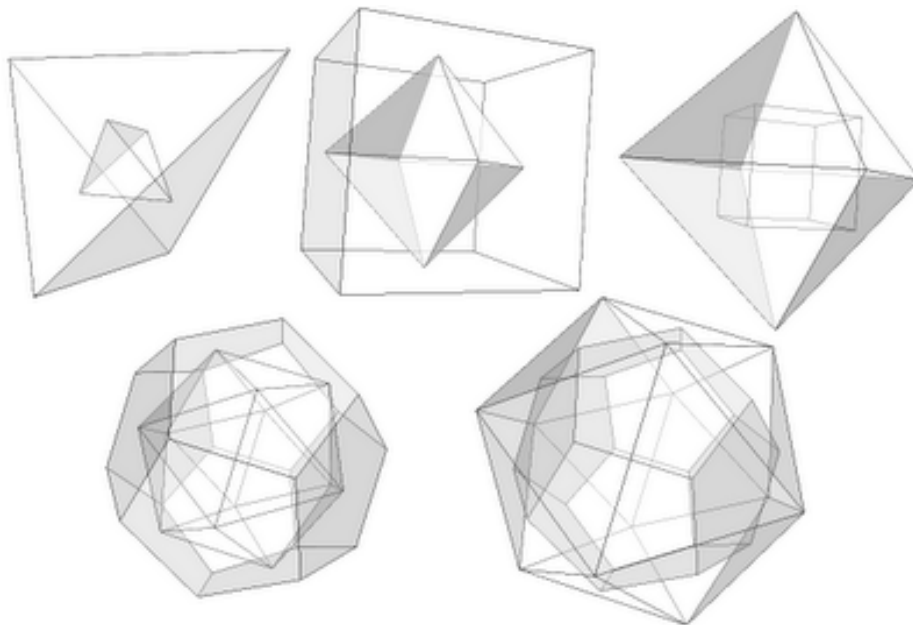


Figure 4.2.: The tetrahedron is dual to itself, the hexahedral and the octahedral are dual, and the icosahedral and the dodecahedral are dual. [120]

The hexahedron is dual to the octahedron. In other words, if one inscribes a octahedron in a sphere and considers the tangent spaces of the points of intersection, one obtains a hexahedron. Two polyhedra which fulfill this property are called **dual** (see Figure 4.2). Regular polyhedra which are dual have the same symmetry group. Thus, \mathcal{O} is the symmetry group of \square_6 . The same situation occurs if we consider the icosahedron and the dodecahedron.

Theorem 4.3.1.3. *Every finite subgroup of $SO_3(\mathbb{R})$ is a cyclic, dihedral, tetrahedral, octahedral or icosahedral group. If two finite subgroups of $SO_3(\mathbb{R})$ are isomorphic then they are conjugate in $SO_3(\mathbb{R})$.*

4.4. Euclidean Space Forms

4.4.1. Affine Spaces

An **affine space** is a set E together with a vector space V acting on E

$$V \times E \rightarrow E, \quad (v, x) \mapsto x + v.$$

For two points $x, y \in E$, there is a unique $v \in V$ with $x + v = y$ and, therefore, every vector v can be written as $v = y - x$. The map

$$T_v : E \rightarrow E, \quad x \mapsto x + v$$

is called **the translation by v** . The **space of all translations** of E is denoted by $V = \mathcal{T}E$.

If E and F are two affine spaces, a map $f : E \rightarrow F$ is called an **affine map** if there is a point $x_0 \in E$ and a linear map $A : \mathcal{T}E \rightarrow \mathcal{T}F$ such that $f(x_0 + v) = f(x_0) + Av$. In this case,

$$f(x + v) = f(x) + Av \quad \forall x \in E, v \in \mathcal{T}E.$$

A is called the linear part of f , denoted by Lf . $\mathcal{T}E$ is the tangent space at every point and Lf is the tangent map of f at every point of E .

$f : E \rightarrow F$ is an **affine isomorphism** if and only if $Lf : \mathcal{T}E \rightarrow \mathcal{T}F$ is a linear isomorphism. In this situation E and F are called **affine equivalent**.

The group of all affine automorphisms, which is the group of all affine transformations of E is isomorphic to the semidirect product of V with the general linear group of V :

$$Aff(E) \approx V \rtimes GL(V).$$

An **affine structure** on a manifold is a maximal atlas consisting of affine charts. Thus, an **affine manifold** is a manifold with an affine structure. An affine manifold has a torsion-free connection with vanishing curvature. Therefore, affine manifolds are also called flat affine

manifolds. [111]

Assume E is an affine space with $\mathcal{T}E = V$ and let F be the vector space defined by $\{(v, 1) | v \in V\}$. This is an affine space with $\mathcal{T}F = V$. The map $\tau_x : E \rightarrow F$ given by $\tau_x(x + v) = (v, 1)$ defines an isomorphism. Thus, we can think of an affine space of dimension n as a hyperplane of a vector space of dimension $n+1$. [1]

The simply-connected Euclidean space is an affine space with $V = \mathbb{R}^n$ and $Aff(\mathbb{E}) = \mathbb{R}^n \times GL_n(\mathbb{R})$. $Aff(\mathbb{E})$ contains the Euclidean group $E(n)$ as a subgroup.

\mathbb{E}^n has the normal covering $\pi : E(n) \rightarrow E(n)/O_n(\mathbb{R}) = \mathbb{E}^n$. An element of $E(n)$ is mapped through the covering on its value at the point 0: $\pi(A, t_a) = a = (A, t_a)(0)$, $A \in O_n(\mathbb{R})$; $t_a \in \mathbb{R}^n$. Any Euclidean space form is given by the normal covering

$$\pi' : \mathbb{E}^n \rightarrow \mathbb{E}^n/\Gamma = M,$$

where Γ is the group of deck transformations with respect to the universal covering. As we have seen that $\Gamma \subset E(n)$ is a discrete group acting freely on \mathbb{E}^n (4.3.0.4, p.81).

Lemma 4.4.1.1. *Let Γ be a subgroup of the Euclidean group $E(n)$. If Γ is closed, Γ acts freely if and only if Γ is torsion-free, that is, if it has no elements of finite order. [111]*

For a proof see, for instance, [111, p.99].

4.4.2. Compact Euclidean Space Forms

In this section we require $M = \mathbb{E}^n/\Gamma$ to be compact. Combining 4.3.0.4 and 4.4.1.1, we conclude that candidates for Γ are exactly the torsion-free, discrete, cocompact subgroups of $E(n)$.

Definition 4.4.2.1 (crystallographic group). *An n -dimensional **crystallographic group** is a cocompact discrete group of isometries of \mathbb{E}^n . Torsion-free crystallographic groups are called **Bieberbach groups**. [99, p.222]*

Remark 4.4.2.2. [111] [103]

1. A crystalline structure is a three-dimensional pattern produced by the atomic arrays in ideal crystals. The crystalline structure is determined by the crystal (unit cell) and its symmetry group. The symmetry group of a geometric structure is the group of motions taking the figure to itself. The crystal is a geometric figure given by the lattice parameters. The symmetry group of the crystalline structure is a discrete, cocompact group of motions of the three-dimensional Euclidean space and therefore a three-dimensional crystallographic group – this explains the name. There are 14 crystallographic groups which are the full symmetry group of a crystalline structure (up to affine equivalence). They were found by Bravais [12] in 1849. The lattices according to this symmetry groups are called Bravais lattices. See Figure 4.3.

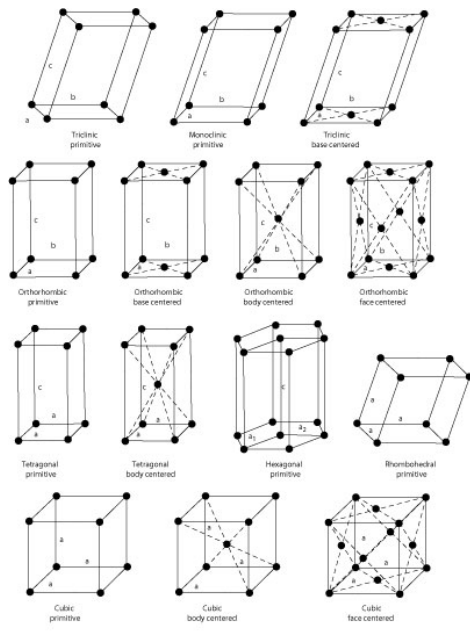
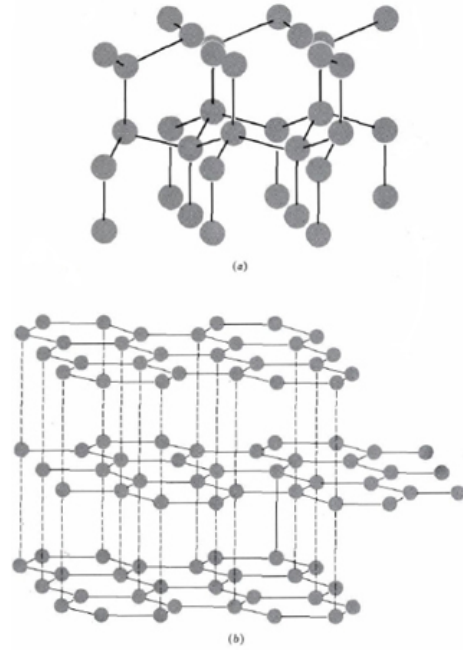


Fig.3 The fourteen bravais lattices. Source: Ref 1

(a) Bravais lattices [121]



(b) Crystalline Structure of (a) graphite (b) diamond [122]

Figure 4.3.: Crystalline structures

2. In higher dimensions, where $\Gamma \subset E(n)$ is equally discrete and cocompact, the set $c_\gamma = \{x \in \mathbb{E}^n : \|\gamma(0) - x\| \leq \|\gamma'(0) - x\|, \forall \gamma' \in \Gamma\}$ defines a so-called crystal for every $\gamma \in \Gamma$. The symmetry group of the crystalline structure $\{c_\gamma\}$ contains Γ as a subgroup of finite index.

Theorem 4.4.2.3 (Bieberbach). *Let Γ be a group isomorphic to a discrete group of isometries of \mathbb{E}^n for some n .*

1. Γ is a crystallographic group if and only if the subgroup T of translations of Γ is a free abelian and normal subgroup of finite index.
2. If Γ and Γ' are crystallographic groups of dimension n and n' that are isomorphic as groups, we have $n = n'$ and there is an affine isomorphism $a : \mathbb{E}^n \rightarrow \mathbb{E}^{n'}$ conjugating Γ to Γ' .
3. For any given n , there are only a finite number of n -dimensional crystallographic groups, up to affine equivalence. [99, p.222] [84]

This theorem was first proven by Bieberbach ([9], [10]). We can now state:

Corollary 4.4.2.4 (classification of Euclidean manifolds). *Diffeomorphism classes of closed Euclidean n -dimensional manifolds are in one-to-one correspondence via their fundamental*

groups with torsion-free groups containing a subgroup of finite index isomorphic to \mathbb{Z}^n . [99, p.222]

Finding all Euclidean space forms by sorting out crystallographic groups which are acting freely on \mathbb{E}^n is a lot of work. There are 219 three-dimensional crystallographic groups, which were found independently by Federov (1949, [29]), Schönflies (1891, [90]) and Barlow (1894, [7]). Only ten of them are acting freely on \mathbb{E}^3 , which was examined by Nowacki (1934, [81]). These give exactly the ten closed locally Euclidean manifolds. If Γ does not include glide reflections the manifold is orientable. There are six of them. In 1935, W. Hantzsche and H. Wendt developed a direct classification of the three-dimensional Euclidean space forms ([41]).

Alternatively we can consider the maximal abelian subgroup of finite index described in 4.4.2.3, which we denote by $\Gamma^* = \Gamma \cap \mathbb{R}^n$. Then

$$\mathbb{E}^n \rightarrow \mathbb{E}^n/\Gamma^* = \mathbb{T}^n$$

is a normal covering. \mathbb{T}^n is a torus, since Γ^* consists only of translations.

In this situation we have:

Theorem 4.4.2.5. *Let Γ be an n -dimensional torsion-free crystallographic group, then Γ is isomorphic to the fundamental group of a compact, connected, flat Riemannian manifold M of dimension n . In that case, we view Γ in $E(n)$. Then $M = \mathbb{E}^n/\Gamma$, $\Gamma^* = \Gamma \cap \mathbb{R}^n$, and Γ/Γ^* is the group of deck transformations of the normal Riemannian covering $\mathbb{E}^n/\Gamma^* \rightarrow M$ by a flat torus.*

Remark 4.4.2.6. Let M be a complete, connected, flat manifold. An element $\gamma \in \Gamma$ can be decomposed as $\gamma = (A_\gamma, t_{a_\gamma})$. Then the linear holonomy group Ψ (3.2.2.6, p.61) consists of all A_γ such that $\gamma = (A_\gamma, t_{a_\gamma}) \in \Gamma$. Ψ is therefore isomorphic to the group Γ/Γ^* and is finite, since Γ^* is of finite index in Γ . This is because in Euclidean spaces the parallel transport along homotopic loops are the same. Therefore, the restricted holonomy group Ψ_0 is always trivial. [111]

Corollary 4.4.2.7. *Let M be a compact connected Riemannian manifold. M is flat if and only if it has finite linear holonomy.*

Remark 4.4.2.8. It is a theorem of Auslander and Kuranishi that the converse is also true: any finite group is the holonomy group of a flat, compact, connected Riemannian manifold. (See, for instance, [111, p.110].)

4.4.2.1. Three-Dimensional Orientable, Compact Euclidean Space Forms

Considering only orientable manifolds, we see that Ψ is a finite subgroup of $SO_3(\mathbb{R})$ and therefore cyclic, dihedral, tetrahedral, octahedral or icosahedral (see section 4.3.1). It turns

out that the only ones which have to be considered are:

Cyclic groups: \mathbb{Z}_m , $m \in \{1, 2, 3, 4, 6\}$ and the dihedral group $\mathbb{Z}_2 \times \mathbb{Z}_2$.

For details see [111, p.116]. These give exactly the six flat, compact, connected and orientable three-dimensional Riemannian manifolds.

Theorem 4.4.2.9. *There are just six diffeomorphism classes of compact connected orientable flat three-dimensional Riemannian manifolds. They are represented by the manifolds \mathbb{E}^3/Γ , where Γ is one of the groups given below. Here, Λ is the translation lattice, $\{a_1, a_2, a_3\}$ are its generators, and $t_i = t_{a_i}$, and $\Psi = \Gamma/\Gamma^*$ is the holonomy.*

\mathcal{G}_1 : $\Psi = \{1\}$, Γ consists only of translations and is generated by $\{t_1, t_2, t_3\}$ with a_i linear independent.

\mathcal{G}_2 : $\Psi = \{\mathbb{Z}_2\}$,

Γ is generated by $\{\alpha, t_1, t_2, t_3\}$. The relations among the generators are given by:

$$\alpha^2 = t_1, \alpha t_2 \alpha^{-1} = t_2^{-1}, \alpha t_3 \alpha^{-1} = t_3^{-1}$$

Lattice: a_1 orthogonal to a_2 and a_3 ; $\alpha = (A, t_{a_1/2})$ with

$$A(a_1) = a_1, A(a_2) = -a_2, A(a_3) = -a_3.$$

\mathcal{G}_3 : $\Psi = \{\mathbb{Z}_3\}$,

Γ is generated by $\{\alpha, t_1, t_2, t_3\}$. The relations among the generators are given by:

$$\alpha^3 = t_1, \alpha t_2 \alpha^{-1} = t_3, \alpha t_3 \alpha^{-1} = t_2^{-1} t_3^{-1}$$

Lattice: $a_1 \perp a_2$; $a_1 \perp a_3$; $\|a_2\| = \|a_3\|$, $\{a_2, a_3\}$ define a hexagonal plane lattice.

$\alpha = (A, t_{a_1/3})$ with

$$A(a_1) = a_1, A(a_2) = a_3, A(a_3) = -a_2 - a_3.$$

\mathcal{G}_4 : $\Psi = \{\mathbb{Z}_4\}$,

Γ is generated by $\{\alpha, t_1, t_2, t_3\}$. The relations among the generators are given by:

$$\alpha^4 = t_1, \alpha t_2 \alpha^{-1} = t_3, \alpha t_3 \alpha^{-1} = t_2^{-1}$$

Lattice: a_1, a_2, a_3 mutually orthogonal; $\|a_2\| = \|a_3\|$, $\alpha = (A, t_{a_1/4})$ with

$$A(a_1) = a_1, A(a_2) = a_3, A(a_3) = -a_2.$$

$\mathcal{G}_5: \Psi = \{\mathbb{Z}_6\}$,

Γ is generated by $\{\alpha, t_1, t_2, t_3\}$. The relations among the generators are given by:

$$\alpha^6 = t_1, \quad \alpha t_2 \alpha^{-1} = t_3, \quad \alpha t_3 \alpha^{-1} = t_2^{-1} t_3$$

Lattice: $a_1 \perp a_2; a_1 \perp a_3; \|a_2\| = \|a_3\|$, $\{a_2, a_3\}$ define a hexagonal plane lattice, $\alpha = (A, t_{a_1/6})$ with

$$A(a_1) = a_1, \quad A(a_2) = a_3, \quad A(a_3) = a_3 - a_2.$$

$\mathcal{G}_6: \Psi = \{\mathbb{Z}_2 \times \mathbb{Z}_2\}$,

Γ is generated by $\{\alpha, \beta, \gamma, t_1, t_2, t_3\}$. The relations among the generators are given by:

$$\alpha^2 = t_1, \quad \alpha t_2 \alpha^{-1} = t_2^{-1}, \quad \alpha t_3 \alpha^{-1} = t_3^{-1}$$

$$\beta t_1 \beta^{-1} = t_1^{-1}, \quad \beta^2 = t_2, \quad \beta t_3 \beta^{-1} = t_3^{-1}$$

$$\gamma t_1 \gamma^{-1} = t_1^{-1}, \quad \gamma t_2 \gamma^{-1} = t_2^{-1}, \quad \gamma^2 = t_3.$$

Lattice: a_1, a_2, a_3 mutually orthogonal; $\alpha = (A, t_{a_1/2})$, $\beta = (B, t_{(a_2+a_3)/2})$, $\gamma = (C, t_{(a_1+a_2+a_3)/2})$, with

$$A(a_1) = a_1, \quad A(a_2) = -a_2, \quad A(a_3) = -a_3$$

$$B(a_1) = -a_1, \quad B(a_2) = a_2, \quad B(a_3) = -a_3$$

$$C(a_1) = -a_1, \quad C(a_2) = -a_2, \quad C(a_3) = a_3$$

Remark 4.4.2.10. All Euclidean translations are Clifford translations. Since the fundamental group of the torus (\mathcal{G}_1) consists only of translations, it is the only globally homogeneous Euclidean manifold.

4.4.3. Open Euclidean Space Forms

If $M = \mathbb{E}^n/\Gamma$ is non-compact, $\Gamma^* = \Gamma \cap \mathbb{R}^n$ is not isomorphic to \mathbb{Z}^n . But Γ^* is a discrete group of pure translations and therefore isomorphic to \mathbb{Z}^m for a $m < n$. $N = \mathbb{E}^m/\Gamma^*$ is an m -dimensional torus. Every $\gamma \in \Gamma$ can be decomposed into $\gamma = (\gamma_1, \gamma_2)$, where $\gamma_1 \in \mathbb{R}^m$ and $\gamma_2 \in O(n-m)$. To ensure that γ_2 does not contain a translation part it may be necessary to choose an appropriate origin. M is then isometric to $\mathbb{E}^{n-m} \times \mathbb{E}^m/\Gamma^*$. We only consider orientable manifolds. Thus, $\Gamma \subset \mathbb{R}^n \times SO_n(\mathbb{R})$ does not contain glide reflections.

4.4.3.1. Open Three-Dimensional Euclidean Space Forms

The classification of non-compact three-dimensional flat space forms was made by Wolf, [111].

Theorem 4.4.3.1. *The affine diffeomorphism classes of complete, connected, non-compact, flat, orientable, three-dimensional Riemannian manifolds are represented uniquely by the manifolds $M = \mathbb{E}^3/\Gamma$ with Γ given below. Here, $\{v_1, v_2, v_3\}$ is a fixed orthonormal basis of \mathbb{E}^3 .*

$$\mathcal{E}: \Gamma = \{1\}, \text{ thus, } M = \mathbb{E}^3,$$

\mathcal{S}^θ , $0 \leq \theta \leq \pi$: Γ generated by a screw motion $S = (\sigma, t_{v_3})$ with:

$$S(v_1) = \cos(\theta)v_1 + \sin(\theta)v_2, \quad S(v_2) = -\sin(\theta)v_1 + \cos(\theta)v_2, \quad S(v_3) = v_3.$$

\mathcal{T} : Γ generated by the translations t_{v_1}, t_{v_2} .

\mathcal{K} : Γ generated by a translation t_{v_1} and a screw motion $\beta = (B, t_{v_2})$, with:

$$B(v_1) = -v_1, \quad B(v_2) = v_2, \quad B(v_3) = -v_3.$$

Motivation of 4.4.3.1: We already know that M is isometric to $\mathbb{E}^{3-m} \times \mathbb{E}^m/\Gamma^*$, $m \in \{0, 1, 2\}$.

$m = 0$: $M = \mathbb{E}^3$ and $\Gamma = \{1\}$, N is a point. We get case \mathcal{E} .

$m = 1$: There is only one compact, one-dimensional, flat Riemannian manifold: the cycle \mathbb{S}^1 . A $\gamma \in \Gamma$ can be decomposed into a rotation $\gamma_2 \in O_2(\mathbb{R})$ and a one-dimensional translation, which can be taken in the direction of v_3 without loss of generality. After choosing an appropriate origin and an orthonormal basis, this defines a screw motion with $0 \leq \theta \leq \pi$ (we exclude the possibility of a glide reflection). We get case \mathcal{S}^θ .

$m = 2$: There are two compact, two-dimensional, flat Riemannian manifolds:

- a) The two-dimensional torus: Γ^* is generated by two independent translations, for example, t_{v_1}, t_{v_2} . Then Γ is generated by $(U, t_{v_1}), (V, t_{v_2})$, with:

$$U(t_{v_1}) = V(t_{v_1}) = v_1, \quad U(t_{v_2}) = V(t_{v_2}) = v_2, \quad U(t_{v_3}) = \pm v_3, V(t_{v_1}) = \pm v_3.$$

The manifold is only orientable if $U(t_{v_3}) = V(t_{v_1}) = v_3$. We get \mathcal{T} .

- b) The Klein bottle: We have to ensure that every element of Γ preserves the orientation. Let Γ^* be generated by t_{v_1} and $\beta = (B, t_{v_2})$ with $B(v_1) = -v_1$ and $B(v_2) = v_2$. \mathbb{E}^1 is generated by t_{v_3} . Γ is again generated by $\gamma = (U, t_{v_1})$ and $\gamma' = (V, t_{v_2})$ with:

$$U(v_1) = -V(v_1) = v_1, \quad U(v_2) = V(v_2) = v_2, \quad U(v_3) = \pm v_3, V(v_3) = \pm v_3.$$

The only possibility to make both γ and γ' orientation-preserving is taking

$$\gamma = t_{v_1}, \text{ then } U(v_3) = v_3, \quad \gamma' = \beta, \text{ with } V(v_3) = -v_3$$

We get \mathcal{K} .

Remark 4.4.3.2. If M and M' are manifolds as described in 4.4.3.1, they are homeomorphic if and only if they are diffeomorphic or they are of types $\mathcal{S}^\theta, \mathcal{S}^{\theta'}$, with $\theta \neq \theta'$. A complete $(E(3), \mathbb{E}^3)$ -manifold is uniquely determined by its fundamental group given by Γ .

4.5. Three-Dimensional Spherical Space Forms

Every spherical space form is given by the quotient \mathbb{S}^3/Γ , where $\Gamma \subset SO_4(\mathbb{R})$ acts freely on \mathbb{S}^3 . Γ is isomorphic to the fundamental group and the holonomy group of the manifold. Since \mathbb{S}^3 is a closed and orientable manifold, spherical space forms are always closed and orientable. As a discrete and closed subgroup of a compact group, Γ is finite. This leaves us to find all the finite subgroups of $SO_4(\mathbb{R})$ which act freely on \mathbb{S}^3 .

4.5.1. Finite Subgroups of $SO_4(\mathbb{R})$

Literature references for this section are [111], [99] and [103].

First, the finite subgroups of $SO_4(\mathbb{R})$ were classified by Threlfall and Seifert. Since $\mathbb{S}^3 = SO_4(\mathbb{R})/SO_3(\mathbb{R})$, the three-dimensional sphere is a topological group, just as the circle. Just as the circle can be described by complex numbers, the three-sphere can be described by quaternions, which we introduce now:

Quaternions: The quaternions \mathcal{H} can be constructed by the set \mathbb{R}^4 with a non-commutative but associative multiplication $\mathcal{H} \times \mathcal{H} \rightarrow \mathcal{H}$. The multiplication is bilinear and is therefore uniquely defined by its effects on a basis $\{1, i, j, k\}$:

$$i^2 = j^2 = k^2 = -1, \quad ij = k = -ji, \quad jk = i = -kj, \quad ki = j = -ik.$$

The subspace spanned by $\{1\}$ can be identified with \mathbb{R} and its elements are called **real quaternions**. A quaternion of the form $q = \mathbb{R}i + \mathbb{R}j + \mathbb{R}k$ is called a **pure quaternion**. The conjugate of $q = a + bi + cj + dk$ is the quaternion $\bar{q} = a - bi - cj - dk$. A norm can be defined by $|q| = q\bar{q}$, which coincides with the standard norm of \mathbb{E}^4 . If $|q| = 1$, q is called a **unit quaternion**. Therefore, the three-sphere is the set of unit quaternions:

$$\mathbb{S}^3 = \{q \in \mathcal{H} \mid |q| = 1\} = \mathcal{H}'.$$

[99, p.105]

Since $\mathbb{S}^3/\{\pm 1\} \cong SO_3(\mathbb{R})$, one can define a covering by

$$\pi : \mathcal{H}' \rightarrow SO_3(\mathbb{R}), \quad \pi(q)(q') = qq'q^{-1},$$

which is a two-to-one map, since $\pi(q) = \pi(-q)$.

The only finite subgroups of $SO_3(\mathbb{R})$ are the cyclic, dihedral and polyhedral subgroups (4.3.1.3, p.85). The groups:

$$D_m^* := \pi^{-1}(\mathcal{D}_m), \quad T^* := \pi^{-1}(\mathcal{T}), \quad O^* := \pi^{-1}(\mathcal{O}), \quad I^* := \pi^{-1}(\mathcal{I})$$

are finite groups of \mathcal{H}' . They are called the **binary dihedral/polyhedral groups**. It turns out that these, together with the cyclic groups, are the only finite subgroups of \mathcal{H}' .

First, the connection between the binary groups and the spherical space forms was seen by H. Hopf ([44]), but the main step was taken by W. Threlfall and H. Seifert ([104], [105]):

$SO_4(\mathbb{R})$ is locally isomorphic to $SO_3(\mathbb{R}) \times SO_3(\mathbb{R})$. We have already seen that the universal covering of $SO_3(\mathbb{R})$ is \mathcal{H}' . Let us denote the universal covering space of $SO_4(\mathbb{R})$ with $Spin(4)$ and the covering by $p : Spin(4) \rightarrow SO_4(\mathbb{R})$. There is an isomorphism:

$$\phi : Spin(4) \rightarrow \mathcal{H}' \times \mathcal{H}' \tag{4.2}$$

which we shall give in detail below. We denote the composition of ϕ with the projection on the i^{th} factor with ϕ_i .

If $\Gamma \subset SO_4(\mathbb{R})$ is finite, $\Gamma_i = \phi_i(p^{-1}(\Gamma)) \subset \mathcal{H}'$ is finite. Since all finite subgroups of \mathcal{H}' are known and we have the isomorphism ϕ , we can construct all finite subgroups of $SO_4(\mathbb{R})$. The subgroups which act freely remain to be found.

A. Hattori reformulated the Threlfall-Seifert classification in terms of quaternions. For unit quaternions a, b we define the homomorphism:

$$F(a, b) : \mathcal{H} \rightarrow \mathcal{H}, \quad q \mapsto aqb^{-1}.$$

F is a two-to-one homomorphism from $\mathcal{H}' \times \mathcal{H}' \rightarrow SO_4(\mathbb{R})$ with kernel $\{(1, 1), (-1, -1)\}$. The above-given isomorphism 4.2 is determined by $F = p\phi^{-1}$.

For $\Gamma \subset SO_4(\mathbb{R})$ is finite, $\Gamma^* = F^{-1}(\Gamma)$ and Γ_i is the projection of Γ^* on the i^{th} factor. Thus, $\Gamma_i \subset \mathcal{H}'$. A theorem by Vincent states that a group Γ acts freely on \mathbb{S}^3 if and only if it is fixed-point-free (see [111]). Since $F(a, b)q = q, q \neq 0$ if and only if $a = qbq^{-1}$, $F(a, b)$ has a fixed point if and only if a and b are conjugates in \mathcal{H}' . Thus, $\Gamma \subset SO_4(\mathbb{R})$ acts freely if the corresponding subgroup in $\Gamma_1 \times \Gamma_2 \subset \mathcal{H}' \times \mathcal{H}'$ has no element (a, b) such that a and b are conjugates.

4.5.2. Classification of the Three-Dimensional Spherical Space Forms

In this section we closely follow [33].

The finite subgroups of $SO_4(\mathbb{R})$ are isomorphic to the finite subgroups $L \times R \subset \mathcal{H}' \times \mathcal{H}'$. If one of the components is trivial, the action is called **single action**. If none of the subgroups L, R are trivial, the group L acts as left translations, whereas the group R acts as right translations. There are two possibilities: either every element of L is allowed to act simultaneously with every element of R , or we restrict the set of elements of R which occur with an element of L . In the first case, we obtain a **double action**, whereas we obtain a **linked action** in the second case. There are three categories of spherical space forms in correspondence to the three different types of actions of Γ on \mathbb{S}^3 :

Single Action Manifolds: A finite, discrete group $\Gamma \subset SO_4(\mathbb{R})$, consisting only of pure Clifford translations, acts on \mathbb{S}^3 . Corresponding to the finite subgroups of $SO_4(\mathbb{R})$, there are five classes of these spherical space forms: the lens spaces, prism spaces and three classes of polyhedral spaces:

Lens Spaces $L(n,1)$ $\Gamma \approx \mathbb{Z}_p$, the cyclic group

Prism Spaces $\Gamma \approx D_m^*$, the binary dihedral group

Polyhedral Spaces: Truncated Cube Space: $\Gamma \approx T^*$, the binary tetrahedral group

Octahedral Space: $\Gamma \approx O^*$, the binary octahedral group

Dodecahedral Space: $\Gamma \approx I^*$, the binary icosahedral group

The names of the spaces correspond to the covering group. As their fundamental group consists only of clifford translations, the manifolds are globally homogeneous.

Double Action Manifolds: Here, $\Gamma = L \times R$, where $L, R \subset SO_4(\mathbb{R})$ are different, finite subgroups. Where L acts as left-handed Clifford translations and R acts as right-handed Clifford translations. In order to obtain a free action, we have to ensure that R and L do not contain a nontrivial element of the same order. Since each of the polyhedral groups contains an element of order four, they cannot be paired with one another. Thus, without loss of generality, L has to be a cyclic group. R is therefore cyclic or a polyhedral group. We assume L has no elements of order four and therefore, $L = \mathbb{Z}_p$ or $L = \mathbb{Z}_{2p}$, p odd. We can think of \mathbb{Z}_{2p} as the set $\{q^i\}_{0 \leq i < p} \cup \{-q^i\}_{0 \leq i < p}$. If R contains the element -1 , the group $\mathbb{Z}_p \times R$ gives the same group as $\mathbb{Z}_{2p} \times R$. If R does not contain -1 , R is a cyclic group of odd order and we may, therefore, switch the roles of L and R . We can assume L to be a cyclic group of odd order. There are the following possibilities:

Remark 4.5.2.1. We denote the greatest common divisor of the integers n and m with (n, m) .

$R = \mathbb{Z}_m, L = \mathbb{Z}_p, (m, p) = 1$ yields a lens space $L(m, n)$.

$R = D_m^*, L = \mathbb{Z}_p, (4m, p) = 1$: yields a quotient of a prism manifold.

$R = T^*, L = \mathbb{Z}_p, (24, p) = 1$: yields a quotient of the truncated cube space.

$R = O^*, L = \mathbb{Z}_p, (48, p) = 1$: yields a quotient of the octahedral space.

$R = I^*, L = \mathbb{Z}_p, (120, p) = 1$: yields a quotient of the dodecahedral space .

All these spaces can also be constructed as a quotient of a lens space $L(p, 1)$, since their covering spaces are not simply-connected. The holonomy groups of two manifolds can be isomorphic even if the manifolds are non-homeomorphic. For example, the lens spaces $L(5, 1)$ and $L(5, 2)$ both have a holonomy group isomorphic to \mathbb{Z}_5 , but the spaces are not homeomorphic.

Linked Action Manifolds Here, the groups L and R are chosen just as in the case of double action manifolds, but now we allow a $r \in R$ to pair only with a restricted set of elements of L . Combinations producing fixed points are avoided. We shall not go into further detail, but see [\[33\]](#).

To conclude the classification of spherical space forms, we give a list of all groups up to the order 120 which generate three-dimensional spherical space forms and a list of the space forms themselves. First, we list the holonomy groups acting on the space form. The first column gives the order of the holonomy group; the second the holonomy group itself. As pointed out before, isomorphic holonomy groups can generate non-homeomorphic manifolds through different group actions.

4. Locally Isotropic Riemannian Manifolds

Order	Single Action	Double Action	Linked Action
1	\mathbb{Z}_1		
2	\mathbb{Z}_2		
3	\mathbb{Z}_3		
4	\mathbb{Z}_4		
5	\mathbb{Z}_5		\mathbb{Z}_5
6	\mathbb{Z}_6		
7	\mathbb{Z}_7		\mathbb{Z}_7
8	$\mathbb{Z}_8, \mathcal{D}_2^*$		\mathbb{Z}_8
...			
12	$\mathbb{Z}_{12}, \mathcal{D}_3^*$	$\mathbb{Z}_3 \times \mathbb{Z}_4$	
...			
72	$\mathbb{Z}_{72}, \mathcal{D}_{18}^*$	$\mathbb{Z}_8 \times \mathbb{Z}_9, \mathcal{D}_2^* \times \mathbb{Z}_9$	$\mathbb{Z}_{72}, T^* \times \mathbb{Z}_9, \mathcal{D}_9^* \times \mathbb{Z}_8$
...			
120	$\mathbb{Z}_{120}, \mathcal{D}_{30}^*, I^*$	$\mathbb{Z}_{40} \times \mathbb{Z}_3, \mathbb{Z}_{24} \times \mathbb{Z}_5,$ $\mathbb{Z}_8 \times \mathbb{Z}_{15}, T^* \times \mathbb{Z}_5,$ $\mathcal{D}_6^* \times \mathbb{Z}_5, \mathcal{D}_2^* \times \mathbb{Z}_{15}, \mathcal{D}_{10}^* \times \mathbb{Z}_3,$	$\mathbb{Z}_{120}, \mathcal{D}_3^* \times \mathbb{Z}_{40},$ $\mathcal{D}_5^* \times \mathbb{Z}_{24},$ $\mathcal{D}_{15}^* \times \mathbb{Z}_8$
...			

We now list the corresponding space forms. Isomorphic manifold can be reconstructed by different types of group actions. We list isomorphic manifolds only once. For example, the lens space $L(7, 2)$ and $L(7, 3)$ are isomorphic.

Order	Single Action	Double Action	Linked Action
1	\mathbb{S}^3		
2	$L(2, 1)$		
3	$L(3, 1)$		
4	$L(4, 1)$		
5	$L(5, 1)$		$L(5, 2)$
6	$L(6, 1)$		
7	$L(7, 1)$		$L(7, 2)$
8	$L(8, 1)$		$L(8, 3)$
...			
12	$L(12, 1)$	$L(12, 5)$	
...			
72	$L(72, 1)$	$L(72, 17)$	$L(72, 5) + 5$ more
...			
120	$L(120, 1)$	$L(120, 31), L(120, 41), L(120, 49)$	$L(120, 7) + 7$ more
...			

4.6. Three-Dimensional Hyperbolic Space Forms

Hyperbolic geometric structures are much more complicated than in the Euclidean or spherical case. Therefore, there is no classification of three-dimensional hyperbolic manifolds, not even for dimension two. In 1979, Riley found an algorithm which lists compact hyperbolic manifolds for the first time. Even if there is no structural classification, there exists a rich theory of hyperbolic geometric structures. We shall only present the main theorems. For an in-depth study on this topic, the following literature is recommended: [98], [99], [39], [84].

Mostow's Rigidity Theorem states that the geometric structure of hyperbolic manifolds is uniquely determined by its fundamental group.

Theorem 4.6.0.2 (Mostow Rigidity Theorem). *Suppose M_1 and M_2 are compact hyperbolic manifolds of dimension $n \geq 3$ for which there is an isomorphism*

$$\Phi : \pi_1(M_1) \rightarrow \pi_1(M_2).$$

Then there exists an isometry $F : M_1 \rightarrow M_2$ which induces the isomorphism Φ (up to conjugacy) between the fundamental groups. [98]

The fundamental group of a three-dimensional hyperbolic manifold is of infinite order. From Thurston's Geometrization Theorem follows that a closed three-dimensional manifold is hyperbolic if and only if it is prime with an infinite fundamental group which contains no $\mathbb{Z} \oplus \mathbb{Z}$. Recall that a prime manifold is a manifold which cannot be written as a connected sum of non-trivial manifolds of the same dimension. [73]

The group of orientation-preserving isometries of \mathbb{H}^3 is isomorphic to the group $PSL_2(\mathbb{C})$. (See 3.1.0.15 on page 56.) Discrete subgroups of $PSL_2(\mathbb{C})$ are called **Kleinian groups**. They act freely on \mathbb{H}^3 if and only if they have no element of finite order. Thus, a classification of the hyperbolic space forms is equivalent to a classification of torsion-free Kleinian groups. To date, no classification is known.

The only Clifford translation is the identity. Thus, the simply-connected open space \mathbb{H}^3 is the only globally homogeneous space form. [98]

4.6.1. Thick-Thin Decomposition

Let M be a complete, hyperbolic manifold of dimension n with covering $p : \mathbb{H}^n \rightarrow M$ and Γ , which is the group of deck transformations. Let us denote the lifts of an $x \in M$ in \mathbb{H}^3 as $\tilde{x}, \tilde{x}', \tilde{x}'', \dots$. Since Γ is a discrete group, there is a shortest distance $d := d(\tilde{x}^i, \tilde{x}^j)$, $i \neq j$ between two lifts. This length is exactly the length of the shortest non-null-homotopic loop based on x . The ball of radius $r(x) = \frac{1}{2}d$ with center x is the biggest ball which can be embedded in the UCS. We call $r(x)$ the **injectivity radius** of M at x . The ball centered at x with radius $r(x)$ is the biggest domain on which the exponential map is injective. Then

M can be decomposed in:

$$M_{\geq\epsilon} = \{x \in M | r(x) \geq \frac{1}{2}\epsilon\}, \text{ the thick part and}$$

$$M_{<\epsilon} = \{x \in M | r(x) < \frac{1}{2}\epsilon\}, \text{ the thin part.}$$

This decomposition is called **the Thick-Thin decomposition**. The thin part can be classified. It is the union of components of four different types (see [99]). One of them is called **the cusp**, which can be thought of as the neighbourhood of a point at infinity.

It is known that the manifold is of finite volume if and only if the thick part is compact $\forall \epsilon > 0$. There is a theorem of Thurston (see, for instance, [39] or [98]) which states that there are only countably many hyperbolic manifolds of finite volume and that there are only finitely many non-homeomorphic manifolds of a given volume V . Therefore, there exists a finite amount of hyperbolic manifolds with minimal volume V_1 . The second lowest volume of hyperbolic manifolds is V_2 , then there is V_3 and so on until the first accumulation point V_ω , which is the lowest volume of hyperbolic manifolds with one cusp. The sequence continues with $V_{\omega+1}, V_{\omega+2}, V_{\omega+3}, \dots$ until the second accumulation point V_{ω^2} , which is the lowest volume of a hyperbolic manifold with two cusps. Thus, there is a structural classification in correspondence to the volume of the manifold. [98]

4.7. Conclusion

We have seen that the model geometries \widetilde{M} for three-dimensional locally isotropic Riemannian manifolds are the three spaces $\mathbb{H}^3, \mathbb{E}^3, \mathbb{S}^3$. Thus, the geometry is modeled on one of the three simply-connected Riemannian manifolds of constant curvature. Since any three-dimensional space form can be written as \widetilde{M}/Γ , we are left with classify the discrete $\Gamma \subset Isom(\widetilde{M})$ acting freely on \widetilde{M} .

For Euclidean space forms, Γ is a torsion-free, discrete group of Euclidean isometries. The compact Euclidean space forms correspond to the ten three-dimensional Bieberbach groups from which six are oriented. Additionally, there are four non-compact Euclidean spaces. Spherical space forms can be identified with the finite subgroups Γ of $SO_4(\mathbb{R})$, for which there is a correspondence to the finite subgroups of $SO_3(\mathbb{R}) \times SO_3(\mathbb{R})$. According to the type of action of Γ on \mathbb{S}^3 , the infinite amount of three-dimensional spherical space forms are grouped in three classes of manifolds: single action, double action and linked action manifolds, whereas, for single action manifolds one component of the corresponding subgroup in $SO_3(\mathbb{R}) \times SO_3(\mathbb{R})$ is trivial. Three-dimensional orientable hyperbolic space forms correspond to torsion-free and discrete subgroups $\Gamma \subset PSL_2(\mathbb{C})$. So far, no classification of Kleinian groups has been found.

5. Gluing Manifolds

We shall now present the mathematical basics for the next chapter, where we focus on **Cosmic Topology**. In Chapter 4, we have developed a list of candidates for \mathcal{M}_3 . How can we decide which space we are sitting in? In order to visualize three-dimensional manifolds, we shall develop a procedure in dimension three.

5.1. Gluings – Geometry of Discrete Groups

Remark 5.1.0.1 (Notation). In this chapter, X shall always refer to an arbitrary metric space and \widetilde{M} to one of the spaces $\mathbb{S}^n, \mathbb{H}^n, \mathbb{E}^n$. Γ denotes a discrete group of isometries of X or \widetilde{M} (2.2.1.5, p.42). A space form shall be denoted by M .

We start with an example in dimension two:

Example 5.1.0.2. Take a rectangle and glue the top side and the bottom side together such that we get a cylinder. Gluing the two circles at the top and the bottom gives us a two-dimensional torus \mathbb{T}_F^2 (see Figure 5.1(a)). Here, the rectangle is called the fundamental domain or fundamental polyhedron of the torus. It is not the only polygon which gives a torus by gluing its sides, we can also use a hexagon or parallelogram for constructing \mathbb{T}_F^2 . [2]

The different choices of the fundamental polyhedron have the following background: take an infinite amount of rectangles, labeled as in Figure 5.1(a). Start with taking one rectangle and add one after the other by identifying edges of the new ones with similarly labeled edges of those placed already. Following this rule, each new polygon fits in a unique way. The resulting pattern is called a regular tessellation of the Euclidean plane. For tiling the Euclidean plane, triangles, parallelograms or hexagons can also be used (see fig. 5.1(b)).

Since the rectangle is a fundamental polyhedron for the torus and tiles the (simply-connected) Euclidean plane, \mathbb{E}^2 is the universal covering space of the torus. The covering map identifies corresponding points in each rectangle by the translations $(x, y) \mapsto (x + b, y)$ and $(x, y) \mapsto (x, y + a)$. These translations generate the group of deck transformations Γ . Thus, the torus is the quotient space \mathbb{E}^2/Γ .

As long as a region D of the torus is simply-connected, it is isometric to \mathbb{E}^2 . Thus, we can define an Euclidean metric on D . Therefore, the torus is locally isometric to the Euclidean plane and has an Euclidean geometric structure. [99] (cf. 3.2.1.1, p.56)

The torus is uniquely described by its fundamental domain and the identifications of its sides by pairs. This concept can be extended further, as we shall see in the following. [2]

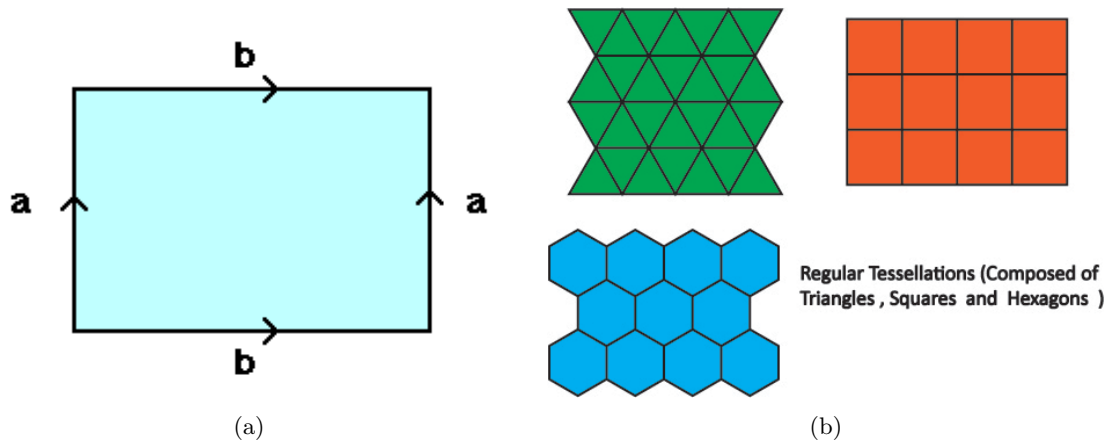


Figure 5.1.: (a): By identifying opposite sides of a rectangle in the Euclidean plane, a flat torus is obtained. [123] (b): Regular tessellations of the Euclidean plane. [124]

Remark 5.1.0.3 (Assumption:). We assume M to be compact and oriented.

5.1.1. Metric on Space Forms

Let $M = \widetilde{M}/\Gamma$ be a space form. That way, M is the orbit space of the action of Γ on the metric space \widetilde{M} :

$$M = \{\Gamma x \mid x \in \widetilde{M}\}.$$

Definition 5.1.1.1. We assuming A and B to be subsets of a metric space X . The distance from A to B in X is defined to be

$$dist(A, B) := \inf\{d(x, y) \mid x \in A, y \in B\}.$$

Remark 5.1.1.2. The **orbit space distance function** $d_\Gamma : \widetilde{M}/\Gamma \times \widetilde{M}/\Gamma \rightarrow \mathbb{R}$ is defined as:

$$d_\Gamma(\Gamma x, \Gamma y) := dist(\Gamma x, \Gamma y).$$

d_Γ defines a metric on an orbit space if and only if every orbit is closed in \widetilde{M} . For a space form $M = \widetilde{M}/\Gamma$, Γ is properly discontinuous. According to Lemma 4.3.0.4 (p.81), Γ is discontinuous (2.3.1.3, p.48) and, thus, every orbit is closed in \widetilde{M} and d_Γ defines a metric on M . [84]

5.1.2. The Fundamental Polyhedron

The geometric properties of a simply-connected domain in M are the same as those of its development in the universal covering space \widetilde{M} . [55]

Definition 5.1.2.1. *A subset R of a metric space X is a **fundamental region** for a group Γ of isometries of X if and only if*

1. *the set R is open in X ;*
2. *the members of $\{\gamma R \mid \gamma \in \Gamma\}$ are mutually disjoint;*
3. *$X = \bigcup\{\gamma \overline{R} \mid \gamma \in \Gamma\}$, where \overline{R} denotes the closure of R . [84]*

Definition 5.1.2.2. *A subset D of a metric space X is a **fundamental domain** for a group of isometries Γ of X if and only if D is a connected fundamental region for Γ . [84]*

Recall the definition of a locally finite set (2.2.1.5, p.42).

Definition 5.1.2.3. *A fundamental region R for a group Γ of isometries of a metric space X is **locally finite** if and only if $\{\gamma \overline{R} \mid \gamma \in \Gamma\}$ is a locally finite family of subsets of X . [103]*

If Γ is a discrete subgroup of the group of isometries of \widetilde{M} , there exists a convex and locally finite fundamental domain R for Γ . R is isometric to a simply-connected domain in the UCS through the above-defined metric (5.1.1.2). Thus, we get the geometry of the UCS \widetilde{M} on the quotient space $M = \widetilde{M}/\Gamma$. Not only does R give the geometry, it is also representative for the topology of M :

Theorem 5.1.2.4. *If R is a fundamental region for a discontinuous group Γ of isometries of a metric space X , the inclusion $\iota : \overline{R} \rightarrow X$ induces a continuous bijection $\kappa : \overline{R}/\Gamma \rightarrow X/\Gamma$ and κ is a homeomorphism if and only if R is locally finite. [84]*

Remark 5.1.2.5. The quotient space \widetilde{M}/Γ is compact if and only if the fundamental domain for Γ is compact. [103]

Definition 5.1.2.6. *The set*

$$D(x) := \{y \in X : d(y, x) \leq d(y, \gamma(x)) \forall \gamma \in \Gamma\}$$

*is called the **Dirichlet domain** for Γ with center x . [103]*

Remark 5.1.2.7. 1. It is very common to produce a fundamental domain by constructing a Dirichlet domain for Γ .

2. The Dirichlet domain of a simply-connected manifold is the manifold itself. For a space form $M = \widetilde{M}/\Gamma$ it is a locally finite fundamental domain for Γ .

3. By changing the center of the Dirichlet domain we obtain another fundamental domain for the same manifold. By changing the lengths of the Dirichlet domain, we obtain another manifold of the same geometric and topological class (and therefore another fundamental domain). [37]

Remark 5.1.2.8 (Fundamental Polyhedron). In order to define a fundamental polyhedron we need several other definitions, which we shall present in this remark.

1. A subset C of \widetilde{M} is called **convex** if it contains the geodesic joining any two points in it.
2. A **side** of a convex set C is a nonempty, maximal, convex subset of the (topological) boundary $\partial_T C$ of C . A side is always closed and two sides meet only along their boundaries.
3. The **interior** of a convex set is defined as $C^\circ = C \setminus \partial_T C$. [84]

Definition 5.1.2.9. A **convex polyhedron** P in \widetilde{M} is a nonempty, closed, convex subset of \widetilde{M} such that the collection \mathcal{S} of its sides is locally finite in \widetilde{M} . [84]

Remark 5.1.2.10 (Faces of Polyhedra). 1. Every **side** of an m -dimensional convex polyhedron is an $(m - 1)$ -dimensional convex polyhedron. [84] They are sometimes called **facets**. [55]

2. We shall inductively define k -faces for $0 \leq k \leq m$ of an m -dimensional convex polyhedron P . The only m -face of P is P itself. Assuming that $(k + 1)$ -faces have already been defined, a k -face is a side of a $(k + 1)$ -face. A k -face is a k -dimensional convex polyhedron.
3. A **vertex** of a polyhedron is a point of a 0-face of P . A side of a polyhedron P is an $(m - 1)$ -face. A **ridge** of a convex polyhedron P is a side of a side of P , that is an $(m - 2)$ -face.
4. We assume P to be a three-dimensional polyhedron. The two-faces are called facets or simply faces, the one-faces are called **edges**, and the zero-faces vertices. [84]

Definition 5.1.2.11. A **flag** of an n -dimensional convex polyhedron P is a sequence

$$\mathcal{F} = \{F_0, F_1, \dots, F_{n-1}\},$$

where F_i is an i -dimensional (closed) face of P , and $F_{i-1} \subset F_i$ for $i = 1, 2, \dots, n - 1$. [103]

Remark 5.1.2.12. We recall the definition of a symmetry group $\mathcal{S}(Y)$ of a set Y (4.3.1.1, p.82). Bear in mind that we denote the collection of the sides of a polyhedron with \mathcal{S} , whereas the symmetry group of a polyhedron P is denoted by $\mathcal{S}(P)$.

Definition 5.1.2.13. A convex polyhedron P is said to be regular if for any two flags \mathcal{F} and \mathcal{F}' there is a unique motion g of the symmetry group of the polyhedron $\mathcal{S}(P)$ taking \mathcal{F} into \mathcal{F}' . [103]

Definition 5.1.2.14. A **convex fundamental polyhedron** for a discrete group Γ of isometries of \widetilde{M} is a convex polyhedron P in \widetilde{M} , the interior of which is a locally finite fundamental domain for Γ . [84]

Remark 5.1.2.15. The closure of any convex, locally finite fundamental domain for Γ is a fundamental polyhedron for Γ . Thus, the closure of a Dirichlet domain $\overline{D(x)}$ for Γ , in particular, is a convex fundamental polyhedron for Γ . It is called the **Dirichlet polyhedron** for Γ with center x . [84]

Corollary 5.1.2.16. Any discrete group of motions of \widetilde{M} has a convex fundamental domain and therefore a convex fundamental polyhedron. [103]

Definition 5.1.2.17. A convex fundamental polyhedron P for Γ is **exact** if and only if for each side S of P there is an element $\gamma \in \Gamma$ such that $S = P \cap \gamma P$. [84]

Theorem 5.1.2.18. Let P be an exact, convex fundamental polyhedron for Γ . Then Γ is generated by the set

$$\Phi = \{\gamma \in \Gamma \mid P \cap \gamma P \text{ is a side of } P\}. [84]$$

Remark 5.1.2.19. The group Γ is generated finitely if its fundamental polyhedron is finite-sided [84].

5.1.3. Tessellation

Definition 5.1.3.1. A **tessellation** of \widetilde{M} is a collection \mathcal{P} of n -dimensional convex polyhedra in \widetilde{M} such that

1. the interiors of the polyhedra in \mathcal{P} are mutually disjoint,
2. the union of the polyhedra in \mathcal{P} is \widetilde{M} and
3. the collection \mathcal{P} is locally finite. [84]

Remark 5.1.3.2. Using arbitrary closed domains instead of convex polyhedra in the definition given above we obtain a **decomposition** of the space. [103]

Definition 5.1.3.3. A tessellation \mathcal{P} of \widetilde{M} is **exact** if and only if each side S of a polyhedron P in \mathcal{P} is a side of exactly two polyhedra P and Q in \mathcal{P} . [84]

Definition 5.1.3.4. A collection \mathcal{P} of n -dimensional polyhedra in \widetilde{M} is said to be **connected** if and only if for each pair P, Q in \mathcal{P} there is a finite sequence P_1, \dots, P_m in \mathcal{P} such that $P = P_1$, $Q = P_m$, and P_{i-1} and P_i share a common side for each $i > 1$. [84]

- Remark 5.1.3.5.**
1. Every exact tessellation is connected. [84]
 2. An exact decomposition is sometimes called a normal decomposition.
 3. Any tessellation can be **normalized** by introducing **false faces**. Here, we define any nonempty intersection which does not contain any other intersection of the same dimension as being a false face. The **bricklaying (brick tessellation)** (see Figure 5.2) becomes an exact tessellation by viewing the rectangles as hexagons. [103]

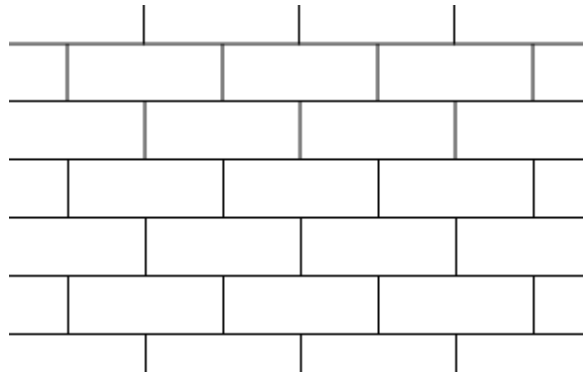


Figure 5.2.: The brick tessellation is an example for a non-exact tessellation. [125]

Theorem 5.1.3.6. *Let P be an n -dimensional convex polyhedron in \widetilde{M} and let Γ be a group of isometries of \widetilde{M} . Then Γ is discrete and P is an (exact) fundamental polyhedron for Γ if and only if*

$$\mathcal{P} = \{\gamma P \mid \gamma \in \Gamma\}$$

is an (exact) tessellation of \widetilde{M} .

Remark 5.1.3.7. The polyhedra $\gamma P, \gamma \in \Gamma$ are said to be **chambers** or **cells** of the tessellation. [103]

5.2. Gluings

We now have a sufficient theoretical basis for developing a construction of metric spaces by gluing the sides of convex polyhedra – gluings. While we consider the theoretical background for gluings in section 5.2.1, we shall focus on the necessary preconditions of a gluing being a manifold in section 5.2.2.

5.2.1. Theoretical Background

In this section, we closely follow [84].

5.2.1.1. Side-Pairing

Let P be an n -dimensional convex fundamental polyhedron and \mathcal{S} the set of all its sides. From the definition of an exact (5.1.2.17, p.103) and convex fundamental polyhedron P for Γ follows directly that if S is a side of P there is a uniquely determined nontrivial element $\gamma_S \in \Gamma$ such that

$$S = P \cap \gamma_S P$$

and $S' = \gamma_S^{-1} S$ is a side of P . The side S' is said to be **paired** to the side S by the element $\gamma_S \in \Gamma$. Since $S' = \gamma_S^{-1} S$, S is paired to S' by γ_S^{-1} and we have $S'' = S$.

The set

$$\Phi = \{\gamma_S \mid S \in \mathcal{S}\}$$

is called the Γ -**side-pairing** (cf. 5.1.2.18) and its elements are the **side-pairing transformations**.

For every side $S' \in \mathcal{S}$, there is a $\gamma_S \in \Phi$ such that $\gamma_S(S') = S$. It follows immediately that $\gamma_S \gamma_{S'} = \gamma_S \gamma_S^{-1} = id$.

Two points x, x' of P are said to be **paired** by Φ if and only if there are sides S, S' such that $x \in S, x' \in S'$ and $\gamma_S(x) = x'$. We write $x \simeq x'$. If $x \simeq x', \gamma_{S'}(x') = x$, and thus, $x' \simeq x$. Two points x, y are said to be **related** by Φ ($x \sim y$), if either $x = y$ or there is a finite sequence of points x_1, \dots, x_m of points of P such that

$$x = x_1 \simeq x_2 \simeq \dots \simeq x_m = y.$$

Being related by Φ is an equivalence relation on the set P . The equivalence classes are called **cycles** of Φ . For the cycle containing x we shall write $[x]$.

If P is an exact, convex fundamental polyhedron for Γ , the cycle for every point x is finite and is given by $[x] = P \cap \Gamma x$.

[84]

5.2.1.2. Dihedral Angle

Remark 5.2.1.1. 1. **Assumption:** From now on we require the dimension of any space mentioned in the following to be of dimension $n > 1$.

2. A hyperplane of a space \widetilde{M} is a flat subset of \widetilde{M} of codimension 1, here $(n - 1)$.

Definition 5.2.1.2. Sides S and T of an n -dimensional convex polyhedron are said to be **adjacent** if and only if $S \cap T$ is a side of both S and T .

Let S and T be sides of the n -dimensional convex polyhedron P in \widetilde{M} and $\langle S \rangle, \langle T \rangle$ the hyperplanes of \widetilde{M} such that $S \subset \langle S \rangle$ and $T \subset \langle T \rangle$. Then $\langle S \rangle$ and $\langle T \rangle$ divide \widetilde{M} in four

half-spaces, one of which contains P . It is

$$\langle S \rangle \cap \langle T \rangle = \langle S \cap T \rangle.$$

For an $x \in S \cap T$, we denote the geodesic lines which satisfy

1. $\lambda(0) = x = \mu(0)$,
2. λ, μ are normal to $\langle S \rangle, \langle T \rangle$,
3. $\lambda'(0), \mu'(0)$ are directed away from the half-space of \widetilde{M} containing P

with $\mu, \lambda : \mathbb{R} \rightarrow \widetilde{M}$. The angle α between λ and μ does not depend on the choice of the point x .

Definition 5.2.1.3. *The dihedral angle $\Theta(S, T)$ between two sides S and T of a convex fundamental polyhedron P is defined as*

- $\Theta(S, T) = \pi$ if $S = T$,
- $\Theta(S, T) = 0$ if S and T are non-adjacent, distinct sides,
- $\Theta(S, T) = \pi - \alpha$ if S and T are adjacent sides of P .

Remark 5.2.1.4. In general, the dihedral angle $\Theta(S, T)$ satisfies $0 \leq \Theta(S, T) \leq \pi$. If $0 < \Theta(S, T) < \pi$, the dihedral angle is said to be **proper**. This is the case if and only if the sides are distinct adjacent sides. [84]

5.2.1.3. Cycle Relations and Cycles of Polyhedra

Definition 5.2.1.5. *A cycle of polyhedra in \widetilde{M} is a finite set*

$$\mathcal{C} = \{P_0, \dots, P_{m-1}\}$$

of n -dimensional convex polyhedra in \widetilde{M} such that for each $i \pmod{m}$

1. *there are adjacent sides S_i, S_{i+1} of P_i such that $P_i \cap P_{i+1} = S_{i+1}$,*
2. *$\sum_{i=0}^{m-1} \Theta(S_i, S_{i+1}) = 2\pi$, and*
3. *$R = \bigcap_{i=0}^{m-1} P_i$ is a side of $S_i \forall i$.*

Remark 5.2.1.6. Let R be a ridge of a polyhedron P in an exact tessellation \mathcal{P} of \widetilde{M} . Then the set of all polyhedra in \mathcal{P} containing R forms a cycle, the intersection of which is R .

Definition 5.2.1.7. Let R be a side of a side S of P . We define a sequence $\{S_i\}_{i=1}^{\infty}$ of sides of P inductively as follows:

1. Let $S_1 = S$.
2. Let S_2 an adjacent side to S'_1 such that $\gamma_{S_1}(S'_1 \cap S_2) = R$.
3. Let S_{i+1} be an adjacent side to S'_i such that $\gamma_{S'_i}(S'_i \cap S_{i+1}) = S'_{i-1} \cap S_i$.

We call $\{S_i\}_{i=1}^{\infty}$ the **sequence of sides** of P determined by R and S .

Theorem 5.2.1.8. Let R be a side of a side S of an exact, convex, fundamental polyhedron P for Γ and let $\{S_i\}_{i=1}^{\infty}$ be the sequence of sides of P determined by S and R . Then there is at least a positive integer l and a positive integer k such that

1. $S_{i+l} = S_i, \forall i$,
2. $\sum_{i=1}^l \Theta(S'_i, S_{i+1}) = 2\pi/k$ and
3. the element $\gamma_{S_1} \dots \gamma_{S_l}$ has order k .

The finite sequence $\{S_i\}_{i=1}^l$ is called the **cycle of sides** determined by R and S of P and the corresponding element $\gamma_{S_1} \gamma_{S_2} \dots \gamma_{S_l}$ of Γ is called the **cycle transformation**. It determines a **cycle relation**

$$(\gamma_{S_1} \gamma_{S_2} \dots \gamma_{S_l})^k = 1$$

of Γ . Since Γ is torsion-free if \widetilde{M} is \mathbb{H}^n or \mathbb{E}^n (4.4.1.1, p.86) and fixed-point-free if $\widetilde{M} = \mathbb{S}^n$ (mentioned in Chapter 4, p.92), $k = 1$. Thus, we have the cycle relation of Γ :

$$\gamma_{S_1} \gamma_{S_2} \dots \gamma_{S_l} = 1.$$

$S_1 S_2 \dots S_l$ is called the **word** in \mathcal{S} corresponding to the cycle relation $\gamma_{S_1} \gamma_{S_2} \dots \gamma_{S_l}$.

Each side S of P determines a **side-pairing relation**:

$$g_S g_{S'} = id. \text{ [84]}$$

5.2.2. Gluing Manifolds

Remark 5.2.2.1 (Notation). Let G be a group of isometries of the three-dimensional space \widetilde{M} and \mathcal{P} a finite family of disjoint convex polyhedra in \widetilde{M} .

Definition 5.2.2.2. A G -side-pairing for \mathcal{P} is a subset

$$\Phi = \{g_S : S \in \mathcal{S}\},$$

of G , indexed by the collection \mathcal{S} of all sides of the polyhedra in \mathcal{P} such that for each side $S \in \mathcal{S}$,

1. there is a side S' in \mathcal{S} such that $g_S(S') = S$,
2. the isometries g_S and $g_{S'}$ satisfy the relation $g_{S'} = g_S^{-1}$,
3. if S is a side of P in \mathcal{P} and S' is a side of P' in \mathcal{P} , then

$$P \cap g_S(P') = S.$$

Remark 5.2.2.3. S' is uniquely determined by S . Here Φ defines an equivalence relation on $\Pi = \bigcup_{P \in \mathcal{P}} P$. The equivalence classes are called **cycles**.

Remark 5.2.2.4 (Solid Angle). Let P be a polyhedron of \mathcal{P} and $x \in P$. Let r be the radius of the open ball with center x : $B(x, r) = \{y \in P \mid d(x, y) < r\}$ such that $B(x, r)$ does not intersect with any side of P not containing x . We define the **solid angle** ω subtended by P at x to be the real number:

$$\omega = 4\pi \frac{\text{Vol}(P \cap B(x, r))}{\text{Vol}(B(x, r))}.$$

For a finite cycle $[x] = \{x_1, \dots, x_m\}$ let P_i be the polyhedron containing x_i and ω_i the solid angle subtended by P_i at x_i for every $1 \leq i \leq m$. The **solid angle sum** is defined by

$$\omega[x] = \omega_1 + \dots + \omega_m.$$

If $x \in P^\circ$, $P \in \mathcal{P}$, the cycle $[x]$ consists only of the point x , and thus, $[x] = \{x\}$. Therefore, $\frac{\text{Vol}(P \cap B(x, r))}{\text{Vol}(B(x, r))} = 1$ and $\omega[x] = 4\pi$. If x is in the interior of a side of a polyhedron $P \in \mathcal{P}$, then $[x] = \{x, x'\}$ and $\frac{\text{Vol}(P \cap B(x, r))}{\text{Vol}(B(x, r))} = \frac{1}{2}$. Here, either $x = x'$ and $\omega[x] = 2\pi$, or $x \neq x'$ and $\omega = 2\pi + 2\pi = 4\pi$.

Remark 5.2.2.5 (Dihedral Angle Sum). If x is a point in the interior of an edge of a polyhedron P° in \mathcal{P} , every point of the cycle $[x]$ is in the interior of an edge of a polyhedron in \mathcal{P} . In this case, the cycle $[x]$ is called **edge cycle** of Φ . The **dihedral angle sum** of the edge cycle $[x]$ is defined to be the real number

$$\Theta[x] = \Theta_1 + \dots + \Theta_m,$$

where Θ_i is the dihedral angle of P_i along the edge containing x_i for each i .

It is $\omega_i = 2\Theta_i$ and therefore, $\omega[x] = 2\Theta[x]$.

Definition 5.2.2.6. A G -side-pairing Φ for \mathcal{P} is **proper** if and only if each cycle of Φ is finite and has a solid angle sum of 4π .

Definition 5.2.2.7. Let G be a group of isometries of \widetilde{M} . A space M obtained by gluing together a finite family \mathcal{P} of disjoint convex polyhedra in \widetilde{M} by a proper G -side-pairing Φ is the quotient space of $\Pi = \bigcup_{P \in \mathcal{P}} P$ by cycles of Φ . The space M is said to be obtained by gluing together the polyhedra in \mathcal{P} by Φ . We call M a **gluing**.

Remark 5.2.2.8. A (\widetilde{M}, G) -map is a continuous map f between two (\widetilde{M}, G) -manifolds N, M such that if $\varphi : U \subset M \rightarrow \widetilde{M}$ is a chart of M and $\psi : V \subset N \rightarrow \widetilde{M}$ is a chart of N with $U \cap f^{-1}(V)$ not empty, the function $\psi \circ f \circ \varphi^{-1}$ agrees locally with an element of G .

Theorem 5.2.2.9. Let G be a group of isometries of \widetilde{M} and let M be a gluing of polyhedra \mathcal{P} by Φ . Then M is a three-dimensional manifold with an (\widetilde{M}, G) -structure such that the natural injection of P° into M is an (\widetilde{M}, G) -map for each P in \mathcal{P} .

Remark 5.2.2.10. 1. If the gluing M is a manifold it is said to be a **gluing manifold**.

2. The identifications $S \rightarrow S'$ give the generators of the holonomy group Γ of $M = \widetilde{M}/\Gamma$.
3. The triplets (S, γ_S, S') are called gluing data and the quotient space M is completely described by the fundamental polyhedron and the gluing data.

To prove if a given G -side-pairing is indeed proper, there is a very useful theorem:

Theorem 5.2.2.11. Let G be a group of orientation-preserving isometries of \widetilde{M} and let $\Phi = \{g_S : S \in \mathcal{S}\}$ be a G -side-pairing for a finite family \mathcal{P} of disjoint convex polyhedra in \widetilde{M} . Φ is proper if and only if

1. each cycle of Φ is finite,
2. the isometry g_S fixes no point of S' for each S in \mathcal{S} , and
3. each edge cycle of Φ has dihedral angle sum 2π .

Remark 5.2.2.12. Under which circumstances is a gluing complete? A spherical gluing is always complete since it is compact. An Euclidean gluing is complete if and only if the fundamental polyhedron is finite-sided. The hyperbolic case is more complex. A necessary condition for a hyperbolic gluing is that the fundamental polyhedron is finitely sided. The sufficient conditions can be read in [84, p.508].

Every compact manifold of constant curvature can be described by a convex fundamental polyhedron which determines the manifold's geometry, and the gluing data which gives the topology of M . The converse is stated in **Poincaré's Polyhedron Theorem**:

Theorem 5.2.2.13 (Poincaré’s Polyhedron Theorem). *Let Φ be a proper $\text{Isom}(\widetilde{M})$ -side-pairing for an n -dimensional convex polyhedron P in \widetilde{M} such that the $(\text{Isom}(\widetilde{M}), \widetilde{M})$ -manifold M , obtained by gluing together the sides of P by Φ , is complete. Then the group Γ generated by Φ is discrete and acts freely. Furthermore, P is an exact, convex fundamental polyhedron for Γ . If \mathcal{S} is the set of sides of P and \mathcal{R} the set of words in \mathcal{S} corresponding to all the side-pairings and cycle relations of Γ , then $(\mathcal{S}, \mathcal{R})$ is a group representation for Γ under the mapping $S \mapsto \gamma_S$.*

5.2.3. Volumes of Space Forms

Proposition 5.2.3.1. If a fundamental domain D of a group Γ satisfies

$$\text{vol } D^\circ = \text{vol } D, \tag{5.1}$$

then

$$\text{vol } X/\Gamma = \text{vol } D.$$

In particular, $\text{vol } X/\Gamma < \infty$ if and only if $\text{vol } D < \infty$. [103]

Corollary 5.2.3.2. *The volumes of all fundamental domains of the group Γ satisfying condition (5.1) are equal. [103]*

5.3. Euclidean Space Forms

We already know that there are six compact, orientable, three-dimensional Euclidean manifolds according to the six orientation-preserving Bieberbach groups (see section 4.4.2.1, p.88). We shall describe these manifolds as gluings.

There are two regular tessellations of the three-dimensional Euclidean space. The fundamental polyhedron of a flat space form is either a parallelepiped or a hexagonal prism. The topology of the manifolds depends on the way facets are identified by pairs.

Remark 5.3.0.3. We shall use the notation used in section 4.4.2.1, p.88.

5.3.0.1. Fundamental Polyhedron: Parallelepiped

For a visualization of fundamental polyhedra and the side-pairing see Figure 5.3(a). We shall use the notation introduced in 4.4.2.9 (p.89).

\mathcal{G}_1 , the Three-Dimensional Torus: opposite facets are identified by translations.

Holonomy Group: $\{1\}$;

Side-Pairing:

$$ABCD \longleftrightarrow A'B'C'D', \quad ABB'A' \longleftrightarrow DCC'D', \quad ADD'A' \longleftrightarrow BCC'B'$$

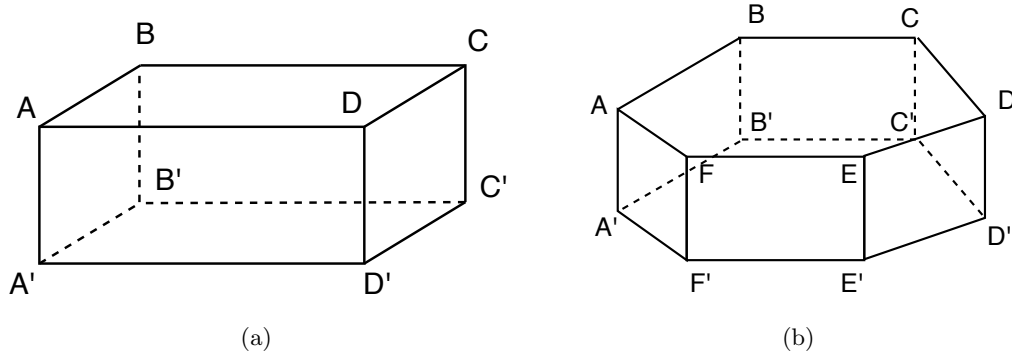


Figure 5.3.: Fundamental polyhedra for Euclidean space forms. (a): the parallelepiped; (b): the hexagonal prism. [55]

\mathcal{G}_2 , **the Half-Turn Cube Space**: opposite facets are identified; one pair being rotated by π .

Holonomy Group: \mathbb{Z}_2 ;

Side-Pairing:

$$ABCD \longleftrightarrow C'D'A'B', \quad ABB'A' \longleftrightarrow DCC'D', \quad ADD'A' \longleftrightarrow BCC'B'$$

\mathcal{G}_4 , **the Quarter-Turn Cube Space**: opposite facets are identified; one pair being rotated by $\pi/2$. Without loss of generality, we can assume the top and bottom facet to be rotated by a quarter turn. To avoid distortions, these facets must be chosen to be squares.

Holonomy Group: \mathbb{Z}_4 ;

Side-Pairing:

$$ABCD \longleftrightarrow B'C'D'A', \quad ABB'A' \longleftrightarrow DCC'D', \quad ADD'A' \longleftrightarrow BCC'B'$$

\mathcal{G}_6 , **the Double Cube Space (Hantzsche-Wendt manifold)**: one pair of opposite facets are identified and the four remaining facets are identified in such a way that each pair consists of adjacent sides. All pairs are rotated by π . See Figure 5.4.

Holonomy Group: $\mathbb{Z}_2 \times \mathbb{Z}_2$;

Side-Pairing:

$$ADD'A' \longleftrightarrow C'B'BC, \quad ABB'A' \longleftrightarrow CDAB, \quad DD'C'C \longleftrightarrow C'D'A'D'$$

Every edge cycle consists of exactly four points. All dihedral angles Θ_i are $\pi/2$. Thus, the dihedral angle sum of each edge cycle is $\Theta = 2\pi$. Hence, the obtained gluings are manifold by Theorem 5.2.2.11.

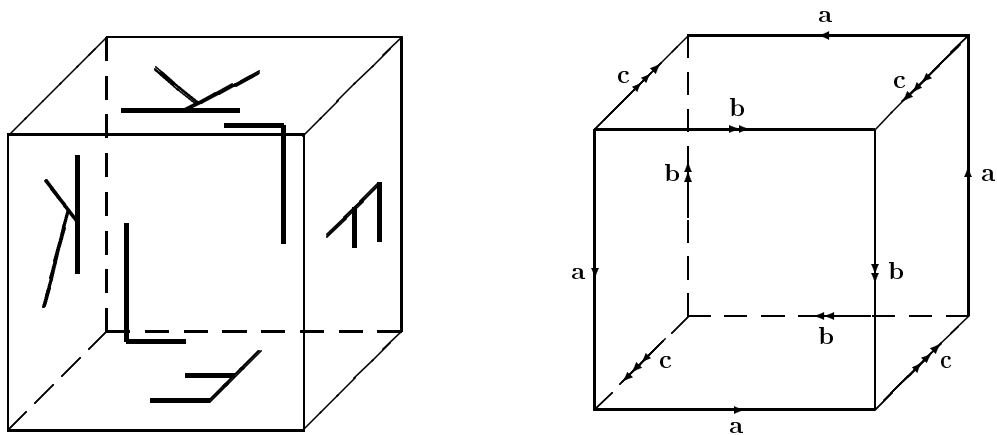


Figure 5.4.: The space form \mathcal{G}_6 as gluing manifold. Left: Facets are identified by pairs. Right: Edge cycles. [37]

5.3.0.2. Fundamental Polyhedron: Hexagonal Prism

See Figure 5.3(b) for a visualization of the fundamental polyhedron and the side-pairing.

\mathcal{G}_3 , the Third-Turn Hexagonal Prism Space: opposite facets are identified. The top facet is rotated by the angle $\frac{2\pi}{3}$ with respect to the bottom face.

Holonomy Group: \mathbb{Z}_3 ;

Side-Pairing:

$$ABCDEF \longleftrightarrow C'D'E'F'A'B', \quad AA'F'F \longleftrightarrow CC'D'D, \quad EE'D'D \longleftrightarrow AA'B'B$$

\mathcal{G}_5 , the Sixth-Turn Hexagonal Prism Space: opposite facets are identified. The top facet is rotated by the angle $\frac{\pi}{3}$ with respect to the bottom face.

Holonomy Group: \mathbb{Z}_6 ;

Side-Pairing:

$$ABCDEF \longleftrightarrow B'C'D'E'F'A', \quad AA'F'F \longleftrightarrow CC'D'D, \quad EE'D'D \longleftrightarrow AA'B'B$$

[55], [84], [2]

5.4. Spherical Space Forms

In this section we follow [33] if not cited otherwise.

In Chapter 4 we classified all the three-dimensional spherical space forms. We shall describe a selected number of them as gluings.

Remark 5.4.0.4. The volumes of spherical space forms is given by:

$$\text{vol } \mathbb{S}^n/\Gamma = \frac{\text{vol } \mathbb{S}^n}{|\Gamma|} = \frac{2\pi^2 R^3}{|\Gamma|},$$

where R is the radius of the three-dimensional sphere. [103]

5.4.1. Lens Spaces

A **lens space** $L(p, q)$, with p and q relatively prime and $0 < q < p$, is obtained by identifying the lower surface of a lens-shaped solid to the upper surface with a q/p twist (see Figure 5.5).

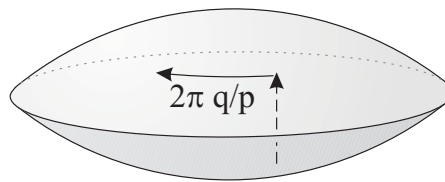


Figure 5.5.: The fundamental domain of a lens space $L(p, q)$ [33]

Since \mathbb{S}^3 is compact, it is tiled by a finite account of fundamental domains. If we consider the lens space $L(p, q)$, the UCS is tiled by p copies of the lens-shaped fundamental domain.

Two lens spaces $L(p, q)$, $L(p', q')$ are homeomorphic if and only if $p = p'$ and either $q = \pm q' \pmod{p}$ or $qq' = 1 \pmod{p}$.

The following finite groups of $SO(4)$ are isomorphic to the holonomy group of a lens space:

$\Gamma = \mathbb{Z}_n$: acts by single action and gives a lens space $L(n, 1)$.

$\Gamma = \mathbb{Z}_n \times \mathbb{Z}_m$: acts by double action and gives a lens space $L(mn, q)$ (see Chapter 4 for a detailed list).

$\Gamma = L \times R$ with L, R cyclic groups: acts by linked action of \mathbb{S}^3 and gives a lens space $L(p, q)$.

The majority of spherical space forms are lens spaces.

5.4.2. Polyhedral Spaces

Prism Manifold: $\Gamma = D_m^*$ acts by single action; the fundamental domain is a $2m$ -sided prism; $4m$ of which tile \mathbb{S}^3 .

Truncated Cube Space: $\Gamma = T^*$ acts by single action; the fundamental domain is a regular octahedron; 24 of which tile \mathbb{S}^3 .

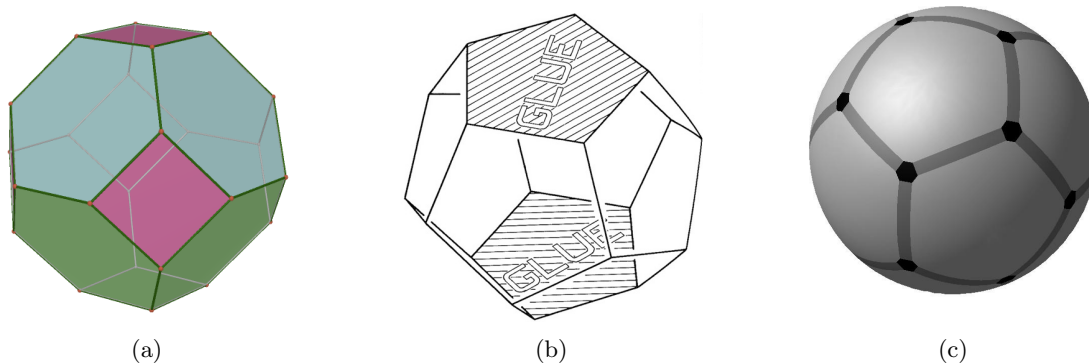


Figure 5.6.: (a): The fundamental domain of the octahedral space. [126] (b): Side-pairing of the fundamental polyhedron for the Poincaré dodecahedral space. [127] (c): Dodecahedron with dihedral angle 180° . [55]

Octahedral Space: $\Gamma = O^*$ acts by single action; the fundamental domain is a truncated cube (see Figure 5.6(a)); 48 of which tile \mathbb{S}^3 .

Remark 5.4.2.1. The names for \mathbb{S}^3/O^* and \mathbb{S}^3/T^* are not unique in the literature. Some authors name the space in order of their fundamental domain, others name the spaces base on their covering group Γ . We chose the latter usage.

Poincaré Dodecahedral Space (PDS): $\Gamma = I^*$ acts by single action; the fundamental domain is a regular dodecahedron; 120 of which tile \mathbb{S}^3 . Therefore, the globally homogeneous space form has a volume of $V_{PDS} = 1/120 \cdot V_{sphere}$.

Because of the importance of the Poincaré dodecahedral space in cosmology, we ought to consider this space in more detail: let us denote the regular spherical dodecahedron inscribed in with $\mu, \lambda : \mathbb{R} \rightarrow \widetilde{M}$ the two-dimensional sphere of radius r , with $0 < r \leq \pi/2$, as $D(r)$. The dihedral angle of the Euclidean regular dodecahedron is approximately $116^\circ 34'$. The dihedral angle $\Theta(r)$ of $D(r)$ is, in general, bigger than that of a Euclidean regular dodecahedron. If r is small, $\Theta(r)$ is approximately $116^\circ 34'$. If r is increasing, $\Theta(r)$ increases continuously. The biggest dihedral angle $\Theta(\pi/2) = \pi$ is obtained if the facets of the dodecahedron lie on \mathbb{S}^2 (see fig. 5.6(c)). The function $r \mapsto \Theta(r)$ is continuous, thus, there is an r such that $\Theta(r) = 120^\circ$. Let us denote this dodecahedron as P . We define an $Isom(\mathbb{S}^3)$ -side-pairing Φ by identifying opposite sides with a twist of $\pi/5$ (see fig. 5.6(b)). Here, every edge cycle consists of three points, each of which having a dihedral angle of $2\pi/3$ (see fig. 5.7(b)). Therefore, the dihedral angle sum $\Theta(r) = 2\pi$. Hence, the space obtained by gluing together the sides of P by Φ is a spherical three-dimensional manifold. [84]

5.5. Hyperbolic Space Forms

Since there is no classification of hyperbolic space forms, we shall give several examples of these manifolds.

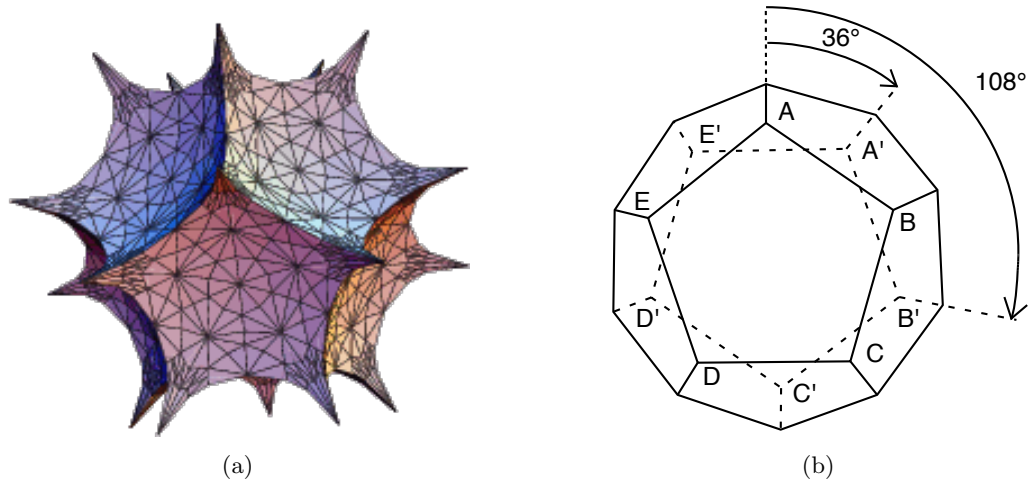


Figure 5.7.: (a): A hyperbolic dodecahedron. [128] (b): The side-pairing of the Poincaré dodecahedral space or the Seifert-Weber dodecahedral space. [55]

Seifert-Weber dodecahedral space: The fundamental polyhedron of the Seifert-Weber dodecahedral space is a hyperbolic dodecahedron (see fig 5.7(a)). As in the spherical space, we denote the dodecahedron inscribed on the two-dimensional sphere with radius $0 < r < 1$ as $D(r)$. If r is small, the dihedral angle $\Theta(r)$ is approximately $116^\circ 34'$, but smaller. Increasing r to 1 leads to a decreasing of $\Theta(r)$ to its minimal value of 60° . Since, as before, the map $r \mapsto \Theta(r)$ is continuous, there is an $r \in (0, 1)$ such that $\Theta(r) = 2\pi/5$. Let us denote this hyperbolic dodecahedron as P . We define a proper $Isom(\mathbb{H}^3)$ -side-pairing Φ by identifying opposite sides with a twist of $3\pi/5$. Every edge cycle consists of five points, each having a dihedral angle of $2\pi/5$ (see fig. 5.7(a) Right). Thus, the dihedral angle sum is 2π . Hence, the space obtained by gluing P by Φ is a hyperbolic three-dimensional manifold. [84]

Löbell Space: The fundamental polyhedron of the Löbell space is a polyhedron with 14 sides. Two faces of which are regular rectangular hexagons and the twelve others are regular rectangular pentagons (see fig 5.8(a)). Around each vertex, eight such polyhedra can be glued together and build a tessellation of \mathbb{H}^3 . There are infinitely many proper \mathbb{H}^3 -side-pairings Φ which refer to a hyperbolic three-dimensional manifold. [55]

Best Space: The fundamental polyhedron of Best Space is a regular icosahedron. The

side-pairing (see fig. 5.8(b)) is given by:

$$\begin{aligned}
 ADI &\longleftrightarrow BGC, & ICA &\longleftrightarrow ABC, & EFL &\longleftrightarrow DIK, & DEL &\longleftrightarrow KLD, \\
 GFB &\longleftrightarrow HJK, & FGJ &\longleftrightarrow GJH, & ABE &\longleftrightarrow LJF, & FEB &\longleftrightarrow CGH \\
 AED &\longleftrightarrow KIH, & JKL &\longleftrightarrow CHI & [55]
 \end{aligned}$$

Weeks Space: The fundamental polyhedron of Weeks Space is a polyhedron with 26 vertices and 18 faces (see fig 5.8(c)). Amongst which there are twelve pentagons and six tetragons. So far, the Weeks Space is the hyperbolic manifold with the smallest known volume. Its has a volume of $\text{vol}(\text{WS}) = 0.94272R^3$. The **side-pairing** is given by:

$$\begin{aligned}
 ABTCD &\longleftrightarrow HLDAO, & SEFBA &\longleftrightarrow FMPJE, & RHIJE &\longleftrightarrow IKQLH, \\
 FMXTB &\longleftrightarrow UKZVN, & WNUYC &\longleftrightarrow IJPZK, & CYQLD &\longleftrightarrow MXWNV, \\
 CTXW &\longleftrightarrow HOGR, & KQYU &\longleftrightarrow ERGS, & MPZV &\longleftrightarrow ASGO & [55]
 \end{aligned}$$

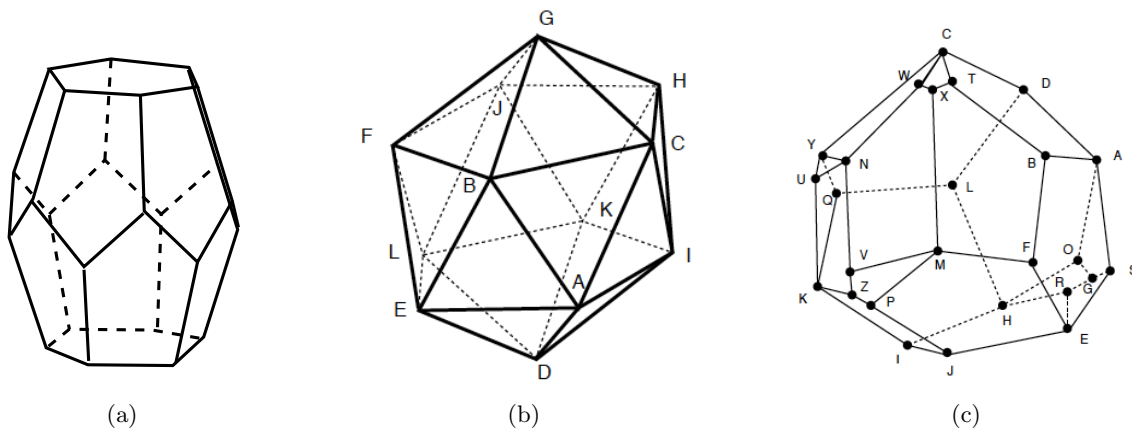


Figure 5.8.: Fundamental polyhedron of the (a) Löbell space (left), (b) Best Space, (c) Weeks Space. [55]

5.6. Conclusion

Any compact Riemannian manifold of constant curvature can be represented as a gluing manifold. Thus, if we assume the spatial part of the universe to be locally isotropic and compact, \mathcal{M}_3 can be obtained by identifying the sides of a convex polyhedron as pairs. This construction enables us to derive methods for detecting the topology of the three-dimensional

manifold we are sitting in. If we determine the fundamental polyhedron and the proper G -side-pairing of the spatial part of the universe, the manifold would be determined completely.

6. Observing the Geometry and Topology of the Universe

In the previous chapters we developed a classification of all geometric structures which are candidates for the geometry of the spatial part \mathcal{M}_3 of space-time \mathcal{M}_4 . For the three-dimensional locally homogeneous and locally isotropic Riemannian manifolds we even developed a classification of their topologies.

As we have explained in Chapter 1, several observational data, such as γ -ray and X -ray maps, the CMB-radiation map, maps of galaxy-distribution in the visible light and the count of radio sources are in confirmation with a locally homogeneous and locally isotropic spatial part of space-time [107]. In Figure 6.1, a map of the distribution of galaxies from the Sloan Digital Sky Survey illustrates the homogeneity and isotropy of the distribution of galaxies.

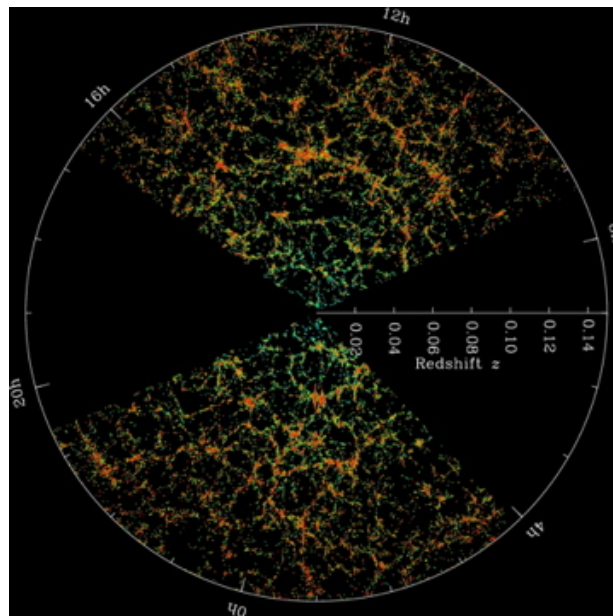


Figure 6.1.: The distribution of galaxies of the Sloan Digital Sky Survey. The earth is located at the center and the radius amounts to two billion light years. Every point represents a galaxy. The black regions are those parts of the universe which we cannot observe, because of dust in the milky way. [129]

The observational data cannot be seen as a proof for local isotropy and local homogeneity of space. It is remarkable that we can detect galaxies which formed approximately 1 Gyr after the Big Bang, which corresponds to a redshift of $z \approx 10$. For a comparison, the first stars and galaxies formed $100 - 270 \text{ Myr}$ after the Big Bang ($z \approx 15 - 30$) [86]. Nevertheless, the part of the universe which we are able to observe will always remain a small portion of our past light-cone. Thus, we are forced to restrict cosmological models by making philosophical assumptions [107].

In the history of cosmology we recognized further and further that our position in the universe is not special. We are on a medium-sized planet, surrounding a medium-sized star, which is located in an arm of a medium galaxy, situated in a medium galaxy cluster. So far, the **Copernican principle** has not been proven wrong. Since additionally isotropy is in confirmation with observational data, it is suitable to assume homogeneity and isotropy. [107] [43]

As pointed out in the first Chapter, standard models of cosmology assume these properties as global properties. This global assumption is called **the cosmological principle**. However, we assume them as local properties since they are derived from observational data. A locally homogeneous and locally isotropic space does not contradict the observational data.

The possible geometric structures and therefore the physics in locally homogeneous and locally isotropic spaces are the same as in globally homogeneous and isotropic spaces. By assuming isotropy and homogeneity as local properties, geometry constrains the topology, but does not dictate it. If global homogeneity and global isotropy are assumed, geometry dictates the topology. [18]

A non-simply-connected shape of the universe cannot be excluded. Geometry determines an exact solution of Einstein's field equations. All spaces with the same geometric structure, the simply-connected and the non-simply-connected ones, are locally identical, and therefore, lead, among others, to the same kinematics, dynamics and inner geometry (angles, distances, area and so forth).

In order to develop an exact solution of Einstein's field equations (see Chapter 1, equation 1.15, p.24), we shall work in the Universal Covering Space (UCS) (2.3.0.15, p.45 and 2.3.0.24, p.46). Since we assume \mathcal{M}_3 to be complete (3.2.3.3, p.62), the UCS is in fact globally homogeneous and globally isotropic. We call the UCS the **physical universe**. If the spatial part of space-time is simply-connected, the covering is trivial. In this case, the UCS $\widetilde{\mathcal{M}}_3$ and the quotient space $\mathcal{M}_3 = \widetilde{\mathcal{M}}_3/\Gamma$ coincide. According to the common designation in cosmology, we shall call space-time models with a simply-connected \mathcal{M}_3 **simply-connected cosmological models (SCM)**. A cosmological model is called **multi-connected (MCM)** if \mathcal{M}_3 is not simply-connected. For a cosmological model with spatial part $\widetilde{\mathcal{M}}_3/\Gamma$, the cosmological model with the same physics, but spatial part of space-time $\widetilde{\mathcal{M}}_3$, is called the **corresponding simply-connected cosmological model** for a MCM $\widetilde{\mathcal{M}}_3/\Gamma$.

The **observational universe** is a sphere with radius $R = \chi_{LSS}$, which is the radius

of the last scattering surface (LSS) (see section 1.3.2, p.34). The last scattering surface determines the limits of observational possibilities, as the universe was opaque before. Every observer in the universe is located at the center of a sphere with $R = \chi_{LSS}$, describing his observational universe. Actual calculations suggest the redshift of the last scattering surface to be $z_{LSS} \approx 1090$ [52]. [55]

6.1. Geometry of the Universe – The State of the Art of Standard Cosmology

6.1.1. Robertson-Walker Metric

We denote by \mathcal{M}_3 the spatial part of the universe at present, i.e. at cosmic time t_0 . Space-time can be seen as foliated by surfaces of homogeneity \sum_t with $t = const.$. Thus, $\sum_{t_0} = \mathcal{M}_3$ [107]. We require the \sum_t to be diffeomorphic $\forall t \in \mathbb{R}_+$ (1.2.6.19, p.29). Thus, the topology and the geometry (up to diffeomorphism) do not change during evolution of the universe. Therefore, we shall write for all \sum_t , \mathcal{M}_3 .

In order to avoid preferred directions, these surfaces of homogeneity must be orthogonal to the worldlines of free-falling observers u^a attending cosmic expansion in an isotropic universe. The metric g_{ab} on \mathcal{M}_4 induces a metric h_{ab} on \mathcal{M}_3 by restricting the action of g_{ab} at each point $p \in \mathcal{M}_3$ to vectors tangent to \mathcal{M}_3 . (See 1.1.5.6, p.20.) [107]

We have seen in Chapter 4 that the only geometric structures for locally homogeneous and locally isotropic Riemannian manifolds are those of constant curvature. (See discussion starting at page 77.) Thus, the UCS of the spatial part of space-time \mathcal{M}_3 is one of \mathbb{E}^3 , \mathbb{S}^3 , \mathbb{H}^3 (4.1.1.2, p.79). The Riemannian curvature tensor (1.1.3.9, p.17), which is constructed from h_{ab} on \mathcal{M}_3 , is of the form

$$R_{ab}^{cd} = K \cdot \delta_{[c}^d \delta_{a]}^b$$

with a scalar K . The trace of R_{ab}^{cd} is the scalar curvature of \mathcal{M}_3 (1.1.3.12, p.18).

Since isotropic observers are orthogonal to the surfaces of homogeneity, the four-dimensional Lorentzian metric of space-time can be written as

$$g_{ab} = -u_a u_b + h_{ab}(t).$$

If we express the last equations in terms of suitable physical coordinates, we get

$$ds^2 = -dt^2 + dl^2, \tag{6.1}$$

where dl^2 describes the metric on \mathcal{M}_3 . [107]

In cosmology it is common to use **comoving coordinates**. Comoving coordinates are coordinates which do not change for a free-falling observer attending cosmic expansion. If \vec{r}

are physical coordinates, the corresponding comoving coordinates \vec{x} are given by

$$\vec{r} = a(t)\vec{x},$$

where $a(t)$ is the **Robertson-Walker scale factor**, which describes the expansion of the universe at cosmic time t . Since we required homogeneity, the scale factor depends only on time and is independent of the spatial position in \mathcal{M}_3 .

By scaling $a(t)$ we obtain the scalar curvature to be one of $+1, 0, -1$, which corresponds to the three possibilities of constant curvature. [60]

The expansion of the universe is often described by **Hubble's scale factor**

$$H(t) = \frac{\dot{a}(t)}{a(t)}.$$

$H(t)$ evaluated at present time t_0 gives the **Hubble constant** H_0 [109].

We shall choose spherical comoving coordinates (χ, Θ, Φ) and a time coordinate t , which represents cosmic time. In spherical coordinates, the proper distance from an observer to an object evaluated at present time t_0 is $d_{proper} = a(t_0)\chi$.

The metric of comoving space is given by $a_0^2 dl^2$, where $a_0 = a(t_0)$ [55]. The geometry of space expands proportionally to the scale factor $a(t)$, which is the same for a multi-connected model and its corresponding simply-connected model. The spaces at time t and t_0 are absolutely homothetic with ratio

$$\frac{a(t)}{a(t_0)} = \frac{1}{1+z},$$

where z is the corresponding redshift at the time t .

Remark 6.1.1.1 (Assumption:). We shall remark that the redshift can be taken as cosmic time since we can assign to each cosmic time t after the Big Bang a unique redshift. To any point P at time t corresponds a point P_{t_0} at time t_0 . In order to avoid confusion of spatial properties of different time, we shall use comoving space.

With comoving coordinates the metric given by equation 6.1 can be written as

$$ds^2 = -c^2 dt^2 + a^2(t) dl^2, \tag{6.2}$$

where c denotes the speed of light.

Corresponding to the scalar curvature K , d_l^2 is one of the following:

- $K=0 \Rightarrow$ Euclidean space;

Cartesian Coordinates: $dl^2 = dx^2 + dy^2 + dz^2$

Spherical Coordinates: $dl^2 = d\chi^2 + \chi^2 d\Theta^2 + \chi^2 \sin^2 \Theta d\Phi^2$, $\chi \in [0; \infty]$.

- $K = +1 \Rightarrow$ Spherical space; spherical (comoving) coordinates are obtained by embedding a three-dimensional sphere with radius $a > 0$ in \mathbb{E}^4 (cf. 1.1.2.21, p.13). The metric dl^2 is given by:

$$dl^2 = d\chi^2 + \sin^2 \chi d\Theta^2 + \sin^2 \chi \sin^2 \Theta d\Phi^2, \quad \chi \in [0; 2\pi].$$

- $K = -1 \Rightarrow$ Hyperbolic space; spherical (comoving) coordinates are obtained by embedding a three-dimensional sphere with radius $-a < 0$ in \mathbb{E}^4 (cf. 1.1.2.21, p.13). The metric dl^2 is given by:

$$dl^2 = d\chi^2 + \sinh^2 \chi d\Theta^2 + \sinh^2 \chi \sin^2 \Theta d\Phi^2, \quad \chi \in [0; \infty].$$

We recall the usage of the convention $c = 1$. In conclusion, the metric given by equation 6.2 can be written as

$$dl^2 = -dt^2 + a^2(t)(d\chi^2 + f^2(\chi)(d\Theta^2 + \sin^2 \Theta d\Phi^2)),$$

with

$$f(\chi) = \begin{cases} \sin \chi & \text{if } K = +1, \\ \chi & \text{if } K = 0, \\ \sinh \chi & \text{if } K = -1. \end{cases}$$

This metric is called **Robertson-Walker metric** and it is the unique metric for (locally) homogeneous and isotropic space-times. Thus, we can choose coordinates such that the metric of space-time has the form given above. According to this metric, the matrix corresponding to g_{ab} has just diagonal entrances due to isotropy:

$$g_{\chi\chi} = \frac{a^2(t)}{1 - K\chi^2}, \quad g_{\Theta\Theta} = a^2(t)\chi^2, \quad g_{\Phi\Phi} = a^2(t)\chi^2 \sin^2 \Theta, \quad g_{00} = -1. \quad [109]$$

6.1.2. Friedmann-Lemaître Universe

Now, we shall derive a family of special solutions of Einstein's field equations for an isotropic and homogeneous universe. In order to derive a solution for \mathcal{M}_3 , we develop a solution for the UCS $\widetilde{\mathcal{M}}_3$, which are then equivalent. At this point it may be recommendable to recall section 1.2.5 (p.22).

The homogeneous and isotropic distribution of matter enables us to treat matter in good approximation as perfect fluid.

Perfect fluid is defined as a medium for which at every point there is a locally inertial Cartesian frame of reference, moving with the fluid, in which the fluid appears the same in all directions. [109, p.521]

Therefore, the energy-momentum tensor T_{ab} (see Chapter 1, p.23) has the form of perfect fluid, which is

$$T_{ab} = \rho u_a u_b + p(g_{ab} + u_a u_b), \quad (6.3)$$

where ρ (the energy density) and p (the pressure) are functions of time only.

The first term $\rho u_a u_b$ of the energy-momentum tensor describes an energy-tensor dominated by non-relativistic matter. The second term $p(g_{ab} + u_a u_b)$ describes the part of the energy-momentum tensor which is dominated by relativistic matter (for example radiation). For present time the latter term is negligible, but it was dominant in the early universe where universe was dominated by radiation. [107]

For a detailed deviation of the Christoffel symbols (1.1.3.4, p.16), the energy-momentum tensor and the Ricci tensor (given by equation 1.6, p.18) of the Robertson Walker metric see, for instance, [109] in terms of Cartesian coordinates or [47] in terms of spherical coordinates. All calculations are made in terms of Cartesian coordinates, where the components of the Robertson-Walker metric are of the form:

$$g_{ij} = a^2(t) \left(\delta_{ij} + K \frac{x^i x^j}{1 - Kx^2} \right), \quad g_{00} = -1, \quad g_{i0} = 0.$$

The indices i and j are running from 1 to 3 and denote the spatial components. The index 0 denotes the time coordinate.

In general, to solve Einstein's field equation

$$G_{ab} = R_{ab} - \frac{1}{2} R g_{ab} = 8\pi T_{ab}, \quad (6.4)$$

one has to solve a system consisting of ten equations according to the components of a tensor with two indices. For an isotropic and homogeneous metric, all off-diagonal components vanish. The "space-space" equations take the form:

$$G_{ab} s^a s^b = 8\pi T_{ab} s^a s^b = 8\pi p, \quad (6.5)$$

where s^a is tangent to \mathcal{M}_3 . The "time-time" equation takes the form:

$$G_{ab} u^a u^b = 8\pi T_{ab} u^a u^b = 8\pi \rho, \quad u^a \in \mathcal{M}_3. \quad (6.6)$$

The Christoffel symbols (1.1.3.4, p.16) can be written in terms of the metric g_{ab} as:

$$\Gamma_{ab}^c = \frac{1}{2} g^{cd} (\partial_a g_{bd} + \partial_b g_{ad} - \partial_d g_{ab}).$$

For Robertson-Walker metric, the Christoffel symbols take the form

$$\Gamma_{ij}^0 = \Gamma_{0j}^i = \Gamma_{i0}^j = a\dot{a} \left(\delta_{ij} + K \frac{x^i x^j}{1 - Kx^2} \right), \quad \Gamma_{0j}^i = \frac{\dot{a}}{a} \delta_{ij} \quad \Gamma_{jl}^i = \tilde{\Gamma}_{jl}^i,$$

where $\tilde{\Gamma}$ denotes the Christoffel symbol of the metric h_{ij} . The Ricci tensor (equation 1.6, p.18) calculates to

$$R_{00} = -3\frac{\ddot{a}}{a}, \quad R_{ij} = \left(2\frac{K}{a^2} + \frac{\ddot{a}}{a} + 2\frac{\dot{a}^2}{a^2}\right). \quad (6.7)$$

Thus, the scalar curvature (1.1.3.12, p.18) is

$$R = -R_{00} + 3R_{ij} = 6\left(\frac{K}{a^2} + \frac{\ddot{a}}{a} + \frac{\dot{a}^2}{a^2}\right).$$

Inserting for Robertson-Walker metric in Einstein's field equations gives for the spatial part

$$G_{ij} = R_{ij} - \frac{1}{2}R = -\frac{K}{a^2} - 2\frac{\ddot{a}}{a} - \frac{\dot{a}^2}{a^2} = 8\pi p. \quad (6.8)$$

For the time coordinate, the corresponding equation is

$$G_{00} = R_{00} + \frac{1}{2}R = 3\left(\frac{K}{a^2} + \frac{\dot{a}^2}{a^2}\right) = 8\pi\rho. \quad [107] \quad (6.9)$$

Using equation 6.8 we can write equation 6.9 as

$$3\frac{\ddot{a}}{a} = -4\pi(\rho + 3p). \quad (6.10)$$

The last equation is called **Raychauduri equation** [43]. Equation 6.9 is called **Friedmann's equation**. It can be written as:

$$\dot{a}^2 + K = \frac{8\pi\rho a^2}{3}. \quad (6.11)$$

Friedmann's equation is true on largest scales, where the expansion of the universe dominates the movements and the cosmological principle is assumed. On smaller scales, for example, at scales of our solar system, of course, movements cannot be described by Friedmann's equation nor atoms in our body expand with time [107] [43]. Cosmological models based on Friedmann's equation (6.11) are called **Friedmann(-Lemaître) universes** [107].

From equation 6.10 and equation 6.11 we can derive a conservation law (see Chapter 1, equation 1.12, p.23):

$$0 = \frac{d\rho}{dt} + \frac{3\dot{a}}{a}(\rho + p). \quad (6.12)$$

From Friedmann's equation 6.10 and the conservation law 6.12 we can derive easily a few details about the dynamics of the universe:

Universe is expanding: If we assume $\rho > 0$ and $p \geq 0$ (assumptions for present time) and a constant scale factor $a(t)$, from equation 6.10 we obtain $\rho = -3p$ which is a contradiction. Thus, the scalar factor $a(t)$ cannot be constant and the universe is expanding or contracting [43]. Observational data indicate that the expansion of the

universe is accelerating at present time [109].

Expansion started a finite time ago: Furthermore, we deduce from equation 6.10 with the assumptions $\rho > 0$ and $p \geq 0$ that $\frac{\ddot{a}}{a} \leq 0$. Thus, expansion started a finite time ago. It started at time t with $a(t) = 0$ [43].

Singularity at the beginning: We derive from the conservation law (equation 6.12) that energy density decreases while the universe is expanding. Thus, the energy density was higher in the past with $\lim_{a \rightarrow 0} \rho = \infty$. In this limit, the worldlines of all particles intersect. The known physical laws break down. This defines a singularity of space-time, and therefore, it has to be excluded from space-time. This singularity cannot be omitted for cosmological models with $(\rho + 3p) > 0$ and where the vacuum energy density is not too large. Hawking and Ellis state (see [43]) that singularities may occur in any reasonable space-time. [43]

By inserting $K = 0$ in Friedmann's equation 6.11, we define the **critical density** of the universe for present time:

$$\rho_{crit,0} = \frac{3H_0^2}{8\pi}. \quad (6.13)$$

Remark 6.1.2.1. Notation: The index 0 always denotes the value for present time t_0 .

If the total energy density ρ_0 of the universe is

- $< \rho_{crit,0} \Rightarrow K = -1$: the universe expands forever and the expansion is accelerating.
- $= \rho_{crit,0} \Rightarrow K = 0$: the universe expands forever with $\lim_{t \rightarrow \infty} \dot{a}(t) = 0$.
- $> \rho_{crit,0} \Rightarrow K = +1$: the expansion of the universe will stop in a finite time and will contract until a **Big Crunch** or it will start to expand at a critical density again. Latter scenario is known as **(Big) Bounce**. [109]

Remark 6.1.2.2. We shall remark that the Big Bang and the Big Crunch cannot be identified since any identifications on the time axis are forbidden (see Chapter 1, section 1.2.6.2, p.28). Nevertheless, events as the Big Bang and a probably future Big Crunch are singularities, and therefore, they are excluded from space-time. [64]

Cosmological Models with $K = 0$ or $K = -1$ are called **open models** whereas cosmological models with $K = +1$ are called **closed cosmological models**.

Remark 6.1.2.3. The name is quite misleading because of the property of a manifold to be open/closed (1.1.1.5, p.8). Here, an open model is forever expanding, whereas a closed model is recollapsing. [56]

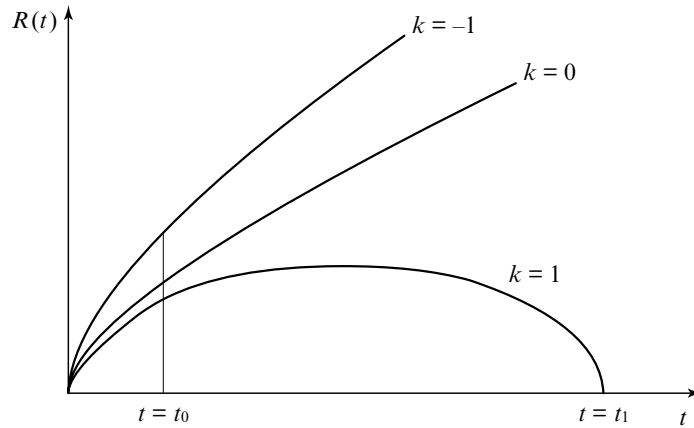


Figure 6.2.: The three different possibilities of long-time evolution of Friedmann-Lemaître universes is presented. For $K = +1$, the universe recollapses at a future time-point. If $K = 0$, universe expands forever with a decreasing velocity. For the case $K = -1$, the universe expands forever. As opposed to the flat case, the velocity does not converge to zero. [47]

The three different possible evolutions of Friedmann-Lemaître universes are visualized in Figure 6.2.

We choose an equation of state of the form $p = w \cdot \rho$ with a time-independent w . If we are inserting $p = w \cdot \rho$ in equation 6.12, we get by solving the differential equation $\rho(t) \propto a^{-3w-3}(t)$. The scalar w depends on the form of energy. We distinguish:

- Cold Matter: non-relativistic matter; for example: dust; pressure is negligible ($p = 0$), and therefore, $\rho \propto a^{-3}$.
- Hot Matter: relativistic matter; for example: radiation; pressure and density are related by $p = \rho/3$, and therefore, $\rho \propto a^{-4}$.
- Vacuum-Energy: In the absence of matter the energy-momentum tensor is proportional to the metric. In this case, we can derive from equation 6.3 for vacuum that there is an energy with $\rho_v = -p_v$. Furthermore, we can deduce from equation 6.12 that the energy density is constant. [109]

According to the three different types of energy (matter, radiation and vacuum), the energy density ρ is composed of the matter density ρ_M , the energy density of radiation ρ_γ and the energy density of vacuum energy ρ_Λ . Thus, we have $\rho = \rho_M + \rho_\Lambda + \rho_\gamma$. Evaluated for the present time and using Hubble's scale factor, Friedmann's equation takes the form:

$$3H_0^2 + 3\frac{K}{a(t_0)^2} = 8\pi(\rho_{M,0} + \rho_{\Lambda,0} + \rho_{\gamma,0}). \quad (6.14)$$

We have developed a formula for the scalar curvature K in terms of the theoretically mea-

surable constants $H_0, \rho_{\gamma,0}, \rho_{\Lambda,0}, \rho_{M,0}$. These are called **cosmological parameters** [108].

It is common, to use the dimensionless numbers

$$\Omega_0 = \frac{\rho_0}{\rho_{crit}}, \Omega_{\Lambda} = \frac{\rho_{\Lambda}}{\rho_{crit}}, \Omega_{\gamma} = \frac{\rho_{\gamma}}{\rho_{crit}} \text{ and } \Omega_M = \frac{\rho_M}{\rho_{crit}}.$$

If $K = 0$, $\Omega_0 = \Omega_{\Lambda} + \Omega_M + \Omega_{\gamma} = 1$. In general, $\Omega_{\Lambda} + \Omega_M + \Omega_{\gamma} + \Omega_K = 1$, where $\Omega_K = \frac{-K}{a_0^2 H_0^2}$.

Previous in this section we have seen that $\rho_m \propto a^{-3}$, $\rho_{\gamma} \propto a^{-4}$ and ρ_{Λ} is constant. Thus,

$$\rho = \rho_{crit,0} \left(\Omega_{\Lambda,0} + \Omega_{M,0} \left(\frac{a_0}{a} \right)^3 + \Omega_{\gamma,0} \left(\frac{a_0}{a} \right)^4 \right). \quad (6.15)$$

An exact solution for Friedmann's equation would be an explicit form of the scale factor $a(t)$. Using equations 6.11, 6.13, 6.15 and $\Omega_K = \frac{-K}{a_0^2 H_0^2}$, we derive

$$H(t) = H_0^2 \left(\Omega_{\Lambda,0} + \Omega_{K,0} \left(\frac{a_0}{a} \right)^2 + \Omega_{M,0} \left(\frac{a_0}{a} \right)^3 + \Omega_{\gamma,0} \left(\frac{a_0}{a} \right)^4 \right).$$

The solution depends on the initial values, i.e. the choice of the cosmological parameters. There exists explicit solutions for the cases $K = 0, \pm 1$. For $K = 0$, the corresponding cosmological model is called **Einstein-de Sitter universe** and the scale factor takes the form $a(t) \propto t^{\frac{2}{3}}$. [109] [108] [43]

6.1.3. Measuring the Cosmological Parameter

In the following, we shall give a short insight into the methods determining the cosmological parameters. There are different methods for every cosmological parameter. We shall present one of them. At the end of each subsection we shall name known problems in calculating the parameter. In general, one has to make a lot of assumptions to measure and calculate the parameters in a sufficient accuracy. We shall quote the values of the cosmological parameters calculated by [52] which assume a Λ CMD model, which is the concordance model today. It is a cosmological model with $\mathcal{M}_3 = \mathbb{E}^3$ which is dominated by vacuum energy and cold dark matter. The authors of [52] combine the 7-year data of WMAP (Wilkinson Microwave Anisotropy Probe) with the distance measurements of BAO (Baryon Acoustic Oscillations), the galaxy distribution derived by Percival et al. (2009) and the measurements of the Hubble constant of Riess et al. (2009). The methods used by [52] require a more complex background than the methods presented here. In this section we shall renounce the convenient choice $c = G = 1$.

6.1.3.1. Hubble Constant H_0

The spectrum of an object is seen with a shift $z = \frac{\lambda - \lambda_0}{\lambda_0}$. Here, λ is the observed wavelength and λ_0 is the emitted wavelength from the source. If $z > 0$, we call z a redshift, whereas $z < 0$ indicates a blueshift. By considering only objects with $z \ll 1$, we can neglect relativistic

phenomena such as time dilation, and therefore, the Lorentz factor γ . If we interpret this shift in terms of the Doppler effect, we can express the shift as a radial velocity $v_r \approx \frac{\lambda - \lambda_0}{\lambda_0} c$.

Empirically, we get: $z = \frac{H_0}{c} d$ for objects with motion which is dominated by the expansion of the universe. Thus, we have $v_r \propto d$ in every direction and for objects with $0.03 < z \ll 1$. The proportional factor H_0 is the above-mentioned **Hubble constant**. For a detailed explanation of the connection between the proportional factor and H_0 see, for instance, [109].

The actual value calculated by [52], where supernovae Ia were used as standard rulers, amounts to

$$H_0 = 70.2 \pm 1.4 \text{ km s}^{-1} \text{ Mpc}^{-1}.$$

Remark 6.1.3.1. Parsec, denoted by [pc], is an often used distance unit in astronomy. It is the parallax to the angular $\varphi = 1''$. Mpc is therefore 10^6 parsec.

Problems: In order to distinguish between motion caused by gravitational effects in the local universe and motion due to cosmic expansion. [108]

Alternative Methods: use Tully-Fisher relation, Faber-Jackson relation, fundamental plane, surface brightness fluctuations and the cosmic microwave background. See [109] for further details.

6.1.3.2. Critical Density ρ_{crit} and Hubble Time T_0

The Hubble constant, gives immediately the critical density:

$$\rho_{crit,0} = \frac{3H_0^2}{8\pi G} = 9.26 \cdot 10^{-27} \text{ kg m}^{-3} = 1.36 \cdot 10^{11} M_\odot \text{ Mpc}^{-3}.$$

Remark 6.1.3.2. The index \odot always denotes the given determinant of the Sun. Hence, M_\odot denotes the mass of the Sun.

If the expansion of the universe has been linear since its beginning, **Hubble time**

$$T_0 < H_0^{-1}.$$

This gives an upper bound for the age of the universe:

$$T_0 = 13.76 \pm 0.11 \text{ Gyr}. [52]$$

Since the expansion of the universe is probably not linear, T_0 serves only as a guidance value.

6.1.3.3. Mass Density ρ_M

Measuring the density of the total amount of matter in the universe is a nontrivial question. Matter in the universe is composed of **luminous matter**, which is directly detectable, and **dark matter**, which is for the major part non-baryonic matter. Baryonic matter is

matter consisting of protons and neutrons. Non-baryonic matter does not consist of the usual nucleons.

Luminous Matter emits radiation and is therefore detectable. The evolution of the stellar energy production as a function of cosmic time z is given by the total luminosity density

$$\epsilon_L(z) = \int_0^\infty L \Phi(L, z) dL \quad z = (z_1, z_2) \dots \text{cosmic time interval} \quad (6.16)$$

$\Phi(L) = n^* \left(\frac{L}{L^*}\right)^\gamma e^{-\frac{L}{L^*}}$ is an approximation of the perturbation of galaxies with luminosity L . This analytic function was derived from Schechter in the 1970s. Thus, this function describes the radiated energy per volume and per time interval. The actual calculated value of ϵ_L is $2 \cdot 10^8 L_\odot Mpc^{-1}$, where an average specific luminosity of $\frac{L}{M} = 0.25 \frac{L_\odot}{M_\odot}$ is assumed. Therefore, we get:

$$\rho_{LM} \approx 5 \cdot 10^{-29} kg m^{-3} \quad \Omega_{LM} \approx 0.005. \quad (6.17)$$

Even if luminous matter was not estimated exactly, we can assume that $\Omega_{LM} \ll 1$.

Problems: We don't know how many radiation is absorbed by dust in galaxies. For measuring we need the best technical equipment available. The precise run of the $\epsilon_l(z)$ is not known, which is a problem for approximating the account of dark energy too. [108]

Dark Matter: 1. The ISM (Interstellar Medium) contains of a view atoms per m^3 . This matter is not bound on galaxies, and therefore, takes part on the galactic expansion.

2. Gravitational Lensing Effect: According to General Theory of Relativity, the paths of light is deflected when it passes through a gravitational field. The angular deflection can be expressed by $\alpha = \frac{4GM_L}{c^2 b}$ where M_L denotes the mass of the gravitational lens and b denotes the transverse distance between the masses center and the path of light. The mass of galaxy clusters indicate that the major part of matter bound in galaxy clusters is dark matter. [108]

The actual value for the density of gravitational mass is approximately

$$\rho_{CDM,0} = 3 \cdot 10^{-27} kg m^{-3} \pm 10 - 15\%, \quad \Omega_{CDM,0} = 0.229 \pm 0.015 \text{ [52]}.$$

Problems: If we calculate the density of baryonic matter which has to be in the universe in conformity with a cosmological model based on a Big Bang scenario, we achieve $\rho_b = 1/10 * \rho_m$ ($\Omega_{b,0} = 0.0458 \pm 0.0016$ [52]). We can conclude that 75 – 80% of the total amount of matter in the universe consists of non-baryonic matter. Potential candidates are: HDM (Hot Dark Matter), for example, relativistic neutrinos; CDM

(Cold Dark Matter), for example, non-relativistic neutrinos and cosmic strings. [108]

Alternative Methods: use the Virial Theorem, anisotropies in the cosmic microwave background, the redshift-luminosity relation of supernovae or X -ray luminosity of clusters and galaxies. For more details see for instance [109].

The actual density parameter of matter amounts to

$$\Omega_M h^2 = 0.1352 \pm 0.0036,$$

where h is the Hubble constant in units of $100 \text{ km s}^{-1} \text{ Mpc}^{-1}$. [52]

6.1.3.4. Radiant Flux Density ρ_γ

We can approximate the radiation produced in all galaxies by $T \cdot \epsilon_L \approx 10^{-15} \text{ J m}^{-3}$, where $T = 15 \pm 3 \text{ Gyr}$ is the age of the universe [108]. The energy density of cosmic microwave background can be calculated by integrating the Rayleigh-Jeans formula and accounts to approximately $4,2 \cdot 10^{-14} \text{ g J m}^{-3}$ [109]. In order to be able to compare these values with mass density we use the famous formula $E = mc^2$ and get:

$$\rho_{\gamma,0} \approx 4 \cdot 10^{-31} \text{ kg m}^{-3} \quad \Omega_{\gamma,0} \approx 4 \cdot 10^{-5} \ll \Omega_{m,0}. \quad (6.18)$$

Thus, we can neglect radiation flux density [108].

6.1.3.5. Energy Density of Vacuum Energy ρ_Λ

Remark 6.1.3.3. Einstein mentioned an additional term $-\Lambda g_{\mu\nu}$ in his field equations, where Λ denotes the **cosmological constant**. He needed a constant because he assumed a steady-state model of the universe, which is a cosmological model which does neither expand nor contract. We have seen that with an isotropic and homogeneous cosmological model this possibility can be ruled out. Therefore, the introduction of the cosmological constant was revised. The observational data of the last ten years indicate an accelerating expansion of the universe. This acceleration is explained by an additional force which satisfies $\rho_v = -p_v$, as we have pointed out in 6.1.2. Thus, the cosmological constant is reintroduced by ρ_Λ . [109]

There are two forces which are accountable for the expansion of the universe: gravity and vacuum energy. These two forces act in reverse directions. While gravity slows expansion down, vacuum energy accelerates it. In order to measure the cosmological constant, we need precise distance measurements to describe expansion of the universe with high accuracy.

If a white dwarf exceeds by mass accretion a certain critical mass, which is called the Chandrasekhar limit, it explodes. This explosion is called a “supernova Ia”. The luminosity function of supernovae Ia are well-studied. The shape of the luminosity function is independent of the time when this space-time event took place. Thus, they are suitable “standard candles” for distances $z > 0.1$.

In 1998, the ‘‘Supernovae Cosmology Project’’ and ‘‘High-z Supernova Search Team’’ compared independently the luminosity distance as a function of redshift derived from observational data of supernovae Ia with the theoretical predictions in a flat universe. The apparent luminosity of supernovae Ia decreases stronger with redshift than expected without vacuum energy. This suggests that the distances are bigger than expected. Best accordance with observable data is achieved with $\Omega_{m,0} = 0.28 \pm 0.1$ and $\Omega_{\Lambda,0} = 1 - \Omega_{m,0}$, which indicates an accelerating expansion of the universe.

It should be noted that it cannot be excluded that the reduction of the apparent luminosity is caused by absorption or light scattering. [109]

The results have been affirmed by several projects. The actual value amounts to

$$\Omega_{\Lambda,0} = 0.725 \pm 0.016. [52]$$

Problems: Dark energy is interpreted as result of quantum fluctuations. ¹ Theoretical calculations obtain a value of $\rho_{\Lambda,0}$ which is 100-times bigger than the value obtained by measurements. [108]

Alternative Methods: Baryonic Acoustic Oscillations (BAO) are used as a standard ruler, which are completely independent from supernovae measurements. Fluctuations of the CMB are compared to today’s density fluctuations calculated with the help of clustering of galaxies. Measurements with the BAO suggest

$$\Omega_0 \approx 1, \Omega_{m,0} \approx 0.3 \Rightarrow \rho_{\Lambda} \approx \Omega_{\Lambda,0} = 0.7.$$

6.1.3.6. Curvature Parameter Ω_K

In conclusion, we shall give an actual estimate of the curvature parameter:

$$-0.0133 < \Omega_k < 0.0084, \text{ (95\% certainty level)}. [52]$$

Recall that $\Omega_k > 0$ corresponds to a scalar curvature $K = -1$ and $\Omega_k < 0$ corresponds to a positive curved space. Thus, today’s observational data prefers slightly a positive curved universe, but no curvature (positive/negative/flat) can be excluded.

6.2. Cosmic Topology

6.2.1. Introduction

By measuring the cosmological parameters, the geometry of universe can be determined. Cosmic Topology focus on the determination of the topology of the universe. Geometry

¹Pairs of Particle-Antiparticle arise spontaneously and discreate immediately. Evidence with the help of the ‘‘Casmir effect’’

does not dictate the topology of space, but topology dictates geometry. Thus, there is hope that Cosmic Topology could derive the curvature of space from the topology of the universe.

In order to measure the cosmological parameters one has to make strong assumptions, as we have seen in the previous section. The concordance model predicts a flat and infinite space, and therefore, a total density parameter of exactly $\Omega_0 = 1$, which is due to measuring inaccuracy not provable. Since it is assumed that the deflection of $\Omega_0 = 1$ ($\Omega_k = 0$) is small, the spatial part of the universe is assumed to be approximately flat. Thus, the curvature radius of \mathcal{M}_3 is assumed to be giant, if it is not infinite. But, giant in correspondence to what? Positively/negatively curved with an enormous curvature radius is still positively/negatively curved. A necessary condition to determine the space's curvature is that the curvature radius is not too big. If the curvature radius is too big or actually infinite, we would not be able to distinguish between a flat and a curved space.

As we have developed in Chapter 5, the space $\mathcal{M}_3 = \widetilde{\mathcal{M}}_3/\Gamma$ can be represented by a fundamental polyhedron with a suitable identification of its sides as pairs. Thus, \mathcal{M}_3 is determined by

1. the Universal Covering Space (UCS) which determines the geometry ($K = 0, -1, 1$),
2. the Fundamental Polyhedron (FP) (5.1.2.14, p.103) and
3. the generators of the holonomy group Γ , which can be interpreted as the identification of the sides of the FP as pairs (5.2.2.10, p.109). The holonomy group is very different for the cases $K = 0, -1, 1$, see 3.4.0.16, p.75. Thus, if we would be able to determine the holonomy group, we would be able to determine geometry. [55]

Before we are able to think of possible methods to determine topology, we have to clarify how a finite three-dimensional space (without boundary) looks from inside. In order to develop an intuition, I recommend the movie “Flatland” (2007) based on the book “Flatland” written by Edwin Abbott Abbott (1884). Furthermore, I can recommend the games of Jeffrey Weeks available on his homepage². Especially the software “Curved Spaces” is recommendable, where a flight through multi-connected universe is simulated. The software “SnapPea” is a giant data base of three-dimensional manifolds with diverse properties and features. Jeffrey Weeks lecture available online³ gives a good first introduction. Furthermore, there is Jean-Paul Luminet’s non-technical book “Wrap around universe” [65].

Assume a two-dimensional being, living on the two-dimensional torus. As we have seen in Chapter 3, a torus can be derived from a rectangle by identifying opposite sides. We chose a small rectangle with respect to the size of the being. Starting in the middle of the rectangle and going straight to the upper edge, as soon as the inhabitant has reached the edge, it finds itself at the lower edge. Leaving the rectangle to the left, it enters it from the right. Looking toward the top side, the being sees its own feet, because the top and bottom

²www.geometrygames.org

³<http://www.wpi.edu/academics/Depts/Math/News/conant.html>

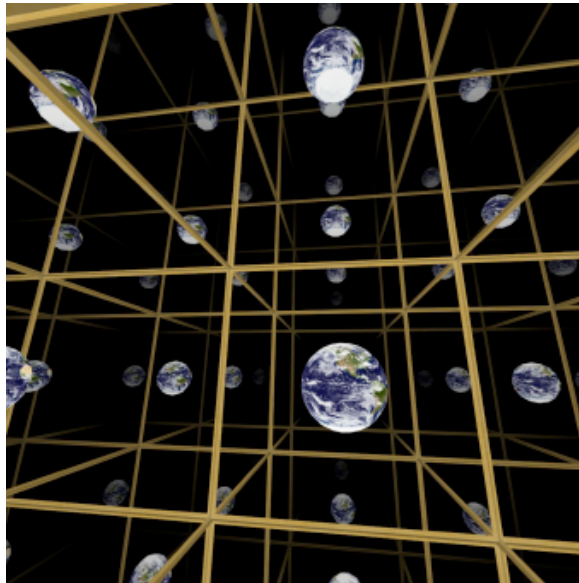


Figure 6.3.: Inner view of a three-dimensional torus. Image was made with the help of the software “Curved Spaces”. [63]

facets are identified. In the same way the being would see its own back if he looks straight ahead. If the FP of the torus is a square, the being sees itself at the same distance if it looks straight up, down, left or right. Looking in the diagonal direction, the distance of its own image is greater. Choosing a general rectangle, the distances of the images derived from the vertical directions differ from those of the horizontal directions. Even if the being sees itself several times, it exists, of course, only once.

We can define an Euclidean metric on the rectangle, and therefore, the surrounding space appears flat and infinite to the being. The point is that the flat torus is locally isometric to \mathbb{R}^2 , because locally we can define an Euclidean metric. The simply-connected infinite Euclidean space and the finite, multi-connected flat torus correspond to the same solution of Einstein’s field equations. As opposed to the global properties, the local properties are the same. While the holonomy group of the Euclidean space is trivial, the generators of the holonomy group of the flat torus is given by two translations which can be interpreted as the side-pairing of the rectangle (see section 5.2.1.1, p.105). Analogously, a three-dimensional torus can be constructed if opposite facets of a parallelepiped are identified (see section 5.3.0.1, p.134). In Figure 6.3 an inner view from a three-dimensional torus is visualized.

Assume a simply-connected domain \mathcal{D} in \mathcal{M}_3 . A path γ in \mathcal{D} starting at x_0 produces a single end point x . The development (see Chapter 3 3.2.2.3, p.60 and Figure 6.4(a)) Δ of \mathcal{D} in the UCS $\widetilde{\mathcal{M}}_3$ does not differ from the original domain. There is a one-to-one correspondence between points in Δ and \mathcal{D} . In the same way, distances between points remain unchanged. If the domain \mathcal{D} is not simply-connected, the path γ produces additional points x', x'', \dots in the UCS. These additional points correspond to the different γ_i which connect the points

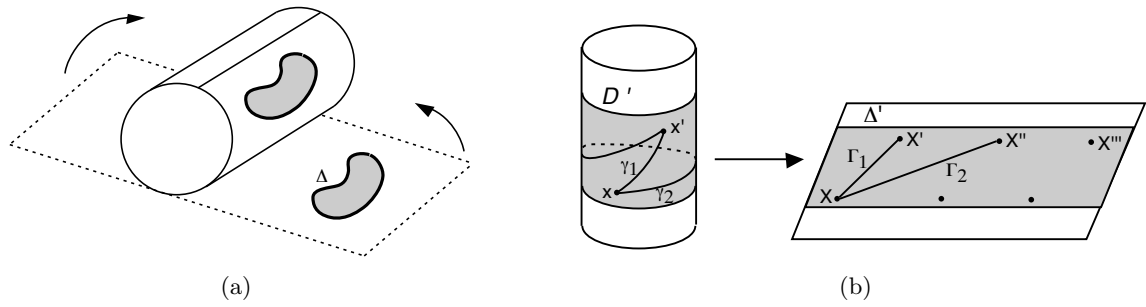


Figure 6.4.: (a) The development Δ of \mathcal{D} , a simply-connected domain on a two-dimensional cylinder, in its UCS, the Euclidean plane, is visualized. (b) If a path is within a simply-connected domain, it produces just a single point x . If the domain is not simply-connected, it produces additional points x', x'' in the UCS. [55]

x_0 and x in \mathcal{D} . (See Figure 6.4(b).) [55]

The FP produces a tessellation $(\gamma FP)_{\gamma \in \Gamma}$ of the UCS with cells γFP (5.1.3.6, p.104). In this context, the FP is called the **fundamental cell**.

According to this discussion, we can describe an important difference between multi-connected and simply-connected cosmological models: the information of an event in space-time reaches us in form of radiation following null geodesics (see section 1.1.4, p.19) starting at the source and ending at the observers position. The proper distance to the events is $d_{proper} = a(t)\chi$. The proper distance shall be independent of the null geodesic. We calculate distances to cosmological events through the redshift z , the luminosity distance d_L or the angular-diameter d_{AD} . All these distances depend on the null geodesic.

In non-compact SCM the null geodesic between a source and an observer is unique. Thus, there is a one-to-one correspondence between real objects in space and events. The only SCM where the null geodesic is not unique is the sphere. Since the sphere is compact, there are several null geodesics connecting an object and an observer.

MCM are compact, and therefore, finite in at least one dimension. Thus, there is no injective correspondence between events with coordinates $S_{obs} = (d_{obs}, \Theta, \Phi)$ and the position of the real objects in space. Because there are in general several null geodesics from a spatial position (object) to an observer, there are associated different images (events) with different redshifts (distances) to a single source. The nearest image is called the “**real object**”, whereas all the others are called “**ghosts**”. See Figure 6.5 for a visualization. The real object and each ghost have a different $S_{obs} = (d_{obs}, \Theta, \Phi)$, but the proper distance is for all the same. If we pass to the (comoving) UCS, we have a one-to-one correspondence between S_{obs} and spatial positions in the UCS. Therefore, the UCS is sometimes called the **observers space**. [55]

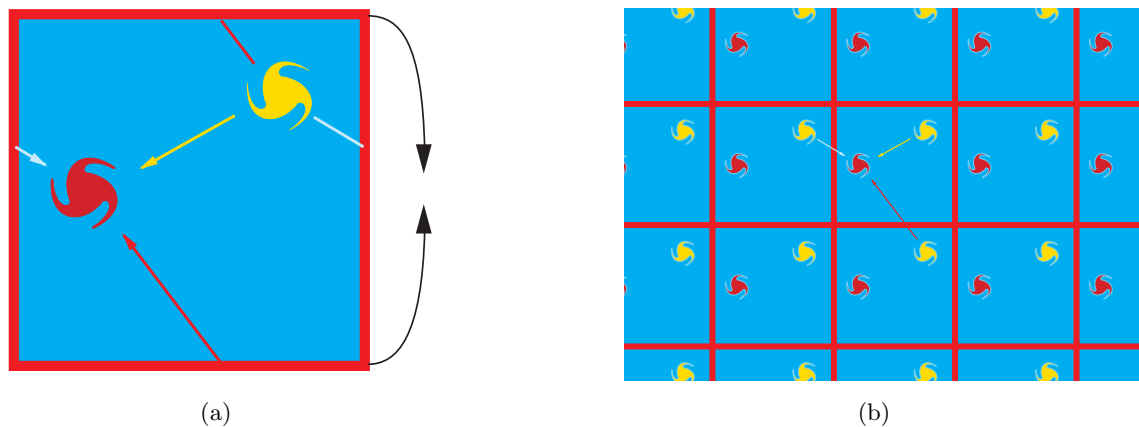


Figure 6.5.: (a): Two galaxies in the fundamental cell of a torus shaped universe. (b): The pattern of these two galaxies produced in the observers space, the UCS. [70]

6.2.2. Finding the Imprints of Multi-Connected Spaces

6.2.2.1. Spatial Scales Associated with the Fundamental Polyhedron

We denote the smallest length associated with the FP, which is the smallest edge, by L_{min} . We call cosmological models with an L_{min} of order $100 - 1,000 Mpc$ a **small universe** [22]. L_{max} denotes the maximum length inscribable in the FP, which is the diameter of the minimal sphere which can be subscribed to the FP. Additionally, we have the same characteristic length as in SCM, for example, χ_{LSS} .

L_{max} is the maximal distance of two images of the same object in adjacent cells. If the observer is located at the center, $\frac{L_{min}}{2}$ or $\frac{L_{max}}{2}$ respectively is the minimal or maximal distance to the boundaries of the FP.

Example 6.2.2.1. For a torus, the FP is a cuboid with length (L_x, L_y, L_z) . In this case $L_{min} = \min\{L_x, L_y, L_z\}$ and $L_{max} = \sqrt{L_x^2 + L_y^2 + L_z^2}$. [55]

6.2.2.2. Distribution of Ghosts in the Observable Universe

We assume the observer to be located at the center of the FP, which is no restriction if space is globally homogeneous. In this case, the nearest possible ghost image is in a distance of $\frac{L_{min}}{2}$. The farthest possible position of a real object is at $\frac{L_{max}}{2}$. Thus, any image nearer $\frac{L_{min}}{2}$ is a real object, images at a distance between $\frac{L_{min}}{2}$ and $\frac{L_{max}}{2}$ can be both real or ghost, and images with a distance greater than $\frac{L_{max}}{2}$ are ghosts.

In general, there are as many ghosts of an object as cells of the FP in the universe. While the number is finite if the geometry is spherical, it is infinite in a universe with flat or hyperbolic geometry. The number of theoretically observable ghosts is the number of cells within the LSS, and therefore, delimited by $(\chi_{LSS}/\sqrt{L_{min}L_{max}})^3$. If we contain the life-time

T of an object in our considerations, the number reduces to $((cT)/\sqrt{L_{min}L_{max}})^3$. Thus, we can only observe ghosts of objects with a life-time $T > L_{min}/c$.

The topology of the universe is not in any case observable. In theory, the topology is detectable if $L_{min} \leq \chi_{LSS}$. If $L_{min} > \chi_{LSS}$, the topology would just be observable if space is not globally homogeneous and we are sitting in a special position. If L_{min} is too big or infinity, we have no chance to detect topology. It is clear that the topology is the easier testable, the smaller the FP is. [55] [66]

6.2.2.3. Searching for Ghosts

If space is small enough for light to have had the time to cross space more than once, than multiple images of one source would occur, as we have argued above. This property of MCM is sometimes called “**topological lensing**” [67]. The obvious method to search for imprints of topology is to search for ghosts. Thus, to find two images, which can be identified as coming from one source. The search for ghosts is no straight forward method and suffers from several problems:

- We know that the only objects for which multiple images could be identified have to have a life-time $T > L_{min}/c$. If we want to identify two images with different redshift to one object, the object should not change much during its life. This restrictions rule out most objects. For example, single galaxies are no good studying objects because their life-time is too short and they change too much during their life-time. Most undertaken experiments used quasars and galaxy clusters. [55]
- The ghost may show the object from another perspective. If geometry is not flat, the ghost could show a compressed or stretched image. These aspects complicate the identification. [18]
- If space is too big, that light could not have crossed space more than once, no ghosts exist.
- Even if there are ghosts which are theoretically observable, it is not clear that we would detect them. Apart from the common limits of observation it suffice that another object is in the path of light between the ghost and the observer. [55]

For a certain project it is advisable to chose a specific topology and search for ghosts in the for this topology favourable directions. There still remain perturbations, which makes the identification harder:

- The favourable directions and distances are calculated in an idealized, homogeneous space. In real space null geodesics are deflected in accordance with the effect of gravitational lensing. Thus, geodesics are deformed (changes in the length) and the images are probably multiplied (gravitational lensing). In MCM, even the real object could effect its own ghosts by gravitational lensing.

- The typical proper velocities are of the order 500km/s . While the light ray turns around a small universe ($t = L_{min}/c$), the real object moves $500 \cdot L_{min}/c$. Thus, the position of the next ghost is shifted. [55]

Several approaches to find ghosts have been made, from which we want to name: [94], [48], [24] and the erratum [25], [20] and [79]. Most projects use catalogues of galaxy clusters as the Zwicky or Abell cluster (limited by $z < 0.2$). Sokolov, Shvartsman [94] and Gott [48] rule out FP with $L_{max} < 600h^{-1}\text{Mpc}$ which corresponds to a redshift $z < 0.2$. Some papers ([11], [74]) deal with extraordinary events like the observation of simultaneous Gamma bursts at antipodal points. For a historic review up to the year 1995 see [55], for instance. None of these approaches was successful. Thus, so far, no ghost could be identified with another and it is not believed that this method will succeed. But, since the search is complicated by so many factors, a negative search for ghosts cannot rule out the possibility for a nontrivial topology. [55]

6.2.3. Cosmic Crystallography

A more promising method is that of cosmic crystallography. The idea of cosmic crystallography is that in spaces with nontrivial topology, equal distances, which are 3D-separations between objects, appear more often than by chance, whatever the curvature of the space form or nature of holonomies are. All crystallographic methods use 3D-data of cosmic objects as quasars or galaxy clusters. The 3D-data is specified by a position on the celestial sphere and a redshift. A redshift-distance relation gives the radial distance to the observer.

In this section, we require space to be compact with a nontrivial topology and a significantly smaller volume than the horizon volume. Spaces satisfying $0.7\chi_{LSS} < L_{min} < 1.2\chi_{LSS}$ have also been examined using crystallographic methods. [26]

Since holonomies are isometries, we can associate to each generator of the holonomy group $\gamma \in \Gamma$ a length λ_γ (related to the size of the fundamental polyhedron). Other holonomies can be represented as a linear combination of the generators of the holonomy group, and therefore, we can associate a length $\Lambda_h = \sum_{\gamma \in \Gamma} N_\gamma \lambda_\gamma$, $N_\gamma \in \mathbb{R}$. For example, the generators of the holonomy group of the three-dimensional torus are translations, and thus, the λ_γ are equal to the lengths of the fundamental parallelepiped L_x, L_y, L_z . [66]

If 3D-separations between images are calculated and plotted in a histogram, lengths associated to a holonomy should produce spikes. Such a histogram is called **Pair Separation Histogram** [66]. In theory, there are two different types of pairs which produce spikes in a histogram:

1. Type I-pairs: Since any holonomy is an isometry, any holonomy satisfies $dist(x, y) = dist(h(x), h(y)), \forall h \in \Gamma$. Thus, $\{h(x), h(y)\}, \forall h \in \Gamma$ produce a peak.
2. Type II-pairs: The image of a real object and a ghost can be taken into each other by

a holonomy. Clifford translations fulfill $dist(x, h(x)) = dist(y, h(y))$. Thus, if h is a Clifford translation, the $\{x, h(x)\}$ produce a peak. [67]

Type I-pairs exist in every space form, but the spike is of the same order as numbers of cells in the catalogue. The until now existing catalogues are too small that a spike due to type I-pairs could produce a significant spike. Type II-pairs exist only in space forms whose holonomy group contains Clifford translations (see Chapter 4, Theorem 4.2.1.2, p.81) [67]. Holonomy groups of hyperbolic manifolds never contain Clifford translation. Thus, for hyperbolic manifolds another method is required [27]. There are different crystallographic methods for the different types of spaces, which we shall present in the following.

As opposed to searching for ghosts, a negative result of a crystallographic method could theoretically rule out that the observational universe is non-simply-connected.

6.2.3.1. Pair Separation Histogram:

If we calculate the 3D-separation of each two objects of a catalogue and plot the numbers of pairs versus the squared 3D-separation in a histogram, there should be a significant peak at the values λ_γ^2 (in comoving distance units). Type II-pairs corresponding to the same holonomy are characterized by their 3D-separation Λ_h . From the distribution and relative height of the sharp peaks, the generators of the holonomy group should be derivable, and therefore, the topology. Thus, the pattern is characteristic for the topology. [66] [67] [56]

The pattern of the PSH depends on the curvature of space and in general on the position of the observer. Only if the space is globally homogeneous, the position of the observer is not relevant. That is, if and only if all holonomies are Clifford translations (see Chapter 4, 4.2.1.2, p.81) [27]. The method works the better, the more holonomies are Clifford translations. For not globally but locally homogeneous spaces there are more, but less sharp spikes.

For a catalogue with N objects, we get $\frac{N(N-1)}{2}$ pairs. If $vol(catalogue) = F \cdot vol(FP)$, $F \in \mathbb{R}$, N/F entries are real objects and the rest of it are ghosts. N Type II-pairs with 3D-separation λ_γ are expected. The more regular the FP is, the more significant is the neat peak. For example, if two or three L_i of the FP of a toroidal universe coincide, the peak is two or three times as strong as if they all take different values. This property manifests in the relative height of the peaks.

First, the method was suggested by Luminet, Uzan and Lehoucq in [66]. We shall explain the method, applying it to the only globally homogeneous Euclidean model — the three-dimensional torus. The generators of the holonomy group are three translations in correspondence to the length L_x, L_y, L_z of the FP, which is a parallelepiped. We shall consider the special case $L = L_x = L_y = L_z$. Thus, we consider the locally Euclidean space form \mathcal{G}_1 , introduced in Chapter 4, Theorem 4.4.2.9 (p.89). ⁴ Here, the pattern shows the sharpest spikes, because all holonomies are Clifford translations and all λ_γ coincide. [26]

⁴The description of the space form as a gluing manifolds was done in 5.3 (p.110).

Luminet, Uzan and Lehoucq distributed randomly 50 objects in a cube with $L = 1500h^{-1}Mpc$ endowed with a flat metric. They set a cut-off redshift at $z = 4$ and calculated the position of the ghosts in the UCS. The simulation produced 45 times more ghosts than objects. The first ghosts appear at a redshift of $z = 0.31$, whereas original objects are seen up to a redshift of $z = 0.63$ [66]. The according pattern can be seen in Figure 6.6.

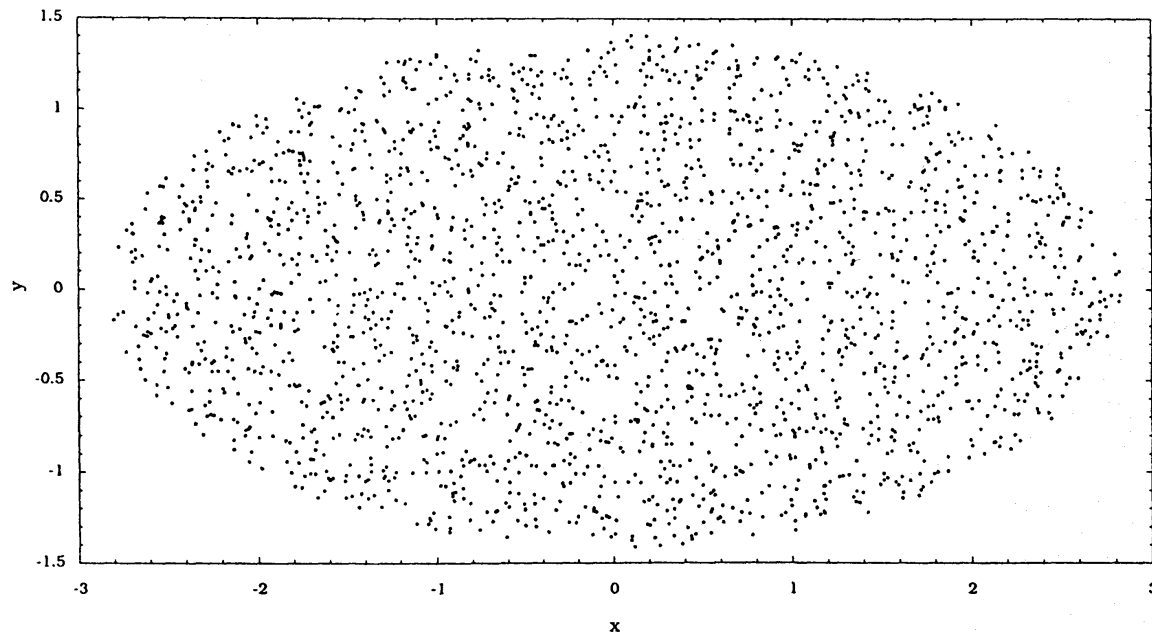


Figure 6.6.: Pattern produced by simulated topological lensing in the space \mathcal{G}_1 with a cubic fundamental polyhedron of size $1500h^{-1}Mpc$ with of 50 randomly distributed objects. [66]

Here, two images X, X' of the same object are related by a translation

$$X = X' + \begin{pmatrix} n_x L \\ n_y L \\ n_z L \end{pmatrix}, n_x, n_y, n_z \dots \text{integers.}$$

Thus, the 3D-separation is of the simple form $d_x^2 + d_y^2 + d_z^2 = L^2(n_x^2 + n_y^2 + n_z^2)$, where $d_x/d_y/d_z$ is parallel to the edge $L_x/L_y/L_z$. In this very special case, the peaks should be located at $\Lambda_h^2 = (a \cdot L)^2$, $a \in \mathbb{N}$. If we plot versus $\Lambda^2/V^{\frac{2}{3}}$ instead of Λ^2 , we get peaks located at

$$\frac{L^2(n_x^2 + n_y^2 + n_z^2)}{L^2} = n_x^2 + n_y^2 + n_z^2 = \Lambda^2/V^{\frac{2}{3}} = \frac{(aL)^2}{L^2} = a^2 \in \mathbb{N}.$$

The boundary of the n_x, n_y, n_z depends on the cut-off redshift. In the here mentioned work, $n_x, n_y, n_z \in \{0, \dots, 5\}$ [66]. The corresponding pattern can be seen in Figure 6.7(a).

The amplitude of the peaks depend on the number of different combinations (n_x, n_y, n_z) producing a certain a^2 . For instance $a^2 = 1$ is produced by the elements $(1, 0, 0), (0, 1, 0)$

and $(0, 0, 1)$, whereas $a^2 = 5$ is produced by $(2, 1, 0)$, $(1, 2, 0)$, $(2, 0, 1)$, $(1, 0, 2)$, $(0, 1, 2)$ and $(0, 2, 1)$.

The PSH of the Euclidean space form with the same topology, but unequal lengths L_x, L_y, L_z shows more, but less intense peaks (see Figure 6.7(b)).

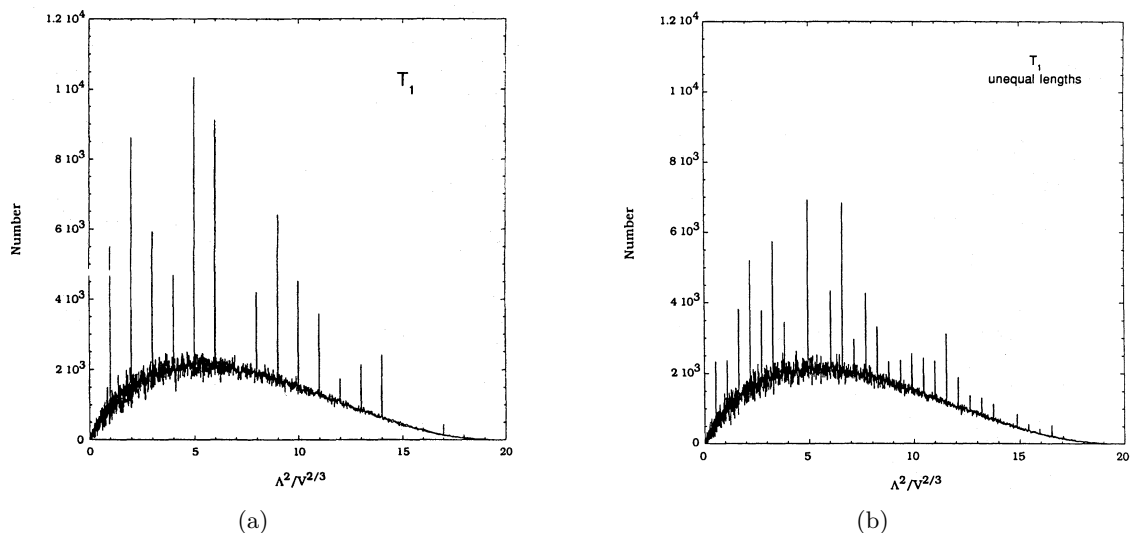


Figure 6.7.: Simulated PSH of a compact Euclidean space form \mathcal{G}_1 with (a) equal lengths (b) unequal length. [66]

Luminet, Uzan and Lehoucq calculated the simulated PSH for all six closed and oriented Euclidean space forms. For $\mathcal{G}_1, \mathcal{G}_2$ and \mathcal{G}_3 , their pattern was affirmed by Fagundes and Gausmann in [26]. For \mathcal{G}_6 , [66] used a wrong holonomy group, which was due a mistake made by Ellis in [22]. Fagundes and Gausmann have not found a characteristic pattern for \mathcal{G}_6 . For \mathcal{G}_4 and \mathcal{G}_5 both, [26] and [66], found characteristic pattern, which do not coincide because of different choices of the fundamental polyhedron.

The simulated analysis was made under very idealized circumstances. In a more realistic scenario, the following problems occur:

- **Aperture Angle:** A realistic catalogue cannot mask the region of the galactic plane. Usually catalogues have an aperture angle of about 120° , consisting of two cones with an angular of about 60° . Luminet, Uzan and Lehoucq [66] found that the signal fades out if the aperture angle goes down to about 20° .
- **Spikes Due to Clustering:** Galaxy clusters produce a significant number of Type II-pairs in correspondence to their separation. In general, an N-body simulation with clustering produces spikes.
- **Calculating Distances:** The calculation of the 3D-separations is strongly sensitive to the choice of the cosmological parameter. Distances which are calculated by using a

redshift-distance relation depend strongly on the Hubble constant.

- Catalogues: Catalogues are not complete and the listed redshifts are contaminated with the redshift of the peculiar motion. But in the simulations, the redshift is taken to be fully due to cosmic expansion. [66]

In order to test the method, the procedure was examined on Bury catalogue in an Einstein-de Sitter universe (see 6.1.2) which consists of all Abell and ACO clusters. The catalogue consists of 901 clusters with a maximal redshift of $z \approx 0.35$ (where just twelve objects have a $z > 0.26$) corresponding to a distance of $840h^{-1}Mpc$. The aperture angle is 120° in form of a double cone. The pattern produced by the entries of Bury catalogue is presented in Figure 6.8(a). The corresponding PSH can be seen in Figure 6.8(b).

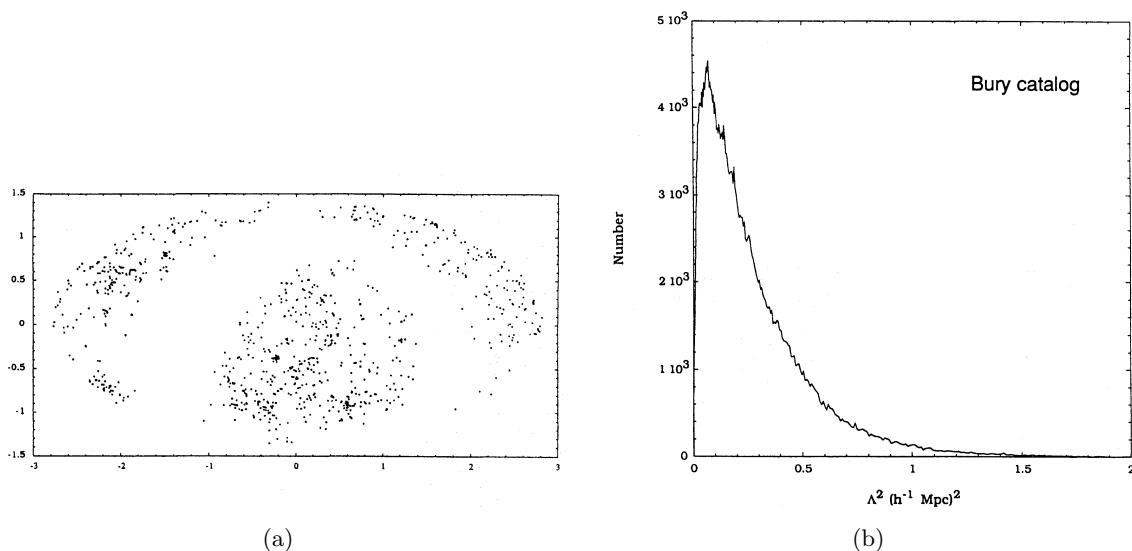


Figure 6.8.: (a): The pattern of the entries of Bury catalogue. (b): The PSH of the same space with data of the Bury cluster catalogue. [66]

They found two suspicious peaks at $270h^{-1}Mpc$ and $382h^{-1}Mpc$. In order to check if these peaks are due to topology, Luminet, Uzan and Lehoucq simulated a catalogue with 30 entries in a cubic fundamental cell with $L = 270h^{-1}Mpc$, $z_{max} = 0.26$. A double cone aperture of 120° was chosen and the number of ghosts was limited to 901. The resulting pattern can be seen in Figure 6.9(a) and the PSH in Figure 6.9(b).

In conclusion, we can say that if the above-mentioned topology would be the topology of space, the peaks would be more significant. Thus, the in Figure 6.8(b) seen peaks are due to noise. [66]

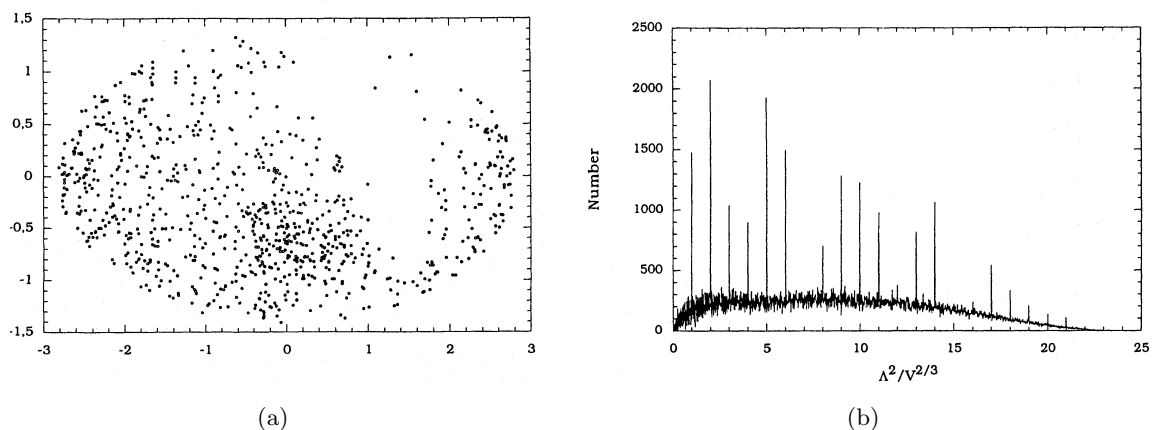


Figure 6.9.: (a): The pattern of the simulated Bury catalogue. (b): The PSH of the simulated Bury catalogue is presented. [66]

6.2.3.2. Collecting Correlated Pair Method CCP:

The Correlated Pair Method was developed by Uzan, Lehoucq and Luminet [67] when the trial to apply the PSH method to several hyperbolic space forms failed. (See, for instance, [26] or [27].) The here explained method works exclusively with type I-pairs, which exist in any space form. We distinguish two different type I-pairs:

1. xy-pairs: $\forall x, y \in \mathcal{M}_3, \forall g \in \Gamma : dist[g(x), g(y)] = dist[x, y]$
2. xg(x)-pairs: $\forall x \in \mathcal{M}_3, \forall g_1, g_2 \in \Gamma : dist[g_1(x), (g_1 \circ g_2)(x)] = dist[x, g_2(x)]$

For a catalogue with N entries, we calculate the 3D-separation d_i of all $P = \frac{N(N-1)}{2}$ pairs and rearrange them such that $d_{i+1} > d_i$. Building the differences $\Delta_i = d_{i+1} - d_i$, all entries with the same distance vanish.

We define the **CCP-index** as

$$R = \frac{\mathcal{N}}{P-1} \quad \text{with} \quad \mathcal{N} = card\{i : \Delta_i = 0\},$$

with *card* denoting the cardinality of the set.

In the above-given definition $\Delta_i = 0$, this is an idealized situation. Working with real data, due to errors in position and redshift, the differences do not vanish but take small values. Therefore, in more realistic situation ϵ -binning is used: $\Delta_i \in [0, \epsilon]$.

If A entries of the N entries in the catalogue are real objects, $N = A(B+1)$ for a $B \in \mathbb{Z}$. Each xy-pair is represented $(B+1)$ -times. Therefore, the $A(A-1)/2$ pairs contribute to $B \cdot A(A-1)/2$ counts in \mathcal{N} . If X is the number of representations of xg-pairs for $A=1$ in \mathcal{N} , the contribution in \mathcal{N} for A real objects is $A^2 \cdot X$. Thus,

$$\mathcal{N}_{min} = A(A-1)B/2 + A^2X.$$

This is just a lower bound, because there are additionally pairs x, y , which have randomly the same separation and if Clifford translations exists in the holonomy group, type II-pairs exist too.

The CCP-index takes values between zero and one. If $B = 0$, space is simply-connected and $R = 0$. If the number of real objects dominates, the index goes to $R \rightarrow \frac{B+2X}{(B+1)^2}$. Thus, the index is representative for the degree of multi-connectedness of the spatial part of the universe.

The CCP-index can be used in the following way: in order to calculate the required radial distances d_i , a redshift-distance relation is needed, which depends on the cosmological parameters Ω_0 and $\Omega_{\Lambda,0}$. If the inaccuracy of these parameters is too big, the topological signal, if existing, is destroyed. We can solve this problem by spanning an $(\Omega_0, \Omega_{\Lambda,0})$ -parameter space and calculating R in terms of Ω_0 and $\Omega_{\Lambda,0}$. The plot of $R(\Omega_0, \Omega_{\Lambda,0})$ produces a spike only if the parameter Ω_0 and $\Omega_{\Lambda,0}$ are chosen exactly. At all other points in the $(\Omega_0, \Omega_{\Lambda,0})$ -plane, the topological signal is destroyed. A simulation showed that with $A = 30$, $\Omega_0 = 0.2$ and $\Omega_{\Lambda,0} = 0.1$, the plot of R produces in Weeks space (see section 5.5, p.116) a big spike at $(0.2, 0.1)$, which vanishes for a small variation of Ω_0 and $\Omega_{\Lambda,0}$. See Figure 6.10(a). In a more realistic situation with an ϵ -binning, the spike is less sharp and the $(\Omega_0, \Omega_{\Lambda,0})$ -plane shows a background noise, see Figure 6.10(b).

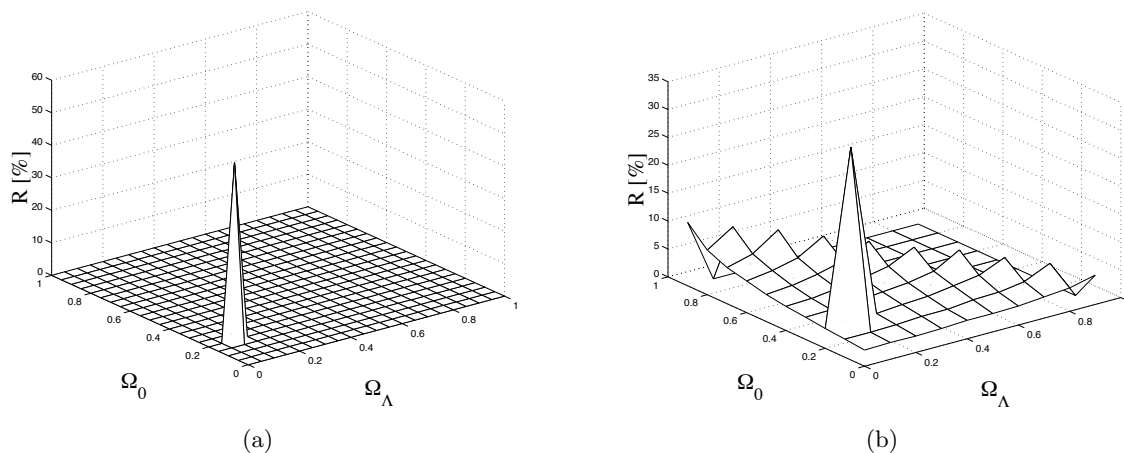


Figure 6.10.: Plot of $R(\Omega_0, \Omega_{\Lambda,0})$ in Weeks manifold with $A = 30$, $\Omega_0 = 0.2$ and $\Omega_{\Lambda,0} = 0.1$; (a): idealized situation ($\epsilon = 0$) (b): More realistic situation with ϵ -binning. [67]

Several tests with real catalogues (Veron-Cetty and Veron 1998 quasar catalogue and Bury cluster catalogue) did not show a topological signal.

The result is not surprising since the binning width and the accuracy of the parameter Ω_0 are correlated by $|\frac{\delta\Omega_0}{\Omega_0}| \approx \epsilon$. Additionally, the accuracy of the parameter Ω_0 is increasing with increasing z_{max} . Thus, one has to find a compromise between the depth of the used catalogue and the error made because of the lack of the required accuracy of Ω_0 . Furthermore, the

greater the inaccuracy in Ω_0 , the greater we have to choose the binning width, which reflects in the computational time. Uzan, Lehoucq and Luminet made trials with $\epsilon = 10^{-5}$, 10^{-6} and 10^{-7} , but were unable to span the $(\Omega_0, \Omega_{\Lambda,0})$ -plane with the required accuracy. Furthermore, the computational time is increasing with increasing entries in the used catalogue and with increasing precision of $(\Omega_0, \Omega_{\Lambda,0})$. For a reasonable precision, the computational time is too long. Thus, the method is not able to determine topology of the universe with the today available data and technical equipment. [67]

6.2.3.3. Cosmic Crystallography with Pull-Back:

This crystallographic method was developed by Fagundes and Gausmann in [28]. The method is applicable to any space form. In [28], they applied it to a hyperbolic space form with a fixed fundamental polyhedron and a fixed orientation in astronomical space. The basic idea is to pull the images back to their position in the FP. This procedure should produce a neat peak located at zero.

As before, working with real data produces a peak near zero instead of at zero, because of inaccuracies in measurement of position and redshift.

The method was applied with idealized, and therefore, complete catalogues to two different hyperbolic manifolds with the same FP, a regular dodecahedron, but different holonomy groups $\Gamma \subset Isom(\mathbb{H}^3)$. Both showed a significant peak near zero, whereas in the simply-connected hyperbolic space, the distribution is Gaussian. See Figure 6.11.

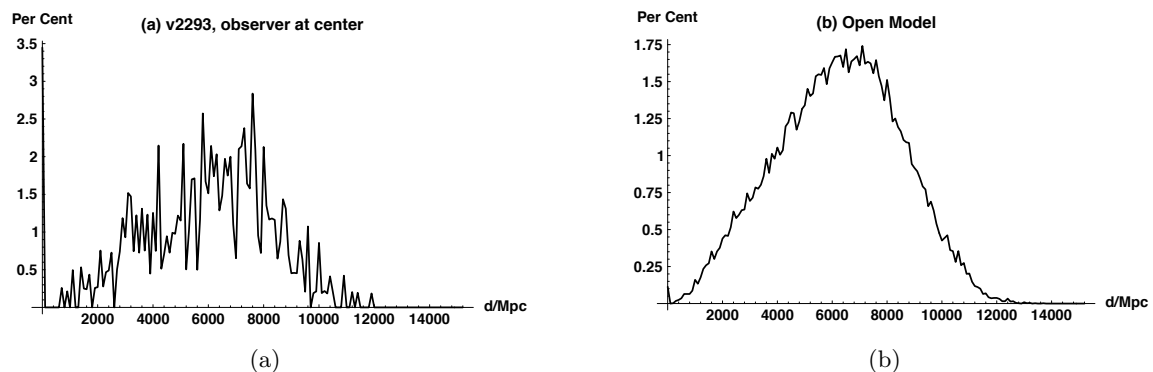


Figure 6.11.: Histogram derived with the pull-back method applied to (a): the hyperbolic manifold with the identification number $v2293(+3, 2)$ (due to the software SnapPea from Jeffrey Weeks) and (b): the simply-connected hyperbolic space. Chosen parameter: $\Omega_{\Lambda} = 0, \Omega_0 = 0.3, H_0 = 65 \text{ km/s/Mpc}$; number of cells: 93; [28]

Another trial was made with a shifted position of the observer. The plots were showing the same result, indicating that the method is independent of the observers position. Further tests showed that the method is strongly dependent on the orientation of the fundamental

domain in astronomical space. If the fundamental domain is rotated by an angle $\beta < 5^\circ$, the peak is less sharp, but visible. A rotation by an angle $\beta > 5^\circ$ destroys the peak. Thus, the topology can just be used to affirm the topology if the orientation of the FP in space is already known up to a high precision. Otherwise, thousands of different orientations have to be examined. [28]

6.2.3.4. Crystallographic Methods Using Filter:

Latest improvements of crystallographic methods use filter. From these methods, we shall present the one derived by Fushii and Yoshii [30], which is based in several aspects on the method presented in [71].

The above-given average frequency of equal separation used with crystallographic methods is caused by topological effects on the one side and stochastic effects on the other side. Here, the idea is to sort out pairs caused by stochastic reasons with the help of filter. In [30] they restrict the objects to shells with $r_1 < \chi < r_2$ and use the following filter:

Filter I: First, pairs $(a_i, a_j), (a_k, a_l)$ are selected with $||a_i - a_j|| - ||a_k - a_l|| < \epsilon$.

Filter II: Secondly, vectorial properties of holonomies are used. Here, specific filters for different types of holonomies are defined. The filters can be defined for very specific properties of a certain kind of holonomies. The more specific a filter, the more free parameter are required. For Euclidean manifolds, five different filter, similar to those used by [71], are applied:

- Translations: If $\gamma \in \Gamma$ is an Euclidean translation and $(a_i, a_j), (a_k, a_l)$ a corresponding quadruplet, $\gamma(a_i, a_j) = (a_k, a_l)$ or $\gamma(a_i, a_j) = (a_l, a_k)$. The filter is constructed as:

$$|(x_i - x_j) \pm (x_k - x_l)| < \epsilon_x, \quad |(y_i - y_j) \pm (y_k - y_l)| < \epsilon_y, \quad |(z_i - z_j) \pm (z_k - z_l)| < \epsilon_z,$$

with $a_r = (x_r, y_r, z_r)$, $r = i, j, k, l$.

- Half-Turn Corkscrew: A half-turn corkscrew in orientable Euclidean spaces is composed by a half-turn rotation followed by a parallel translation. For a quadruplet corresponding to a half-turn corkscrew $\gamma(a_i, a_j) = (a_k, a_l)$ or $\gamma(a_i, a_j) = (a_l, a_k)$, once more. A filter for these holonomies can be defined by:

$$|(x_i - x_j) \pm (x_k - x_l)| < \epsilon_x, \quad |(y_i - y_j) \pm (y_k - y_l)| < \epsilon_y, \quad |(z_i - z_j) \mp (z_k - z_l)| < \epsilon_z.$$

- Nth-Turn Corkscrew for $n = 3, 4, 6$: An nth-turn corkscrew is an nth-turn followed by a parallel translation. These holonomies indicate a specific Euclidean space form. While third-turn corkscrew occur just in third-turn space, only the quarter-turn space has quarter-turn corkscrew and sixth-turn corkscrew exists just in

sixth-turn space. (See section 5.3, p.110, for a description of the mentioned spaces.) The filters are:

$$\begin{aligned} |(x_i - x_j) \cos(2/n) - (y_i - y_j) \sin(2/n) \pm (x_k - x_l)| &< \epsilon_x, \\ |(x_i - x_j) \sin(2/n) + (y_i - y_j) \cos(2/n) \pm (y_k - y_l)| &< \epsilon_y, \\ |(z_i - z_j) \pm (z_k - z_l)| &< \epsilon_z. \end{aligned}$$

As opposed to the filter for translations and half-turn corkscrew, here, the filter does ignore γ^{-1} . Therefore, we have to use additionally the very similar filters

$$\begin{aligned} |(x_i - x_j) \cos(2/n) - (y_i - y_j) \sin(2/n) \pm (x_k - x_l)| &< \epsilon_x, \\ -|(x_i - x_j) \sin(2/n) + (y_i - y_j) \cos(2/n) \pm (y_k - y_l)| &< \epsilon_y, \\ |(z_i - z_j) \pm (z_k - z_l)| &< \epsilon_z. \end{aligned}$$

For hyperbolic or spherical manifolds one can define appropriate filter.

Filter III: Thirdly, as in [71], the last filter is used to select due life-time. Ghost images with life-times t_i, t_j of the same object with a life-time t_{life} satisfy

$$\Delta t_{ij} = |t_i - t_j| < t_{life}.$$

Quadruplets of ghost images $(a_i, a_j), (a_k, a_l)$ with life-times t_i, t_j, t_k, t_l are dropped unless $\Delta t_{il}, \Delta t_{jk} < t_{life}$ or $\Delta t_{ik}, \Delta t_{jl} < t_{life}$.

With the images which have passed the filters, the CCP index and the PSH can be calculated. In theory, this method can detect the topology of manifolds with greater FP than other methods. However, a test [31] has shown that this method is impractical in realistic situations.

6.2.3.5. Possible Sources of Errors of Crystallographic Methods:

Crystallographic methods use 3D-data, as already mentioned. The general approach is to test a specific method on a simulated catalogue and then apply it to a real catalogue. Therefore, the two possible sources of errors are due to errors in the 3D-data and due to the incompleteness of real catalogues.

1. Errors in 3D-data are caused by:

- error in redshift due to spectroscopic imprecision,
- uncertainties in the position due to peculiar motions (correction of redshift),

- uncertainties in the cosmological parameter, especially in H_0 (error in the radial distances) and
- angular displacement due to gravitational lensing.

2. Catalogues are incomplete because

- objects are missing since either their apparent luminosity is too small or dust respectively galactic gas is in the path of light between the source and the observer.
- we do not have access to observational data in the direction of the galactic plane, which reduces the solid angle (5.2.2.4, p.108) to $\omega \ll 4\pi$.

This different sources of errors influence the results more or less dramatic. The uncertainties in the cosmological parameter can be handled by binning. With some methods the required binning however increases the computational time to a not performable value. The displacement of objects due to gravitational lensing is at most one arcsec and therefore negligible. The today's errors in redshift are of magnitude $\Delta z \approx 0.001$ (for quasars, for galaxies the error is smaller) which causes an error $\Delta v \approx 1,000 \text{ km s}^{-1}$.

In [56], the different errors have been added to an idealized catalogue and their effect on the results have been studied for PSH and CCP.

The error in the redshift was assumed to be Gaussian. Δz can be interpreted as error in redshift or position, even if the error in position is greater in real data than that in redshift. The error in incompleteness was realized by randomly throwing out $p\%$ of the sources, but more objects with greater redshift were deleted. Furthermore, a decreasing aperture angle was chosen.

PSH: In order to test the PSH method, a three-dimensional torus was chosen with $L = 3,000 \text{ Mpc}$. Further chosen cosmological parameter: $\Omega_\Lambda = 0.7$, $\Omega_m = 0.3$, $H_0 = 75 \text{ km s}^{-1} \text{ Mpc}^{-1}$. The simulated catalogue consists of 8500 entries which is of the magnitude of the today's quasar catalogues.

The errors in the redshift and velocities were raised until the spikes disappeared. Furthermore, the aperture angular was decreased and $p\%$ of the entries were randomly vanished until the signal faded out. The results are represented in table 6.1.

We can conclude, that the error in the velocity is negligible.

CCP: Here, the test was exemplified with Weeks manifold, $\Omega_\Lambda = 0$, $\Omega_0 = 0.3$. The number of cells within the horizon was chosen to be 190, whereas the number of catalogue entries was delimited to 1300, which defines a compromise between a realistic catalogue and calculation time. Once more the errors were raised until the index fell to noise level. The index fell to noise level for errors in velocity of $\Delta v = 50 \text{ km s}^{-1}$ and redshift $\Delta z \approx 10^{-6}$, the order of the binning width. Were the error in the velocities is a bigger

Table 6.1.: Values of errors at which the spike disappears dependent on the considered maximal redshift.

z_{max}	Δz	$\Delta v [kms^{-1}]$	%	$\Theta [^\circ]$
1	0.002	10,000	70	
2	0.1		80	110
3	0.03		90	80
4	0.08			70
5	0.12	40,000		60

problem than the spectroscopic inaccuracies. The incompleteness has less dramatic effects. [56]

A closing remark to the application of Crystallographic methods to spherical space forms:

There are infinitely many spherical space forms. A lot of crystallographic methods require a choice for the topology which can then be affirmed or rejected. [33] have reviewed the spherical holonomy groups on the aspect of their degree of difficulty to be detectable.

Single action manifolds: The holonomy group of single action manifolds consists only of Clifford translation. Therefore, these space forms could be detected with the PSH method. For cyclic groups \mathcal{C}_n and binary dihedral groups D_m^* , the minimal translation distance is $\frac{2\pi}{n}$ or $\frac{2\pi}{2m}$. Thus, the minimal translation distance is arbitrary small for high n or m respectively. Therefore, cyclic and binary dihedral groups are the easiest holonomy groups to be detected, whereas binary tetrahedral/octahedral and icosahedral groups are more difficult.

Double action manifolds: If one of the factors is cyclic or binary dihedral, the holonomy group is likely to be detected. The PSH of a double action manifold shows all spikes produced by a single action manifold of one of the factors.

Linked action manifolds: These manifolds are the most difficult to detect, because they have a very specific pattern.

6.3. Anisotropies in the Cosmic Microwave Background

In principal, there are two different kinds of data from which the topology of the universe should be theoretically derivable. First, the three-dimensional data (position, redshift) of objects used in crystallographic methods. The other kind of data is the Cosmic Microwave Background (CMB), briefly introduced in Chapter 1. In order to describe methods based

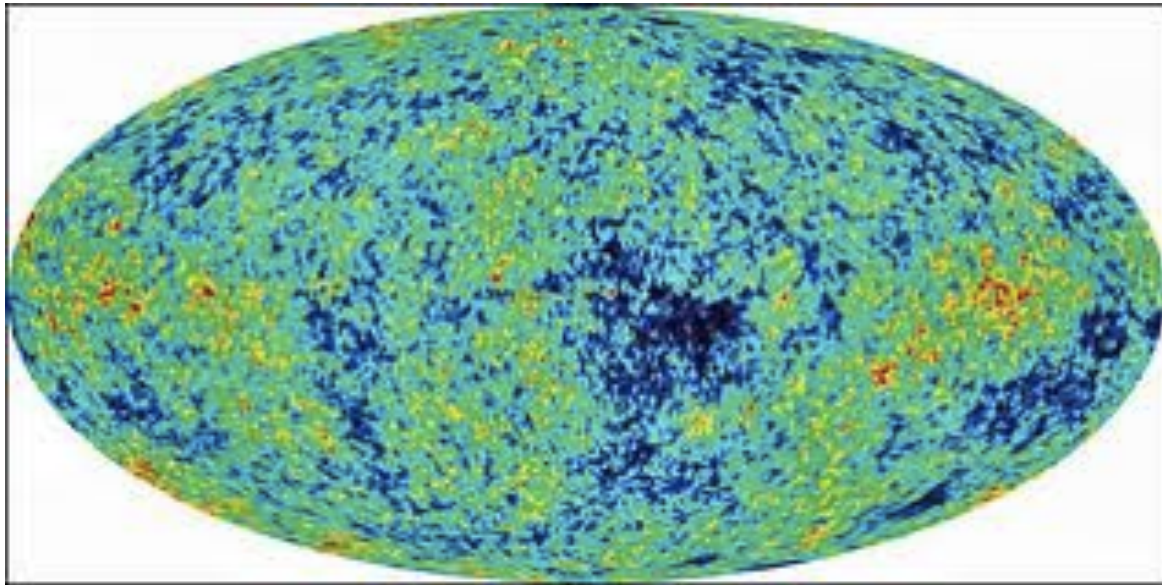


Figure 6.12.: Image of the CMB anisotropies made by WMAP [130]. As CMB is observable on a sphere around us, the shape can be seen in the same way as a chart of the earth visualizes the surface of a two-dimensional sphere.

on CMB data, we have to go into further detail on anisotropies of the CMB. Since this is a complicated and wide field of science, we shall only mention the most important points. For more details [57] and [109] are recommended.

As we have explained in Chapter 1, the microwave background radiation is the remnant of the radiation emitted at the time of last scattering. Light could not propagate before recombination. At the time of the last scattering (which is more precisely a time interval) radiation could propagate freely for the first time. During cosmic expansion, radiation also expanded. Today, we detect its remnants in the microwave range of the spectrum. The light received at earth has travelled the same distance in every direction since last scattering and therefore defines a sphere around us [57]. Figure 6.12 shows an image of the CMB from WMAP. Since it is the most extended source known in the universe, it is an excellent studying object for Cosmic Topology.

The CMB was propagated when radiation was in thermal equilibrium with hot matter, caused by numerous rapid collisions of electrons and photons. The number density of photons in equilibrium with matter of a temperature T and a frequency between ν and $\nu + d\nu$ is given by the **black body spectrum**

$$n_z(\nu)d\nu = \frac{8\pi\nu^2 d\nu}{\exp(h\nu/k_B T) - 1}$$

where h denotes Planck's constant, k_B denotes Boltzmann's constant and the convention $c = 1$ is used. As the universe has expanded, the radiation has cooled down, but has not

changed its distribution. Thus, the CMB still has an almost perfect black body spectrum. See Figure 6.13. The mean temperature has cooled down from approximately $3,000K$ to $2.725K \approx 3,000K \cdot a(t_{LSS})/a(t)$ [109].

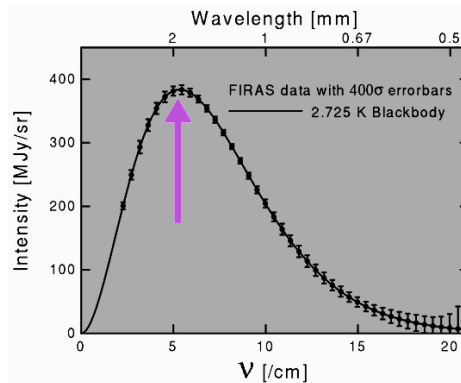


Figure 6.13.: The black body spectrum of the CMB. [131]

The CMB is remarkable homogeneous and isotropic. For the first time FIRAS on COBE detected anisotropies within the background radiation [91]. A few years later, WMAP were able to detect the anisotropies in a higher resolution, see Figure 6.12 [8]. The anisotropies are of magnitude $\frac{\delta T}{T} = 10^{-5}$, and therefore, the CMB remains remarkable homogeneous and isotropic. The anisotropies are caused by numerous effects, from which we shall only mention the most important ones. There are primary anisotropies and anisotropies in the observed CMB, which are caused by effects in the recent universe.

The source of the anisotropy depends mainly on the scale, meaning that anisotropies of a certain angular scale are dominated by a particular effect. Therefore, the parameter ℓ is used, which is called the **multipole**. It is the angular wave number and corresponds to an angular fluctuation θ with $\ell \sim \pi/\theta$. Small ℓ correspond to large angular correlations, whereas fluctuations on small scales correspond to high ℓ [57]. See Figure 6.14 for an illustration.

6.3.1. Anisotropies Caused by Effects in the Recent Universe:

6.3.1.1. Dipole Anisotropy:

The CMB is comoving with cosmic expansion. Since the earth has a peculiar velocity, we move with respect to the CMB. The motion of the earth with respect to CMB is composed of the motion of the galaxy with respect to the local group, the motion of the solar system within the galaxy and the motion of the earth within the solar system. The motion of the earth with respect to the CMB is estimated to be of order $10^{-3} \cdot c$. The maximal apparent temperature is measured in the direction we are moving to. WMAP satellite experiment found a maximal deviation of the mean temperature of CMB of about $\delta T = 3.372 \pm 0.014 mK$, which indicates that we are moving with a net velocity of $370 km/sec$ [8]. The motion with

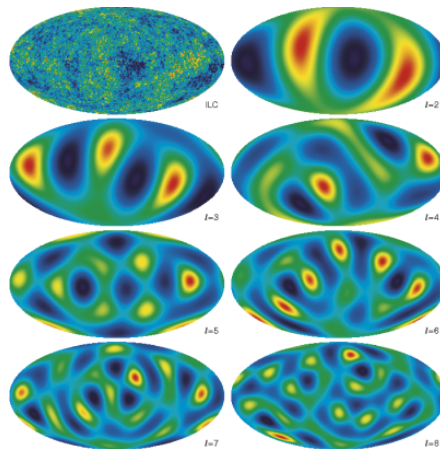


Figure 6.14.: Visualization of the multipole ℓ . [132]

respect to the CMB causes the dipole anisotropy due to the Doppler effect which dominates the temperature fluctuation with $\ell = 1$ ($\theta = 180^\circ$). The visual effect of the dipole anisotropy can be seen in Figure 6.15 [109].

6.3.1.2. Sunyaev-Zel'dovich Effect:

Along the line of sight, CMB photons are scattered by electrons in intergalactic space within clusters of galaxies and therefore cause anisotropies. The Sunyaev-Zel'dovich effect does not lower the amount of photons we are receiving, but it decreases the temperature and the sharpness of the peak. Radio astronomers can distinguish between temperature anisotropies caused by Sunyaev-Zel'dovich effect and primary anisotropies, which we shall explain in the following. Fluctuations with $\ell > 200$ are corrupted by the Sunyaev-Zel'dovich effect. As we shall see, these are not interesting for Cosmic Topology. [109]

6.3.2. Primary Anisotropies

Apart from intrinsic temperature fluctuations in the electro-nucleon plasma at the time of last scattering and the Doppler effect due to velocity fluctuations in the plasma at last scattering, the primary anisotropies of the CMB are caused by the Sachs-Wolf (SW) effect and the integrated Sachs-Wolf (ISW) effect, which we shall describe in more detail. [109]

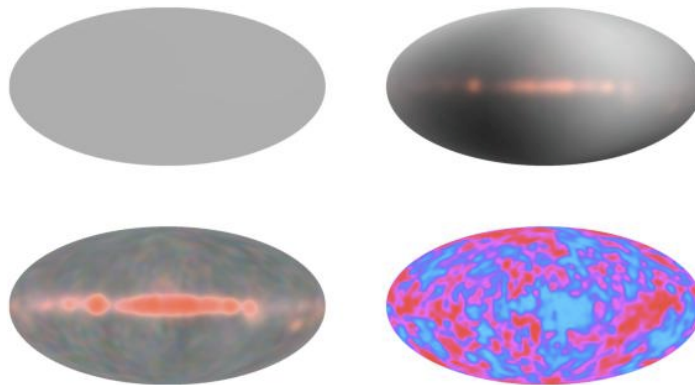


Figure 6.15.: (top left) The CMB has a isotropic temperature all over the universe; (top right) A higher resolution shows the dipole pattern caused by the motion of the earth versus the CMB. The red coloured balk is the plane of the milky way. CMB has to be mask for this region. (bottom left) Dipole pattern is reduced; (bottom right) Milky Way is reduced and the anisotropies of the CMB can be seen. [133]

6.3.2.1. Sachs-Wolf Effect:

In the early universe acoustic waves propagated and caused by superposition density anisotropies in the primordial plasma. These gravitational fluctuations at the time of last scattering are one origin of temperature fluctuations in the CMB. Photons coming from a denser region had to compete more strongly against gravity, and therefore, are reaching us cooler. Whereas photons coming from a less dense region are reaching us hotter. These anisotropies have stretched to macroscopic scales during a possible era of inflation. [18] [55]

It is widely accepted that these primordial density fluctuations are the origin of density fluctuations today, as, for example, galaxies or galaxy clusters [60].

In a first approximation, this effect can be treated with Newtonian physics. The perturbation of the gravitational potential, expressed in comoving coordinates, is a time independent function $\delta\Phi(x)$ which can be written as a combination of components of $\delta g_{\mu\nu}$ [57]. The perturbation has two effects:

- Gravitational Redshift: The energy of a photon emitted at the time of last scattering is shifted by an amount $\delta\Phi(x)$. When we observe it in the direction \vec{n} , it differs from the average by an amount

$$\left(\frac{\delta T(\vec{n})}{T_0}\right)_1 = \delta\Phi(\vec{n}\chi_{LSS}). \quad (6.19)$$

- The perturbation of the gravitational potential changes the rate at which the universe expands. We observe the redshift of the last scattering surface shifted by approximately

$\frac{1}{1+z}$. In a matter dominated universe, the shift in $1+z$ causes a shift of

$$\left(\frac{\delta T(\vec{n})}{T_0}\right)_2 = -\frac{2}{3}\delta\Phi(\vec{n}\chi_{LSS}). \quad (6.20)$$

Equations 6.19 and 6.20 add to the Sachs-Wolf effect:

$$\left(\frac{\delta T(\vec{n})}{T_0}\right)_{SW} = \frac{1}{3}\delta\Phi(\vec{n}\chi_{LSS}). \quad (6.21)$$

Sachs-Wolf effect dominates the fluctuations for $10 \leq \ell \leq 50$.

6.3.2.2. Integrated Sachs-Wolf Effect:

The perturbation is not strictly time-independent. The time-dependent part is due to the integrated Sachs-Wolf effect and describes the gravitational red-/blueshift due to time-dependent fluctuations in the gravitational potential between the time of last scattering and today. It dominates the temperature fluctuations for $\ell \leq 10$. [109]

6.3.3. Mathematical Description of Anisotropies

We expand the deviations of the CMB temperature in the direction of the unit vector \vec{n} from the mean temperature T_0 in spherical harmonics:

$$\delta T(\vec{n}) = T(\vec{n}) - T_0 = \sum_{\ell, m} a_{\ell m} Y_{\ell}^m(\vec{n}),$$

with ℓ positive definite integers, $m \in \{-\ell, \dots, \ell\}$ and

$$T_0 = \frac{1}{4\pi} \int d^2 \vec{n} T(\vec{n}).$$

The coefficients $a_{\ell m}$ describe what happened at the last scattering surface for the position of the earth in universe. Since we do not have access to such specific information, we are forced to focus on averages over time and position. The Ergodic Theorem states that these averages can be handled as only one average, which we shall denote by \langle, \rangle . [109]

We can describe the anisotropies of the CMB by considering the **angular (temperature two-point) correlation function**. It describes the difference in temperature of the CMB between any two points on the sphere and is given by

$$C(\theta) = C(\vec{n}, \vec{n}') = \langle \delta T(\vec{n}), \delta T(\vec{n}') \rangle,$$

with $\vec{n} \cdot \vec{n}' = \cos(\theta)$. The $C(\vec{n}, \vec{n}')$ can be derived by theoretical considerations to compare them to the observed C^{obs} . [57]

The coefficients of the angular correlation function define the **correlation matrix**:

$$C_{\ell m}^{\ell' m'} = \langle a_{\ell m}, a_{\ell' m'} \rangle.$$

In Standard Cosmology, \mathcal{M}_3 is assumed to be simply-connected and isotropic. In this case, $\langle \delta T(\vec{n}) \rangle$ is independent on the direction \vec{n} and

$$\langle a_{\ell m}, a_{\ell' m'} \rangle = \delta_{\ell, \ell'} \delta_{m, -m'} C_\ell, \quad (6.22)$$

with C_ℓ being the **multipole coefficient** which can be written as

$$C_\ell = \sum_{m=-\ell}^{\ell} \frac{|a_{\ell m}|^2}{2\ell + 1}. \quad [57]$$

With these assumptions, the angular correlation function can be written as:

$$\langle \delta T(\vec{n}), \delta T(\vec{n}') \rangle = \sum_{\ell m} C_\ell Y_\ell^m(\vec{n}) Y_\ell^{-m}(\vec{n}') = \sum_{\ell} C_\ell \left(\frac{2\ell + 1}{4\pi} \right) P_\ell(\vec{n}, \vec{n}')$$

with P_ℓ denoting the Legendre polynomials.

The observed multipole coefficients C_ℓ^{obs} are averaged over m but not over the position. Of course we cannot have the average over position, since we just have access to one observing position. The C_ℓ and C_ℓ^{obs} satisfy

$$\left\langle \left(\frac{C_\ell - C_\ell^{obs}}{C_\ell} \right)^2 \right\rangle = \frac{2}{2\ell + 1}, \quad \left\langle \left(\frac{C_\ell - C_\ell^{obs}}{C_\ell} \right) \left(\frac{C_{\ell'} - C_{\ell'}^{obs}}{C_{\ell'}} \right) \right\rangle = 0. \quad [109]$$

For $\ell \geq 4$, the multipole coefficients C_ℓ can be expressed with the help of the **Harrison-Zel'dovich spectrum**:

$$C_\ell = \frac{24\pi Q^2}{5\ell(\ell + 1)} \quad (6.23)$$

where Q denotes the **quadrupole moment**. [109]

In simply-connected, isotropic and homogeneous spaces it suffices to calculate the C_ℓ . In non globally isotropic and homogeneous spaces, the correlation matrix $C_{\ell, \ell'}^{m, m'}$ may have off-diagonal entries. Here, the angular correlation matrix is not rotationally invariant. Therefore, it depends on the orientation of the manifold with respect to the coordinate system.

In order to calculate the coefficients $C_{\ell, \ell'}^{m, m'}$, the eigenmodes $\Upsilon_k^{[\mathcal{M}_3]}$ of $\mathcal{M}_3 = \widetilde{\mathcal{M}}_3/\Gamma$ have to be calculated. In particular, these are the eigenmodes of the **Laplace operator** $\Delta = \nabla^2$ on $\widetilde{\mathcal{M}}_3/\Gamma$, where ∇ is the covariant derivative corresponding to the metric h_{ab} on \mathcal{M}_3 (1.1.3.7, p.17) with the Harrison-Zel'dovich spectrum as initial data [62]. Thus, they are the solutions of the **Helmholtz equation**:

$$\Delta \Upsilon_k^{[\mathcal{M}_3]} = E_k \Upsilon_k^{[\mathcal{M}_3]},$$

with E_k denoting the eigenvalue corresponding to the integer k , which can be interpreted as the wave number [14]. For space forms, $E_k = k^2 - K$, where K is positive, zero or negative depending on whether the space form is spherical, flat or hyperbolic. Any other function on $\widetilde{\mathcal{M}}_3/\Gamma$ can then be developed on its eigenmodes. [102]

In general, the space of eigenmodes of a space form $\widetilde{\mathcal{M}}/\Gamma$, is a subspace of the space of eigenmodes of the UCS $\widetilde{\mathcal{M}}$. The subspace is defined as the space of all eigenmodes which are invariant under Γ . In other words, they satisfy the fundamental periodicity condition $\mathcal{Y}(\gamma(x)) = \mathcal{Y}(x) \forall \gamma \in \Gamma$ where $x \in \mathcal{M}$ and \mathcal{Y} is an eigenmode of the UCS $\widetilde{\mathcal{M}}$ [5]. The multiplicity of a mode is at most equal to the multiplicity in the UCS. If $\{\mathcal{Y}_{klm}^{\widetilde{\mathcal{M}}}\}$ is a basis of eigenmodes of $\widetilde{\mathcal{M}}$,

$$\Upsilon_{ks}^{[\mathcal{M}]} = \sum_{\ell=0}^{\infty} \sum_{m=-\ell}^{\ell} \xi_{klm}^{[\mathcal{M}]s} \mathcal{Y}_{klm}^{\widetilde{\mathcal{M}}}$$

with s indexing the eigenmodes to the eigenvalue E_k . The topological information is encoded in the coefficients ξ_{klm} . Thus, we are implementing the topology by performing the substitution

$$\mathcal{Y}_{klm}^{\widetilde{\mathcal{M}}} \rightarrow \Upsilon_{ks}^{[\mathcal{M}]},$$

where s is a subset of $\{\ell, m\}$.

For Euclidean space forms ([102]), the determination of the space of eigenmodes can be done analytically. For hyperbolic space forms, one is left to numerical methods. For spherical space forms, the eigenmodes of prism spaces and lens spaces can be done analytically ([13]), otherwise one is left to numerical methods. For compact space forms, the set of eigenvalues E_k and the set of coefficients ξ_{klm} are discrete.

With the help of perturbation equations, which are local differential equations and therefore the same for SCM and MCM, the coefficients $C_{\ell, \ell'}^{m, m'}$ can be calculated. Furthermore, the C_{ℓ} can be determined, which are rotationally invariant. [102]

6.3.4. Detecting-Methods using CMB-Maps

If you sprinkle fine sand on a drum and let it vibrate, the sand rearranges in a certain pattern which is called the **Chaldi pattern**. The Chaldi pattern depends on the size and shape of the drum. It is caused by the way acoustical waves are reflected. The early universe was filled with acoustic waves, generated soon after the Big Bang. The primordial universe vibrated for 380,000 years before the radiation could escape. These vibrations left their imprints in the primordial plasma in the form of small density fluctuations. These density fluctuations are detectable today as temperature anisotropies in the CMB. Thus, the temperature fluctuations of the CMB can be interpreted as a Chaldi pattern of the early universe which vibrated over 380,000 years. As the Chaldi pattern of a drum depends on its size and shape, the pattern of the CMB depends on the shape and size of the universe. The challenge is to reconstruct geometrical and topological properties by studying the pattern

of the CMB. [62]

In order to develop methods using CMB-maps, simulating maps with the topological signal of a brought variety of topologies are required to test the method. These maps can be used to estimate the run-time of the method and the significance of the topological signal. In order to mask the CMB for different space forms, the whole correlation matrix has to be calculated. The predicted C_ℓ depend on

1. the model of structure formation, which fixes the initial conditions for perturbations,
2. the matter content and geometry, which is given by the cosmological parameter and
3. the topology.

In a MCM the CMB map is expected to differ from the CMB map in a SCM in the following aspects:

1. Existence of $\ell - \ell'$ and $m - m'$ correlations, which reflect the break down of global isotropy. Thus, the correlation matrix $C_{\ell,\ell'}^{m,m'}$ is not diagonal.
2. Existence of a cut-off frequency in the CMB angular correlation spectrum on large angular scales if $L_{min} < \chi_{LSS}$.
3. Existence of patterns such as matched circles if $L_{min} < \chi_{LSS}$. These are the circles of intersection of the last scattering surface with itself, where the temperature fluctuations are assumed to be strongly correlated.

[102]

6.3.4.1. Circles-in-the-Sky

Every observer is located at the center of a sphere with radius χ_{LSS} , the last scattering surface, which determines the physical horizon. The last scattering surfaces of two observers intersect along circles, because spheres always intersect along circles (or single points). If space is non-simply-connected, there is the possibility that the fundamental cell intersects the last scattering surface (along circles). In this case, the last scattering surfaces of two observer in adjacent cells must have the same distribution of temperature fluctuations due to the ordinary SW effect along these circles of intersection (up to a phase). Of course the two observers are in reality only one observer and the circles are one circle observed in different directions in the sky. Thus, if we live in a multi-connected universe with a fundamental cell of size smaller or equal to the size of the last scattering surface, circles with the same temperature distribution due to SW effect must exist in the CMB. These circles are called **a pair of matched circles**. [19]

Just the temperature fluctuations caused by the ordinary SW effect are strongly correlated along matched circles. The dipole anisotropy as well as the anisotropies caused by the

integrated SW effect are in general anti-correlated since they depend on the null geodesic and the circles are seen in different directions in the observers space. The correlation would be perfect if the last scattering surface would be a two-dimensional sphere. Since the time of last scattering is a time interval instead of a sharp time-point, the last scattering surface has a finite width. These perturbations are probably negligible because the considered correlations are on larger scales than the thickness of the last scattering surface. [102]

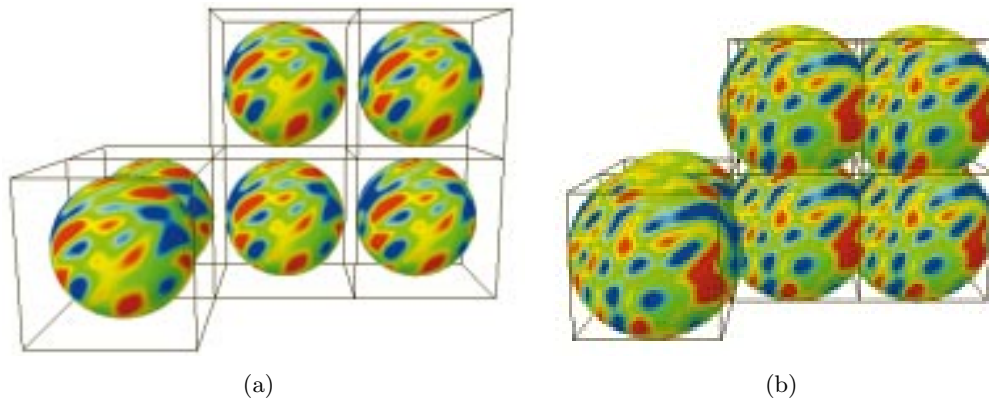


Figure 6.16.: Whether matched circles exist or not, depends on the size of the fundamental cell. In Figure (a), the fundamental cell is bigger than the last scattering surface and therefore no matched circles occur. In Figure (b), the fundamental cell is small enough to enable the existence of matched circles. [70]

As already mentioned, matched circles would only exist if the fundamental cell has an appropriate size. There are three different cases, depending on the size of the fundamental cell (see Figure 6.16(a) and 6.16(b)):

1. If the LSS is smaller than the size of the fundamental cell and does not intersect, no matched circles would be observable. If $2\chi_{LSS} < L_{min}$, no signal would have reached us. See Figure 6.16(a).
2. If the LSS fits exactly within the fundamental cell, there would be just points of intersections. In a toroidal universe, there would be three pairs of points with exactly the same temperature.
3. If the LSS intersects the fundamental cell along circles, we would detect pairs of circles with correlated temperature anisotropies. The pattern of the locations of the circles depends on the topology. For a torus, we would detect three pairs of antipodal matched circles. See Figure 6.16(b). [18]

Circles-in-the-sky methods, first mentioned by [18], assume the universe to be not too small such that the fundamental cell intersects the LSS. Then, the method is independent of the topology, because the intersection of two spheres with the same radius is always a

circle. The position, distance and number of matched circles is then representative for the topology of the universe. [18]

The search for matched circles is time-consuming. The WMAP data ([8]) consists of $3 \cdot 10^6$ independent points. Each point can be the center of a circle with radius $0 \leq \nu \leq 90^\circ$. The Fourier transform $\sum_m T_{i,m} \exp(im\Phi)$, where $T_{i,m}$ is the m th harmonic of the i th circle, of each circle has to be calculated. The temperature fluctuation of circles with the same radius are compared where a possible phase ϕ between 0° and 360° has to be taken into account. [51]

A statistic

$$S_{ij}(\Theta, \Phi) = \frac{2 \sum_m m T_{i,m}(\Theta) T_{j,m}^*(\Theta) e^{-im\Phi}}{\sum_n n [|T_{i,n}(\Theta)|^2 + |T_{j,n}^*(\Theta)|^2]}$$

has been defined in [19] (first mentioned in [18]) which compares fluctuations of all scales along circles with the same radius. The index satisfies $S_{ij} = 1$ for a perfect match and expectation value of 0 if random circle are compared. The method was tested with a simulated CMB sky for a finite cubic three-dimensional torus of $L = 0.513\chi_{LSS}$ where the Sachs-Wolf effect was included. The algorithm found almost perfect matched circles with $S = 0.99$. The algorithms applied to real data shall not show such perfect values. The statistic is widely used in papers dealing with the circles-in-the-sky method, for example, in [51], [6] and [59].

There have been attempts to search for antipodal circles in the sky ([19], [51]), without result. Roukema et al. ([59]) claimed the detection of six pairs of dodecahedral shaped circles of radius $11 \pm 1^\circ$ with a phase shift of 36° as predicted for the Poincaré dodecahedral space. The promised analysis of the statistic methods was not made and was doubt by [51]. Then [97] made the analysis and found out that the ILC⁵ maps, used in [59], reduce foreground not sufficiently enough to use the map for the circles-in-the-sky method. The statistical significance was doubt by Roukema himself in [58]. The authors of [19] rule out the possibility of a dodecahedral topology.

First, Aurich, Lustig and Steiner remarked in [6] that the correlated fluctuations due to the ordinary SW effect could be degraded by the integrated SW effect and the dipole-anisotropy. The in Figure 6.17 illustrated three contributions to the temperature fluctuations lead to a deviation of a perfect match of temperature fluctuations along the circles. See also Figure 6.18.

Aurich, Lustig and Steiner [4] and Lew and Roukema [58] found a marginally hint for Poincaré dodecahedral space, for which we shall present a detailed review in the end of this chapter.

Recently, the deviation for matched circles from being antipodal has been calculated. The results show that at least for Euclidean manifolds, the circles do not have to be antipodal at all [77], [76]. The results for Euclidean space forms is presented in Figure 6.19(b).

⁵The ILC (Internal Linear Combination) maps are formed from weighted linear combinations of five smoothed I-maps with minimized galactic foreground contribution. See Lambda Homepage (http://lambda.gsfc.nasa.gov/product/map/dr1/internal_linear_comb.cfm) for more detailed information.

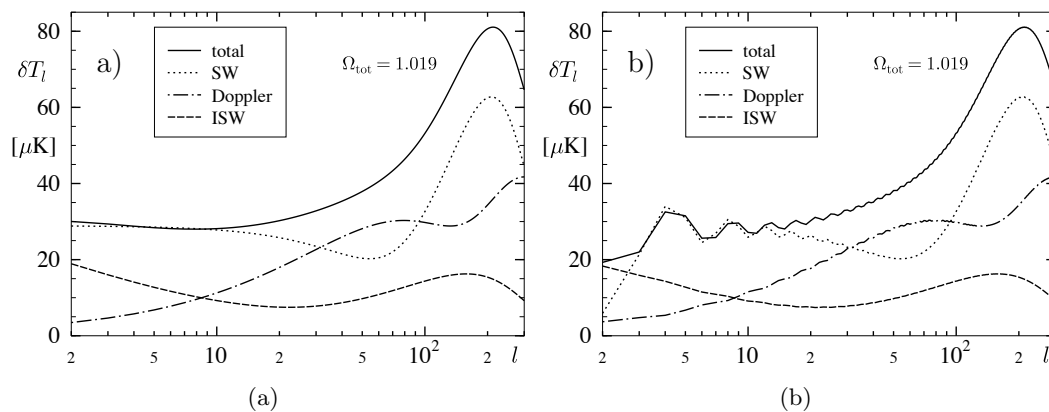


Figure 6.17.: The dipole anisotropies and the anisotropies caused by the ordinary SW effect as well as the integrated SW effect are illustrated for the sphere (a) and the dodecahedral space (b). Used cosmological parameter: $\Omega_0 = 1.019$, $h = 0.70$, $\Omega_m = 0.28$. For further informations of the simulations see [6]. For the lowest modes, the ISW effect dominates over the ordinary SW effect for the dodecahedral space, which may avoid the detection of matched circles. [6]

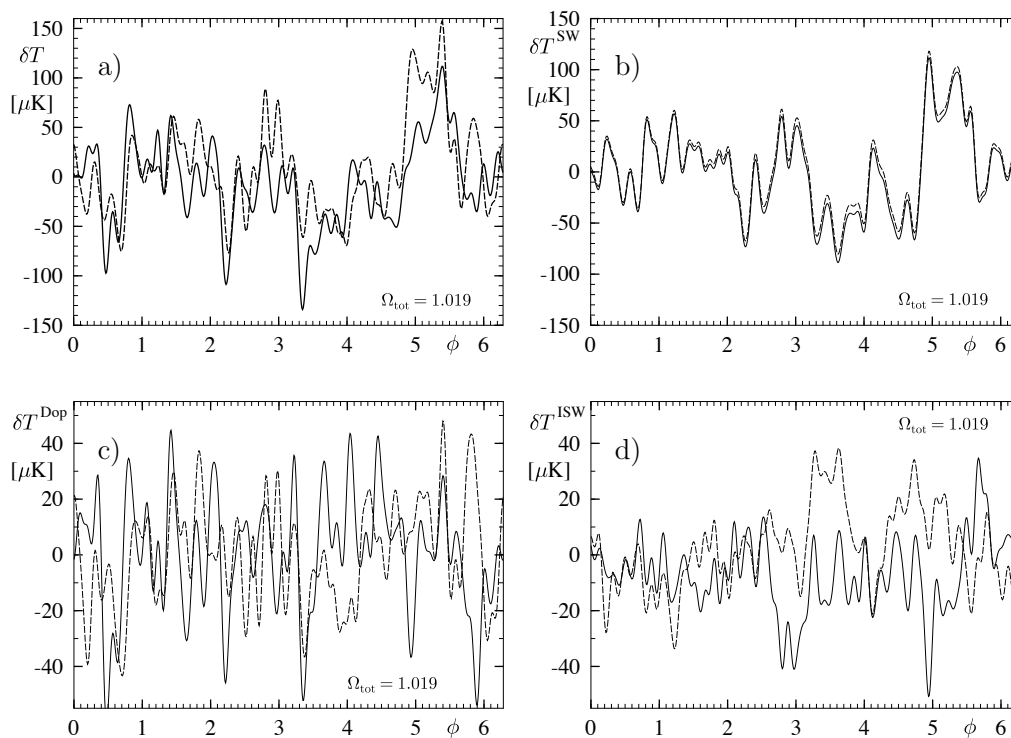


Figure 6.18.: In panel a), the total temperature fluctuations of two matched circles are visualized. In panel b), c) and d) the according fluctuations due to SW effect, ISW effect and dipole anisotropy respectively can be seen. The anisotropies due to the SW effect give a perfect fit. The total anisotropies is not matched perfectly well, because of the contribution of ISW and dipole anisotropies. [6]

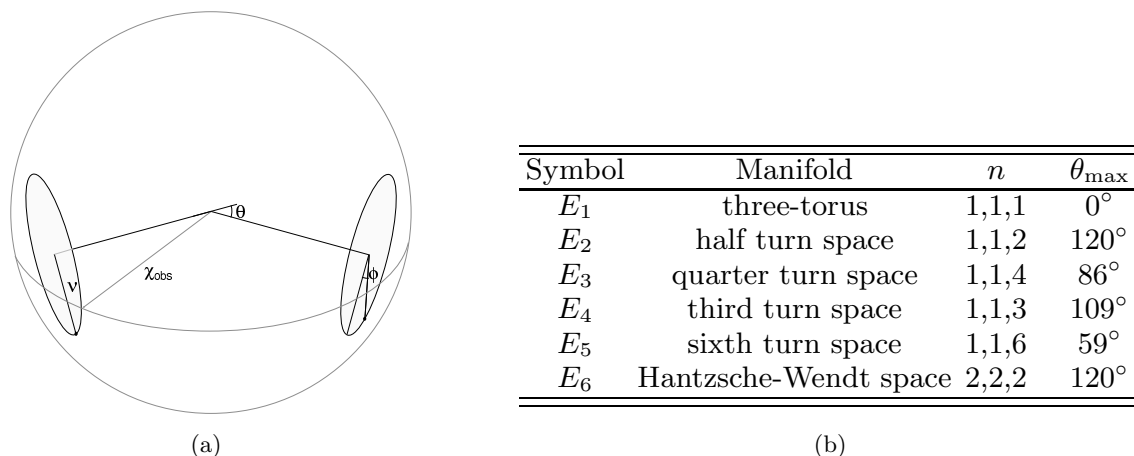


Figure 6.19.: (a): Two matched circles are determined by the coordinates of one of the circles and three angles describing the relative position of the second. (b): Maximal possible deviation of matched circles of being antipodal for Euclidean space forms. E_i denotes the Euclidean space form \mathcal{G}_i introduced in Chapter 4, Theorem 4.4.2.9, p.89 except for $i = 3$ and 4. $E_3 = \mathcal{G}_4$ and $E_4 = \mathcal{G}_3$. The description as gluing manifolds was done in 5.3 (p.110). [77]

In a further investigation, Mota, Rebouças and Tavakol showed in [78], how to reconstruct topology if one pair of matched circles is found in an Euclidean space ⁶:

Matched circles corresponding to an element of the holonomy group $\gamma \in \Gamma$ are characterized by three angles giving the position of the first circle and the following three angles determining the relative position of the second (see also Figure 6.19(a)):

1. deviation angle of antipodicity ($0 \leq \Theta \leq \pi$),
2. angular radius of the circle ($0 \leq \nu \leq \pi/2$) and
3. phase-shift: angle between correlated points on the circle ($0 \leq \phi \leq \pi$).

It is easy to see, that the nearer the circles are, the bigger the radius of the circles. For a flat universe, a holonomy is a screw-motion, which consists of a rotation and a translation. Thus, any Euclidean holonomy is determined by the following parameter:

1. α : The angle of the rotation, which can only take the discrete values $\alpha = \frac{2\pi}{n}$, $n = 1, 2, 3, 4, 6$ according to the space form $\mathcal{G}_1, \mathcal{G}_2, \mathcal{G}_3, \mathcal{G}_4$ or \mathcal{G}_5 .
2. L : the length of the translation,
3. r : the distance of the observer to the axis of rotation.

⁶Mota, Rebouças and Tavakol considered in [78] just flat universes because of there negative attempts in previous work on nearly flat spaces ([19], [51])

The coordinates of the matched circles and the parameter of the holonomy are correlated by the following formulas [78]:

$$\cos \alpha = \frac{(\cos \Phi + 1)(\cos \Theta + 1)}{2} - 1, \quad L = 2\chi_{LSS} \cos \nu \sqrt{\frac{\cos \Theta - \cos \alpha}{1 - \cos \alpha}}, \quad r = \sqrt{2}\chi_{LSS} \cos \nu \frac{\sqrt{1 - \cos \Theta}}{1 - \cos \alpha}$$

First equation, defines contour lines in the (Φ, Θ) -plane, see Figure 6.20.

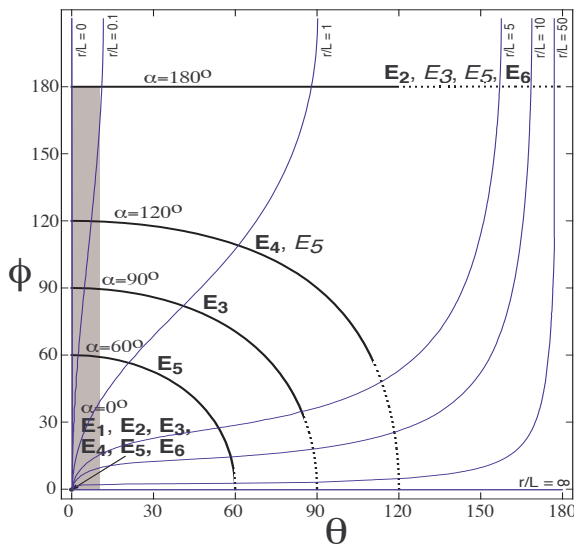


Figure 6.20.: The correlation of the twist parameter α of an Euclidean holonomy and the coordinates Θ, Φ of a pair of matched circles define a contour plot in the (Θ, Φ) -plane. The correlation is not one-to-one onto between the contour curves and the topology of the Euclidean space forms. See Figure 6.19(b) for the corresponding names of the space forms. [78]

We assume a pair of matched circles with coordinates (ν, Θ, Φ) . If (Θ, Φ) lie on one of the contour curves of Figure 6.20, it indicates that the geometry of space is actually Euclidean. If they do not lie on one of the curves, this is an indication for a non-flat geometry. Uncertainties of coordinates have to be taken into account by working with real data.

Suppose (Θ, Φ) lies on one of the contour curves, then α gives us a first restriction on the topology, see Figure 6.20. But the correlation is not one-to-one onto. If we assume the matched circles to be the nearest pair, we get a one-to-one onto relation except for the cases $\alpha = 0^\circ$ and $\alpha = 180^\circ$. If $\alpha = 0^\circ$, any of the six Euclidean topologies is possible. If $\alpha = 180^\circ$, the found matched circles are the nearest circles for \mathcal{G}_2 and \mathcal{G}_6 . Thus, in this case another pair of matched circles has to be found. This case is unlikely because of the several negative searches for antipodal circles.

Otherwise the pair of matched circles determines uniquely the topology. If we assume,

for instance, that a pair of matched circles with $\alpha = 120^\circ$ was found. Figure 6.20 tells us, that the possible topologies are \mathcal{G}_3 and \mathcal{G}_5 . \mathcal{G}_5 has a generator of the holonomy group with $\alpha = 60^\circ$. The corresponding matched circles to the holonomy with $\alpha = 60^\circ$ is nearer and therefore easier detectable. Thus, we would properly already have found it. If we have not found it, we can calculate the position of these matched circles and search for them. If the search result is negative, we have an indication that the topology of the universe is \mathcal{G}_3 . [78]

6.3.4.2. Power Spectrum

In the **power spectrum**, the multipole is plotted versus the **anisotropy power**

$$\delta T_\ell^2 = \frac{\ell(\ell+1)}{2\pi} C_\ell. \quad [5]$$

If space is simply-connected, the C_ℓ contain all the information. Otherwise, the $C_{\ell m}^{\ell' m'}$ have to be calculated to derive full information. In this case, the C_ℓ can be taken as an estimation for the values of the average power spectrum. [57]

The power spectrum of the CMB can be seen in Figure 6.21. The power spectrum does not change if a multi-connected space is considered instead of a simply-connected one. Just the number of modes which exist is lowered.

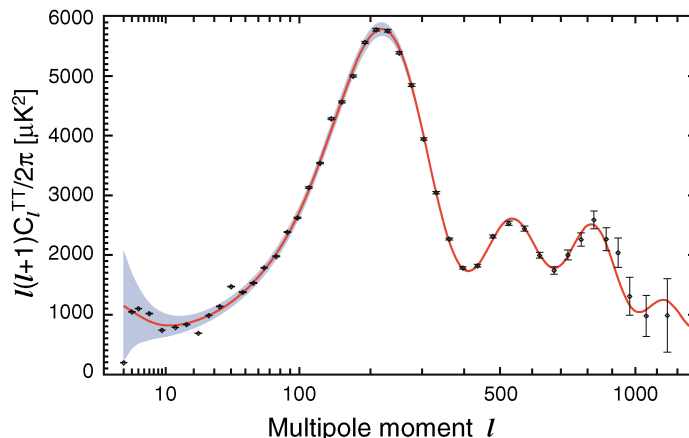


Figure 6.21.: The power spectrum of the CMB visualizes the temperature anisotropies of different angular scales. From left to right, the angular decreases, while the multipole increases. For $\ell < 10$, the wide-angular anisotropies are dominated by the integrated Sachs-Wolf effect. For $10 < \ell < 50$, the Sachs-Wolf effect causes the Sachs-Wolf Plateau. The dots are the anisotropy power derived by WMAP data. It is visible that the quadrupole and octopole are significantly smaller than the expected value. The here presented power spectrum uses the 7-year WMAP data. [134]

The measurements of the C_ℓ^{obs} for $4 \leq \ell \leq 40$ are in accordance with formula 6.23 [109]. The observed power spectrum is consistent with an infinite, flat universe at small and mean

scales. Thus, the power spectrum of the CMB can be explained by Standard Cosmology except for the multipole coefficients with $\ell = 2$ and $\ell = 3$. The first observable harmonic is the quadrupole, which corresponds to the multipole $\ell = 2$. The harmonic corresponding to $\ell = 1$ is not observable because the dipole caused by the Doppler effect is 100 times greater than that caused by primary anisotropy [69]. The measured value of the quadrupole is seven times weaker than expected by integrated Sachs-Wolf effect. The value of the harmonic corresponding to $\ell = 3$, which is called the octopole, is just 72% of the expected value [102], [3]. These unexpected low values for temperature fluctuations on large scales ($\theta > 60^\circ$) have been detected for the first time by WMAP [95] [109]. Thus, long wavelengths are missing. There are three possible explanations:

1. There are unknown physical laws in the early universe, see for example [101].
2. Space is not big enough to sustain long wavelength. This argument was first suggested by [95] after they found the low wide-angular correlation.
3. The small values are due to errors in analysis. See for example [21].

[102] [3]

In the following we shall take the values of the observed C_ℓ s as real.

In an infinite space all wavelengths are allowed, and therefore, fluctuations must be present on all scales. In a finite universe, the maximal wavelength is as long as the diameter of space [62]. A power spectrum for different spaces can be simulated and compared to the observed pattern.

For many homogeneous topologies, the eigenmodes can be thought of as harmonics of the FP with identified facets. For example, the eigenstates of the three-dimensional torus with equal fundamental lengths L are the discrete values $\sin(k \cdot r)$ and $\cos(k \cdot r)$, where $k = \left(\frac{2\pi n_x}{L}, \frac{2\pi n_y}{L}, \frac{2\pi n_z}{L}\right)$, with n_x, n_y, n_z being integers. The minimum wave number is $k_{min} = \frac{2\pi}{L}$ and the corresponding maximum wavelength is given by $\lambda_{max} = L$. Thus, no fluctuation larger than the topology scale L can occur [68]. For hyperbolic manifolds the situation is different, because there are no discrete orbits and therefore no cut-off wavelength [18]. We shall not go into further details here. For a more detailed description see [102], [3] and references there.

If the whole correlation matrix is determined, the $C_\ell = \frac{1}{2\ell+1} \sum_m C_{\ell m}^{\ell' m'}$ can be calculated. The multipole coefficients then include all the sufficient information [102].

The size of the FP has to be of the size of the last scattering surface. If it is significantly smaller, higher modes (smaller angles) would be suppressed more strongly. If it is significantly larger than the LSS, no effect on the CMB map from topology would be detectable.

In a MCM, the smaller the FP, the fewer modes are supported. In comparison with the corresponding SCM, all modes are suppressed. The small values for low-order modes could be caused by a FP, which suppresses the low modes more than the higher modes. Weeks

et al. have considered the question which shapes of the FP could cause the observed power spectrum. [68]

If we shrink the fundamental length L to a value L' in a regular three-dimensional torus, the power spectrum does not change its shape, but the spectrum occurs on smaller wavelengths (larger multipoles). If $L' \gg \chi_{LSS}$ no effect is visible. If $L > \chi_{LSS}$ and $L' < \chi_{LSS}$ the quadrupole is suppressed. A further shrinking of L' causes properly the loss of support of the octopole as well. Here, the low modes are more suppressed than the high modes. If we shrink the fundamental length in one dimension, for example L_x to a value L'_x while leaving the other lengths unchanged, $L_y = L_z = L$, the lowest mode remains unchanged, but its multiplicity is lowered by the factor $2/3$. The overall density of modes has dropped by the factor L_x/L . Thus the relative strength of the low modes with respect to the high modes is $\frac{2L}{3L_x}$. For $L_x \rightarrow 0$ and $\frac{2L}{3L_x} \rightarrow \infty$, the low modes are boosted. [68]

Spaces with a fundamental polyhedron of approximately equal fundamental lengths are called **well-proportioned spaces**, whereas spaces with at least one fundamental length significantly larger than the others are called **oddly-proportioned**. The result derived by [68] is that well-proportioned spaces suppress low modes more than high modes. In oddly-proportioned spaces low modes are boosted relative to high modes. This conclusion has been confirmed by simulations including the SW effect, ISW effect and dipole anisotropy.

For spherical spaces, lens spaces are oddly-proportioned whereas binary polyhedral spaces are well-proportioned. The simulated power spectra of these homogeneous spaces fit the observed powers spectrum better than a torus-universe, which fits the observed power spectrum better than the concordance model. From the binary polyhedral spaces, the data is fitted the best by Poincaré dodecahedral space.

Aurich and Lustig calculated in [3] the angular correlation function $C(\theta)$ for different flat space forms. In order to compare their predicted $C^p(\theta)$ to the observed $C^{obs}(\theta)$, they used the **weighted temperature correlation difference**: for $\theta \in [0^\circ, 180^\circ]$

$$I := \int_{-1}^1 d\cos(\theta) \frac{(C^p(\theta) - C^{obs}(\theta))^2}{Var(C^p(\theta))}$$

$$Var(C(\theta)) \approx \sum_{\ell} \frac{2\ell + 1}{8\pi^2} [C_{\ell} P_{\ell}(\cos\theta)]^2.$$

Their results are presented in Figure 6.22. They independently derived the result that a multi-connected space fits the power spectrum better than the concordance model. They obtained best fit for the half-turn space.

6.4. The Poincaré Dodecahedral Space

For a mathematical description of Poincaré dodecahedral space see Chapter 5 (5.4.2, p.114).

Apart from the three-dimensional torus, the most discussed non-simply-connected space in

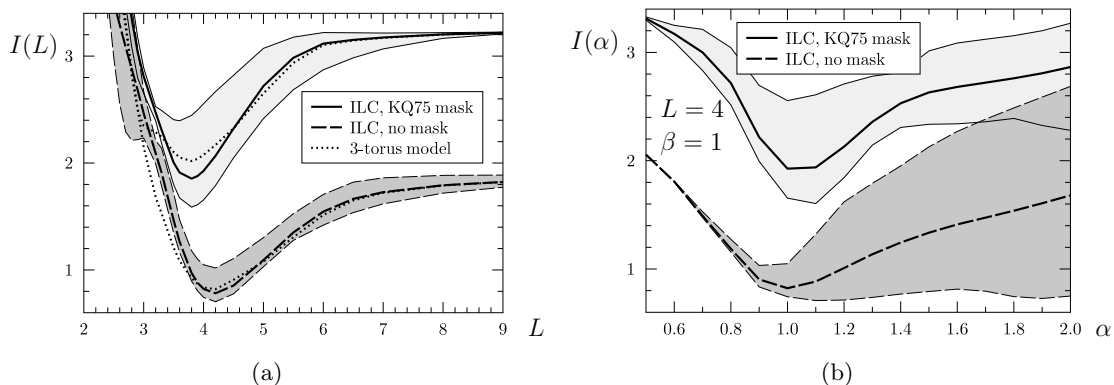


Figure 6.22.: (a) The weighted temperature correlation difference $I(L)$ for the cubic half-turn space and the cubic torus is plotted versus the topological length L , characteristic for the fundamental cell. L is given in units of the Hubble length $L_{Hubble} = c/H_0$, which takes here the value $L_{Hubble} = 4.28 \text{ Gpc}$. Used cosmological parameter: $\Omega_b = 0.0474$, $\Omega_{CDM} = 0.243$, $\Omega_\Lambda = 0.709$ and $h = 0.697$. The plots using the ILC 7yr map [34] with and without using the KQ75 7yr mask, which masks the galactic plane, are shown. The bands show the variance of the function if the position of the observer is changed. It is striking that the half-turn space fits the data better than the torus and the infinite space, which can be compared with $L = 9$. Best fit is achieved for $L = 4$. (b) Shows the plot of the weighted temperature correlation difference depending on the angular scale, here denoted by α , for the best fit of plot (a), the half-turn space with $L = 4$. A better result is achieved with using the maps without the KQ75 7yr mask. [3]

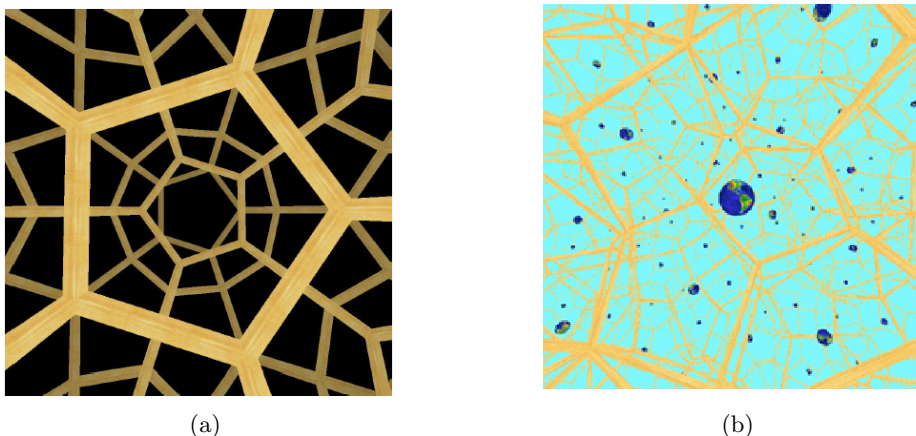


Figure 6.23.: Inner view of the Poincaré dodecahedral space. [64]

cosmology is Poincaré Dodecahedral Space (PDS). We shall present the scientific discussion of the last ten years to conclude this chapter. In Figure 6.23, the inner view of the PDS is visualized.

The eigenvalues of the three-dimensional sphere build a discrete set since the sphere is compact [6]. They can be expressed in terms of the wave number k by $E_k = k^2 - 1$ with multiplicity k^2 . For a fixed space form \mathbb{S}^3/Γ , the eigenvalues are the same, but the wave number k cannot take all integer numbers and the multiplicity is may lowered. The eigenvalues of PDS are $E_k = k^2 - 1$ with

$$k \in \{1, 13, 21, 25, 31, 33, 37, 41, 43, 45, 49, 51, 53, 55, 57\} \cup \{2n + 1, n > 30, n \in \mathbb{N}\}$$

with multiplicity

$$k \left(\left[\frac{k-1}{10} \right] + \left[\frac{k-1}{6} \right] + \left[\frac{k-1}{4} \right] - \frac{k-3}{2} \right). \quad [6]$$

Using the method described in [102], Luminet et al. ([69]) calculated the value of the quadrupole and octopole numerically using the eigenmodes corresponding to the wave numbers $k < 30$ for the PDS. They found that the low modes fit the first-year WMAP data ([95]) better than the standard model, see Figure 6.24.

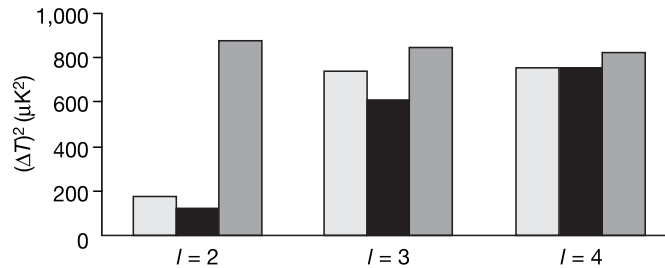


Figure 6.24.: Comparison of the low modes for first-year WMAP data (black) from [95], expectations for an infinite flat space (dark grey) and those for PDS (light grey) [69]

Furthermore, they remarked the strong dependence of the low modes on the density parameter Ω_0 . Determining $\Omega_m = 0.28$ and $\Omega_\Lambda = \Omega_0 - \Omega_m$, they conclude that the expected quadrupole and octopole for PDS fit the first-year WMAP data ([8]) for $1.012 < \Omega_0 < 1.014$, which is consistent with the density parameter derived by [8]. See Figure 6.25(a). In 2005, they plotted the multipoles in dependence of Ω_0 with the first-year data and found the best fit at $\Omega_0 = 1.016$, see Figure 6.25(b) [64]. For $\Omega_0 = 1.02$, the smallest volume of the fundamental polyhedron of the PDS is just 80% of the volume of the last scattering surface and $L_{min} = 43 \text{ GPC}$. This is a theoretically testable model. [63]

The Poincaré dodecahedral space was affirmed, when Roukema et al. ([59]) found six pairs of matched circles in a pattern predicted by the PDS. As already remarked in section

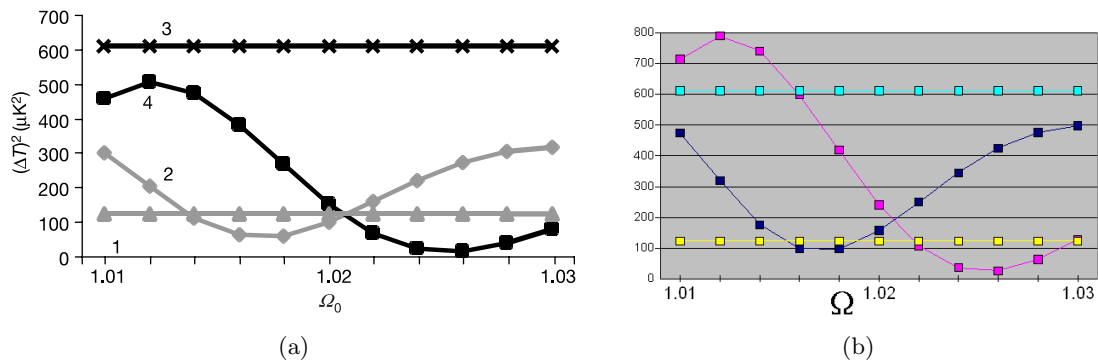


Figure 6.25.: (a): The modes for $\ell = 2$ and $\ell = 3$ for WMAP first-year data [8] are plotted as constant lines denoted by (1) respectively (3). The expectations for the low modes for PDS are denoted by (2) for $\ell = 2$ and (4) for $\ell = 3$. [69] (b): Comparison of the low modes for WMAP first-year data (light blue for the octopole and yellow for the quadrupole) with the expectations for PDS-model (pink for the octopole and dark blue for the quadrupole). [64]

6.3.4.1, the statistical significant has not been approved and the result is argumentative.

In 2005, Aurich, Lustig and Steiner considered spherical space forms in their investigations [5] and [6]. Instead of using just the first three wave numbers 13, 21 and 25 (59 eigenfunctions) as [69], they were able to consider 10 521 eigenfunctions of the PDS corresponding to the wave numbers up to $k = 155$. The used algorithm to calculate the eigenmodes is described in [6]. The dipole effect as well as the Sachs-Wolf and the integrated Sachs-Wolf effect have been considered. A suppression of the low modes was only found for all polyhedral spaces. First, they made investigations to derive the optimal value of Ω_0 to obtain the best fit to the WMAP data for the polyhedral spaces. The value of Ω_0 can be taken as indication of one of the polyhedral spaces. While $\Omega_0 \in [1.06; 1.07]$ for the binary tetrahedral space, $\Omega_0 \in [1.03; 1.04]$ for the octahedral space and $\Omega_0 \in [1.015; 1.02]$ for the dodecahedral space (PDS). Furthermore, a map of the temperature fluctuation for the three spaces was simulated and from them the angular power spectrum. The used cosmological parameter are listed in table 6.2.

Table 6.2.: cosmological parameter used in [5]

Space form	k_{max}	Ω_0	Ω_Λ	h
\mathbb{S}/T^*	155	1.065	0.785	70
\mathbb{S}/O^*	161	1.038	0.785	70
\mathbb{S}/I^*	185	1.018	0.785	70

They found a strong suppression of the low modes for the PDS and could affirm the results made by [69]. An even stronger suppression was found for the binary octahedral space. See

Figure 6.26. For the optimal cosmological parameter, the power spectrum of both spaces lie within the $1\text{-}\sigma$ band, thus, future restrictions of Ω_0 may exclude at least one model.

The search for matched circles in [6] brought just a marginally hint for the PDS. As discussed in 6.3.4.1, the statistical significance is not granted.

Furthermore, the angular correlation function was calculated and plotted for different values of Ω_0 , see Figure 6.27. It is striking, that the PDS-model fits the WMAP data better than the concordance model. The WMAP data is within the $1\text{-}\sigma$ region of the simulated angular correlation function of the PDS for angles $\theta < 170^\circ$ in Figure 6.27 b) and c). Thus, just the largest negative correlation of WMAP data cannot be explained by the PDS-model, where the dipole anisotropy and Doppler effect dominate the data.

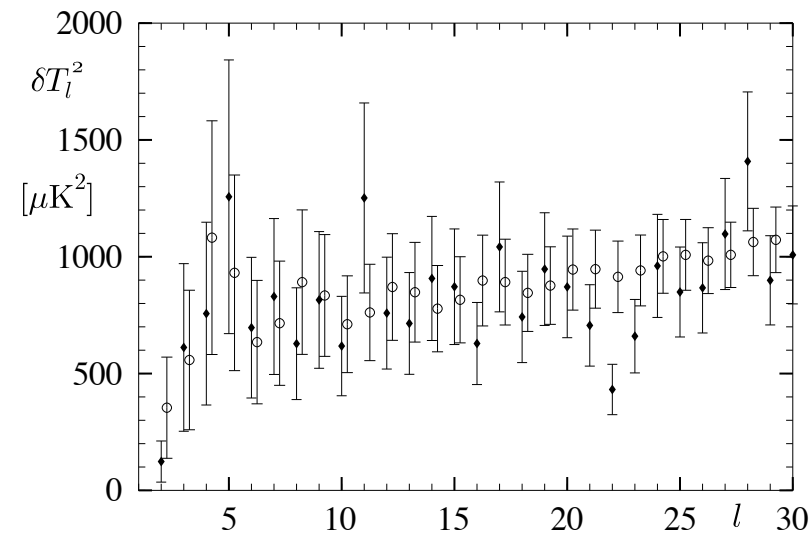
The results presented in [6] have been confirmed by Caillerie and Lachièze-Rey et al. in [14], which find an optimal fit for $\Omega_0 = 1.018$. They used the analysis derived by [6], but used more recent data from 2007. See Figure 6.28.

Roukema with partially co-authors argued in [88], [87] and [89] that because of the residual gravity accelerating effect, which we shall not explain here, polyhedral spaces are favourable. From those, the Poincaré dodecahedral space fits the data the best.

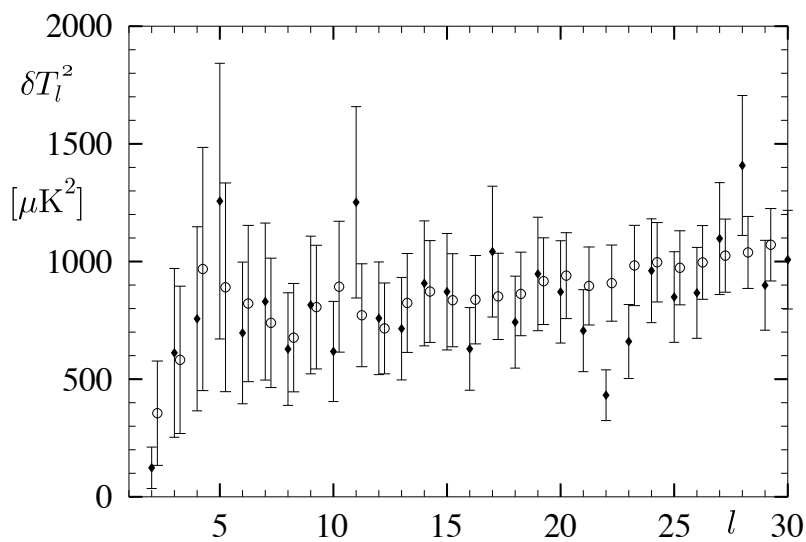
There are, of course, also critical article, from which we shall mention [80].

6.5. Conclusion

We presented the derivation of Friedmann's equation as a special solution of Einstein's field equation for isotropic and homogeneous $\widetilde{\mathcal{M}}_3$. We have seen that Friedmann's equation enables us to determine the geometry of the universe by determining the cosmological parameter, which is aimed by Standard Cosmology. Cosmic Topology tries to determine the topology of the universe. Therefore, two different types of data are used: three-dimensional data of cosmic objects for crystallographic methods and the CMB-anisotropies for the circles-in-the-sky method and methods using the power spectrum. Up to now, these methods were not able to determine the topology of space, but they indicate that MCMs fit the observational data better than SCMs. The power spectrum and the angular correlation function of MCM, as for example the PDS, fit the real data better than the concordance model. For a proof of this indication, deeper catalogues, better technical equipment and data with a higher accuracy are required. Future data from Planck and further developments of the methods constraining the topology of the universe shall answer the until today open questions.



(a)



(b)

Figure 6.26.: The angular power spectrum for the space (a) \mathbb{S}/I^* and (b) \mathbb{S}/O^* are shown. The open circles correspond to the simulated power spectrum derived by [6] with the error bars visualizing the fluctuation due to different realizations. In order to enable a comparison with the WMAP data the simulated power spectrum is shifted by $\Delta l = 0.25$. The full diamonds correspond to the data of the first-year WMAP with the $1 - \sigma$ errors.

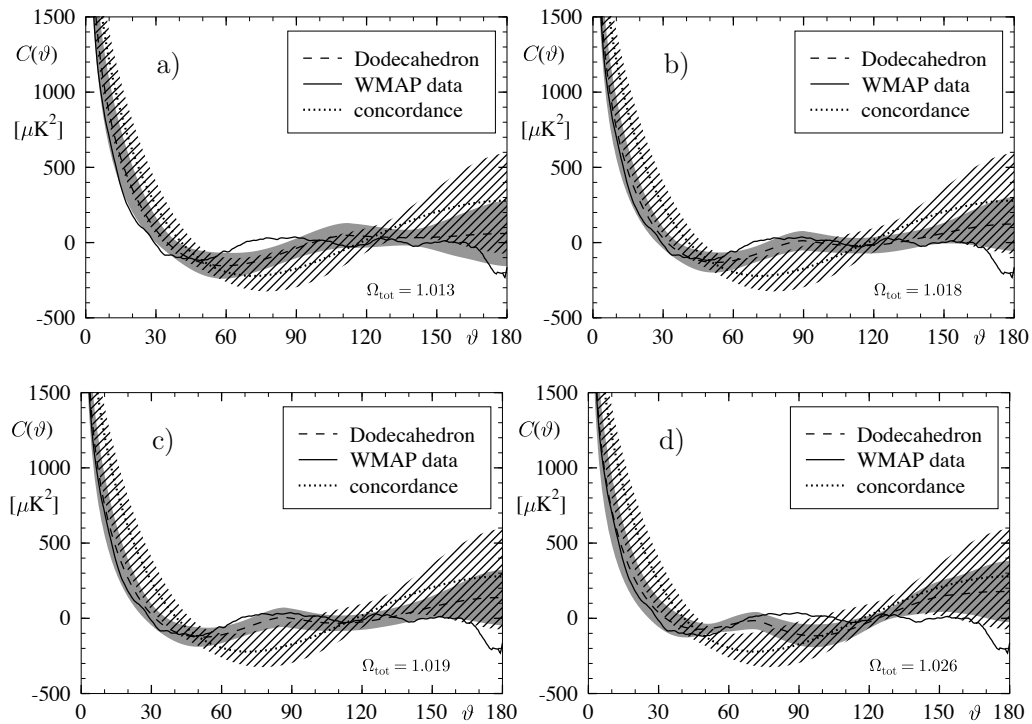


Figure 6.27.: The temperature correlation function $C(\theta)$ for the concordance model, the WMAP data and for the PDS with cosmological parameter $h = 0.70$, $\Omega_m = 0.28$ for different Ω_0 is plotted. The grey region corresponds to the $1\text{-}\sigma$ -deviation caused by the 500 performed simulations. The curve for the concordance model is, as the curve for the WMAP data, taken from LAMBDA Homepage (<http://lambda.gsfc.nasa.gov>) the dashed region corresponded to the $1\text{-}\sigma$ deviation of the concordance model. [6]

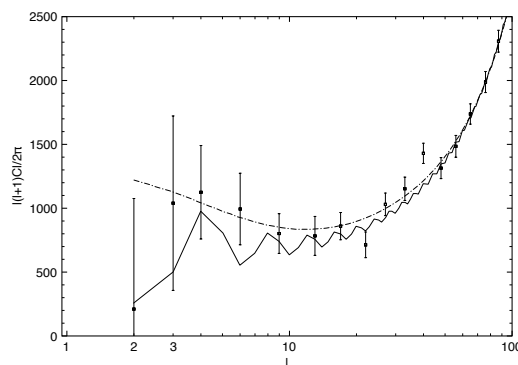


Figure 6.28.: The power spectrum as a function of the multipole ℓ . The dots with error bars correspond third-year WMAP data from 2007. The solid curve represents PDS-model with cosmological parameter $h = 0.70$, $\Omega_m = 0.27$ and $\Omega_0 = 1.018$. The dashed curve represents the concordance model. [14]

Bibliography

- [1] H. Abels. Properly Discontinuous Groups of Transformations: A Survey. Geometriae Dedicata, 87:309–333, 2001. [86](#)
- [2] C. Adams and J. Shapiro. The Shape of the Universe: Ten Possibilities. American Scientist, 89:443–453, 2001. [99](#), [100](#), [112](#)
- [3] R. Aurich and S. Lustig. Cosmic microwave anisotropies in an inhomogeneous compact flat universe. Classical Quantum Gravity, 28(085017), 2011, arXiv:1009.5880v2. [164](#), [165](#), [166](#)
- [4] R. Aurich, S. Lustig, and F. Steiner. The circles-in-the-sky signature for three spherical universes. Monthly Notices of the Royal astronomical Society MNRAS, 369:240–248, 2005, arXiv:astro-ph/0510847v1. [30](#), [159](#)
- [5] R. Aurich, S. Lustig, and F. Steiner. CMB Anisotropy of Spherical Spaces. Classical Quantum Gravity, 22(3443 - 3460), 2005, arXiv:astro-ph/0504656v1. [156](#), [163](#), [168](#)
- [6] R. Aurich, S. Lustig, and F. Steiner. CMB Anisotropy of the Poincaré Dodecahedron. Classical Quantum Gravity, 22(2061 - 2083), 2005, arXiv:astro-ph/0412569v2. [159](#), [160](#), [167](#), [168](#), [169](#), [170](#), [171](#)
- [7] W. Barlow. Über die geometrischen Eigenschaften homogener starrer Strukturen und ihre Anwendung auf Kristalle. Zeitschrift für Krystallographie und Mineralogie, 23, 1894. [88](#)
- [8] C. Bennett et al. First-Year Wilkinson Microwave Anisotropy Probe (WMAP) Observations: Preliminary Maps and Basic Results. Astrophysical Journal Supplement Series, 148:1–27, 2003, arXiv:astro-ph/0302207v3. [151](#), [159](#), [167](#), [168](#)
- [9] Bieberbach. Über die Bewegungsgruppen euklidischer Räume i. Mathematische Annalen, 70:297–336, 1911. [87](#)
- [10] Bieberbach. Über die Bewegungsgruppen euklidischer Räume ii. Mathematische Annalen, 72:400–412, 1912. [87](#)

- [11] M. Biesiada. Gamma-Ray Bursts and Topology of the Universe. 1993, arXiv:astro-ph/9310005v1. [138](#)
- [12] A. Bravais. Mémoire sur les poly'edres de form symétrique. Journal de Mathematiques Pures et Appliquées, 14:141–180, 1849. [86](#)
- [13] S. Caillerie and M. L. Rey. Laplacian eigenmodes for spherical spaces. Classical and Quantum Gravity, 22(4):695–708, 2005, arXiv:astro-ph/0501419v1. [156](#)
- [14] S. Caillerie, M. L. Rey, J.-P. Luminet, et al. A new analysis of the Poincaré dodecahedral space model. Astronomy and Astrophysics, 476(2):691–696, 2007, arXiv:0705.0217v2 [astro-ph]. [156](#), [169](#), [171](#)
- [15] A. Cap. Algebraische Topologie. Vorlesungsskript, 2004. [44](#), [45](#), [46](#)
- [16] A. Cap. Lie groups. Vorlesungsskript, 2004. [40](#), [41](#), [42](#), [43](#), [70](#), [72](#), [191](#), [192](#), [193](#)
- [17] A. Cap. Lie algebras and Representative Theory. Vorlesungsskript, 2009. [40](#), [189](#), [190](#)
- [18] N. Cornish, D. Spergel, and G. Starkman. Circles in the Sky: Finding Topology with the Microwave Background Radiation. Classical and Quantum Gravity, 15:2657 – 2670, 1998, arXiv:gr-qc/9602039v2. [36](#), [120](#), [137](#), [153](#), [158](#), [159](#), [164](#)
- [19] N. Cornish, D. Spergel, G. Starkman, and E. Komatsu. Constraining the Topology of the Universes. Physical Review Letters, 92(20):201302, 2005, arXiv:astro-ph/0310233. [157](#), [159](#), [161](#)
- [20] M. Demianski and M. Lapucha. On the problem of topological structure of the universe. Monthly Notices of the Royal astronomic Society MNRAS, 224:527–536, 1987. [138](#)
- [21] G. Efsathiou, Y. Ma, and D. Hanson. Large-Angle Correlation in the Cosmic Microwave Background. Monthly Notices of the Royal astronomic Society MNRAS, 407(2530), 2010, arXiv:0911.5399. [164](#)
- [22] G. Ellis. Topology and cosmology. General Relativity and Gravitation, 2(1):7 – 21, 1971. [25](#), [26](#), [31](#), [136](#), [141](#)
- [23] J. B. Etnyre. Introductory lectures on Contact Geometry. Proceedings Symposium Pure Mathematics, Georgia Topology Conference, 71:81–107, 2003, arXiv:math/0111118. [71](#)
- [24] H. Fagundes. Quasar-galaxy associations with discordant redshifts as a topological effect. ii - A closed hyperbolic mode. Astrophysical Journal, 338(1):618–629, 1989. [138](#)

-
- [25] H. Fagundes. Erratum to “quasar-galaxy associations with discordant redshifts as a topological effect. ii - A closed hyperbolic mode”. *Astrophysical Journal*, 349:678, 1990. [138](#)
- [26] H. Fagundes and E. Gausmann. On closed Einstein - de Sitter Universes. *Physical Letters A*, 238:235 – 238, 1998, arXiv:astrp-ph/9811368. [138](#), [139](#), [141](#), [143](#)
- [27] H. Fagundes and E. Gausmann. Cosmic Crystallography in Compact Hyperbolic Universes. *Astronomy and Astrophysics*, 351:766 – 774, 1999, arXiv:astrp-ph/9811368. [139](#), [143](#)
- [28] H. V. Fagundes and E. Gausmann. Cosmic Crystallographic method with a pull-back. *Physics Letters A*, 261(5-6):235–239, 1999, arXiv:astro-ph/9906046. [145](#), [146](#)
- [29] E. S. Fedorov. *Symmetry of crystals*. American Crystallographic Association, New York, 1949. [88](#)
- [30] H. Fujii and Y. Yoshii. An improved cosmic crystallography method to detect holonomies in flat spaces. *Astronomy and Astrophysics*, 529:A121, 2011, arXiv:1103.1466. [146](#)
- [31] H. Fujii and Y. Yoshii. On the possibility for constraining cosmic topology from the celestial distribution of astronomical objects. *Astronomy and Astrophysics*, 531, 2011, arXiv:1105.2337. [147](#)
- [32] R. Gamkrelidze. *Geometry I*, volume 1. Springer Verlag, 1988. [21](#), [39](#), [40](#), [41](#), [42](#), [43](#), [194](#)
- [33] E. Gausmann, R. Lehoucq, J.-P. Luminet, J.-P. Uzan, and J. Weeks. Topological Lensing in Spherical Spaces. *Classical and Quantum Gravity*, 18:5155–5186, 2001, arXiv:gr-qc/0106033v1. [94](#), [95](#), [112](#), [113](#), [149](#)
- [34] B. Gold et al. Seven-Year Wilkinson Microwave Anisotropy Probe (WMAP) Observations: Galactic Foreground Emission. 2011, arXiv:1001.4555v3 [astro-ph.GA]. [166](#)
- [35] W. M. Goldman. Geometric structures on manifolds and varieties of representations, in Geometry of group representations. *American Mathematical Society Contemporary Mathematics*, 74:169–198, 1988. [62](#)
- [36] W. M. Goldman. Locally homogeneous geometric manifolds. *Proceedings of the 2010 International Congress of Mathematicians, Hyderabad*, pages 717–744, 2010, arXiv:math.DG/1003.2759. [54](#), [70](#), [74](#)
- [37] G. Gómero. Fundamental Polyhedron and Glueing Data for the Sixth Euclidean, Compact, Orientable 3-manifold. Workshop: A Estrutura Topológica do Universo

- Universidade Federal do Rio Grande do Norte (UFRN), Natal, RN-Brasil, 1996. [102](#), [112](#)
- [38] A. Gray. A generalization of Schur's theorem. Journal of the Mathematical Society of Japan, 21(3):454–457, 1969. [78](#)
- [39] M. Gromov. Hyperbolic manifolds according to Thurston and Jørgenson. Bourbaki Seminar, 546:40–53, 1979-1980. [97](#), [98](#)
- [40] S. Gudmundsson. An Introduction to Riemannian Geometry. Lecture Notes in Mathematics, 2010. [78](#), [190](#), [195](#)
- [41] H. W. H. Hantschke. Dreidimensionale euklidische Raumformen. Mathematische Annalen, 110:593–611, 1935. [88](#)
- [42] A. Hatcher. Algebraic Topology. Princeton University Press, 2002. [20](#), [44](#), [45](#), [46](#), [48](#), [186](#)
- [43] S. Hawking and G. Ellis. The large scales of space-time. Cambridge University Press, 1973. [1](#), [5](#), [8](#), [9](#), [10](#), [11](#), [13](#), [15](#), [16](#), [18](#), [20](#), [21](#), [22](#), [23](#), [24](#), [25](#), [27](#), [28](#), [29](#), [30](#), [31](#), [32](#), [120](#), [125](#), [126](#), [128](#)
- [44] H. Hopf. Zum Clifford-Kleinschen Raumproblem. Mathematische Annalen, 95:253–297, 1925. [93](#)
- [45] E. Hubble. The Law of Red Shift (George Darwin Lecture). Monthly Notices of the Royal Astronomic Society MNRAS, 113:658, 1953. [1](#)
- [46] J. M. I. Moerdijk. Introduction to foliations and Lie grupoids. Cambridge University Press, 2003. [69](#), [70](#)
- [47] J. N. Islam. AN INTRODUCTION TO MATHEMATICAL COSMOLOGY. Cambridge University Press, 2nd edition, 2004. [124](#), [127](#)
- [48] I. J. Richard Gott. Chaotic cosmologies and the topology of the Universe. Monthly Notices of the Royal astronomic Society MNRAS, 193:153 – 169, 1980. [30](#), [36](#), [138](#)
- [49] K. Jaenich. Topologie. Springer-Verlag Berlin Heidelberg, 8 edition, 2005. [185](#), [186](#)
- [50] H. B. L. Jr. Foliations. Bulletin American Mathematical Society, 80:369–418, 1974. [71](#)
- [51] J. S. Key, N. Cornish, D. Spergel, and G. Starkman. Extending the WMAP bound on the size of the Universe. Physical Review D, 75:084034, 2007, arXiv:astro-ph/0604616. [159](#), [161](#)

-
- [52] E. Komatsu, K. Smith, et al. Seven-Year Wilkinson Microwave Anisotropy Probe (WMAP) Observations: Cosmological Interpretation. Astrophysical Journal Supplement Series, 192:18–75, 2011, arXiv:1001.4538v3 [astro-ph.CO]. [121](#), [128](#), [129](#), [130](#), [131](#), [132](#)
- [53] B. Kostant. Holonomy and the Lie algebra of infinitesimal motions of a Riemannian manifold. Proceedings of the National Academy of Sciences of the United States of America, 42(5):258–261, 1956. [62](#)
- [54] A. Kriegl. Differentialgeometrie 1. Vorlesungsskript, 2004. [7](#), [13](#), [40](#), [43](#), [56](#), [68](#), [71](#), [190](#), [191](#)
- [55] M. Lachi eze-Rey and J.-P. Luminet. Cosmic Topology. Physics Reports, 254:135–214, 2003, arXiv:gr-qc/9605010v2. [5](#), [6](#), [20](#), [26](#), [31](#), [33](#), [36](#), [44](#), [46](#), [101](#), [102](#), [111](#), [112](#), [114](#), [115](#), [116](#), [121](#), [122](#), [133](#), [135](#), [136](#), [137](#), [138](#), [153](#)
- [56] R. Lehoucq, J.-P. Luminet, and J.-P. Uzan. Limits of crystallographic methods for detecting space topology. Astronomy and Astrophysics, 363:1 – 8, 2000, arXiv:astro-ph/0005515v1. [126](#), [139](#), [148](#), [149](#)
- [57] J. Levin. Topology and the Cosmic Microwave Background. Physical Reports, 365:251–333, 2002, arXiv:gr-qc/0108043v2. [150](#), [151](#), [153](#), [154](#), [155](#), [163](#)
- [58] B. Lew and B. Roukema. A test of the Poincar e dodecahedral space topology hypothesis with WMAP CMB data. Astronomy and Astrophysics, 482:747–753, 2008, arXiv:0801.1358v2 [astro-ph]. [159](#)
- [59] B. Lew, B. Roukema, M. Cechowska, et al. A Hint of Poincar e Dodecahedral Topology in the WMAP First Year Sky Map. Astronomy and Astrophysics, 423:821, 2004, arXiv:astro-ph/0402608v4. [159](#), [167](#)
- [60] A. Liddle. An Introduction to Modern Cosmology. John Wiley and Sons Ltd., 2. edition, 2003. [33](#), [122](#), [153](#)
- [61] A. Lucchini. Group Theory. Vorlesungsskript (Padova), 2009. [187](#)
- [62] J.-P. Luminet. Geometry and Topology in Relativistic Cosmology. Proceedings ”New Trends in Geometry, and Its Role in the Natural and Life Sciences”, 2005, arXiv:0704.3374v1 [astro-ph]. [5](#), [155](#), [157](#), [164](#)
- [63] J.-P. Luminet. The Shape and Topology of the Universe. Proceedings of conference ”Tessellations : The world a jigsaw”, Leyden (Netherlands), 2006, arXiv:astro-ph/0802.2236v1. [134](#), [167](#)
- [64] J.-P. Luminet. The Shape of Space after WMAP data. Brazilian Journal of Physik, 36:107–114, 2006, arXiv:astro-ph/0501189v. [30](#), [31](#), [126](#), [166](#), [167](#), [168](#)
-

- [65] J.-P. Luminet. The Wraparound Universe. A K Peters, 2008. [133](#)
- [66] J.-P. Luminet, M. Lachièze-Rey, and R. Lehoucq. Cosmic Crystallography. Astronomy and Astrophysics, 313:339–346, 1996, arXiv:grqc/9604050. [137](#), [138](#), [139](#), [140](#), [141](#), [142](#), [143](#)
- [67] J.-P. Luminet, J. Uzan, and R. Lehoucq. A new crystallographic method for detecting space topology. Astronomy and Astrophysics, 351:766–776, 1999, arXiv:astro-ph/9903155v2. [137](#), [139](#), [143](#), [144](#), [145](#)
- [68] J.-P. Luminet, J. Weeks, A. Riazuelo, and R. Lehoucq. Well-proportioned universes suppress CMB quadrupole. Monthly Notices of the Royal Astronomic Society MNRAS, 352:258–268, 2004, arXiv:astro-ph/0312312v2. [164](#), [165](#)
- [69] J.-P. Luminet, J. Weeks, A. Riazuelo, R. Lehoucq, and J. Uzan. Dodecahedral space topology as an explanation for weak wide-angle temperature correlations in the cosmic microwave background, 2003, arXiv:astro-ph/0310253v1. [164](#), [167](#), [168](#)
- [70] J.-P. Luminet, J. Weeks, and G. D. Starkman. Is space finite? Scientific American, pages 90–97, April, 1999. [136](#), [158](#)
- [71] A. Marecki, B. Roukema, and S. Bajtlik. Cosmic Crystallography using short-lived objects - Activ Galactic Nuclei. Astronomy and Astrophysics, 435(2):427 – 435, 2005, arXiv: astro-ph/0412181. [146](#), [147](#)
- [72] J. Mather et al. Measurement of the cosmic microwave background spectrum by the COBE FIRAS instrumente. Astrophysical Journal, 420:439, 1994. [35](#)
- [73] J. Milnor. Toward the Poincaré Conjecture and the Classification of 3-Manifolds. Notices of the American Mathematical Society, 50(10):1226–1233, 2003. [74](#), [97](#)
- [74] C. Misner. Magic without Magic. Freeman, San Francisco, 1972. [138](#)
- [75] J. W. Morgan and F. T.-H. Fong. Ricci Flow and Geometrization of 3-Manifolds. American Mathematical Society, 2010. [74](#)
- [76] B. Mota, M. Rebouças, and R. Tavakol. Circles-in-the-sky searches and observable cosmic topology in a flat universe. Physical Review D, 81:103516, 2010, arXiv:1002.0834. [159](#)
- [77] B. Mota, M. Rebouças, and R. Tavakol. Observable circles-in-the-sky in flat universes. 2010, arXiv:1007.3466. [159](#), [161](#)
- [78] B. Mota, M. Rebouças, and R. Tavakol. What can the detection of a single pair of circles-in-the-sky tell us about the geometry and topology of the Universe? Physical Review D, 84:083507, 2011, arXiv:1108.2842. [161](#), [162](#), [163](#)

-
- [79] J. Narlikar and T. Seshadri. Counterimages in closed elliptical Friedmann universes. *Astrophysical Journal*, 288:43–49, 1985. [138](#)
- [80] A. Niarchou and A. Jaffe. Imprints of spherical non-trivial topologies on the CMB. *Phys.Rev.Lett.*, 99(081302), 2007, arXiv:astro-ph/0702436v2. [169](#)
- [81] W. Nowacki. Die euklidischen, dreidimensionalen, geschlossenen und offenen Raumformen. *Commentarii Mathematici Helvetici*, 7:81–93, 1934. [88](#)
- [82] A. Penzias and R. Wilson. Measurement of the Flux Density of CAS a at 4080 Mc/s. *Astrophysical Journal*, 42:1149, 1965. [35](#)
- [83] P. Peterson. *Riemannian Geometry*. New York: Springer, 1998. [13](#), [43](#), [62](#)
- [84] J. Ratcliffe. *On the foundations of hyperbolic geometry*. Vieweg Verlag, Sohn Verlag, GWV Fachverlage GmbH, Wiesbaden, 2004. [12](#), [13](#), [14](#), [32](#), [43](#), [48](#), [53](#), [54](#), [55](#), [56](#), [61](#), [62](#), [64](#), [65](#), [87](#), [97](#), [100](#), [101](#), [102](#), [103](#), [104](#), [105](#), [106](#), [107](#), [109](#), [112](#), [114](#), [115](#), [185](#)
- [85] F. Raymond and A. Vasquez. 3-manifolds whose universal coverings are Lie groups. *Topology and its Applications*, 12:161–179, 1981. [73](#)
- [86] B. E. Robertson, R. S. Ellis, et al. Early star-forming galaxies and the reionization of the Universe. *Nature*, 468:55, 2010. [120](#)
- [87] B. Roukema. Does gravity prefer the Poincaré’ dodecahedral space? *International Journal of Modern Physics D*, 18:2237–2241, 2009, arXiv:0905.2543v1 [astro-ph.CO]. [169](#)
- [88] B. Roukema. Some spaces are more equal than others. *Annalen der Physik*, 522:340–343, 2010, arXiv:0910.5837v1 [astro-ph.CO]. [169](#)
- [89] B. Roukema and P. Rozanski. The residual gravity acceleration effect in the Poincaré’ dodecahedral space. *Astronomy and Astrophysics*, 502:27–35, 2009, arXiv:0902.3402v4 [astro-ph.CO]. [169](#)
- [90] A. Schönflies. *Krystallsysteme und Krystallstruktur*. Teubner Verlag, Leipzig, 1891. [88](#)
- [91] G. Scott, C. Bennett, et al. STRUCTURE IN THE COBE DIFFERENTIAL MICROWAVE RADIOMETER FIRST-YEAR MAPS. *Astrophysical Journal*, 396:L1–L5, 1992. [35](#), [151](#)
- [92] P. Scott. The Geometries of 3-Manifolds. *Bull.Mathematical Society*, 15:401–487, 1983. [53](#), [56](#), [63](#), [67](#), [69](#), [72](#), [73](#), [74](#)
- [93] I. Singer. Infinitesimally homogeneous spaces. *Communications on Pure and Applied Mathematics*, 13:685–697, 1960. [63](#)
-

- [94] D. Sokoloff and V. Shvartsman. An estimate of the size of the universe from a topological point of view. JETP, 39:196, 1974. [138](#)
- [95] D. Spergel et al. First-Year Wilkinson Microwave Anisotropy Probe (WMAP) Observations: Determination of Cosmological Parameter. Astrophysical Journal Supplement Series, 148(175-194), 2003, arXiv:astro-ph/0302209v3. [164](#), [167](#)
- [96] J. L. Sylvestre Gallot, Dominique Hulin. Riemannian Geometry. Springer-Verlag Berlin Heidelberg, 3 edition, 2004. [7](#), [8](#), [9](#), [25](#), [33](#), [43](#), [54](#), [62](#), [64](#), [66](#), [71](#), [80](#), [190](#), [191](#)
- [97] H. Then. Foreground contamination of the WMAP CMB maps from the perspective of the matched circle test. Monthly Notices of the Royal astronomical Society MNRAS, 000:1–7, 2006, arXiv:astro-ph/0511726v2. [159](#)
- [98] W. P. Thurston. Three dimensional manifolds, Kleinian groups and hyperbolic geometry. Bulletin (New Series) of the American Mathematical Society, 6(3):357–381, 1982. [97](#), [98](#)
- [99] W. P. Thurston. Three-Dimensional Geometry and Topology. Princeton University Press, 1997. [38](#), [39](#), [40](#), [47](#), [49](#), [50](#), [55](#), [56](#), [59](#), [60](#), [61](#), [62](#), [63](#), [64](#), [65](#), [66](#), [67](#), [69](#), [70](#), [72](#), [73](#), [75](#), [77](#), [86](#), [87](#), [88](#), [92](#), [97](#), [98](#), [99](#)
- [100] F. Tricerri. Locally homogeneous Riemannian manifolds. Rend.Seminar Mat. Univ. Poitec. Torino, pages 411–426, 1992. [62](#)
- [101] S. Tsujikawa, R. Maartens, and R. Brandenberger. Non-commutative inflation in the CMB. Physical Letters B, 574:141–148, 2003, arXiv:astro-ph/0308169v2. [164](#)
- [102] J.-P. Uzan, J. Weeks, A. Riazuelo, and R. Lehoucq. Simulating cosmic microwave background maps in multi connected spaces. Physical Review D, 69(103514), 2004, arXiv:astro-ph/0212223v2. [156](#), [157](#), [158](#), [164](#), [167](#)
- [103] E. Vinberg, editor. Geometry II, volume 29. Springer-Verlag Berlin-Heidelberg-New York, 1993. [8](#), [13](#), [14](#), [42](#), [54](#), [62](#), [63](#), [68](#), [78](#), [79](#), [80](#), [81](#), [86](#), [92](#), [101](#), [102](#), [103](#), [104](#), [110](#), [113](#)
- [104] H. S. W. Threlfall. Topologische Untersuchung der Diskontinuitätsbereiche endlicher Bewegungsgruppen des dreidimensionalen sphärischen Raumes. Mathematische Annalen, 104:1–70, 1930. [93](#)
- [105] H. S. W. Threlfall. Topologische Untersuchung der Diskontinuitätsbereiche endlicher Bewegungsgruppen des dreidimensionalen sphärischen Raumes (Schluss). Mathematische Annalen, 107:543–586, 1932. [93](#)
- [106] P. Wagner, G. Reischl, and G. Steiner. Einführung in die Physik. Facultas Verlags- und Buchhandels AG, 2010. [26](#)

-
- [107] R. M. Wald. General Relativity. The University of Chicago Press, 1984. 1, 6, 7, 8, 9, 10, 11, 12, 13, 15, 16, 17, 18, 19, 21, 22, 23, 24, 25, 27, 28, 29, 30, 31, 32, 119, 120, 121, 124, 125
- [108] A. Weigert, H. Wendker, and L. Wisotzki. Astronomie und Astrophysik. WILEY-VCH-Verlag, 2005. 128, 129, 130, 131, 132
- [109] S. Weinberg. Cosmology. Oxford University Press, 2008. 21, 24, 33, 34, 35, 122, 123, 124, 126, 127, 128, 129, 131, 132, 150, 151, 152, 154, 155, 163, 164
- [110] H. Whitney. Differentiable Manifolds. Annals of Mathematics, 37:645–680, 1936. 38, 39
- [111] J. A. Wolf. Spaces of Constant Curvature. Publish or Perish, 4 edition, 1977. 33, 48, 49, 50, 69, 77, 80, 81, 86, 88, 89, 90, 92, 93
- [112] G. Wüstholtz. Algebra. Vieweg Verlag, Sohn Verlag, GWV Fachverlage GmbH, Wiesbaden 2004, 2004. 82, 83
- [113] J. Yadav, S. Bharadwaj, B. Pandey, and T. Seshadri. Testing homogeneity on large scales in the Sloan Digital Sky Survey Data Release One. Monthly Notices of the Royal Astronomical Society, 364:601–606, 2005. 32
- [114] http://de.wikipedia.org/wiki/Differenzierbare_Mannigfaltigkeit. 7
- [115] <http://www.cyberclassroom.de/module/faecher/mathematik.html>. 25
- [116] <http://www.mth.uct.ac.za/omei/gr/chap1/node7.html>.
- [117] http://hendrix2.uoregon.edu/~imamura/123/lecture-5/Universe_expansion.gif. 34
- [118] <http://en.wikipedia.org/wiki/Torus>. 57
- [119] www.unitaryflow.com/2009/06/polyhedra-and-groups.html. 83
- [120] www.light-weaver.com/vortex/5geometry.html. 84
- [121] <http://www.asminternational.org/portal/site/www/SubjectGuideItem/?vgnextoid=ad7cdc8cc359d2187>. 87
- [122] http://wiki.chemeddl.org/mediawiki/index.php/Main_Page. 87
- [123] <http://www.math.uconn.edu/~alozano/talks/infinity/finiteuniverse.html>. 100
- [124] <http://www.xploreandxpress.blogspot.com/2010/12/fun-with-mathematics-tessellations.html>. 100
- [125] www.mathcs.slu.edu/escher/index.php/Wallpaper_Patterns.html. 104
-

- [126] <http://www.apollonius.math.nthu.edu.tw/d1/gc08-exe/9621261>. 114
- [127] <http://www.rudyrucker.com/blog/2008/04/20/is-the-universe-infinite>. 114
- [128] <http://www.mathworld.wolfram.com/HyperbolicDodecahedron.html>. 115
- [129] www.sdss.org. 119
- [130] '<http://backreaction.blogspot.com/2010/07/non-gaussianities-in-cmb.html>'. 150
- [131] <http://planck.caltech.edu/epo/epo-cmbDiscovery3.html>. 151
- [132] <http://blog.lib.umn.edu/mill1974/EGAD/images/Minn06/WMAP-tempF14.png>. 152
- [133] <http://www.astro.ucla.edu/~wright/DMRsky4up.jpg>. 153
- [134] http://lambda.gsfc.nasa.gov/product/map/current/pub_papers/sevenyear/basic_results/wmap_7yr_basic_results_images.cfm. 163

I have attempted to locate the copyright holders of images used in this publication and to obtain permission for using their work. In case of an incorrect identification of the true right-holder, please bring this to my attention immediately.

Ich habe mich bemüht, sämtliche Inhaber der Bildrechte ausfindig zu machen und ihre Zustimmung zur Verwendung der Bilder in dieser Arbeit eingeholt. Sollte dennoch eine Urheberrechtsverletzung bekannt werden, ersuche ich um Meldung bei mir.

Appendix

A. Topology

Definition A.0.0.1 (Topological Space). *A topological space is a pair (X, \mathcal{O}) consisting of a set X and a set of open subsets \mathcal{O} of X such that:*

1. *An arbitrary union of open sets in \mathcal{O} is open.*
2. *The intersection $O_1 \cap O_2$ of two open sets $O_1, O_2 \subset \mathcal{O}$ is open.*
3. *The empty set \emptyset and the entire set X are open. [49]*

Remark A.0.0.2. 1. Let X be a metric space (1.1.2.16, p.12) with metric d . The open ball with center $a \in X$ and radius r is defined to be the set

$$B(a, r) = \{x \in X \mid d(a, x) < r\}.$$

2. A subset $U \subset X$ is open in X if and only if for each point $x \in U$, there is an $r > 0$ such that $B(x, r) \subset U$.
3. The collection of all open sets of a metric space X is a topology on X , called the *metric topology* of X . [84]

Definition A.0.0.3 (Basis of a Topology). *A basis of a topological space is a set $\mathcal{B} \subset \mathcal{O}$ of open sets such that any open set $O \subset \mathcal{O}$ can be represented as a union of open sets of \mathcal{B} . [49]*

Definition A.0.0.4. *A map $f : X \rightarrow Y$ between topological spaces is continuous if preimages of open sets are open. Thus, if $V \subset Y$ is open, $f^{-1}(V)$ is open in X . [49]*

Remark A.0.0.5 (Quotient Space). Let X be a set and \sim an equivalence relation on X . X/\sim denotes the set of all equivalence classes. The equivalence class of $x \in X$ shall be denoted by $[x] \in X/\sim$ and $\pi : X \rightarrow X/\sim, x \mapsto [x]$ is the canonical projection.

Definition A.0.0.6 (Quotient Topology). *Let X be a topological space and \sim an equivalence relation on X . A subset $U \subset X/\sim$ is called open with respect to the quotient topology if $\pi^{-1}(U)$ is open in X . X/\sim with this topology is called the quotient space of X with respect to \sim . It is the finest topology such that the projection π is continuous. [49, p.39]*

Definition A.0.0.7. A homeomorphism between topological spaces X, Y is a bijective map $f : X \rightarrow Y$ such that f and f^{-1} are continuous. Here X and Y are called homeomorphic, denoted by $X \simeq Y$. [49]

Definition A.0.0.8 (Path). A path in a space X is a continuous map $f : I \rightarrow X$, with I the unit interval $[0, 1]$. A path with the same starting point as end point $x_0 = f(0) = f(1) \in X$ is called a loop with base point x_0 . [42]

Definition A.0.0.9 (Path-Connected). A space X is path-connected if, for all $x, y \in X$, there is a path α in X which takes x to y , thus, $\alpha(0) = x$ and $\alpha(1) = y$.

Remark A.0.0.10. 1. A space X is called locally path-connected if $\forall x \in X$ and for any neighbourhood $U \subset X$ of x there is a path-connected neighbourhood $V \subset U$ of x . [49]

2. In mathematics, connectedness is defined in different, non-equivalent ways. A space X is called connected if it cannot be written as the disjoint union of nonempty, open subsets. A path-connected space is naturally connected, the converse is in general not true. Take, for example, the space $\{(x, \sin(\ln x)) \in \mathbb{R} \mid x > 0\} \cup (0 \times [-1, 1])$. However, for a topological manifold these properties are equivalent. [49]

A.1. Topological Groups

Definition A.1.0.11. G is a **topological group** if

(i) G is a group and

(ii) G is a topological space

such that the maps

$$G \times G \xrightarrow{\mu} G \quad (x, y) \mapsto xy \quad G \xrightarrow{i} G \quad x \mapsto x^{-1} \quad (\text{A.1})$$

are continuous. In particular, they are homeomorphisms. Thus, for every open/closed subgroup X in G the right or left cosets are open/closed too.

Proposition A.1.0.12. Let H be a subgroup of G .

1. If H is open $\Rightarrow H$ is closed.
2. If H is closed and the Index $[G : H] < \infty \Rightarrow H$ is open.
3. If G is compact and H open in $G \Rightarrow |G : H| < \infty$.

Proof. Every group can be represented as a disjoint union of cosets. Thus, $G = \overset{\circ}{\bigcup}_{t \in T} Ht$ with

T is transversal. Therefore, G can be written as $G = H \overset{\circ}{\bigcup}_{\substack{t \in T \\ t \notin H}} (\bigcup)$.

1. If H is open $\Rightarrow Ht$ is open for all $t \in T, t \notin H \Rightarrow \bigcup_{t \in T, t \notin H} Ht$ is open $\Rightarrow H = G \setminus \bigcup_{t \in T, t \notin H} Ht \Rightarrow H$ is closed.
2. If H is closed $\Rightarrow Ht$ is closed $\Rightarrow \bigcup Ht$ is closed, because $[G:H]$ is finite $\Rightarrow H$ is open.
3. Because G is compact, there is a finite covering consisting of open sets. For instance, take the set of all left or right cosets of H , which have to be disjoint \Rightarrow Index is finite.

□

Remark A.1.0.13. Let G be a topological group

1. If $H \leq G$, H is a topological group with the subspace topology.
2. If $N \trianglelefteq G$, G/N is a topological group with the quotient topology. [61]

Definition A.1.0.14. A topological space X is Hausdorff if $\forall a, b \in X, a \neq b \exists U, V$ open in X with $a \in U, b \in V$ and $U \cap V = \emptyset$.

Proposition A.1.0.15. Let G be a topological group, G is Hausdorff if and only if $\{1\}$ is closed.

Proof. (\Rightarrow) If X is Hausdorff and $x \in X$, take an $y \in X \setminus \{x\}$ thus, $x \neq y$. There is an open subset $U \subset X \setminus \{x\}$. Since y was arbitrary, $X \setminus \{x\}$ is open as the union of open sets. Therefore, $\{x\}$ is closed and in particular $\{1\}$.

(\Leftarrow) Assume $\{1\}$ is closed and $a \neq b$ then, $\{1\}a^{-1}b = \{a^{-1}b\}$ is closed. Since $1 \notin \{a^{-1}b\}$, there is an $U \subset G \setminus \{a^{-1}b\}$.

The multiplication μ is continuous and $\mu(1, 1) = 1$. Since U is open, there is an open neighbourhood $V \times W$ of $(1, 1)$ in $G \times G$, which is mapped inside U . $VW^{-1} = V(V \times W) \subset U$ and $a^{-1}b \notin VW^{-1} \subset U$. It follows that $aV \cap bW = \emptyset$, because otherwise there are $v \in V$ and $w \in W$ such that $av = bw \Rightarrow vw^{-1} = a^{-1}b$. This is a contradiction. Since $1 \in V, W, a \in aV$ and $b \in bW$ and $aV \cap bW = \emptyset$, G is Hausdorff □

We conclude:

Corollary A.1.0.16. G/K is Hausdorff if and only if K is closed.

B. The Correspondence of Lie Groups and Lie Algebras

B.1. Representation of Lie Groups

Before we focus on the correspondence between Lie groups (2.2.0.6, p.39) and Lie algebras, we introduce “representation of Lie groups”: A representation of a group G on a vector space V over a field K is an action (2.2.1.1, p.40) of G on a \mathbb{K} -vector space V by linear maps. If we describe an action as a homomorphism between the group and the set of all bijections on V (2.2.1.3 (2), p.41), a representation of a group G on a vector space V over a field K is a group homomorphism from G to $GL(V)$. [17]

Example B.1.0.17 (Standard Representation). Consider the group $GL_n(\mathbb{R})$ and its action on \mathbb{R}^n given by

$$GL_n(\mathbb{R}) \times \mathbb{R}^n \rightarrow \mathbb{R}^n, \quad (A, x) \mapsto Ax.$$

This is the standard representation of $GL_n(\mathbb{R})$ on \mathbb{R}^n .

B.2. Correspondence between Lie Groups and Lie Algebras

Definition B.2.0.18 (Lie algebra). (i) A **Lie algebra** over $\mathbb{K} = \mathbb{R}$ or \mathbb{C} is a \mathbb{K} -vector space \mathfrak{g} together with a bilinear map $[\cdot, \cdot] : \mathfrak{g} \times \mathfrak{g} \rightarrow \mathfrak{g}$, called the **Lie bracket** of \mathfrak{g} , which is skew symmetric and satisfies the Jacobi identity:

$$[X, [Y, Z]] = [[X, Y], Z] + [Y, [X, Z]] \quad \forall X, Y, Z \in \mathfrak{g}. \quad (\text{B.1})$$

(ii) Let $(\mathfrak{g}, [\cdot, \cdot])$ be a Lie algebra. A **Lie subalgebra** of \mathfrak{g} is a linear subspace $\mathfrak{h} \subset \mathfrak{g}$, which is closed under the Lie bracket, denoted by $\mathfrak{h} < \mathfrak{g}$. Of course, $(\mathfrak{h}, [\cdot, \cdot])$ is a Lie algebra too.

(iii) If \mathfrak{g} and \mathfrak{h} are Lie algebras, a homomorphism $\varphi : \mathfrak{g} \rightarrow \mathfrak{h}$ of Lie algebras is a linear map which is compatible with the brackets, i.e. such that $[\varphi(X), \varphi(Y)] = \varphi([X, Y]) \forall X, Y \in \mathfrak{g}$.

(iv) An **isomorphism** of Lie algebras is a bijective homomorphism. Here, the inverse is a homomorphism too. If there is an isomorphism $\varphi : \mathfrak{g} \rightarrow \mathfrak{h}$, \mathfrak{g} and \mathfrak{h} are called isomorphic and we write $\mathfrak{g} \approx \mathfrak{h}$.

[17, S.13]

B.2.1. The Tangent Space and the Vector Space of Vector Fields

We recall the definition of a manifold M (1.1.1.1, p.6) and a tangent space $T_x M$ (1.1.2.4, p.9).

Definition B.2.1.1. Let M be a manifold. A map $\partial : C^\infty(M, \mathbb{R}) \rightarrow \mathbb{R}$ is a derivation over $x \in M$ if it is linear and for $f, g \in C^\infty(M, \mathbb{R})$ and $\alpha \in \mathbb{R}$:

1. $\partial(f + g)(x) = (\partial f + \partial g)(x)$
2. $\partial(\alpha \cdot f)(x) = \alpha \cdot (\partial f)(x)$
3. $\partial(f \cdot g)(x) = (\partial f \cdot g + f \cdot \partial g)(x)$

The vector space of all derivations over $x \in M$ will be denoted by $\mathcal{D}_x(C^\infty(M, \mathbb{R}), \mathbb{R})$ or $\mathcal{D}_x(M)$. [54, .114]

Definition B.2.1.2. For a point $x \in M$, a manifold M , a differentiable map $f : M \rightarrow M$ and an element $\xi \in T_x M$ of the tangent space over $x \in M$, we define the **Lie derivative** in the direction ξ as:

$$L_\xi(f) := T_x f \cdot \xi.$$

Theorem B.2.1.3. The map $\xi \mapsto L_\xi$ is a linear isomorphism between $T_x M$ and $\mathcal{D}_x(M)$. [96, p.20]

Remark B.2.1.4. 1. The fundamental theorem for the proof of B.2.1.3 is the following:

(U, x) be a local chart on M and $\{e_k \mid k = 1, \dots, n\}$ a basis of \mathbb{R}^n . For an arbitrary point $p \in U$ we define $\frac{\partial}{\partial x_k}$ in $T_p M$ as:

$$\left(\frac{\partial}{\partial x_k}\right)_p : f \mapsto \frac{\partial f}{\partial x_k}(p) = \partial_{e_k}(f \circ x^{-1})(x(p)).$$

Then the set

$$\left\{ \frac{\partial}{\partial x_k} \mid k = 1, \dots, n \right\}$$

is a basis for the tangent space $T_p M$ of M at p . [40, p.26] Therefore, any derivation can be written as

$$\delta(f) = \sum_{j=1}^n \delta(x^j) \left(\frac{\partial f}{\partial x^j} \right) \Big|_0.$$

2. The tangent space of a manifold M at the point $x \in M$ is therefore sometimes defined as the vector space:

$$T_x M := \mathcal{D}_x(C^\infty(M, \mathbb{R}), \mathbb{R}). \text{ [54, p.116]}$$

Let (U, Φ) be a chart around $m \in M$, (x^1, \dots, x^n) are the corresponding coordinate functions and $f : M \rightarrow \mathbb{R}$ a differentiable function, then

$$\left(\frac{\partial}{\partial x^j}\right) \Big|_m (f) = \left(\frac{\partial}{\partial x^j}\right)(f \circ \Phi^{-1})(\Phi(m)).$$

In this way a map from $U \rightarrow TU$, $m \mapsto \left(\frac{\partial}{\partial x^j}\right)(f \circ \Phi^{-1})(\Phi(m)) \in T_m M$ is defined. Thus, this defines a vector field (1.1.2.7, p.9). In general, if X^1, \dots, X^n are smooth functions from U to \mathbb{R} , a vector field is given by:

$$X = \sum_{i=1}^n X^i \left(\frac{\partial}{\partial x^i}\right).$$

Consider the map

$$L_X : C^\infty(M) \rightarrow C^\infty(M), f \mapsto \sum_{i=1}^n X^i \left(\frac{\partial f}{\partial x^i}\right).$$

Theorem B.2.1.5. *The map*

$$\chi(M) \rightarrow \mathcal{D}(M), X \mapsto L_X,$$

is an isomorphism between the set of all vector fields of a manifold and the vector space of all derivations.

Definition B.2.1.6. *The bracket of two vector fields X and Y , denoted by $[X, Y]$, is the vector field corresponding to the derivation $L_X L_Y - L_Y L_X$.*

Lemma B.2.1.7. *The bracket of vector fields X, Y, Z on M achieve the Jacobi identity:*

$$[X, [Y, Z]] + [Y, [Z, X]] + [Z, [X, Y]] = 0.$$

Proposition B.2.1.8. Since the bracket is a bilinear map, achieves the Jacobi identity and is obviously screw symmetric, the vector space $\chi(M)$ of all vector fields forms a Lie algebra with the Lie bracket defined in B.2.1.6. The set of all left-invariant vector fields (3.3.2.9, p.70) $\chi_l(M)$ is closed under the Lie bracket and therefore a subalgebra. [96]

B.2.2. The Lie Algebra of the Lie Group G

For details see [16] or [96].

We begin by recalling the left translation of a Lie group G as the map:

$$l_g : G \rightarrow G, h \mapsto g \cdot h,$$

where \cdot denotes the group multiplication.

For an element of the tangent space at the identity $\xi \in T_e G$, we define the vector field

$$X_\xi : G \rightarrow TG, X_\xi(g) = T_e l_g \cdot \xi.$$

Observe that $T_e l_g \cdot \xi$ is an element in $T_g G$.

By construction this vector field is left-invariant and determined by its value at the identity, thus, the map:

$$T_e G \rightarrow \chi_l(G), \xi \mapsto X_\xi,$$

is an isomorphism between the tangent space at the identity and the space of all left-invariant vector fields of G . This isomorphism induces the Lie algebra structure on $T_e G$. Thus, we have:

Proposition B.2.2.1. Let G be a Lie group. For ξ in $T_e G$, the expression $X_\xi(g) = T_e l_g \cdot \xi$ defines a left-invariant vector field on G . The map $\xi \mapsto X_\xi$ is an isomorphism between $T_e G$ and the vector space of left-invariant vector fields. The latter has the structure of Lie algebra as a subalgebra of the Lie algebra of all vector fields.

Definition B.2.2.2. Let G be a Lie group. The space of all left-invariant vector fields of G , which is isomorphic to $T_e G$, is denoted by \mathfrak{g} and called the **tangent Lie algebra** of the Lie group G .

Example B.2.2.3. Let $G = GL_n(\mathbb{R})$, the Lie group of all linear maps from \mathbb{R}^n to itself. The corresponding Lie algebra is $\mathfrak{gl}_n(\mathbb{R})$. $\mathfrak{gl}_n(\mathbb{R})$ is the set of all $(n \times n)$ matrices with entries in \mathbb{R} under the commutator $[x, y] = x \cdot y - y \cdot x$.

B.2.3. Consequences

The following statements shall not be proven here. We state them to give an overview of the strength of the correspondence.

Theorem B.2.3.1. Let \mathfrak{g} be a finite-dimensional Lie algebra, there exists a unique (up to isomorphism) simply-connected Lie group \tilde{G} with Lie algebra \mathfrak{g} . Any other Lie group G with Lie algebra \mathfrak{g} (or isomorphic to it) is isomorphic to the quotient of \tilde{G} by a discrete normal subgroup $H \subset \tilde{G}$ which is contained in the center $Z(\tilde{G})$. [16, p.30]

Remark B.2.3.2. Thus, there is an one-to-one correspondence between Lie algebras and simply-connected Lie groups.

Lie Group Homomorphism – Lie Algebra Homomorphism : Assume G and H to be Lie groups and \mathfrak{g} and \mathfrak{h} their corresponding Lie algebras. For a smooth homomorphism $\varphi : G \rightarrow H$, the linear map $T_e\varphi =: \varphi' : \mathfrak{g} \rightarrow \mathfrak{h}$ is a Lie algebra homomorphism which is compatible with the Lie bracket, i.e. $\varphi'([X, Y]) = [\varphi'(X), \varphi'(Y)]$.

Representations If $\varphi : G \rightarrow GL_n(\mathbb{K})$ is a representation of the Lie group G , the derivative $\varphi' : \mathfrak{g} \rightarrow L_n(\mathbb{K})$ is a representation of \mathfrak{g} .

Example B.2.3.3 (The Adjoint Representation). Consider the smooth function given by conjugation with a fixed $g \in G$:

$$c_g : G \rightarrow G, h \mapsto ghg^{-1}.$$

Since this is a group homomorphism in a natural way, its derivative is a Lie algebra homomorphism:

$$Ad(g) : \mathfrak{g} \rightarrow \mathfrak{g},$$

Furthermore we consider the map

$$Ad : G \mapsto GL(\mathfrak{g}), g \mapsto Ad(g),$$

which is a smooth homomorphism and in particular a representation of G on \mathfrak{g} . Its corresponding representation of its Lie algebra \mathfrak{g} : $ad : \mathfrak{g} \rightarrow L(\mathfrak{g}, \mathfrak{g})$ is called the adjoint representation of the Lie algebra \mathfrak{g} .

Lie Subgroups – Lie Subalgebras

Theorem B.2.3.4. *Let G be a Lie group with Lie algebra \mathfrak{g} and let $\mathfrak{h} \subset \mathfrak{g}$ be a subalgebra. Then, there is a unique connected virtual Lie subgroup $H \rightarrow G$ with tangent space at the identity is \mathfrak{h} . [16, p.26]*

H' is called a virtual Lie subgroup of G if it is the image $i(H)$ of some smooth injective homomorphism $i : H \rightarrow G$ from some Lie group H .

Consider a connected Lie subgroup H of a simply-connected Lie group G . For the corresponding Lie algebras holds: $\mathfrak{h} = T_e H \subset \mathfrak{g} = T_e G$.

Conversely let \mathfrak{h} be the corresponding Lie algebra of the Lie group G and let \mathfrak{h} be a subalgebra of \mathfrak{g} . There exists a connected Lie subgroup $H \subset G$ with Lie algebra \mathfrak{h} . Further more, there exists an injective homomorphism $i : H \rightarrow G$ such that $i' : \mathfrak{h} \rightarrow \mathfrak{g}$ is the inclusion. If $i(H)$ is closed in G , $i : H \rightarrow i(H)$ is an isomorphism.

Example B.2.3.5. Consider the subgroup $O_n(\mathbb{R}) \subset GL_n(\mathbb{R})$. We already now that the corresponding Lie algebra to $GL_n(\mathbb{R})$ is $\mathfrak{gl}_n(\mathbb{R})$. The corresponding Lie algebra of $O_n(\mathbb{R})$ is the Lie algebra of all screw symmetric matrices: $\mathfrak{so}_n(\mathbb{R}) = \{A \in \mathfrak{gl}_n(\mathbb{R}) \mid A^t + A = 0\}$. It is of dimension $dim(O_n(\mathbb{R})) = dim(\mathfrak{so}(n)) = \frac{n(n-1)}{2}$.

B.2.4. Homogenous Spaces and their Lie Algebras

Let G act locally effectively on the homogeneous space G/H . If the group G is simply-connected, its corresponding Lie algebra \mathfrak{g} is uniquely determined. (If G is not simply-connected, one can pass to the universal cover.) G/H is a simply-connected homogenous space if and only if H is connected. Here, the tangent algebra \mathfrak{h} of the stabilizer H is a subalgebra of the Lie algebra \mathfrak{g} and uniquely determined. In this way, the simply-connected homogenous space G/H is uniquely determined by the pair $(\mathfrak{g}, \mathfrak{h})$.

Conversely determines a pair $(\mathfrak{g}, \mathfrak{h})$, where \mathfrak{h} is a subalgebra of an arbitrary Lie algebra \mathfrak{g} , a simply-connected homogenous space G/H such that \mathfrak{g} is the Lie algebra of G and \mathfrak{h} corresponds to a closed, connected subgroup of G . [32, p.98–99]

C. Sectional Curvature

In this section I follow [40] if not cited otherwise. In the following, we shall use the notation of Chapter 1, where the basic definitions necessary for this section are given.

Definition C.0.4.1. *Let (M, g) be a Riemannian manifold then the map*

$$\nabla : \chi(M) \times \chi(M) \rightarrow \chi(M)$$

given by:

$$2g(\nabla_X Y, Z) = \{X(g(Y, Z)) + Y(g(X, Z)) - Z(g(X, Y)) + g([Z, X], Y) + g([Z, Y], X) + g(Z, [X, Y])\}$$

is called the Levi-Civita connection on M .

Remark C.0.4.2. The Levi-Civita connection is the unique torsion-free and metric connection described in Chapter 1 (1.1.3.7, p.17).

Remark C.0.4.3. 1. The Riemannian curvature can be written in terms of the Levi-Civita connection as

$$R(X, Y)Z = \nabla_X \nabla_Y Z - \nabla_Y \nabla_X Z - \nabla_{[X, Y]} Z.$$

Definition C.0.4.4. *Let (M, g) a Riemannian manifold and $p \in M$. A section V at p is a two-dimensional subspace of the tangent space $T_p M$. The set of all section*

$$G_2(T_p M) := \{V \mid V \text{ is a section of } T_p M\}$$

*is called the **Grassmanian** of two-dimensional planes at p .*

Definition C.0.4.5. *Let (M, g) be a Riemannian manifold and $p \in M$. Then the function*

$$K_p : G_2(T_p M) \rightarrow \mathbb{R}, \text{span}_{\mathbb{R}}\{X, Y\} \mapsto \frac{g(R(X, Y)Y, X)}{|X|^2|Y|^2 - g(X, Y)^2}$$

is called the sectional curvature at p .

Remark C.0.4.6. If $X, Y, Z, W \in T_p M$ be tangent vectors at p such that the two sections $\text{span}_{\mathbb{R}}\{X, Y\}$ and $\text{span}_{\mathbb{R}}\{Z, W\}$ are identical, it holds:

$$\frac{g(R(X, Y)Y, X)}{|X|^2|Y|^2 - g(X, Y)^2} = \frac{g(R(Z, W)W, Z)}{|Z|^2|W|^2 - g(Z, W)^2}.$$

Thus, the definition C.0.4.5 is well-defined.

Definition C.0.4.7. Let (M, g) be a Riemannian manifold, $p \in M$ and K_p the sectional curvature. We define the functions: $\delta, \Delta : M \rightarrow \mathbb{R}$ by

$$\delta : p \mapsto \min_{V \in G_2(T_p M)} K_p(V), \text{ and } \Delta : p \mapsto \max_{V \in G_2(T_p M)} K_p(V).$$

The Riemannian manifold is said to be of

- positive curvature if $\delta(p) \geq 0, \forall p \in M$,
- strictly positive curvature if $\delta(p) > 0, \forall p \in M$,
- negative curvature if $\delta(p) \leq 0, \forall p \in M$,
- strictly negative curvature if $\delta(p) < 0, \forall p \in M$,
- constant curvature if $\delta = \Delta$ is constant
- flat $\delta \equiv \Delta \equiv 0$

Remark C.0.4.8. The curvature of a Riemannian manifold can be written in terms of local coordinates with the help of the so called Christoffel symbols. Thus, the curvature is completely described by the local geometry of a manifold.

Index

- $L(V)$: set of linear maps on the vector space V , [39](#)
 (\mathbb{G}, \mathbb{M}) -structure, [54](#)
 C° : interior of C , [102](#)
 C^r -diffeomorphism, [38](#)
 C^r -extension, [31](#)
 C^∞ , [38](#)
 set of all infinitely continuous maps, [6](#)
 D_m^* , T^* , O^* , I^* : binary dihedral/polyhedral groups, [93](#)
 G : gravitational constant, [21](#)
 $GL(\mathbb{R}^n)$: set of invertible linear maps on \mathbb{R}^n , [39](#)
 $Isom(M)$: isometry group of the manifold M , [41](#)
 $L(\mathbb{R}^n)$: set of linear maps on \mathbb{R}^n , [39](#)
 $L(n, m)$: lens space, [94](#)
 $M(X)$: group of Möbius transformations of the space X , see Möbius group, [55](#)
 $O_n(\mathbb{R})$: orthogonal group, [40](#)
 $O_{n,1}(\mathbb{R})$: Lorentz group, [43](#)
 $PO_{n,1}(\mathbb{R})$: positive Lorentz group, [43](#)
 $PSL_2(\mathbb{R}), PSL_2(\mathbb{C})$: projective special linear group, [56](#)
 $SL_n(\mathbb{R})$: special linear group, [40](#)
 $SO_n(\mathbb{R})$: special orthogonal group, [40](#)
 TM : tangent bundle of a manifold, see tangent bundle, [9](#)
 $T_x M$: tangent space of a point on a manifold, see tangent space, [9](#)
 $\Gamma(\tilde{X}/X)$: group of deck transformations, see deck transformations, [48](#)
 Γ_{ab}^c : Christoffel symbol, see Christoffel symbol, [16](#)
 ΛCMD model, [128](#)
 \approx : isomorphic, [49](#)
 $\chi(\mathcal{M})$: set of all vector fields of a manifold, see vector field, [9](#)
 χ_{LSS} : comoving radius of the last scattering surface, [120](#)
 \cong : diffeomorphic, [42](#)
 \mathbb{E}^n : n-dimensional Euclidean space, see Euclidean space, [13](#)
 \mathbb{G} -isomorphism, [38](#)
 \mathbb{H}^n : n-dimensional hyperbolic space, see hyperbolic space, [14](#)
 \mathbb{S}^n : n-dimensional sphere, see spherical space, [13](#)
 \mathbb{T}^n : n-dimensional torus, see torus, [56](#)
 \mathbb{T}_E^n : n-dimensional embedded torus, see torus, [56](#)
 \mathbb{T}_F^n : n-dimensional flat torus, see torus, [56](#)
 \mathcal{C}_m : cyclic group of order m , [83](#)
 \mathcal{D}_m : dihedral group, [83](#)
 \mathcal{H} : quaternions, [92](#)
 \mathcal{I} : icosahedral group, [84](#)
 \mathcal{M}_3 : spatial part of the universe, a three-dimensional, connected and smooth Riemannian manifold without boundary, [29](#)

- \mathcal{M}_4 : space-time, a four-dimensional, connected and smooth Lorentzian manifold, 20
- \mathcal{O} : octahedral group, 83
- $\mathcal{S}(Y)$: symmetry group of the set Y , 82
- \mathcal{T} : tetrahedral group, 83
- \mathcal{TE} : space of all translations of the affine space E ., 85
- $\partial\mathcal{M}$: boundary of a manifold, see manifold, 8
- $\pi_1(X, x_0)$: fundamental group, see fundamental group, 44
- \sim : If $f \sim g$, f is homotopic to g ., 44
- \simeq : homeomorphic, 176
- $\widetilde{SL}_2(\mathbb{R})$, 72
- c : speed of light, 21
- $x \sim x'$: related points, 105
- $x \simeq x'$: paired points, 105
- $GL_n(\mathbb{R})$: linear group, 39
- $\mathbb{R}^{1,n}$: Lorentzian space, 14
- $E(n)$: Euclidean group, 42
- acausal set, 28
- achronical set, 27
 - edge, 27
- action
 - discontinuous, 48
 - free, 48
 - properly discontinuous, 48
- affine equivalent, 85
- affine space, 85
- analytic continuation, 59
- angular correlation function, 154
- antipodal, 14
- atlas, 7
 - equivalent atlases, 7
 - foliation atlas, 70
 - maximal atlas, 7
- baryonic matter, 129
- basis of a topology, 175
- Best Space, 115
- Bianchi identities, 18
- Bieberbach group, 86
- Big Bang, 33
- big crunch, 126
- binary dihedral/polyhedral groups, 93
- bounce model, 126
- Cauchy development, 29
- Cauchy problem, 30
- Cauchy surface, 29
- causal future/past, 27
- causality
 - local causality, 25
- causality condition, 29
 - strong causality condition, 29
- change of scale, 53
- chart, 7
 - compatible, 7
 - foliation chart, 70
- Christoffel symbol, 16
- chronological future/past, 26
- chronology condition, 28
- chronology violating set, 28
- circles-in-the-sky, 157
- Clifford translation, 81
- Clifford-Klein space form problem, 80
- Collecting Correlated Pair Method, 142
- comoving coordinates, 121
- complete, 62
 - complete metric space, 62
 - geodesically complete, 32
- component group, 39
- connection, 15
 - Levi-Civita connection, 185
- continuous map, 175
- convex set, 102
 - interior of a convex set, 102
 - side of a convex set, 102

-
- coordinate change, 7
 - coordinate system, 7
 - Copernican principle, 32, 120
 - cosmic microwave background, 34
 - cosmic time, 29
 - cosmological constant, 131
 - cosmological model
 - open/closed, 126
 - simply-/multi-connected, 120
 - cosmological parameters, 127
 - cosmological principle, 35, 120
 - covering group, 48
 - covering space, 45
 - critical density, 126, 129
 - crystallographic group, 86
 - curvature
 - Ricci tensor, 18
 - scalar curvature, 18
 - Riemannian curvature tensor, 17
 - sectional curvature, 78, 185
 - curve
 - C^r -curve, 8
 - causal curve, 13
 - null curve, 13
 - space-like curve, 13
 - time-like curve, 13
 - cuspidal, 97
 - cyclic group, 83
 - dark matter, 130
 - deck transformation, 48
 - decomposition, 103
 - decoupling, 35
 - density
 - mass density, 129
 - radiant flux density, 131
 - vacuum energy, 131
 - derivation, 180
 - derivative operator, 15
 - ordinary derivative, 15
 - torsion-free, 15
 - developing map, 59
 - definition, 60
 - developing pair, 61
 - diffeomorphism, 21
 - dihedral angle, 106
 - dihedral angle sum, 108
 - proper dihedral angle, 106
 - dihedral group, 83
 - dipole anisotropy, 152
 - Dirichlet domain, 101
 - Dirichlet polyhedron, 103
 - discrete subgroup, 42
 - displacement function, 81
 - dodecahedral space
 - Seifert-Weber dodecahedral space, 115
 - dodecahedral space, see also Poincaré dodecahedral space, 94
 - domain of dependence, 29
 - double action, 94
 - dual basis, 9
 - dual vector, 9
 - dual vector space, 9
 - Einstein tensor, 19
 - Einstein's field equations, 24
 - Einstein-de Sitter universe, 128
 - embedding, 20
 - energy-momentum tensor, 23
 - equivalence principle, 21
 - Euclidean space, 13, 43
 - expansion of the universe, 33
 - fiber, 65
 - fiber bundle, 65
 - foliation, 69
 - Friedmann's equation, 125
 - Friedmann-Lemaître universe, 125
 - fundamental cell, 135
 - fundamental domain, 101
-

- fundamental group, [44](#)
- fundamental polyhedron, [103](#)
 - exact fundamental polyhedron, [103](#)
- fundamental region, [101](#)
- future endpoint, [28](#)
- future-inextendible curve, [28](#)
- future-oriented curve, [26](#)
- geodesic, [19](#)
 - geodesic equation, [19](#)
- geodesic deviation equation, [24](#)
- geodesic hypothesis, [22](#)
- geometry, [64](#)
 - equivalent geometries, [65](#)
 - geometric structure, [56](#)
 - affine structure, [85](#)
 - model geometry, [65](#)
- ghost, [135](#)
- globally hyperbolic, [30](#)
- gluing, [109](#)
- group action, [40](#)
 - co-compact (uniform), [49](#)
 - co-finite, [49](#)
 - effective, [40](#)
 - sharply transitive, [42](#)
 - transitive, [42](#)
- group of deck transformations, [48](#)
- group of similarities, [54](#)
- group representation, [179](#)
 - adjoint representation, [183](#)
 - Standard representation, [179](#)
- Hantzsche-Wendt manifold, [111](#)
- Harrison-Zel'dovich spectrum, [155](#)
- Hausdorff, [177](#)
- Heisenberg group, [72](#)
- Helmholtz equation, [155](#)
- holonomy, [61](#)
- holonomy group, [61](#)
 - restricted holonomy group, [61](#)
 - linear holonomy group, [61](#)
- holonomy representation, [62](#)
- homeomorphism, [176](#)
 - homeomorphic, [176](#)
- homogeneity problem, [36](#)
- homogeneous space, [42](#)
- homotopic, [44](#)
 - null-homotopic, [44](#)
- homotopy, [44](#)
- homotopy class, [44](#)
- Hubble constant, [33](#), [122](#), [128](#)
- Hubble time, [129](#)
- Hubble's law, [33](#)
- Hubble's scale factor, [122](#)
- Hyperbolic space, [14](#), [43](#)
- hyperbolic space
 - upper half-space model, [55](#)
- hypersurface, [20](#)
 - null, [20](#)
 - space-like, [20](#)
 - time-like, [20](#)
- icosahedral group, [84](#)
- immersion, [20](#)
- inextendible, [31](#)
 - locally inextendible, [31](#)
- injectivity radius, [97](#)
- isometry group, [41](#)
- isotropic
 - locally isotropic, [77](#)
- isotropy group, [40](#), [41](#)
- Jacobi identity, [179](#)
- kernel of ineffectiveness, [41](#)
- Kleinian group, [97](#)
- Löbell space, [115](#)
- Laplace operator, [155](#)
- last scattering surface, [35](#), [120](#)
- leave, [70](#)

-
- Leibnitz rule, 15
 - lens space, 94, 113
 - Lie algebra, 179
 - Lie bracket, 179
 - Lie derivative, 180
 - Lie group, 39
 - Lie algebra of a Lie group, 182
 - Lie group of transformations, 41
 - lift, 45
 - homotopy lifting property, 45
 - homotopy lifting theorem, 45
 - unique lifting property, 45
 - light cone, 27
 - linear group, 39
 - linked action, 94
 - local coordinates, 7
 - local trivialization, 65
 - locally finite, 8
 - locally homogeneous, 33
 - locally path-connected, 176
 - Lorentz group, 43
 - Lorentzian space, 14

 - Möbius group, 55
 - manifold, 6
 - (G, \mathbb{M}) -manifold, 54
 - C^r -manifold, 7, 38
 - affine manifold, 85
 - boundary of a manifold, 8
 - closed/open manifold, 8
 - Euclidean manifold, 55
 - foliated manifold, 70
 - G-manifold, 38
 - geometric manifold, 64
 - gluing manifold, 109
 - hyperbolic manifold, 55
 - interior of a manifold, 8
 - Lorentzian manifold, 12
 - metric manifold, 56
 - paracompact, 8
 - product of manifolds, 8
 - real-analytic manifold, 38
 - Riemannian manifold, 12
 - smooth manifold, 7, 38
 - spherical manifold, 55
 - map, 19
 - March's principle, 21
 - matched circles, 157
 - matrix groups, 40
 - matter
 - luminous matter, 129
 - matter
 - dark matter, 129
 - metric, 12
 - G -invariant metric, 54
 - Lorentzian metric, 12
 - Riemannian metric, 12
 - signature, 12
 - Minkowski space, 21
 - motion equation, 22, 23
 - multipole, 151
 - multipole coefficient, 154

 - Nil geometry, 72
 - null-homotopic, 44

 - observational universe, 120
 - observers space, 135
 - octahedral group, 83
 - octahedral space, 94, 113, 114
 - oddly-proportioned spaces, 165
 - one-point-compactification, 55
 - orbit, 40
 - orbit space, 41
 - orbit space distance function, 100
 - orientable, 25
 - space-orientable, 31
 - time-orientable, 26
 - locally time-orientable, 26
 - total-orientable, 31
-

- orthonormal basis, 12
- page, 70
- Pair Separation Histogram, 138
- parallel transport, 16
- past-oriented curve, 26
- path, 176
- path-connected, 176
- perfect fluid, 123
- physical universe, 120
- Poincaré dodecahedral space, 114
- Poincaré's Polyhedron Theorem, 109
- Poincaré's Theorem, 74
- polyhedral group, 83
- polyhedral spaces, 94, 113
- polyhedron, 102
 - cycles of polyhedra, 106
 - edge of a polyhedron, 102
 - faces of a polyhedron, 102
 - flag of a polyhedron, 102
 - regular polyhedron, 103
 - ridge of a polyhedron, 102
 - side of a polyhedron see side, 102
 - vertex of a polyhedron, 102
- power spectrum, 163
- principal bundle, 67
- prism space, 94, 113
- proper points, 102
- pseudogroup, 37
- quadrupole moment, 155
- quaternions, 92
- quotient space, 175
- Raychaudhuri equation, 125
- recombination, 35
- reflection, 55
- relaxation, 38
- Robertson-Walker metric, 123
- Robertson-Walker scale factor, 122
- rotational group, 82
- Sachs-Wolf effect, 153
- Sachs-Wolfe effect
 - integrated Sachs-Wolf effect, 154
- scalar field, 9
- section, 185
- Seifert-manifolds, 73
- side of a polyhedron, 102
 - adjacent sides, 105
 - cycle of sides, 107
 - cycle relation, 107
 - cycle transformation, 107
 - G-side-pairing, 108
 - related points, 105
 - sequence of sides, 107
 - side-pairing, 105
 - side-pairing transformations, 105
- similarity, 53
- simply-connected, 45
 - semi-locally simply-connected, 45
- single action, 93
- small universe, 136
- smooth, 38
- smoothing, 38
- Sol geometry, 73
- solid angle, 108
 - solid angle sum, 108
- space form, 80
 - homogeneous space form, 81
 - Euclidean space form, 80, 110
 - compact, 89
 - non-compact, 90
 - hyperbolic space form, 80, 96, 115
 - spherical space form, 80, 93, 112
- space of constant curvature, 68
- spherical harmonics, 154
- spherical space, 13, 43
- stabilizer, 40
- stably causal, 29
- steady-state cosmological model, 131

-
- stiffening, [38](#)
 - stress tensor, [10](#)
 - Sunyaev-Zel'dovich effect, [152](#)
 - symmetry group, [82](#)

 - tangent bundle, [9](#)
 - tangent space, [9](#)
 - tangent vector, [8](#)
 - tensor, [10](#)
 - abstract index notation, [11](#)
 - component notation, [10](#)
 - contraction, [11](#)
 - outer product, [10](#)
 - transformation law, [10](#)
 - tensor field, [11](#)
 - tessellation, [103](#)
 - brick tessellation, [104](#)
 - cells (chambers) of a tessellation, [104](#)
 - connected tessellation, [103](#)
 - exact tessellation, [103](#)
 - normalized tessellation, [104](#)
 - test body, [22](#)
 - tetrahedral group, [83](#)
 - Thick-Thin Decomposition, [97](#)
 - Thurston's Geometrization Theorem, [74](#)
 - time-preserving, [26](#)
 - topological group, [176](#)
 - topological lensing, [137](#)
 - topological space, [175](#)
 - topology
 - metric topology, [175](#)
 - quotient topology, [175](#)
 - torsion tensor, [15](#)
 - torsion-free, group, [86](#)
 - torus, [40](#), [56](#), [99](#)
 - embedded torus, [56](#)
 - flat torus, [56](#)
 - transformation, [21](#)
 - transition function, [7](#)
 - truncated cube space, [94](#), [113](#)

 - unimodular, [40](#)
 - universal covering space (UCS), [47](#)
 - upper half-space, [55](#)

 - vector
 - contravariant, [9](#)
 - covariant, [9](#)
 - null vector, [13](#)
 - space-like, [13](#)
 - time-like, [13](#)
 - vector bundle, [66](#)
 - vector field, [9](#)
 - left-invariant, [70](#)
 - integral curve, [71](#)

 - Weeks Space, [116](#)
 - well-proportioned spaces, [165](#)
 - worldline, [22](#)
-

Curriculum Vitae



Lebenslauf

Gudrun Weisz

geboren

am 13.12.1984 in Wien, Österreich

E-Mail

gudi.weisz@me.com

Ausbildung

- seit 10/2003** Diplomstudium Mathematik an der Universität Wien
- *Erster Studienabschnitt: Abschluss im März 2006*
 - *Zweiter Studienabschnitt: Schwerpunkt Algebra*
- 04/2012** Abschluss des Bakkalaureatsstudium Astronomie an der Universität Wien mit Auszeichnung
- 06/2003** GRG 21 Ödenburgerstraße, Abschluss mit Matura

Berufserfahrung

- 10/2010 – 10/2012** Studienassistentz an der Universität für Bodenkultur Wien für die Lehrveranstaltungen “Mathematik für LMBT” bei Ao.Univ.Prof Dr.phil. Wolfgang Ruppert, Betreuung von Übungsgruppen

Auslandserfahrung

- Sommersemester 2009** Austauschsemester im Rahmen des Erasmus-Programm an der Università degli Studi di Padova